

# UC San Diego

## UC San Diego Electronic Theses and Dissertations

### Title

Metal binding pharmacophore library yields discovery of inhibitors of the proteasome subunit Rpn11 and human Glyoxalase 1

### Permalink

<https://escholarship.org/uc/item/6961q7fj>

### Author

Perez, Christian

### Publication Date

2018

Peer reviewed|Thesis/dissertation

UNIVERSITY OF CALIFORNIA SAN DIEGO

**Metal binding pharmacophore library yields discovery of inhibitors of the proteasome subunit Rpn11 and human Glyoxalase 1**

A dissertation submitted in partial satisfaction of the requirements for the degree  
Doctor of Philosophy

in

Chemistry

by

Christian Perez

Committee in charge:

Professor Seth M. Cohen, Chair  
Professor Kamil Godula  
Professor Vivian Y.H. Hook  
Professor Charles L. Perrin  
Professor Jeffrey Rinehart

2018



The Dissertation of Christian Perez is approved, and it is acceptable in quality and form for publication on microfilm and electronically:

---

---

---

---

---

Chair

University of California San Diego

2018

## **DEDICATION**

To my family, thank you for supporting me

## TABLE OF CONTENTS

Signature Page.....	iii
Dedication.....	iv
Table of Contents .....	v
List of Symbols and Abbreviations .....	viii
List of Figures.....	xii
List of Schemes .....	xv
List of Tables .....	xviii
Acknowledgements .....	xx
Vita .....	xxii
Abstract of the Dissertation .....	xxxiii
<u>Chapter 1. Introduction</u> .....	1
1.1 Metalloenzymes as Medicinal Targets .....	2
1.2 Utilizing a Fragment-Based Drug Discovery Approach for Development of Metalloenzyme Inhibitors.....	5
1.3 Inhibitors of the Proteasome and Rpn11 as Cancer Therapeutics....	10
1.4 Inhibitors of Glyoxalase as Novel Treatments for Depression and Anxiety.....	16
1.5 Outlook.....	20
1.6 References .....	22
<u>Chapter 2: Discovery of an Inhibitor of the Proteasome Subunit Rpn11</u> .....	32

2.1 Introduction.....	33
2.2 Results and Discussion .....	35
2.2.1 Two Screenings Yield Inhibitors for Rpn11 .....	35
2.2.2 MBP Library Hits are Investigated as Potential Rpn11 Inhibitors ..	38
2.2.3 Investigating the Mechanism of Inhibition of 8-TQ .....	43
2.2.4 Synthesis of Methyl Derivatives and Cross Inhibition Studies.....	48
2.3 Conclusions.....	51
2.4 Experimental.....	53
2.5 Acknowledgements .....	78
2.6 References .....	79
 <u>Chapter 3: Capzimin is a potent and specific inhibitor of proteasome</u>	
<u>isopeptidase Rpn11 .....</u>	<u>83</u>
3.1 Introduction.....	84
3.2 Results and Discussion .....	85
3.2.1 Synthesis of an 8-TQ Sublibrary.....	85
3.2.2 Synthesis and Evaluation of Control Compounds .....	98
3.3 Conclusions.....	103
3.4 Experimental.....	105
3.5 Acknowledgements .....	138
3.6 References .....	139
 <u>Chapter 4: Discovery of Novel Glyoxalase 1 Inhibitors .....</u>	
4.1 Introduction.....	144

4.2 Results and Discussion .....	145
4.2.1 Screening of the MBP Library.....	145
4.2.2 Synthesis, Computational Docking, and Evaluation of a 3,4-HOPTO Library.....	149
4.2.3 Synthesis, Computational Docking, and Evaluation of a 2-BTP Library .....	154
4.3 Conclusion.....	163
4.4 Experimental.....	164
4.5 Acknowledgements .....	181
4.6 References .....	182
<u>Chapter 5: Computer Aided Design of Novel Potent Glyoxalase 1 Inhibitors</u> .....	186
5.1 Introduction.....	187
5.2 Results and Discussion .....	188
5.2.1 Investigating the Mechanism of Inhibition .....	188
5.2.2 Development of a GLO1 Computational Model .....	190
5.2.3 8-Sulfonamidequinoline Analogs .....	195
5.2.4 5-Aryl/Cyclic-8-(Methylsulfonylamino)quinoline Derivatives .....	198
5.2.5 Merged Compounds .....	202
5.3 Conclusions.....	205
5.4 Experimental.....	206
5.5 Acknowledgements .....	242

5.6 References .....	243
----------------------	-----

## LIST OF SYMBOLS AND ABBREVIATIONS

Ac	Acetyl
AcOH	Acetic Acid
ACN	Acetonitrile
AHC-GSH	<i>S</i> -( <i>N</i> -Aryl- <i>N</i> -hydroxycarbamoyl) Glutathione
2-BTP	2-(benzo[ <i>d</i> ]thiazol-2-yl)phenol
<i>t</i> -BuSH	<i>tert</i> -Butyl Thiol
CAD	Computer Aided Design
CDI	Carbonyl Diimidazole
Chugai-3d	6-Phenyl-7-azaindole- <i>N</i> -hydroxypyridinone
CP	Core Particle
Cyclen	1,4,7,10-Tetraazacyclododecane
CZM	Capzimin
DIPA	Diisopropylamine
DMF	<i>N</i> - <i>N</i> '-Dimethylformamide
DMSO	Dimethylsulfoxide
DNA	Deoxyribonucleic Acid
DTT	Dithiothreitol
DUB	Deubiquitinating Enzyme
E1	Ubiquitin-Activating Enzyme
E2	Ubiquitin-Conjugating Enzyme
E3	Ubiquitin-Ligase Enzyme

EDC	1-Ethyl-3-(3-dimethylaminopropyl)carbodiimide
EDTA	Ethylenediaminetetraacetic Acid
ESI-MS	Electrospray Ionization Mass Spectrometry
EtOH	Ethanol
EtOAc	Ethyl Acetate
FBDD	Fragment-Based Drug Discovery
FDA	Food and Drug Administration
FRET	Förster Resonance Energy Transfer
GABA	<i>gamma</i> -Aminobutyric acid
GFP	Green Fluorescent Protein
GLO1	Glyoxalase 1
GLO2	Glyoxalase 2
GSH	Glutathione
h	Hour
HATU	1-[Bis(dimethylamino)methylene]-1H-1,2,3-triazolo[4,5-b]pyridinium 3-oxid hexafluorophosphate
hCAII	Human Carbonic Anhydrase II
HCT	Human Colon Carcinoma
HDAC	Histone Deacetylase
HMDSO	Hexamethyldisiloxane
HOBT	Hydroxybenzotriazole
3,4-HOPTO	3-Hydroxy-1,2-dimethylpyridine-4(1 <i>H</i> )-thione

HPLC	High-Performance Liquid Chromatography
HRMS	High Resolution Mass Spectrometry
HTS	High-throughput screening
Hz	Hertz ( $s^{-1}$ )
IC <sub>50</sub>	Half Maximal Inhibition Concentration
<i>J</i>	Coupling Constant
LasB	<i>Pseudomonas Aeruginosa</i> elastase B
LE	Ligand Efficiency
LLE	Lipophilic Ligand Efficiency
5-LO	5-Lipoxygenase
MBP	Metal-Binding Pharmacophore
<i>p</i> -MBSH	4-Methoxyphenyl)methanethiol
MeOH	Methanol
min	Minute
MG	Methylglyoxal
M-GFN	Methyl Gerfelin
mL	Milliliter
mM	Millimolar
μM	Micromolar
MM	Multiple Myeloma
mmol	Millimoles
MMP	Matrix Metalloproteinase

MOE	Molecular Operating Environment
MS	Mass Spectrometry
8-MSQ	8-(Methylsulfonylamino)quinoline
MW	Molecular Weight
NMR	Nuclear Magnetic Resonance Spectroscopy
ROS	Reactive Oxygen Species
RP	Regulatory Particle
SBD	Structure Based Design
SAR	Structure Activity Relationship
sec	Second
Ub	Ubiquitin
UPS	Ubiquitin-Proteasome System
VS	Virtual Screening
TBAF	Tetrabutylammonium Fluoride
TFA	Trifluoroacetic Acid
THF	Tetrahydrofuran
Trp	Tris(pyrazolyl)borate
8-TQ	8-Thioquinoline
X-Phos	2-Dicyclohexylphosphino-2',4',6'-triisopropylbiphenyl

## LISTS OF FIGURES

- Figure 1-1.** A MBP fragment library designed for FBDD against metalloenzymes. Adapted from Jacobsen, J.A.....10
- Figure 1-2.** Structure of the 26S proteasome highlighting the 20S core and 19S regulatory particles. The  $\beta_5$  active site utilizes the N-terminal threonine for proteolysis. All three FDA approved proteasome inhibitors preferentially bind to this site.....12
- Figure 1-3.** Structure of the three FDA approved proteasome inhibitors.....14
- Figure 1-4.** Structure of the 26S proteasome highlighting the 20S core and 19S regulatory particle. The Rpn11 active site utilizes a catalytic  $Zn^{2+}$  to cleave the isopeptide bond between ubiquitin and the protein to be degraded.....15
- Figure 1-5.** The glyoxalase pathway.....17
- Figure 1-6.** Molecular structures of previously reported GLO1 inhibitors with their corresponding inhibition values.....19
- Figure 2-1.** Mechanism of degradation of polyubiquitinated proteins by the proteasome. In red is highlighted the specific step a Rpn11 inhibitor would prevent. Adapted from Li, J.....34
- Figure 2-2.** Screening results from a MBP library (Figure 1-1) against Rpn11. Lines represent percent enzyme inhibition for a given MBP fragment at a concentration of 200  $\mu$ M.....36
- Figure 2-3.** Screening results from the second generation MBP library against Rpn11. Lines represent percent enzyme inhibition for a given MBP fragment at a concentration of 200  $\mu$ M.....37
- Figure 2-4.** Chemical illustration (*left*) and image of the X-ray structure (*right*) of  $[(Tp^{Ph,Me})Zn(8-TQ)]$ . Thermal ellipsoids are shown at 50% probability. Hydrogen atoms are omitted for clarity. Color scheme: boron (pink), carbon (gray), nitrogen (blue), sulfur (yellow), and zinc (green).....44
- Figure 2-5.** Structure representation of 8-TQ with the quinoline ring positions labeled.....49

<b>Figure 3-1.</b> Cytotoxicity assay against 293T and A549 cancer cell lines with compound <b>43</b> ( <i>top</i> ) and <b>CZM</b> ( <i>bottom</i> ).....	97
<b>Figure 3-2.</b> Inhibition of <b>CZM</b> against Rpn11 in the presence and absence of Zn (cyclen) <sup>2+</sup> .....	99
<b>Figure 4-1.</b> Reaction scheme depicting the GLO1 assay ( <i>top</i> ) screening results of the MBP library against GLO1 using a colorimetric assay ( <i>bottom</i> ). Lines represent percent enzyme inhibition for a given MBP fragment at a concentration of 200 $\mu$ M.....	147
<b>Figure 4-2.</b> Screening results of the MBP library against GLO1 using a colorimetric assay. Lines represent percent enzyme inhibition for a given MBP fragment at a concentration of 50 $\mu$ M.....	148
<b>Figure 4-3.</b> Molecular structures of the three lead fragment hits from the MBP library screen. MBP acronyms and IC <sub>50</sub> values against GLO1 are shown.....	148
<b>Figure 4-4.</b> Superpositioned pose of <b>3,4-HOPTO</b> coordinating to the Zn <sup>2+</sup> ion the GLO1 active site ( <i>left</i> ) and chemical illustration ( <i>right</i> ). A surface outlining the active site pockets is shown in gray. Zn <sup>2+</sup> ion is depicted as an orange sphere and water molecule as a red sphere.....	150
<b>Figure 4-5.</b> Superpositioned pose of <b>3,4-HOPTO</b> coordinating to the Zn <sup>2+</sup> ion the GLO1 active site ( <i>left</i> ) and chemical illustration ( <i>right</i> ). A surface outlining the active site pockets is shown in gray. Zn <sup>2+</sup> ion is depicted as an orange sphere and water molecule as a red sphere.....	152
<b>Figure 4-6.</b> Superpositioned pose of <b>2-BTP</b> coordinating to the Zn <sup>2+</sup> ion the GLO1 active site ( <i>left</i> ) and chemical illustration ( <i>right</i> ). A surface outlining the active site pockets is shown in gray. Zinc is depicted as an orange sphere.....	155
<b>Figure 5-1.</b> Superpositioned pose of <b>8-MSQ</b> coordinating to the Zn <sup>2+</sup> ion the GLO1 active site ( <i>left</i> ) and chemical illustration ( <i>right</i> ). Two possible coordinating poses are shown: pose 1 ( <i>top</i> ) and pose 2 ( <i>bottom</i> ). A surface outlining the active site pockets is shown in gray.....	188
<b>Figure 5-2.</b> Superpositioned pose of compound <b>107</b> coordinating to the Zn <sup>2+</sup> in the GLO1 active site. An image demonstrating the amino acid side chain residues is shown ( <i>left</i> ) with a surface outlining the active site GSH binding pocket is shown in gray and a chemical illustration ( <i>bottom</i> ).....	193

**Figure 5-3.** Superpositioned pose of compound **122** coordinating to the Zn<sup>2+</sup> ion the GLO1 active site. An image demonstrating the amino acid side chain residues is shown (*left*) with a surface outlining the active site GSH binding pocket is shown in gray and a chemical illustration (*bottom*).....196

**Figure 5-4.** Superpositioned pose of **136** coordinating to the Zn<sup>2+</sup> ion the GLO1 active site (*left*) and chemical illustration (*right*). A surface outlining the active site pockets is shown in gray. Zinc is depicted as an orange sphere.....200

**Figure 5-5.** Binding mode of **146** within GLO1 active site (*left*) and a chemical illustration of mode of binding (*right*).....205

## LISTS OF SCHEMES

- Scheme 2-1.** Synthetic route for compounds **6-8**. Reagents and conditions: (a) P<sub>2</sub>S<sub>5</sub>, Hexamethyldisiloxane (HMDSO), Toluene, 110 °C, 8 h (b) Amine, AcOH, H<sub>2</sub>O, EtOH, 165 °C (Microwave Reactor), 1 h.....40
- Scheme 2-2.** Synthetic route for 2-hydroxy-5-methylbenzoic acid analogs. Reagents and conditions: (a) EDC, HOBT, DMF, 25 °C 1 h.....42
- Scheme 2-3.** Synthetic route for pyridine-2,6-dicarboxylic acid analogs. Reagents and conditions: (a) MeOH, H<sub>2</sub>SO<sub>4</sub> (cat.), 75 °C, 24 h (b) MeOH, KOH, 0 °C, 4 h (c) EDC, HOBT, R-NH<sub>2</sub>, 18 h; then 4:1 1 M NaOH/THF, 30 min to 1 h, 4 M HCl (d) EDC, HOBT, MeNH<sub>2</sub>, 18 h.....42
- Scheme 2-4.** Synthesis of 8-(methylthio)quinoline. Reagents and conditions: (a) CH<sub>3</sub>I, EtOH, H<sub>2</sub>O, 2M NaOH, 25 °C.....46
- Scheme 2-5.** Synthesis of quinoline-5-thiol. Reagents and conditions: (a) POCl<sub>3</sub>, 100 °C; (b) *tert*-butylthiol (*t*-BuSH), NaH, DMF, 140 °C; (c) 12M HCl, 100 °C. ....47
- Scheme 2-6.** Synthesis of quinoline-5-thiol. Reagents and conditions: (a) 2,2,6-Trimethyl-4H-1,3-dioxin-4-one (Meldrum's acid), Triethyl orthoformate, 105 °C; (b) Dowtherm A, 250 °C; (c) POCl<sub>3</sub>, Toluene, 110 °C; (d) 4-Methoxyphenyl)methanethiol (*p*-MBSH), NaH, DMF, 25 °C; (e) *m*-Cresol....47
- Scheme 2-7.** Synthesis of 2-, 3-, and 4-methyl-8-thioquinoline. Reagents and conditions: (a) Toluene, 6M HCl, 110 °C; (b) *t*-BuSH, NaH, DMF, 140 °C; (c) 12M HCl, 100 °C.....49
- Scheme 2-8.** Synthesis of 5- and 6-methyl-8-thioquinoline. Reagents and conditions: (a) Glycerol, Nitrobenzene, 150 °C; (b) *t*-BuSH, NaH, DMF, 140 °C; (c) 12M HCl, 100 °C. ....49
- Scheme 3-1.** Synthesis of 2- and 3-carboxyl-8-thioquinoline derivatives. Reagents and conditions: (a) *t*-BuSH, NaH, DMF, 140 °C; (b) 12M HCl, 110 °C; (c) H<sub>2</sub>SO<sub>4</sub>, MeOH, reflux.....86
- Scheme 3-2.** Synthesis of 4-carboxyl-8-thioquinoline. Reagents and conditions: (a) Sodium Pyruvate, 5M NaOH, 110 °C; (b) H<sub>2</sub>O, 170 °C; (c) *t*-BuSH, NaH, DMF, 140 °C; (d) 12M HCl, 110 °C; (e) H<sub>2</sub>SO<sub>4</sub>, MeOH,.....87
- Scheme 3-3.** Synthesis of 3-carboxamide derivatives. Reagents and conditions: (a) CDI, DMF, 25 °C; (b) HATU, Et<sub>3</sub>N, DMF, 60 °C.....87

- Scheme 3-4.** Synthesis of an 8-hydroxyquinoline MBP based analog of lead compound **CZM**. Reagents and conditions: (a) 2-(Thiazol-2-yl)ethan-1-amine, HATU, Et<sub>3</sub>N, DMF, 25 °C.....99
- Scheme 3-5.** Synthesis of a methylated analog of lead compound **CZM**. Reagents and conditions: (a) NaBH<sub>4</sub>, MeOH, 25 °C; (b) CH<sub>3</sub>I, THF.....99
- Scheme 3-6.** Synthesis of a structural-isomer analog of lead compound **CZM**. Reagents and conditions: (a) Crotonaldehyde, Toluene, 6M HCl, reflux; (b) SeO<sub>2</sub>, Pyridine, reflux; (c) Pd(OH)<sub>2</sub>/C, 1M NaOH, MeOH, H<sub>2</sub>, 25 °C; (d) 2-(Thiazol-2-yl)ethan-1-amine, HATU, Et<sub>3</sub>N, DMF, 25 °C.....100
- Scheme 3-7.** Synthesis of a MBP analog of lead compound **CZM**. Reagents and conditions: (a) Meldrum's acid, Triethylformate, 100 °C; (b) Dowtherm A, 250 °C; (c) POCl<sub>3</sub>, Toluene, 110 °C; (d) *p*-MBSH, NaH, DMF, 25 °C; (e) 2-(Thiazol-2-yl)ethan-1-amine, pyridine, EDC, HOBT, DMF, 25 °C.....101
- Scheme 4-1.** Synthetic route for 3-hydroxy-2-methylpyridine-4(1*H*)-thione analogs. Reagents and conditions: (a) P<sub>2</sub>S<sub>5</sub>, HMDSO, toluene, 110 °C, 8 h; (b) amine, AcOH, H<sub>2</sub>O, EtOH, 165 °C (microwave reactor).....152
- Scheme 4-2.** Synthesis of **94**. Reagents and conditions: (a) 2-Aminobenzenethiol, sulfamic acid, H<sub>2</sub>O, MeOH, Acetone, 25 °C; (b) Phenylboronic acid, DIPA, Pd(OAc)<sub>2</sub>, H<sub>2</sub>O, 100 °C.....157
- Scheme 4-3.** Synthesis of **95**. Reagents and conditions: (a) Ethynyltrimethylsilane, Pd(dppf)Cl<sub>2</sub>, CuI, Et<sub>3</sub>N, X-Phos, Dioxane, 80 °C; (b) TBAF, H<sub>2</sub>O, DMF, 25 °C; (c) Benzyl azide, DIPA, CuI, DMF, 25 °C; (d) BBr<sub>3</sub>, CHCl<sub>3</sub>, 25 °C.....159
- Scheme 4-4.** Synthesis of **97**. Reagents and conditions: (a) Benzaldehyde, EtOH, reflux; (b) Dess-Martin periodinane (DMP), CH<sub>2</sub>Cl<sub>2</sub>, 25 °C; (c) BBr<sub>3</sub>, CHCl<sub>3</sub>, 25 °C.....159
- Scheme 4-5.** Synthesis of **98**. Reagents and conditions: (a) Phenylboronic acid, DIPA, Pd(OAc)<sub>2</sub>, H<sub>2</sub>O, 100 °C; (b) (CF<sub>3</sub>SO<sub>2</sub>)<sub>2</sub>O, Pyridine, CH<sub>2</sub>Cl<sub>2</sub>, 0-25 °C; (c) Ethynyltrimethylsilane, Pd(PPh<sub>3</sub>)<sub>2</sub>Cl<sub>2</sub>, CuI, Et<sub>3</sub>N, Dioxane, 80 °C; (d) TBAF, H<sub>2</sub>O, DMF, 25 °C; (e) Benzyl azide, DIPA, CuI, DMF, 25 °C.....162
- Scheme 4-6.** Synthesis of **99**. Reagents and conditions: (a) MeOH, H<sub>2</sub>SO<sub>4</sub>, reflux; (b) Phenylboronic acid, K<sub>2</sub>CO<sub>3</sub>, Pd(dppf)Cl<sub>2</sub>, Dioxane, reflux; (c) Hydrazine, EtOH, reflux; (d) Benzaldehyde, EtOH, reflux; (e) DMP, CH<sub>2</sub>Cl<sub>2</sub>, 25 °C; (f) BBr<sub>3</sub>, CHCl<sub>3</sub>, 25 °C.....162

**Scheme 5-1.** Synthesis of 8-sulfonamide derivatives. (a) R-SO<sub>2</sub>Cl, pyridine, 25 °C; (b) R-SO<sub>2</sub>Cl, pyridine, 25 °C. ).....193

**Scheme 5-2.** Synthesis 5-Aryl/Cyclic/Ethynyl-8-sulfonamide quinoline derivatives. (a) KNO<sub>3</sub>, H<sub>2</sub>SO<sub>4</sub>, 0-25 °C; (b) R-B(OH)<sub>2</sub>, Pd(OAc)<sub>2</sub>, DIPA, H<sub>2</sub>O, 100 °C; (c) R-B(OH)<sub>2</sub>, Pd(PPh<sub>3</sub>)<sub>4</sub>, CH<sub>3</sub>COOK, 1,4-Dioxane 100 °C; (d) R-B(OH)<sub>2</sub>, Pd(dppf)Cl<sub>2</sub>, S-Phos, K<sub>2</sub>CO<sub>3</sub>, H<sub>2</sub>O, 1,4-Dioxane, 100 °C.....200

**Scheme 5-3.** Synthesis 5-Aryl/Cyclic/Ethynyl-8-sulfonamide quinoline derivatives. (a) Acrolein, 6M HCl, toluene, reflux; (b) R-Ethynyl, CuI, Pd(dppf)Cl<sub>2</sub>, X-Phos, Et<sub>3</sub>N, 1,4-Dioxane 90 °C; (c) Pd/C, H<sub>2</sub>, MeOH, 25 °C; (h) Na<sub>2</sub>S<sub>2</sub>O<sub>4</sub>, K<sub>2</sub>CO<sub>3</sub>, H<sub>2</sub>O, MeOH, Acetone 25 °C; (d) R-SO<sub>2</sub>Cl, pyridine.....203

## LISTS OF TABLES

<b>Table 1-1.</b> Examples of metalloenzymes that have attracted attention as therapeutic targets. Adapted from Martin, D.P.....	4
<b>Table 1-2.</b> Examples of lead identification by FBDD. The target protein is indicated as well as the method used for fragment growth. MNEC, maximal non-effective concentration; NMR, nuclear magnetic resonance; SBD, structure-based design; VS, virtual screening. Adapted from Rees, D.C.....	7
<b>Table 2-1.</b> Hits against Rpn11 from the MBP library screens. All values listed are percent inhibition at a concentration of 200 $\mu\text{M}$ .....	40
<b>Table 2-2.</b> Derivatives of hits obtained from the MBP library against Rpn11. All values listed are percent inhibition at a concentration of 200 $\mu\text{M}$ .....	41
<b>Table 2-3.</b> <b>8-TQ</b> fragment derivatives used to examine the role of metal binding in Rpn11 inhibition. . All $\text{IC}_{50}$ values listed are in $\mu\text{M}$ .....	46
<b>Table 2-4.</b> Enzyme inhibition data for <b>8-TQ</b> and derivatives of this MBP hit. Data listed includes inhibitory values against off-target metalloenzymes and cytotoxicity against the HCT 116 cell line. All $\text{IC}_{50}$ values listed are in $\mu\text{M}$ .....	50
<b>Table 3-1.</b> Rpn11 inhibitory activity of <b>8-TQ</b> derivatives functionalized at the 2-, 3-, and 4-positions of the ring system. All $\text{IC}_{50}$ values listed are in $\mu\text{M}$ .....	89
<b>Table 3-2.</b> Inhibitory activity against Rpn11, Csn5, and AMSH for 3-position substituted <b>8-TQ</b> derivatives. Cellular levels of proteasome inhibition are also listed. All $\text{IC}_{50}$ values listed are in $\mu\text{M}$ .....	92
<b>Table 3-3.</b> Inhibitory activity against Rpn11, Csn5, and AMSH for control compounds. Cellular levels of proteasome inhibition are also listed. All $\text{IC}_{50}$ values listed are in $\mu\text{M}$ .....	101
<b>Table 3-4.</b> Summary of CZM $\text{IC}_{50}$ on $\text{Zn}^{2+}$ -dependent metalloenzymes.....	103
<b>Table 4-1.</b> Inhibitory activity against GLO1 for <b>3,4-HOPTO</b> derivatives.....	153
<b>Table 4-2.</b> Inhibitory activity against GLO1 for <b>2-BTP</b> derivatives.....	156
<b>Table 4-3.</b> Inhibitory activity against GLO1 for <b>2-BTP</b> derivatives.....	160
<b>Table 5-1.</b> <b>8-MSQ</b> fragment derivatives used to examine the role of metal binding in GLO1 inhibition. All $\text{IC}_{50}$ values listed are in $\mu\text{M}$ .....	190

<b>Table 5-2. 8-MSQ derivatives used to examine the coordination mode in the computational model. All IC<sub>50</sub> values listed are in μM.....</b>	<b>194</b>
<b>Table 5-3. 8-MSQ fragment derivatives probing functionalization at the 8-position. All IC<sub>50</sub> values listed are in μM.....</b>	<b>197</b>
<b>Table 5-4. 8-MSQ fragment derivatives used to examine the role of metal binding in GLO1 inhibition. Values shown represent IC<sub>50</sub> (μM).....</b>	<b>201</b>
<b>Table 5-5. 8-MSQ fragment derivatives used to examine the role of metal binding in GLO1 inhibition. All IC<sub>50</sub> values listed are in μM.....</b>	<b>204</b>

## ACKNOWLEDGEMENTS

To my mom, thanks for always supporting and believing in me, everything I have achieved is because of you. Thanks to my brother, sister, and friends for pushing me and always supporting me. To my beautiful wife, thank you for putting up with me everyday. Lastly, to my daughter Natalia, I did this for you.

I want to thank Professor Seth M. Cohen for allowing me to be part of your lab. I have learned so much about science, life and myself through being a Cohen lab member, so thank you for giving me this chance. Thank you to the former Cohen lab members Professor Matthieu Rouffet, Dr. David P. Martin, and Dr. David Puerta for always answering my questions and being great mentors. A special thanks to Dr. Kevin B. Daniel for being a great mentor and friend, lab was always fun while you were around brah. I would also like to give a special thanks to the current Cohen lab members for their help and support. Lastly, I would like to acknowledge my “BFF” Allie Y. Chen and the smartest mentee there is, Peter F. Glatt, both of you made my final years in graduate school fun and tolerable.

Collaborators have been crucial to my success as a graduate student. Dr. Yongxuan Su is one of the most talented analytical chemists I know, and I thank you for all of your hard work with my projects. I would like to thank Professor Raymond Deshaies and Dr. Jing Li for their work and contribution with the Rpn11 project. Thank you to Professor Abraham Palmer and Amanda Barkley-Levenson for their guidance and work in the glyoxalase project. I also would like to thank Benjamin Dick for his helpful discussions and assistance with

crystallography in our glyoxalase project. Lastly, again thanks to Peter F. Glatt for all your assistance with the glyoxalase assays.

Chapter 2 and 3, in part, is a reprint of the materials published in the following paper: Christian Perez, Jing Li, Francesco Parlati, Matthieu Rouffet, Yuyong Ma, Andrew L. Mackinnon, Tsui-Fen Chou, Raymond J. Deshaies, and Seth M. Cohen. “Discovery of an Inhibitor of the Proteasome Subunit Rpn11”, *J. Med. Chem.* **2017**, *60*, 1343-1361. The permission to reproduce materials is granted by American Chemical Society. The dissertation author was the primary researcher for the data presented. The co-authors listed in these publications also participated in the research.

Chapter 4 and 5, highlights the work of a publication currently in preparation. The manuscript in preparation was authored by the following: Christian Perez, Benjamin Dick, Peter F. Glatt, and Seth M. Cohen with a planned title of “Metal-Binding Pharmacophore Library Yields Discovery of a Novel Glyoxalase 1 Inhibitor.” The dissertation author was the primary researcher for the data presented. The co-authors listed in these publications also participated in the research.

## VITA

### EDUCATION

<b>University of California San Diego</b> Ph.D., Chemistry	2018
<b>University of California San Diego</b> M.S., Chemistry	2015
<b>University of California San Diego</b> B.S., Biochemistry/Chemistry	2013

### PUBLICATIONS

1. Perez, C.; Li, J.; Parlati, F.; Rouffet, M.; Ma, Y.; Mackinnon, A. L.; Chou, T-F.; Deshaies, R.J.; S.M., Cohen. "Discovery of an Inhibitor of the Proteasome Subunit Rpn11." *J. Med. Chem.*, **2017**, 60, 1343–1361
2. Li, J.; Yakushi, T.; Parlati, F.; Mackinnon, A. L.; Perez, C.; Ma, Y.; Carter, K. P.; Colayco, S.; Magnuson, G.; Brown, B.; Nguyen, K.; Vasile, S.; Suyama, E.; Smith, L. H.; Sergienko, E.; Pinkerton, A. B.; Chung, T. D. Y.; Palmer, A.; Pass, I.; Hess, S.M.; Cohen, S. M.; Deshaies, R. J. "Capzimin, a potent and specific inhibitor of proteasome isopeptidase Rpn11." *Nat. Chem. Biol.*, **2017**, 13, 486–493
3. Perez, C.; Monserrat, J.P.; Cohen, S.M. "Exploring Hydrogen Peroxide Responsive Thiazolidinone -Based Prodrugs" *Chem. Commun.*, **2015**, 51, 7116-7119
4. Perez, C.; Daniel, K.B.; Cohen, S.M. "Evaluating Prodrug Strategies for Esterase-Triggered Release of Alcohols" *ChemMedChem*, **2013**, 8, 1662-1667

### PATENTS

1. Cohen, S.M.; Deshaies, R.J.; Perez, C.; Li, J. "Inhibitors of Rpn11." Patent No. US 10,005,735 B2, filed August 17, 2016
2. Cohen, S.M.; Puerta, D.T.; Perez, C. "Inhibitors of LpxC." Patent No. US 2017/0088532 A1, filed June 3, 2016.
3. Cohen, S.M.; Perez, C.; Monserrat, J.P. "Reactive Oxygen Species-Based Prodrugs." Patent No. US 2015/0005352, filed June 26, 2014

## **ABSTRACT OF THE DISSERTATION**

Metal binding pharmacophore library yields discovery of inhibitors of the proteasome subunit Rpn11 and human Glyoxalase 1

by

Christian Perez

Doctor of Philosophy in Chemistry

University of California San Diego, 2018

Professor Seth M. Cohen, Chair

Metalloproteins are essential in many biological processes and make up approximately one-third to one-half of the proteome. Metalloproteins utilize a

metal ion cofactor that can serve a structural role, allow electron transfer, or catalyze an enzymatic reaction. Specifically, a metalloprotein that utilizes a metal ion in a catalytic role is referred to as a metalloenzyme. The catalytic activity of certain metalloenzymes has been associated with a number of diseases ranging from diabetes, cancer, depression, anxiety, and pathogenic infections.<sup>4</sup> Therefore the development of novel therapeutics that target specific metalloenzymes in these diseased states is in great need. The use of fragment-based drug discovery (FBDD) through the use of metal-binding pharmacophores (MBP) libraries for metalloenzyme inhibitor development represents a unique opportunity. This dissertation will focus on utilizing FBDD for the discovery of novel metalloenzyme inhibitors. Two therapeutically relevant Zn<sup>2+</sup>-dependent enzymes, Rpn11 and GLO1, were chosen as targets. The use of a modest MBP fragment library to enable the discovery of a novel class of inhibitors for Rpn11 will be presented in Chapter 2. Chapter 3 details a synthetic campaign prompted by the discoveries discussed in Chapter 2, that lead to the development of a first-in-class potent Rpn11 inhibitor. The same FBDD approach was utilized for the development of a novel class of GLO1 inhibitors, which is described in Chapter 4. Lastly, a novel potent GLO1 inhibitor is described in Chapter 5.

## **Chapter 1. Introduction**

## 1.1 Metalloenzymes as Medicinal Targets

Metalloproteins are essential in many biological processes including transcription, protein homeostasis, photosynthesis, detoxification of reactive metabolites, cellular signaling, and many others.<sup>1</sup> It is estimated that approximately one-third to one-half of the proteome is comprised of metalloproteins, wherein the metal ion cofactor can serve a structural role, allow electron transfer, or catalyze an enzymatic reaction.<sup>1-3</sup> Specifically, a metalloprotein that utilizes a metal ion in a catalytic role is referred to as a metalloenzyme. The misregulation of metalloenzymes has been associated with a number of diseases ranging from diabetes, cancer, depression, anxiety, and pathogenic infections.<sup>4</sup> Therefore the development of novel therapeutics that target specific metalloenzymes in these diseased states is in great need. Some clinically relevant metalloenzyme targets along with their metal co-factor and indication are highlighted in Table 1-1. Although many metalloenzymes have been associated with diseases, the clinical success of inhibitors has been limited to only a few classes of metalloenzymes.<sup>5</sup>

An effective strategy for the design of metalloenzyme inhibitors consist of two main components: a metal-binding pharmacophore (MBP) and a backbone substituent(s). A MBP is a functional group that typically possess one or two donor atoms that can coordinate to the active site metal ion and thereby serve as an anchoring point to the rest of the molecule. The backbone component is designed via traditional medicinal chemistry methods to form interactions with the

amino acid residues within the active site. Traditionally, the MBP components of metalloenzyme inhibitors have not been well studied or understood, which is highlighted by the fact that inhibitors typically have relied on only a handful of MBPs. By far the most common MBPs utilized are carboxylic acids, thiols, phosphates, and hydroxamic acids.<sup>6</sup> Although these four classes of MBPs are capable of forming strong coordination bonds with active site metals, they often do not possess the most “drug like” properties and can be a liability in drug design and development.

**Table 1-1.** Examples of metalloenzymes that have attracted attention as therapeutic targets. Adapted from Martin, D.P.<sup>6</sup>

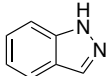
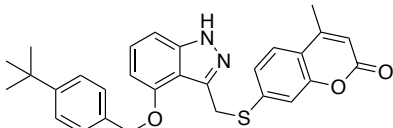
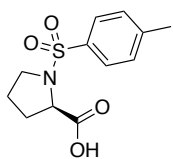
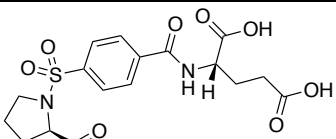
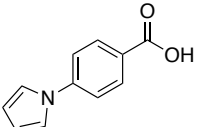
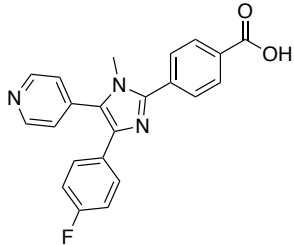
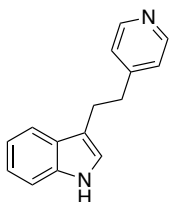
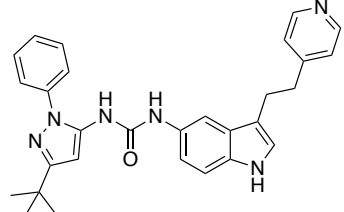
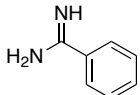
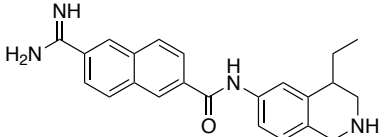
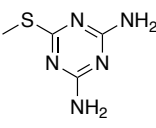
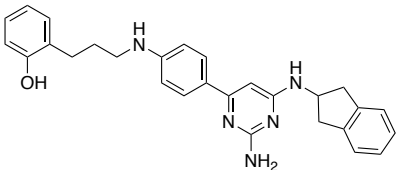
<b>Enzyme</b>	<b>Metal Ion</b>	<b>Disease/Condition</b>
Adamalysin	Zn <sup>2+</sup>	Cancer
Angiotensin converting enzyme	Zn <sup>2+</sup>	Hypertension
Carbonic anhydrase	Zn <sup>2+</sup>	Glaucoma
Catechol- <i>O</i> -methyltransferase	Mg <sup>2+</sup>	Parkinson's disease
Farnesyl transferase	Zn <sup>2+</sup>	Cancer
Glyoxalase 1	Zn <sup>2+</sup>	Cancer
Histone deacetylase	Zn <sup>2+</sup>	Cancer
Histone demethylase	Fe <sup>2+</sup>	Cancer
Indoleamine 2,3-dioxygenase	Fe <sup>2+</sup>	Cancer
KRAS	Mg <sup>2+</sup>	Cancer
5-Lipoxygenase	Fe <sup>2+</sup>	Asthma
Matrix metalloproteinase	Zn <sup>2+</sup>	Cancer, arthritis, inflammation
Methionine aminopeptidase	Mn <sup>2+</sup>	Cancer
Neprilysin	Zn <sup>2+</sup>	Hypertension
Rpn11	Zn <sup>2+</sup>	Cancer
TNF- $\alpha$ converting enzyme	Zn <sup>2+</sup>	Cancer
Tyrosinase	Cu <sup>2+</sup>	Cancer
<b>Pathogenic Enzyme</b>	<b>Metal Ion</b>	<b>Organism</b>
Anthrax Lethal Factor	Zn <sup>2+</sup>	<i>B. anthracis</i>
Botulinum Neurotoxin	Zn <sup>2+</sup>	<i>C. botulinum, butyricum, baratii</i>
HIV integrase	Mg <sup>2+</sup>	Human Immunodeficiency Virus
Influenza endonuclease	Mn <sup>2+</sup>	Influenza Virus
IspC	Mn <sup>2+</sup>	Gram-negative and positive bacteria
IspF	Zn <sup>2+</sup>	Gram-negative and positive bacteria
LasB	Zn <sup>2+</sup>	<i>P. aureginosa</i>
LpxC	Zn <sup>2+</sup>	Gram-negative bacteria
Metallo- $\beta$ -lactamases	Zn <sup>2+</sup>	Gram-negative and positive bacteria
Peptide deformylase	Fe <sup>2+</sup>	Gram-negative and positive bacteria

## 1.2 Utilizing a Fragment-Based Drug Discovery Approach for Development of Metalloenzyme Inhibitors

In the last 20 years, fragment-based drug discovery (FBDD) has emerged as an alternative to traditional drug discovery methods, such as high-throughput screening (HTS), combinatorial chemistry, computer aided design (CAD), and de novo design.<sup>7-10</sup> This method of discovering novel therapeutics has yielded >30 drug candidates, and was validated with the Food and Drug Administration (FDA) approval of two drugs, vemurafenib and venetoclax.<sup>10</sup> Vemurafenib is B-Raf enzyme inhibitor approved in 2011 for the treatment of late-stage melanoma, while venetoclax gained its approval in 2015 for the treatment of chronic lymphocytic leukemia. At a fundamental level, FBDD utilizes libraries of simpler, smaller compounds in order to efficiently probe a broader chemical space than when using complex compounds with higher molecular weight (which is more typical in HTS campaigns). A shortcoming of FBDD is that fragments generally have a poor affinity for the target due to the limited number of interactions it can make with its receptor. However, these interactions are considered to be 'high-quality' interactions, as they must overcome a substantial entropic barrier to binding, relative to their size.<sup>11</sup> Drug discovery from a FBDD approach typically involves the rational design of fragment libraries that follow the "Rule of Three": small fragments with low molecular weight (<300 amu), minimal hydrophobicity and good aqueous solubility (cLogP <3), and limited hydrogen bond donors (<3) and acceptors (<3). Together these set of rules are designed to yield fragments with good physicochemical and pharmacokinetics properties.<sup>11</sup> One obstacle in

utilizing FBDD lies in the challenge of transforming a fragment into a lead compound. Therefore, medicinal chemistry principles should be used early on to assess which fragments to invest in. Fragment structural analysis to determine physicochemical properties such as cLogP and cLogD, as well as ligand efficiency (LE) and lipophilic ligand efficiency (LLE), are effective metrics that help determine the lead fragment.<sup>12-13</sup> LE is a metric that correlates molecular weight with the binding affinity of the ligand, while LLE is a metric that correlates cLogP with binding affinity. Another challenge for FBDD is to determine the binding mode of the fragment to the target, which can be determined via biophysical screening techniques such as NMR or x-ray crystallography. With these methods, the binding mode of a fragment to a target protein can be determined, allowing for development strategy on how to elaborate a simple fragment into a complex molecule that targets additional interactions with the protein active site. Synthetically 'growing' of the fragments can lead to tighter binding molecules with greater activity. A sample of previously reported lead compounds identified via a fragment-growth strategy is highlighted in Table 1-2. For example, Entry 1 in Table 1-2 depicts a fragment that inhibits bacterial DNA gyrase and the methods utilized for fragment growth. An indazole molecule was initially identified with weak affinity (10 mM) and was elaborated via virtual screening (VS) and structure-based design (SBD) into a lead compound with good activity. Entries 2-6 (Table 1-2) depict the protein target, methods utilized for fragment-growth, and the structural elaboration from fragment to lead.

**Table 1-2.** Examples of lead identification by FBDD. The target protein is indicated as well as the method used for fragment growth. MNEC, maximal non-effective concentration; NMR, nuclear magnetic resonance; SBD, structure-based design; VS, virtual screening. Adapted from Rees, D.C.<sup>8</sup>

Entry	Target/Method	Fragment Hit	Lead Compound
1	DNA Gyrase/ VS and SBD	 $K_d = 10 \text{ mM}$	 MNEC = 30 ng/mL
2	Thymidylate synthase/ Tethering and SBD	 $IC_{50} = 1.1 \text{ mM}$	 $IC_{50} = 330 \text{ nM}$
3	p38 kinase/ NMR	 $K_d = 1 \text{ mM}$	 $K_i = 200 \text{ nM}$
4	p38 kinase/ X-ray and SBD	 $IC_{50} = 33 \text{ }\mu\text{M}$	 $IC_{50} = 142 \text{ nM}$
5	Urokinase/ Bioassay and SBD	 $K_i = \text{not reported}$	 $K_i = 6.3 \text{ nM}$
6	Erm methyl transferase/ NMR	 $K_d = 1 \text{ mM}$	 $K_i = 7.5 \text{ }\mu\text{M}$

FBDD for the development of metalloenzyme inhibitors presents a unique method for discovery of novel inhibitors. Metalloenzymes typically utilize divalent catalytic metals with open coordination sites in order to serve their function. A common efficient strategy for developing inhibitors of metalloenzymes is by developing a compound that incorporates a MBP that can coordinate to the catalytic metal and serve as an anchoring point.<sup>5</sup> Because substrate turnover by metalloenzymes generally proceeds through a metal-bound species, blocking the metal-substrate interaction is an effective strategy for inhibition. Targeting the metal ion is an attractive method for initial direct binding of a fragment. The development of libraries of fragments that incorporate donor atoms capable of binding to the metal can be designed to yield MBP fragment libraries.<sup>14</sup> In essence, this provides an ideal method for initial screening efforts because it introduces a bias to where the fragment will bind to the metalloenzyme (i.e., the metal ion active site). Utilizing the principles of inorganic chemistry one can model or assume a binding event between the MBP fragment and the catalytic metal center. If the assumption is made that the MBP fragment is binding to the metal ion and a crystal structure of the target protein has been reported, then a hypothesis on how to elaborate the MBP fragment into a complex molecule can be made. Additionally, metalloenzymes utilize the metals in a catalytic fashion; hence, a MBP fragment that inhibits through coordination can be anticipated to be a competitive inhibitor.

The use of FBDD for the development of metalloenzyme inhibitors was described by Cohen, wherein a small fragment library of 96 MBPs was rationally designed.<sup>14</sup> The library generally consisted of previously reported metal binding motifs such as salicylic acids, hydroxamic acids, hydroxyl pyrones, hydroxypyridinones, hydroxyquinolones, among others (Figure 1-1). In this proof of concept study, the 96 fragments were screened against a small panel of metalloenzymes utilizing commercially available assays. Surprisingly, these screens yielded several hits for each metalloenzyme, which highlights the effectiveness and efficiency of FBDD as an approach for metalloenzyme inhibitors. The hits from the library screening were then linked or grown in order to generate “full length”, active lead compounds. Subsequently, the library generated from this study was utilized to discover novel inhibitors for several metalloenzymes, including *Pseudomonas Aeruginosa* elastase (LasB)<sup>15-16</sup>, human carbonic anhydrase II (hCAII),<sup>17</sup> and influenza endonuclease.<sup>18</sup> The focus of this dissertation is the use of this library and FBDD to develop inhibitors for the proteasome subunit Rpn11, and glyoxalase 1 (GLO1).

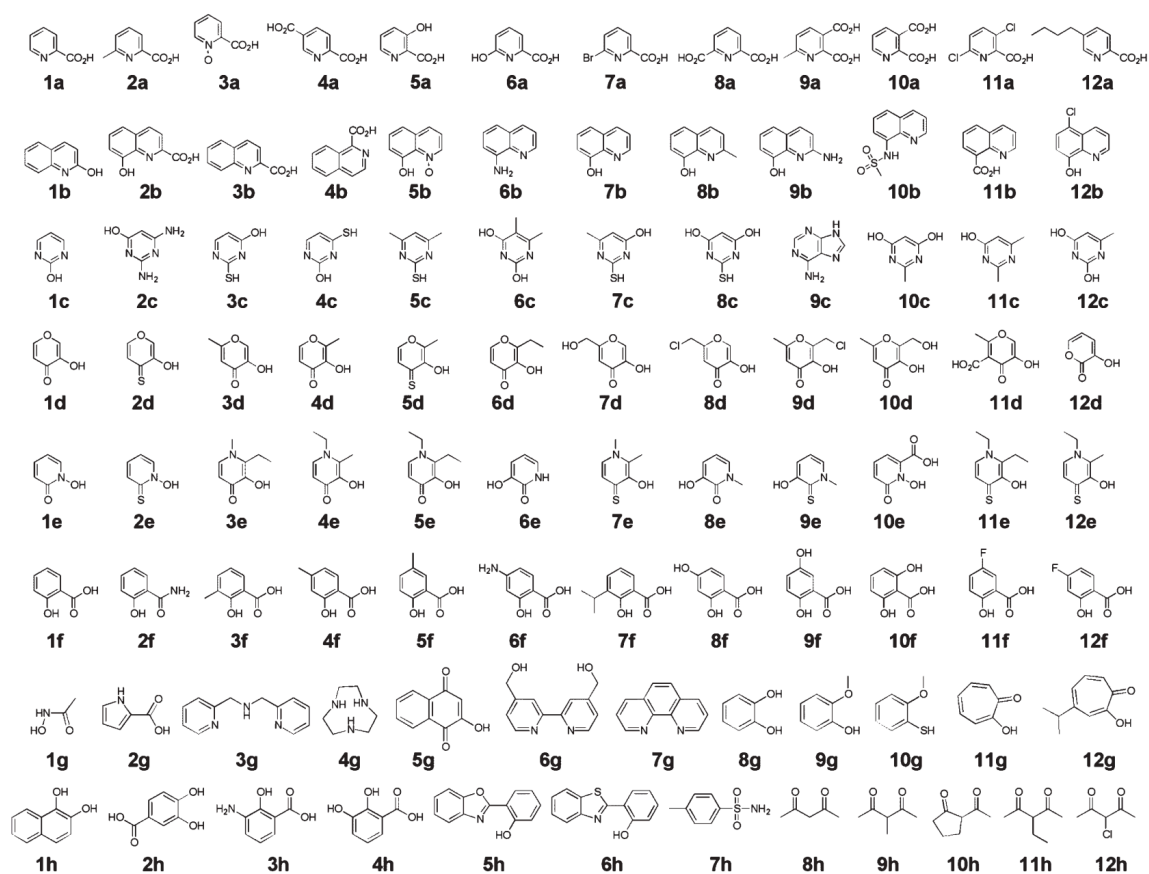


**Figure 1-1.** A MBP fragment library designed for FBDD against metalloenzymes. Adapted from Jacobsen, J.A.<sup>14</sup>

### 1.3 Inhibitors of the Proteasome and Rpn11 as Cancer Therapeutics

Degradation of eukaryotic cell proteins is a highly regulated and complex process that plays a central role in protein homeostasis.<sup>19-21</sup> The majority of cellular proteins become degraded through the ubiquitin-proteasome system (UPS) pathway, which include proteins that help regulate cell cycle, apoptosis, DNA repair, among others.<sup>20-21</sup> Proteins that are destined to become degraded are tagged through conjugation to the small protein ubiquitin through the action of

ubiquitin-activating enzyme (E1), ubiquitin-conjugating enzyme (E2) and ubiquitin-ligase enzyme (E3). Upon conjugation of several ubiquitin domains, the tagged protein will possess a polyubiquitin chain that serves for substrate recognition by the proteasome. The 26S proteasome is a massive cellular machine that degrades ubiquitin-tagged proteins and is found in the nucleus and cytoplasm of eukaryotic cells. The constitutive 26S proteasome consists of two major components: one or two 19S regulatory particles (RP) and the 20S core particle (CP) (Figure 1-2). The polyubiquitin chain bound to the protein set for degradation is recognized by the 19S RP as a substrate, which is then trapped, the polyubiquitin chain is hydrolyzed, and the protein is then unfolded and translocated into the 20S CP. The 19S RP can be divided into a base component, which is composed of a hexameric ring of AAA ATPases (Rpt1-6), and a lid component made up of eight or more regulatory subunits (Rpn).<sup>22</sup> The Rpt subunits promote substrate unfolding, open the channel leading to the 20S core and help translocate the substrates into the 20S CP. The lid subcomplex of the 19S RP is necessary for ubiquitin-dependent degradation. The Rpn subunits aid in substrate recognition, trapping, and hydrolyzing ubiquitin from the protein to be degraded. The 20S CP is structurally composed of four stacked heptameric rings that form a hollow barrel-like shape. Each ring contains seven  $\alpha$ - or  $\beta$ -subunits: the  $\alpha$  subunits serve a structural role while some of the  $\beta$  subunits are catalytically active. The proteasome has three pairs of proteolytically active subunits ( $\beta_1$ ,  $\beta_2$ , and  $\beta_5$ ) each distinguished by type of

substrate it cleaves. At each of the catalytic subunits is found an N-terminal threonine that acts as the nucleophile to cleave the peptide bond. A proximal water molecule acts as a base to facilitate cleavage (Figure 1-2). Once the protein is degraded it is released as oligopeptides.

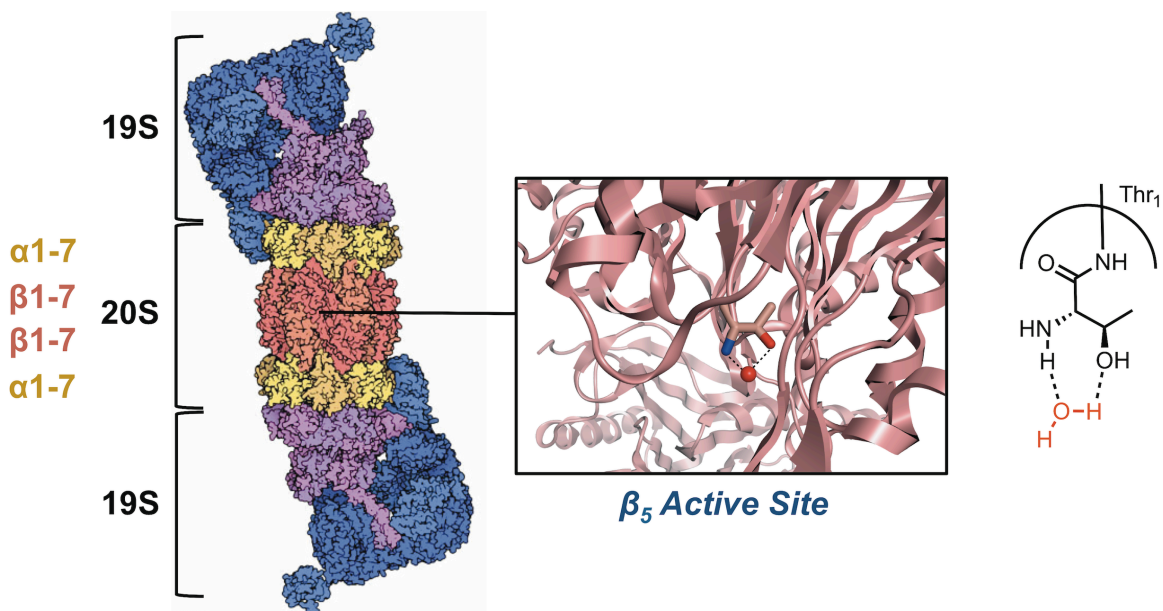


**Figure 1-2.** Structure of the 26S proteasome highlighting the 20S core and 19S regulatory particles. The  $\beta_5$  active site utilizes the N-terminal threonine for proteolysis. All three FDA approved proteasome inhibitors preferentially bind to this site.

In recent years, the proteasome has gathered substantial attention as a possible therapeutic target for oncology treatment.<sup>23-25</sup> Recent reports suggest cancer cells have a heightened dependence on UPS mediated degradation of proteins.<sup>26</sup> Analysis of cancer cell genomes revealed multiple point mutations in protein coding sequences, and through transcription and translation of these

DNA sequences, it yields mutant proteins that are unstable or present improper folding. Additionally, cancer cell genomes typically contain duplications, deletions, inversions, as well as altered copy numbers of chromosomes.<sup>26</sup> Taken together, translation of elevated levels these mutant proteins presents a burden to cancer cells, which in turn places an increased burden on the proteasome to degrade these defective proteins.

Bortezomib is a peptide boronate that was approved by the FDA in 2003 for the treatment of multiple myeloma (MM).<sup>27-28</sup> The boronic acid moiety of Bortezomib preferentially binds the catalytic threonine residue within the  $\beta_5$  subunit of the 20S CP (Figure 1-2, 1-3). The boron acts as a Lewis acid, which allows for bond formation with the hydroxyl functional group of the side chain of the N-terminal threonine. Carfilzomib is a second-generation proteasome inhibitor that utilizes an epoxy ketone functional group to covalently and irreversibly binds the N-terminal threonine of the  $\beta_5$  subunit (Figure 1-3).<sup>24</sup> Lastly, ixazomib similar to bortezomib, utilizes a boronic acid as its warhead (Figure 1-3). The approval of these three proteasome inhibitors has prompted substantial interest in developing novel inhibitors of the proteasome.<sup>24</sup> The majority of published studies have investigated inhibitors that bind one or several of the  $\beta$  subunits within the 20S CP, and to a lesser extent compounds that bind the 19S RP.

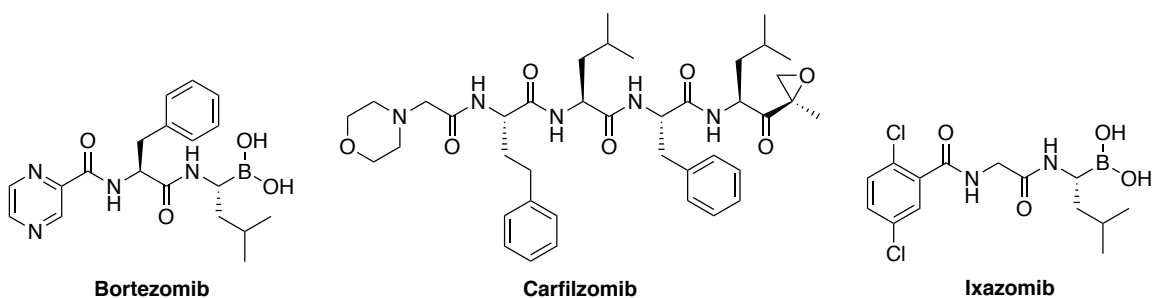


**Figure 1-3.** Structure of the three FDA approved proteasome inhibitors

Rpn11 is a  $Zn^{2+}$ -dependent isopeptidase that is part of the JAMM domain containing deubiquitinating enzymes (DUBs).<sup>29</sup> The JAMM domain is found in 7 different human proteins including the Csn5 subunit of the COP9 signalosome, AMSH, AMSH-LP, the BRCC36 subunit of BRISC, MPND, and MYSM1.<sup>30-36</sup> All of these enzymes cleave the isopeptide linkage that joins ubiquitin (or the ubiquitin-like protein Nedd8 in the case of Csn5) to a second molecule of ubiquitin or to a substrate. The conserved JAMM domain has the consensus sequence  $EX_nHS/THX_7SXXD$ , in which the His, His, and Asp residues coordinate the  $Zn^{2+}$  ion and the fourth coordination site is occupied by a water molecule that is engaged in hydrogen bonding with the conserved Glu (Figure 1-4). The  $Zn^{2+}$  acts as a Lewis acid and increases the nucleophilic character of the bound water enough to allow hydrolytic cleavage of the isopeptide bond.<sup>33, 37</sup>

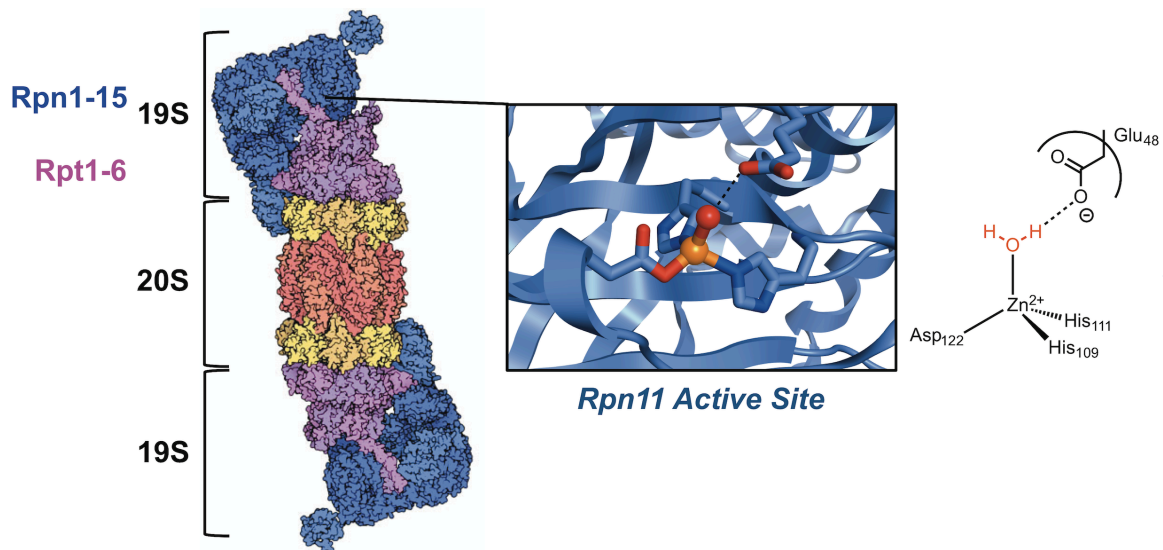


**Figure 1-4.** Structure of the 26S proteasome highlighting the 20S core and 19S regulatory particle. The Rpn11 active site utilizes a catalytic Zn<sup>2+</sup> to cleave the isopeptide bond between ubiquitin and the protein to be degraded.

The main role of Rpn11 is to cleave off the polyubiquitin chain bound to proteins that are to be degraded by the proteasome. Previous reports<sup>38-40</sup> demonstrate that mutations within the conserved JAMM domain or addition of metal chelators to proteasome-dependent degradation reactions does not result in loss of substrate recognition, but impairs degradation of the substrate by blocking insertion into the 20S CP. This impairment occurs due to a failure to remove the bulky ubiquitin chain, the diameter of which is wider (~25 Å) than the entry portal into the 20S CP (~17 Å). The development of an Rpn11 inhibitor that results in a similar blockage could lead to preferential apoptosis of neoplastic cells because these cells are thought to have a higher dependency on proteasome-dependent protein quality control when compared to normal cells.<sup>41-</sup>

<sup>42</sup> Therefore, Rpn11 represents an attractive and novel therapeutic target for proteasome inhibition.

#### **1.4 Inhibitors of Glyoxalase as Novel Treatments for Depression and Anxiety**

GLO1 is a cytoplasmic homodimeric Zn<sup>2+</sup>-dependent isomerase that catalyzes the detoxification of methylglyoxal (MG).<sup>43</sup> GLO1 utilizes endogenous glutathione (GSH) as a co-factor, which spontaneously reacts with MG to form stable hemithioacetals that serve as GLO1 substrates.<sup>44</sup> GLO1 catalyzes the isomerization of the hemithioacetal to a thioester, which is then hydrolyzed by GLO2 releasing a non-toxic D-lactate product and GSH (Figure 1-5). GLO1 and GLO2 work in conjunction to remove cytotoxic MG from cells and together they make up the glyoxalase system (Figure 1-5). MG is a reactive metabolite generated via the degradation of glycolytic intermediates and at high concentrations is capable of forming covalent adducts with proteins and nucleotides which result in advanced glycation end (AGE) products, reactive-oxygen species (ROS), and apoptosis.<sup>45-48</sup> The glyoxalase system is well designed to remove MG from cells, as both enzymes operate near the diffusion-controlled limit under physiological conditions. Presumably, this high level of kinetic efficiency reflects the need to maintain minimal levels of methylglyoxal in cells.<sup>49</sup> Due to the role in AGE formation and cytotoxicity, GLO1 inhibitors have been investigated as potential oncogenic therapeutics, but have not had any clinical success.<sup>50-51</sup>

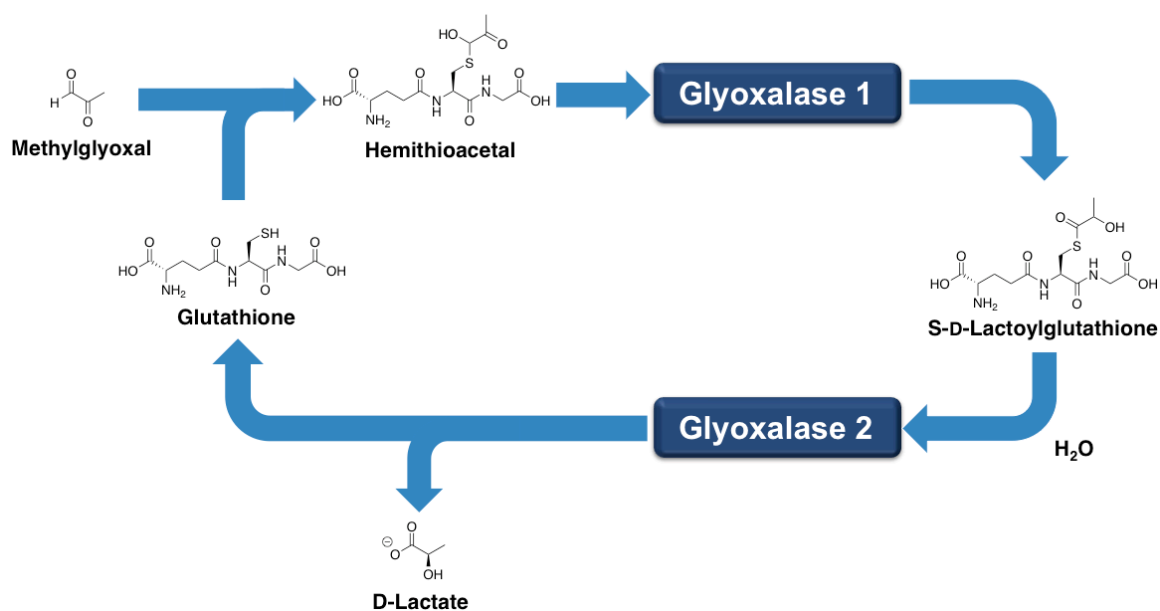


**Figure 1-5.** The glyoxalase pathway.

In 1971, Vince and Daluge first suggested that inhibitors of GLO1 may serve as antitumor agents. An inhibitor of GLO1 would cause an accumulation of MG in cancer cells, which would result in cytotoxicity. Their hypothesis was proven correct, when tumor cells demonstrated exceptional sensitivity to exogenous methylglyoxal.<sup>52-54</sup> It is also hypothesized that cancer cells have elevated levels of GLO1 possibly due to cancer cells having a high rate of glycolysis and therefore producing a high level of MG, rendering cancer cells more sensitive to GLO1 inhibition. These early studies prompted the development of several GLO1 inhibitors throughout the following decades.

The earliest inhibitors described were based on transition state mimics and glutathione analogs.<sup>55-58</sup> Additionally, several natural products and natural

product derivatives have been screened for GLO1 inhibition, but only few have exhibited  $IC_{50}$  values in the low nanomolar range.<sup>59-66</sup> One potent compound is a glutathione-based compound containing a hydroxamic acid MBP, AHC-GSH (Figure 1-6);<sup>67</sup> however, both the hydroxamic acid MBP and glutathione components make this molecule unsuitable as a viable drug candidate. AHC-GSH has been studied for its potential as an anticancer agent, but to achieve cell permeability the inhibitor had to be reformulated as an ester prodrug. Although AHC-GSH shows efficacy in vitro, no clinical therapeutics have been generated from this compound since its discovery >20 years ago, which again is likely due to the poor pharmacokinetic properties of the molecules. A second potent GLO1 inhibitor is methyl gerfelin (M-GFN), which is one of several natural products that have been demonstrated to inhibit GLO1. Lastly, a compound based on the 6-phenyl-7-azaindole-*N*-hydroxypyridinone (Chugai-3d) scaffold showed a best-in-class  $IC_{50}$  value of 11 nM (Figure 1-6); however, to the best of our knowledge, no in vivo studies have been reported with this compound.<sup>68</sup> Although there are several GLO1 inhibitors reported, no GLO1 inhibitor has entered clinical trials.

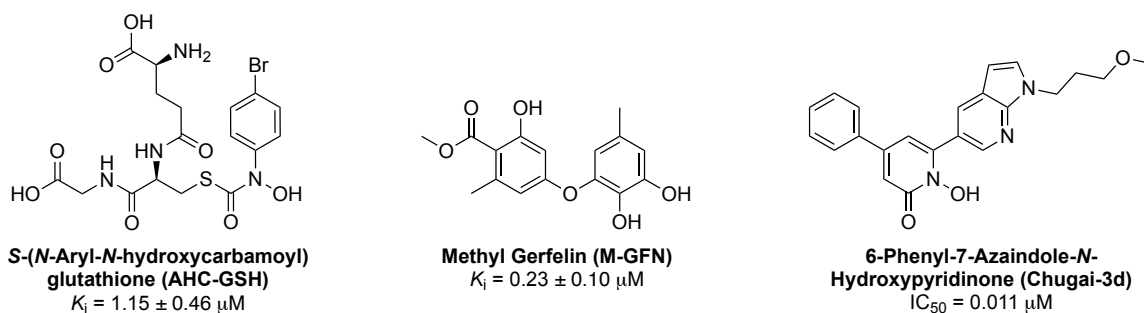


**Figure 1-6.** Molecular structures of previously reported GLO1 inhibitors with their corresponding inhibition values.

The existing inhibitors have been largely developed for oncology purposes, with more recent reports looking at GLO1 as a therapeutic target for other conditions, such as diabetic complications, aging, and depression/anxiety.<sup>45, 69-73</sup> Anxiety and depression are the two most common psychiatric disorders in the US and affect approximately one-in-five adults at some point in their lifetime.<sup>74-75</sup> Currently, there are many FDA approved drugs for both disorders; however, these drugs have several limitations. Some drawbacks associated with anxiolytic drugs include sedating side effects and abuse liability. For antidepressant drugs limitations also include detrimental side effects, lack of efficacy, and a slow onset of therapeutic effects. Therefore, due to the current limitations of available drugs, there is a need for developing alternative therapeutics. Recent studies have linked GLO1 to numerous behavioral phenotypes, including psychiatric diseases such as anxiety and depression.<sup>76-81</sup> Previous reports demonstrate knockdown of *Glo1* or

suppression of GLO1 enzyme activity via inhibitors results in an increase of intracellular concentration of MG and a reduction of anxiety-like behaviors in mice.<sup>82-83</sup> Additionally, MG has been shown to be a competitive partial GABA-A (*gamma*-Aminobutyric acid) receptor agonists, which is the proposed mechanism leading to changes in behavioral phenotypes.<sup>80</sup> These studies suggest that inhibition of GLO1 can cause an accumulation of MG and thereby lead to anti-depressive effects.

## 1.5 Outlook

Although metalloenzymes make up more than one third of the proteome, approximately only about 5% of FDA approved drugs target metalloenzymes.<sup>5</sup> Traditionally, the MBP moiety of metalloenzyme inhibitors has not been well studied or understood. The most commonly utilized MBPs in medicinal chemistry (thiols, hydroxamic acids, phosphinic/phosphonic acids, and carboxylic acids) are not very drug-like functional groups and can become a liability in drug development. The use of FBDD through the use of MBP libraries for metalloenzyme inhibitor development represents a unique opportunity. This dissertation will focus on utilizing FBDD for the discovery of novel metalloenzyme inhibitors. Two therapeutically relevant Zn<sup>2+</sup>-dependent enzymes, Rpn11 and GLO1, were chosen as targets. The use of a modest MBP fragment library to enable the discovery of a novel class of inhibitors for Rpn11 will be presented in

Chapter 2. Chapter 3 details a synthetic campaign prompted by the discoveries discussed in Chapter 2, that lead to the development of a first-in-class potent Rpn11 inhibitor. The same FBDD approach was utilized for the development of a novel class of GLO1 inhibitors, which is described in Chapter 4. Lastly, a novel potent GLO1 inhibitor is described in Chapter 5.

## 1.6 References

1. Holm, R. H.; Kennepohl, P.; Solomon, E. I., Structural and functional aspects of metal sites in biology. *Chem. Rev.* **1996**, *96* (7), 2239-2314.
2. Andreini, C.; Bertini, I.; Cavallaro, G.; Holliday, G. L.; Thornton, J. M., Metal ions in biological catalysis: from enzyme databases to general principles. *J. Biol. Inorg. Chem.* **2008**, *13* (8), 1205-1218.
3. Lill, R., Function and biogenesis of iron-sulphur proteins. *Nature* **2009**, *460* (7257), 831-838.
4. Anzellotti, A. I.; Farrell, N. P., Zinc metalloproteins as medicinal targets. *Chem. Soc. Rev.* **2008**, *37* (8), 1629-1651.
5. Cohen, S. M., A Bioinorganic Approach to Fragment-Based Drug Discovery Targeting Metalloenzymes. *Acc. Chem. Res.* **2017**, *50* (8), 2007-2016.
6. Martin, D. P.; Puerta, D.; Cohen, S. M., *Metalloprotein Inhibitors. In Ligand Design in Medicinal Inorganic Chemistry.* Storr, T., Ed. John Wiley and Sons: Hoboken, NJ, 2014.
7. Erlanson, D. A.; McDowell, R. S.; O'Brien, T., Fragment-based drug discovery. *J. Med. Chem.* **2004**, *47* (14), 3463-3482.
8. Rees, D. C.; Congreve, M.; Murray, C. W.; Carr, R., Fragment-based lead discovery. *Nat. Rev. Drug Discov.* **2004**, *3* (8), 660-672.
9. Joseph-McCarthy, D.; Campbell, A. J.; Kern, G.; Moustakas, D., Fragment-Based Lead Discovery and Design. *J. Chem. Inf. Model.* **2014**, *54* (3), 693-704.
10. Congreve, M.; Chessari, G.; Tisi, D.; Woodhead, A. J., Recent developments in fragment-based drug discovery. *J. Med. Chem.* **2008**, *51* (13), 3661-3680.

11. Jhoti, H.; Williams, G.; Rees, D. C.; Murray, C. W., The 'rule of three' for fragment-based drug discovery: where are we now? *Nat. Rev. Drug Discov.* **2013**, *12* (8), 644-+.
12. Hopkins, A. L.; Groom, C. R.; Alex, A., Ligand Efficiency: A Useful Metric for Lead Selection. *Drug Discov. Today* **2004**, *9* (10), 430-431.
13. Hopkins, A. L.; Keseru, G. M.; Leeson, P. D.; Rees, D. C.; Reynolds, C. H., The role of ligand efficiency metrics in drug discovery. *Nat. Rev. Drug Discov.* **2014**, *13* (2), 105-121.
14. Jacobsen, J. A.; Fullagar, J. L.; Miller, M. T.; Cohen, S. M., Identifying Chelators for Metalloprotein Inhibitors Using a Fragment-Based Approach. *J. Med. Chem.* **2011**, *54* (2), 591-602.
15. Garner, A. L.; Struss, A. K.; Fullagar, J. L.; Agrawal, A.; Moreno, A. Y.; Cohen, S. M.; Janda, K. D., 3-Hydroxy-1-alkyl-2-methylpyridine-4(1H)-thiones: Inhibition of the *Pseudomonas aeruginosa* Virulence Factor LasB. *ACS Med. Chem. Lett.* **2012**, *3* (8), 668-672.
16. Fullagar, J. L.; Garner, A. L.; Struss, A. K.; Day, J. A.; Martin, D. P.; Yu, J.; Cai, X. Q.; Janda, K. D.; Cohen, S. M., Antagonism of a Zinc Metalloprotease Using a Unique Metal-Chelating Scaffold: Tropolones as Inhibitors of *P. aeruginosa* Elastase. *Chem. Commun.* **2013**, *49* (31), 3197-3199.
17. Martin, D. P.; Cohen, S. M., Nucleophile recognition as an alternative inhibition mode for benzoic acid based carbonic anhydrase inhibitors. *Chem. Commun.* **2012**, *48* (43), 5259-5261.
18. Credille, C. V.; Chen, Y.; Cohen, S. M., Fragment-Based Identification of Influenza Endonuclease Inhibitors. *J. Med. Chem.* **2016**, *59* (13), 6444-6454.
19. Goldberg, A. L., Probing the proteasome pathway. *Nat. Biotechnol.* **2000**, *18* (5), 494-496.
20. Gallastegui, N.; Groll, M., The 26S proteasome: assembly and function of a destructive machine. *Trends Biochem. Sci.* **2010**, *35* (11), 634-642.

21. Bedford, L.; Paine, S.; Sheppard, P. W.; Mayer, R. J.; Roelofs, J., Assembly, structure, and function of the 26S proteasome. *Trends Cell Biol.* **2010**, *20* (7), 391-401.
22. Liu, C. W.; Jacobson, A. D., Functions of the 19S complex in proteasomal degradation. *Trends Biochem. Sci.* **2013**, *38* (2), 103-110.
23. Kubiczikova, L.; Pour, L.; Sedlarikova, L.; Hajek, R.; Sevcikova, S., Proteasome inhibitors - molecular basis and current perspectives in multiple myeloma. *J. Cell. Mol. Med.* **2014**, *18* (6), 947-961.
24. Crawford, L. J.; Walker, B.; Irvine, A. E., Proteasome inhibitors in cancer therapy. *J. Cell Commun. Signal.* **2011**, *5* (2), 101-110.
25. Kisselev, A. F.; van der Linden, W. A.; Overkleeft, H. S., Proteasome Inhibitors: An Expanding Army Attacking a Unique Target. *Chem. Biol.* **2012**, *19* (1), 99-115.
26. Deshaies, R. J., Proteotoxic crisis, the ubiquitin-proteasome system, and cancer therapy. *BMC Biol.* **2014**, *12*.
27. Paramore, A.; Frantz, S., Bortezomib. *Nat. Rev. Drug Discov.* **2003**, *2* (8), 611-612.
28. Curran, M. P.; McKeage, K., Bortezomib A Review of its Use in Patients with Multiple Myeloma. *Drugs* **2009**, *69* (7), 859-888.
29. Verma, R.; Aravind, L.; Oania, R.; McDonald, W. H.; Yates, J. R.; Koonin, E. V.; Deshaies, R. J., Role of Rpn11 Metalloprotease in Deubiquitination and Degradation by the 26S Proteasome. *Science* **2002**, *298* (5593), 611-615.
30. McCullough, J.; Clague, M. J.; Urbe, S., AMSH is an Endosome-Associated Ubiquitin Isopeptidase. *J. Cell Biol.* **2004**, *166* (4), 487-492.
31. Nijman, S. M. B.; Luna-Vargas, M. P. A.; Velds, A.; Brummelkamp, T. R.; Dirac, A. M. G.; Sixma, T. K.; Bernards, R., A Genomic and Functional Inventory of Deubiquitinating Enzymes. *Cell* **2005**, *123* (5), 773-786.

32. Zhu, P.; Zhou, W. L.; Wang, J. X.; Puc, J.; Ohgi, K. A.; Erdjument-Bromage, H.; Tempst, P.; Glass, C. K.; Rosenfeld, M. G., A Histone H2A Deubiquitinase Complex Coordinating Histone Acetylation and H1 Dissociation in Transcriptional Regulation. *Mol. Cell* **2007**, *27* (4), 609-621.
33. Ambroggio, X. I.; Rees, D. C.; Deshaies, R. J., JAMM: A Metalloprotease-like Zinc Site in the Proteasome and Signalosome. *PLOS Biol.* **2004**, *2* (1), 113-119.
34. Sobhian, B.; Shao, G. Z.; Lilli, D. R.; Culhane, A. C.; Moreau, L. A.; Xia, B.; Livingston, D. M.; Greenberg, R. A., RAP80 Targets BRCA1 to Specific Ubiquitin Structures at DNA Damage Sites. *Science* **2007**, *316* (5828), 1198-1202.
35. Cope, G. A.; Suh, G. S. B.; Aravind, L.; Schwarz, S. E.; Zipursky, S. L.; Koonin, E. V.; Deshaies, R. J., Role of Predicted Metalloprotease Motif of Jab1/Csn5 in Cleavage of Nedd8 From Cul1. *Science* **2002**, *298* (5593), 608-611.
36. Sato, Y.; Yoshikawa, A.; Yamagata, A.; Mimura, H.; Yamashita, M.; Ookata, K.; Nureki, O.; Iwai, K.; Komada, M.; Fukai, S., Structural Basis for Specific Cleavage of Lys 63-Linked Polyubiquitin Chains. *Nature* **2008**, *455* (7211), 358-362.
37. Shrestha, R. K.; Ronau, J. A.; Davies, C. W.; Guenette, R. G.; Strieter, E. R.; Paul, L. N.; Das, C., Insights into the Mechanism of Deubiquitination by JAMM Deubiquitinases from Cocystal Structures of the Enzyme with the Substrate and Product. *Biochemistry* **2014**, *53* (19), 3199-3217.
38. Reyes-Turcu, F. E.; Wilkinson, K. D., Polyubiquitin Binding and Disassembly By Deubiquitinating Enzymes. *Chem. Rev.* **2009**, *109* (4), 1495-1508.
39. Koulich, E.; Li, X. H.; DeMartino, G. N., Relative Structural and Functional Roles of Multiple Deubiquitylating Proteins Associated With Mammalian 26S Proteasome. *Mol. Biol. Cell.* **2008**, *19* (3), 1072-1082.

40. Guterman, A.; Glickman, M. H., Complementary Roles for Rpn11 and Ubp6 in Deubiquitination and Proteolysis by the Proteasome. *J. Biol. Chem.* **2004**, *279* (3), 1729-1738.
41. Cenci, S.; Oliva, L.; Cerruti, F.; Milan, E.; Bianchi, G.; Raule, M.; Mezghrani, A.; Pasqualetto, E.; Sitia, R.; Cascio, P., Pivotal Advance: Protein Synthesis Modulates Responsiveness of Differentiating and Malignant Plasma Cells to Proteasome Inhibitors. *J. Leukocyte Biol.* **2012**, *92* (5), 921-931.
42. Deshaies, R. J., Proteotoxic Crisis, the Ubiquitin-Proteasome System, and Cancer Therapy. *BMC Biol.* **2014**, *12*, 1-14.
43. Thornalley, P. J., Glyoxalase I - structure, function and a critical role in the enzymatic defence against glycation. *Biochem. Soc. Trans.* **2003**, *31*, 1343-1348.
44. Silva, M. S.; Gomes, R. A.; Ferreira, A. E. N.; Freire, A. P.; Cordeiro, C., The glyoxalase pathway: the first hundred years ... and beyond. *Biochem. J.* **2013**, *453*, 1-15.
45. Brownlee, M., Biochemistry and molecular cell biology of diabetic complications. *Nature* **2001**, *414* (6865), 813-820.
46. Thornalley, P. J., Glyoxalase I--structure, function and a critical role in the enzymatic defence against glycation. *Biochem. Soc. Trans.* **2003**, *31* (Pt 6), 1343-8.
47. Schleicher, E.; Friess, U., Oxidative stress, AGE, and atherosclerosis. *Kidney. Int. Suppl.* **2007**, (106), S17-26.
48. Loh, K. P.; Huang, S. H.; De Silva, R.; Tan, B. K.; Zhu, Y. Z., Oxidative stress: apoptosis in neuronal injury. *Curr. Alzheimer. Res.* **2006**, *3* (4), 327-37.
49. Creighton, D. J.; Zheng, Z. B.; Holewinski, R.; Hamilton, D. S.; Eiseman, J. L., Glyoxalase I inhibitors in cancer chemotherapy. *Biochem. Soc. Trans.* **2003**, *31*, 1378-1382.

50. Creighton, D. J.; Zheng, Z. B.; Holewinski, R.; Hamilton, D. S.; Eiseman, J. L., Glyoxalase I inhibitors in cancer chemotherapy. *Biochem. Soc. Trans.* **2003**, *31* (Pt 6), 1378-82.
51. Thornalley, P. J., Advances in glyoxalase research. Glyoxalase expression in malignancy, anti-proliferative effects of methylglyoxal, glyoxalase I inhibitor diesters and S-D-lactoylglutathione, and methylglyoxal-modified protein binding and endocytosis by the advanced glycation endproduct receptor. *Crit. Rev. Oncol. Hematol* **1995**, *20* (1-2), 99-128.
52. Reiffen, K. A.; Schneider, F., A Comparative-Study on Proliferation, Macromolecular-Synthesis and Energy-Metabolism of Invitro-Grown Ehrlich Ascites Tumor-Cells in the Presence of Glucosone, Galactosone and Methylglyoxal. *J. Cancer Res. Clin. Oncol.* **1984**, *107* (3), 206-210.
53. Ayoub, F. M.; Allen, R. E.; Thornalley, P. J., Inhibition of Proliferation of Human Leukemia 60-Cells by Methylglyoxal Invitro. *Leuk. Res.* **1993**, *17* (5), 397-401.
54. Amicarelli, F.; Bucciarelli, T.; Poma, A.; Aimola, P.; Di Ilio, C.; Ragnelli, A. M.; Miranda, M., Adaptive response of human melanoma cells to methylglyoxal injury. *Carcinogenesis* **1998**, *19* (3), 519-523.
55. Vince, R.; Wadd, W. B., Glyoxalase Inhibitors as Potential Anticancer Agents. *Biochem. Biophys. Res. Commun.* **1969**, *35* (5), 593-&.
56. Vince, R.; Wolf, M.; Sanford, C., Glutaryl-S-(P-Bromobenzyl)-L-Cysteinylglycine - Metabolically Stable Inhibitor of Glyoxalase I. *J. Med. Chem.* **1973**, *16* (8), 951-953.
57. Vince, R.; Brownell, J.; Akella, L. B., Synthesis and activity of gamma-(L-gamma-azaglutamyl)-S(p-bromobenzyl)-L-cysteinylglycine: A metabolically stable inhibitor of glyoxalase I. *Bioorg. Med. Chem. Lett.* **1999**, *9* (6), 853-856.
58. More, S. S.; Vince, R., A metabolically stable tight-binding transition-state inhibitor of glyoxalase-I. *Bioorg. Med. Chem. Lett.* **2006**, *16* (23), 6039-6042.

59. Liu, M.; Yuan, M. G.; Luo, M. X.; Bu, X. Z.; Luo, H. B.; Hu, X. P., Binding of curcumin with glyoxalase I: Molecular docking, molecular dynamics simulations, and kinetics analysis. *Biophys. Chem.* **2010**, *147* (1-2), 28-34.
60. Santel, T.; Pflug, G.; Hemdan, N. Y. A.; Schafer, A.; Hollenbach, M.; Buchold, M.; Hintersdorf, A.; Lindner, I.; Otto, A.; Bigl, M.; Oerlecke, I.; Hutschenreuter, A.; Sack, U.; Huse, K.; Groth, M.; Birkemeyer, C.; Schellenberger, W.; Gebhardt, R.; Platzer, M.; Weiss, T.; Vijayalakshmi, M. A.; Kruger, M.; Birkenmeier, G., Curcumin Inhibits Glyoxalase 1-A Possible Link to Its Anti-Inflammatory and Anti-Tumor Activity. *PLOS One* **2008**, *3* (10).
61. Yadav, A.; Kumar, R.; Sunkaria, A.; Singhal, N.; Kumar, M.; Sandhir, R., Evaluation of potential flavonoid inhibitors of glyoxalase-I based on virtual screening and in vitro studies. *J. Biomol. Struct. Dyn.* **2016**, *34* (5), 993-1007.
62. Kawatani, M.; Okumura, H.; Honda, K.; Kanoh, N.; Muroi, M.; Dohmae, N.; Takami, M.; Kitagawa, M.; Futamura, Y.; Imoto, M.; Osada, H., The identification of an osteoclastogenesis inhibitor through the inhibition of glyoxalase I. *P. Natl. Acad. Sci.* **2008**, *105* (33), 11691-11696.
63. Yuan, M. G.; Luo, M. X.; Song, Y.; Xu, Q.; Wang, X. F.; Cao, Y.; Bu, X. Z.; Ren, Y. L.; Hu, X. P., Identification of curcumin derivatives as human glyoxalase I inhibitors: A combination of biological evaluation, molecular docking, 3D-QSAR and molecular dynamics simulation studies. *Bioorg. Med. Chem.* **2011**, *19* (3), 1189-1196.
64. Zhang, H.; Zhai, J.; Zhang, L. P.; Li, C. Y.; Zhao, Y. N.; Chen, Y. Y.; Li, Q.; Hu, X. P., In Vitro Inhibition of Glyoxalase I by Flavonoids: New Insights from Crystallographic Analysis. *Curr. Top. Med. Chem* **2016**, *16* (4), 460-466.
65. Al-Balas, Q. A.; Hassan, M. A.; Al-Shar'i, N. A.; Mhaidat, N. M.; Almaaytah, A. M.; Al-Mahasneh, F. M.; Isawi, I. H., Novel glyoxalase-I inhibitors possessing a "zinc-binding feature" as potential anticancer agents. *Drug Des. Dev. Ther.* **2016**, *10*, 2623-2629.
66. Takasawa, R.; Takahashi, S.; Saeki, K.; Sunaga, S.; Yoshimori, A.; Tanuma, S. I., Structure-activity relationship of human GLO I inhibitory natural flavonoids and their growth inhibitory effects. *Bioorg. Med. Chem.* **2008**, *16* (7), 3969-3975.

67. Hamilton, D. S.; Creighton, D. J., Inhibition of Glyoxalase I by the Enediol Mimic S-(N-Hydroxy-N-Methylcarbamoyl)Glutathione - the Possible Basis of a Tumor-Selective Anticancer Strategy. *J. Biol. Chem.* **1992**, *267* (35), 24933-24936.
68. Chiba, T.; Ohwada, J.; Sakamoto, H.; Kobayashi, T.; Fukami, T. A.; Irie, M.; Miura, T.; Ohara, K.; Koyano, H., Design and evaluation of azaindole-substituted N-hydroxypyridones as glyoxalase I inhibitors. *Bioorg. Med. Chem. Lett.* **2012**, *22* (24), 7486-7489.
69. Thornalley, P. J., Protecting the genome: defence against nucleotide glycation and emerging role of glyoxalase I overexpression in multidrug resistance in cancer chemotherapy. *Biochem. Soc. Trans.* **2003**, *31*, 1372-1377.
70. Ahmed, N.; Thornalley, P. J., Advanced glycation endproducts: what is their relevance to diabetic complications? *Diabetes Obes. Metab.* **2007**, *9* (3), 233-245.
71. Morcos, M.; Du, X. L.; Pfisterer, F.; Hutter, H.; Sayed, A. A. R.; Thornalley, P.; Ahmed, N.; Baynes, J.; Thorpe, S.; Kukudov, G.; Schlotterer, A.; Bozorgmehr, F.; El Baki, R. A.; Stern, D.; Moehrlen, F.; Ibrahim, Y.; Oikonomou, D.; Hamann, A.; Becker, C.; Zeier, M.; Schwenger, V.; Miftari, N.; Humpert, P.; Hammes, H. P.; Buechler, M.; Bierhaus, A.; Brownlee, M.; Nawroth, P. P., Glyoxalase-1 prevents mitochondrial protein modification and enhances lifespan in *Caenorhabditis elegans*. *Aging Cell* **2008**, *7* (2), 260-269.
72. Fleming, T. H.; Humpert, P. M.; Nawroth, P. P.; Bierhaus, A., Reactive Metabolites and AGE/RAGE-Mediated Cellular Dysfunction Affect the Aging Process - A Mini-Review. *Gerontology* **2011**, *57* (5), 435-443.
73. Distler, M. G.; Plant, L. D.; Sokoloff, G.; Hawk, A. J.; Aneas, I.; Wuenschell, G. E.; Termini, J.; Meredith, S. C.; Nobrega, M. A.; Palmer, A. A., Glyoxalase 1 increases anxiety by reducing GABA(A) receptor agonist methylglyoxal. *J. Clin. Invest.* **2012**, *122* (6), 2306-2315.
74. Kessler, R. C.; Chiu, W. T.; Demler, O.; Walters, E. E., Prevalence, severity, and comorbidity of 12-month DSM-IV disorders in the National Comorbidity Survey Replication. *Arch. Gen. Psychiatr.* **2005**, *62* (6), 617-627.

75. Kessler, R. C.; Petukhova, M.; Sampson, N. A.; Zaslavsky, A. M.; Wittchen, H. U., Twelve-month and lifetime prevalence and lifetime morbid risk of anxiety and mood disorders in the United States. *Int. J. Methods Psychiatr. Res.* **2012**, *21* (3), 169-184.
76. Hovatta, I.; Tennant, R. S.; Helton, R.; Marr, R. A.; Singer, O.; Redwine, J. M.; Ellison, J. A.; Schadt, E. E.; Verma, I. M.; Lockhart, D. J.; Barlow, C., Glyoxalase 1 and glutathione reductase 1 regulate anxiety in mice. *Nature* **2005**, *438* (7068), 662-6.
77. Reiner-Benaim, A.; Yekutieli, D.; Letwin, N. E.; Elmer, G. I.; Lee, N. H.; Kafkafi, N.; Benjamini, Y., Associating quantitative behavioral traits with gene expression in the brain: searching for diamonds in the hay. *Bioinformatics* **2007**, *23* (17), 2239-46.
78. Loos, M.; van der Sluis, S.; Bochdanovits, Z.; van Zutphen, I. J.; Pattij, T.; Stiedl, O.; Neuro, B. M. P. c.; Smit, A. B.; Spijker, S., Activity and impulsive action are controlled by different genetic and environmental factors. *Genes Brain Behav.* **2009**, *8* (8), 817-28.
79. Benton, C. S.; Miller, B. H.; Skwerer, S.; Suzuki, O.; Schultz, L. E.; Cameron, M. D.; Marron, J. S.; Pletcher, M. T.; Wiltshire, T., Evaluating genetic markers and neurobiochemical analytes for fluoxetine response using a panel of mouse inbred strains. *Psychopharmacology* **2012**, *221* (2), 297-315.
80. Distler, M. G.; Plant, L. D.; Sokoloff, G.; Hawk, A. J.; Aneas, I.; Wuenschell, G. E.; Termini, J.; Meredith, S. C.; Nobrega, M. A.; Palmer, A. A., Glyoxalase 1 increases anxiety by reducing GABAA receptor agonist methylglyoxal. *J. Clin. Invest.* **2012**, *122* (6), 2306-15.
81. Distler, M. G.; Palmer, A. A., Role of Glyoxalase 1 (Glo1) and methylglyoxal (MG) in behavior: recent advances and mechanistic insights. *Front. Genet.* **2012**, *3*, 250.
82. Williams, R. t.; Lim, J. E.; Harr, B.; Wing, C.; Walters, R.; Distler, M. G.; Teschke, M.; Wu, C.; Wiltshire, T.; Su, A. I.; Sokoloff, G.; Tarantino, L. M.; Borevitz, J. O.; Palmer, A. A., A common and unstable copy number variant is associated with differences in Glo1 expression and anxiety-like behavior. *PLOS One* **2009**, *4* (3), e4649.

83. McMurray, K. M.; Ramaker, M. J.; Barkley-Levenson, A. M.; Sidhu, P. S.; Elkin, P. K.; Reddy, M. K.; Guthrie, M. L.; Cook, J. M.; Rawal, V. H.; Arnold, L. A.; Dulawa, S. C.; Palmer, A. A., Identification of a novel, fast-acting GABAergic antidepressant. *Mol. Psychiatry*. **2017**.

## **Chapter 2: Discovery of an Inhibitor of the Proteasome Subunit Rpn11**

## 2.1 Introduction

MM is a plasma cell neoplasm that affects thousands of people each year. Currently, there is no cure for MM. Even with a strong regiment of available chemotherapies, average life expectancy from time of diagnosis ranges from 2.5 to 5 years, depending upon the stage of the disease.<sup>1-2</sup> The development of novel chemotherapeutics that inhibit components of the proteasome has proven very successful in extending progression-free and overall survival.<sup>3-4</sup> These drugs inhibit the UPS pathway through binding to one or more of the protease active sites within the proteasome (Figure 1-2).

The UPS plays a major role in protein quality control by degrading unwanted, damaged, or misfolded proteins within eukaryotic cells. It also controls numerous processes including cell cycle, apoptosis, transcription, and DNA repair by modulating the stability of critical regulatory proteins. Due to the UPS playing a central role in cellular metabolism, inhibition of the proteasome has emerged as a powerful strategy for anticancer therapy. Inhibiting this pathway was validated as a clinical target with the FDA approval of bortezomib, followed by carfilzomib, and most recently ixazomib, all for the treatment of MM (Figure 1-3). The success of these small molecules has generated substantial interest in developing inhibitors that target other key elements of the proteasome.<sup>5-9</sup>

The Zn<sup>2+</sup>-dependent JAMM domain of the Rpn11 subunit, found within the 19S RP, cleaves ubiquitin from its substrates, thereby releasing ubiquitin for

recycling (Figure 2-1). Inhibition of Rpn11 impairs degradation of the substrate by the proteasome because it can no longer be inserted into the 20S CP due to failure to remove the bulky ubiquitin chain.<sup>10-11</sup> Therefore, Rpn11 represents an attractive and novel therapeutic target for proteasome inhibition.

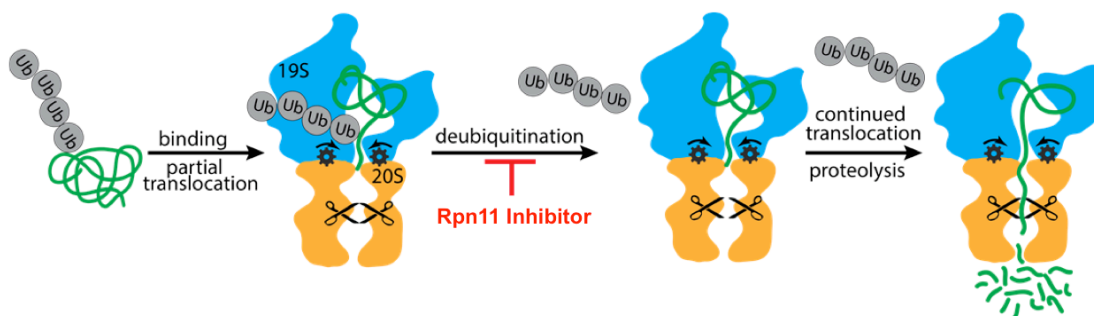


**Figure 2-1.** Mechanism of degradation of polyubiquitinated proteins by the proteasome. In red is highlighted the specific step a Rpn11 inhibitor would prevent. Adapted from Li, J.<sup>23</sup>

In this chapter, the discovery and evaluation of a novel class of fragments that inhibit the proteasome subunit Rpn11 is presented. Two independent drug discovery approaches were utilized to identify inhibitors for Rpn11. A FBDD approach was applied by screening a small library of MBPs. A second, independent approach utilizing HTS was also performed to identify potential inhibitors. Both of these approaches converged on a single fragment, 8-thioquinoline (**8-TQ**) as a promising hit. This initial study reports on a rudimentary structure-activity relationship (SAR), evaluates the mechanism of inhibition of Rpn11, and describes off-target inhibition of metalloenzymes by **8-**

**TQ.** The data presented in this chapter provides the foundation that allowed the development of Capzimin, a first-in-class Rpn11 inhibitor, which is discussed in Chapter 3.

## **2.2 Results and Discussion**

### **2.2.1 Two Screenings Yield Inhibitors for Rpn11**

In order to identify potent MBPs that can serve as initial building blocks for inhibitor design, a first generation chemical library containing 96 MBP fragments<sup>12</sup> (Figure 1-1) was screened against Rpn11 at a fragment concentration of 200  $\mu$ M by utilizing a fluorescence polarization assay (Figure 2-2).<sup>13-14</sup> The fluorescence polarization assay specifically measures the deubiquitinating activity of Rpn11. The assay features a proteasome substrate with four tandem repeats of ubiquitin (Ub<sub>4</sub>) followed by a peptide labeled with Oregon Green on a unique cysteine residue. Incubation of this substrate, Ub<sub>4</sub>peptide<sup>OG</sup>, with the proteasome results in depolarization of Oregon Green fluorescence due to release of the peptide<sup>OG</sup> from Ub<sub>4</sub>.<sup>15</sup> This assay proved to be robust and adaptable for rapid screening.

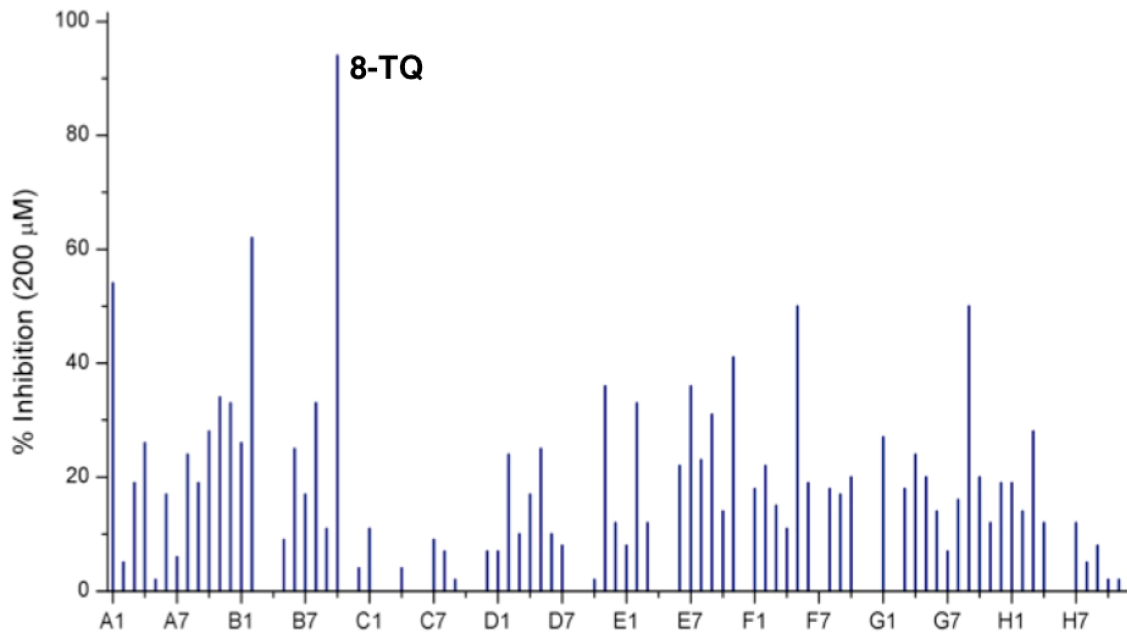


**Figure 2-2.** Screening results from a MBP library (Figure 1-1) against Rpn11. Lines represent percent enzyme inhibition for a given MBP fragment at a concentration of 200  $\mu\text{M}$ .

Initial evaluation of the first generation MBP library (Figure 1-1) revealed three compounds with >50% inhibition, with the majority of the compounds exhibiting 0-30% inhibition (Figure 2-2). One fragment, **8-TQ**, demonstrated essentially complete inhibition at a concentration of 200  $\mu\text{M}$ . Although only three compounds were designated as hits, the results of this screen were encouraging and prompted the development of a second generation MBP library. A second-generation library was then screened that expanded on the structural diversity of the fragments to include a total of 240 fragments (compounds not shown). With an expanded library in hand, a second round of screening against the Rpn11 enzyme was performed, which yielded <10 fragments with >50% inhibition at 200

$\mu\text{M}$  (Figure 2-3). Several of these compounds showed up as hits due to fluorescence artifacts and were not further pursued. Finally, only 4 compounds were determined to be true hits against Rpn11 (Table 2-1). **8-TQ** was the most potent compound even after screening of the second generation MBP library.

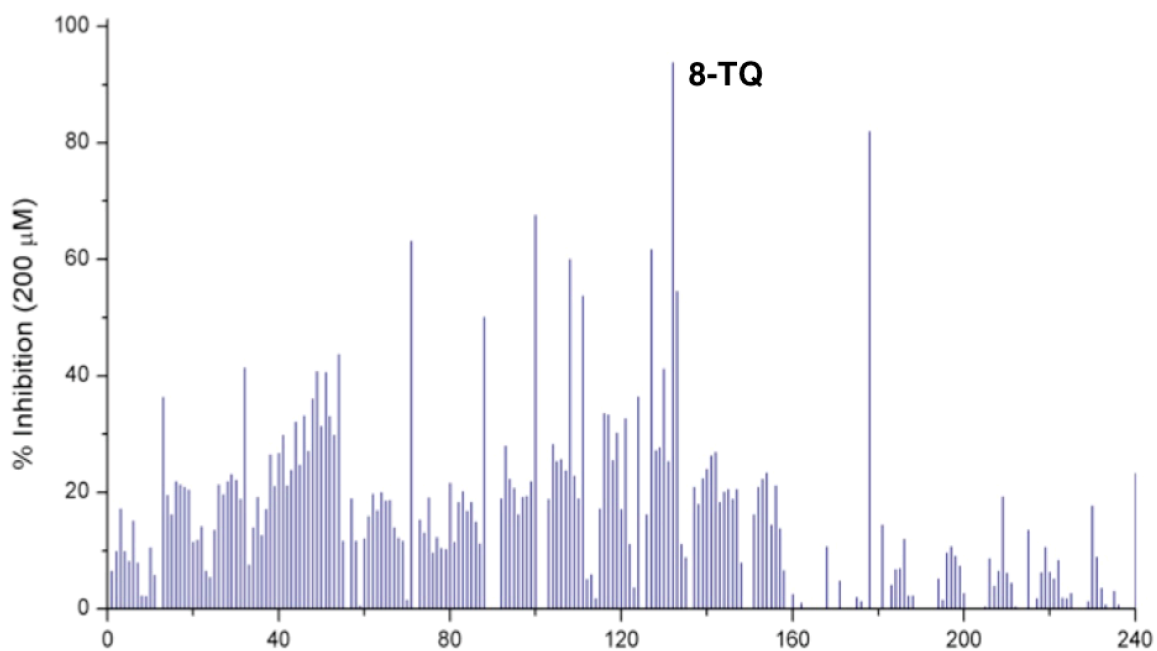


**Figure 2-3.** Screening results from the second generation MBP library against Rpn11. Lines represent percent enzyme inhibition for a given MBP fragment at a concentration of 200  $\mu\text{M}$ .

In addition to fragment based screening, a HTS screening effort was also performed against Rpn11. The laboratory of Prof. Raymond Deshaies (Caltech, collaborator on this project) worked with the National Institutes of Health Molecular Libraries Small-Molecule Repository (independent from the Cohen lab)

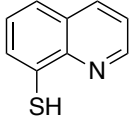
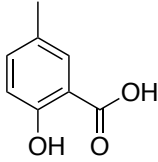
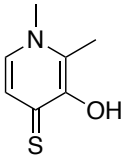
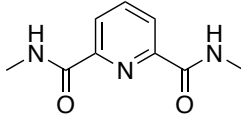
to screen 330,000 compounds at a concentration of 20  $\mu\text{M}$ .<sup>15</sup> The initial hits from the HTS screen were revalidated via dose-dependent response in a 10-point titration assay. A second screen of the hit compounds, eliminated those that inhibited processing of Ub<sub>4</sub>peptide<sup>OG</sup> by thrombin. Due to possible toxicity liabilities, another screen excluded compounds that blocked matrix metalloproteinase 2 (MMP-2) and Rpn11 activity with equal potency. Lastly, the remaining candidates were then tested for their ability to block proteasome-dependent degradation of reporter protein Ub<sup>G76V</sup>-GFP in cells.<sup>16</sup> Upon competition of all these screens, only one compound emerged from this process. Remarkably, this compound, *S*-(quinolin-8-yl)-2-bromobenzothioate, is a thioester derivative of **8-TQ**. Thioesters are inherently unstable in the reducing environment of the cell, suggesting that the active moiety is **8-TQ**. Incredibly both independent studies (HTS and FDBB approaches) yielded the same result of **8-TQ** as a potent inhibitor of Rpn11. This result highlights the efficiency and effectiveness of the FBDD approach utilized from a small MBP library.

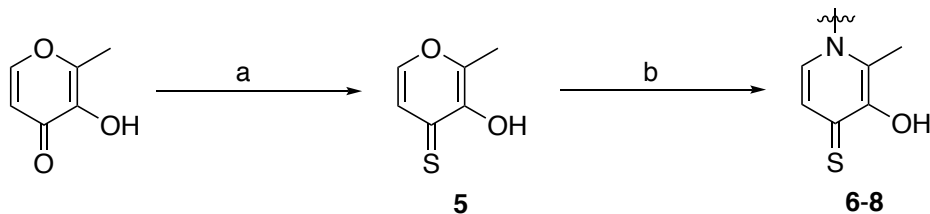
### 2.2.2 MBP Library Hits are Investigated as Potential Rpn11 Inhibitors

The majority of the compounds from the MBP libraries demonstrated weak binding; however, four compounds were validated as hits against Rpn11 (Table 2-1). The result from the screens of the MBP library prompted the development of synthetic analogs of compounds 1-4 (Table 2-1). Compound **2** analogs were

obtained via a two-step reaction synthesis as described in Scheme 2-1. Maltol was utilized as the starting material, where the exocyclic oxygen was transformed to a sulfur atom in the presence of phosphorus pentasulfide to form thiomaltol (**5**). Compound **5** underwent a dehydration reaction via irradiation in a microwave reactor under acidic conditions, along with the corresponding amine to yield compounds (**6-8**). Compounds **6-8** displayed modest inhibition of Rpn11, but failed to increase activity over the parent MBP (**2**). These simple analogs did not yield an appreciable increase in activity, therefore no other analogs were explored. A few simple analogs based off compound **3** were evaluated. Compounds **9-12** (Table 2-2) are salicylic acid derivatives and displayed moderate inhibition of Rpn11. Therefore, direct analogs of compound **3** wherein the acid moiety was converted to a functionalized amide was explored (**13-15**, Scheme 2-2, Table 2-2). These three compounds did not inhibit Rpn11, indicating that the carboxylic acid functional group is necessary for inhibition. Additionally, a few analogs of compound **4** were synthesized (**16-20**) but also failed to exhibit any inhibition of Rpn11. The only remaining hit was **8-TQ**. Because of the particularly strong activity of **8-TQ** the fragment was chosen for lead development. **8-TQ** was determined to have an  $IC_{50}$  value of  $2.8 \pm 0.36 \mu\text{M}$ , which translates to an extremely high ligand efficiency of 0.69.<sup>17</sup>

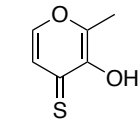
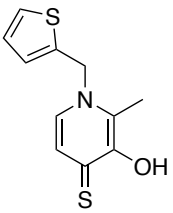
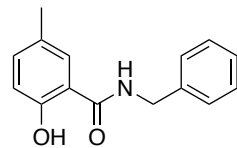
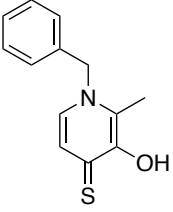
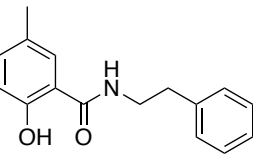
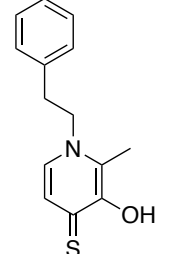
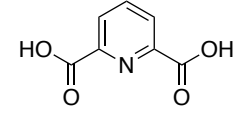
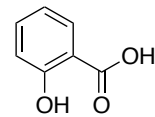
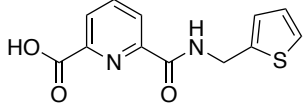
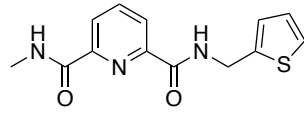
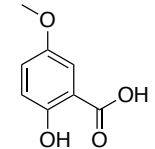
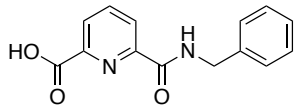
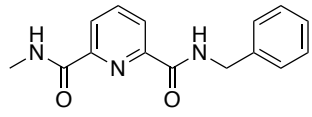
**Table 2-1.** Hits against Rpn11 from the MBP library screens. All values listed are percent inhibition at a concentration of 200  $\mu$ M.

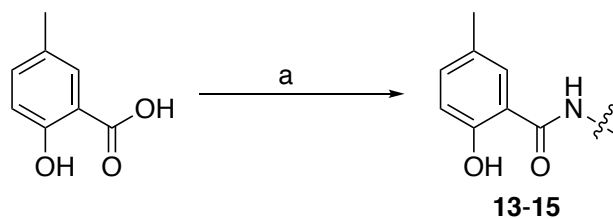
Cmpd	Structure	Inhibition	Cmpd	Structure	Inhibition
<b>1</b> <b>(8-TQ)</b>		94%	<b>3</b>		50%
<b>2</b>		48%	<b>4</b>		60%



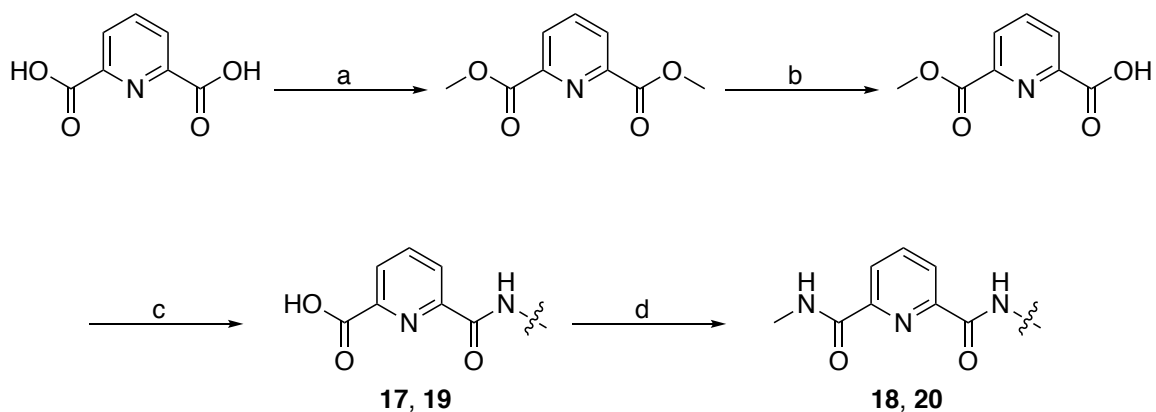
**Scheme 2-1.** Synthetic route for compounds **6-8**. Reagents and conditions: (a)  $P_2S_5$ , Hexamethyldisiloxane (HMDSO), Toluene, 110  $^{\circ}$ C, 8 h (b) Amine, AcOH,  $H_2O$ , EtOH, 165  $^{\circ}$ C (Microwave Reactor), 1 h.

**Table 2-2.** Derivatives of hits obtained from the MBP library against Rpn11. All values listed are percent inhibition at a concentration of 200  $\mu$ M.

Cmpd	Structure	Inhibition	Cmpd	Structure	Inhibition
5		38%	13		0%
6		58%	14		10%
7		58%	15		0%
8		59%	16		40%
9		5%	17		5%
10		12%	18		0%
11		38%	19		0%
12		10%	20		0%



**Scheme 2-2.** Synthetic route for 2-hydroxy-5-methylbenzoic acid analogs. Reagents and conditions: (a) EDC, HOBT, DMF, 25 °C 1 h.



**Scheme 2-3.** Synthetic route for pyridine-2,6-dicarboxylic acid analogs. Reagents and conditions: (a) MeOH, H<sub>2</sub>SO<sub>4</sub> (cat.), 75 °C, 24 h (b) MeOH, KOH, 0 °C, 4 h (c) EDC, HOBT, R-NH<sub>2</sub>, 18 h; then 4:1 1 M NaOH/THF, 30 min to 1 h, 4 M HCl (d) EDC, HOBT, MeNH<sub>2</sub>, 18 h.

### 2.2.3 Investigating the Mechanism of Inhibition of **8-TQ**

Due to the structural similarity of **8-TQ** to the common metal chelator 8-hydroxyquinoline, as well as data on previously reported **8-TQ** metal complexes, it was predicted that **8-TQ** would bind the catalytic  $Zn^{2+}$  ion of Rpn11 in a bidentate fashion through the endocyclic nitrogen and exocyclic sulfur donor atoms (Figure 2-4).<sup>18-20</sup> To validate this hypothesis, a model was sought to allow for structural characterization of the mode of binding. Tris(pyrazolyl)borate (Tp) complexes have been shown to serve as useful metalloenzyme active site mimics, giving some insight into bond lengths and angles for MBPs coordinated to metalloenzyme active site metal ions.<sup>21-26</sup> A  $Zn^{2+}$  complex with the ligand hydrotris(5,3-phenylmethylpyrazolyl)borate ( $Tp^{Ph,Me}$ )<sup>21</sup> was combined with **8-TQ** to obtain the complex  $[(Tp^{Ph,Me})Zn(\mathbf{8-TQ})]$ . The metal complex was readily crystallized and revealed a five-coordinate  $Zn^{2+}$  center with a trigonal bipyramidal coordination geometry (Figure 2-4). **8-TQ** was bound in the expected bidentate manner, with the sulfur donor atom positioned in the equatorial plane (2.29 Å, Zn-S distance) and the endocyclic nitrogen atom serving as an axial donor (2.17 Å, Zn-N distance). The structure of this metalloenzyme model complex supports the hypothesis that **8-TQ** inhibited Rpn11 by metal coordination of the active site  $Zn^{2+}$  ion.

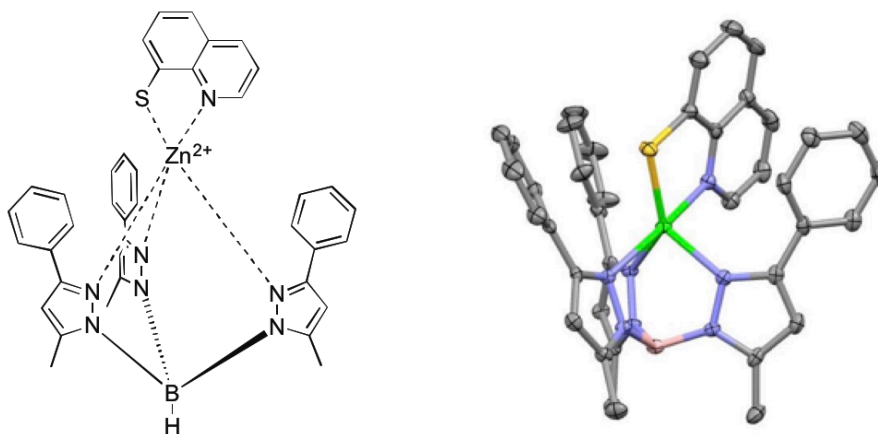


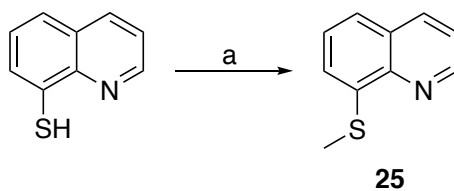
**Figure 2-4.** Chemical illustration (*left*) and image of the X-ray structure (*right*) of  $[(\text{Tp}^{\text{Ph,Me}})\text{Zn}(\mathbf{8-TQ})]$ . Thermal ellipsoids are shown at 50% probability. Hydrogen atoms are omitted for clarity. Color scheme: boron (pink), carbon (gray), nitrogen (blue), sulfur (yellow), and zinc (green).

Additional evidence for the mode of inhibition was obtained from SAR studies using **8-TQ** derivatives. Derivatives of **8-TQ** were prepared including fragments where the metal-coordinating atoms were removed, moved, or otherwise modified (Table 2-3). For example, compound **21** replaced the endocyclic nitrogen with a C-H group, giving a naphthyl derivative, which is incapable of the bidentate mode of binding exhibited by **8-TQ** (Figure 2-4). Similarly, in compounds **22**, **23**, and **24** the thiol moiety was replaced by a methyl, hydroxyl, or amine group, respectively, giving a series of isosteric compounds that lack the requisite thiol donor atom. In compound **25**, the thiol moiety was alkylated with a methyl group (Scheme 2-4), which prevents formation of the anionic thiolate donor atom for binding  $\text{Zn}^{2+}$  (Figure 2-4). Finally, compound **26** places the coordinating nitrogen atom on the opposite side of the

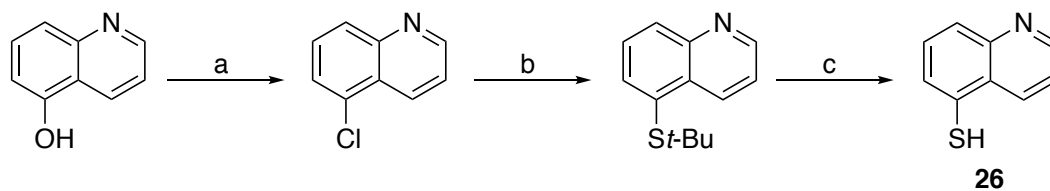
quinoline ring from the thiol moiety (Scheme 2-5), which produces an isosteric compound, but does not allow for bidentate binding of the ligand to the metal ion. As summarized in Table 2-3, compounds **21-26** all exhibited a complete loss of activity ( $IC_{50} >100 \mu\text{M}$ ) against Rpn11, further validating the importance of the bidentate binding of **8-TQ** through the nitrogen and sulfur pair of donor atoms. Further confirmation of this hypothesis was demonstrated by the activity of compound **27**, which has an additional nitrogen atom at the 5-position of the ring (Scheme 2-6), but otherwise can maintain the **8-TQ** binding motif. Compound **27** inhibits Rpn11 with an  $IC_{50}$  value of  $15 \pm 3.4 \mu\text{M}$ . The  $\sim 6$ -fold weaker activity of **27** when compared to **8-TQ** is attributed to the ability of **27** to tautomerize to the 1,5-naphthyridine-4(1*H*)-thione form.

**Table 2-3.** 8-TQ fragment derivatives used to examine the role of metal binding in Rpn11 inhibition. . All IC<sub>50</sub> values listed are in μM.

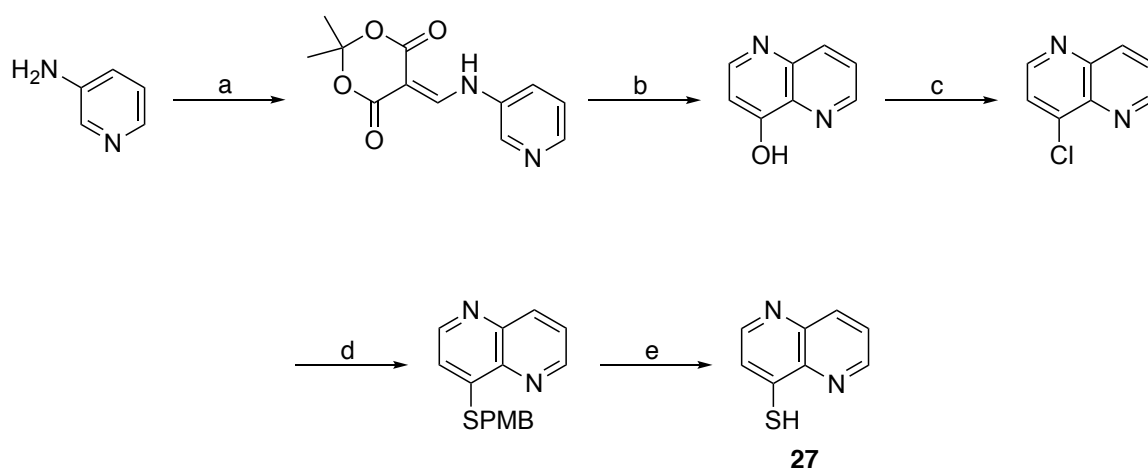
Cmpd	Structure	Rpn11	HCT 116	Cmpd	Structure	Rpn11	HCT 116
8-TQ		2.8±0.36	1.3	24		>100	---
21		>100	>100	25		>100	>100
22		>100	>100	26		>100	>100
23		>100	6	27		15±3.4	---



**Scheme 2-4.** Synthesis of 8-(methylthio)quinoline. Reagents and conditions: (a) CH<sub>3</sub>I, EtOH, H<sub>2</sub>O, 2M NaOH, 25 °C.



**Scheme 2-5.** Synthesis of quinoline-5-thiol. Reagents and conditions: (a)  $\text{POCl}_3$ , 100 °C; (b) *tert*-butylthiol (*t*-BuSH), NaH, DMF, 140 °C; (c) 12M HCl, 100 °C.



**Scheme 2-6.** Synthesis of quinoline-5-thiol. Reagents and conditions: (a) 2,2,6-Trimethyl-4H-1,3-dioxin-4-one (Meldrum's acid), Triethyl orthoformate, 105 °C; (b) Dowtherm A, 250 °C; (c)  $\text{POCl}_3$ , Toluene, 110 °C; (d) 4-Methoxyphenyl)methanethiol (*p*-MBSH), NaH, DMF, 25 °C; (e) *m*-Cresol, TFA, reflux.

## 2.2.4 Synthesis of Methyl Derivatives and Cross Inhibition Studies

Having established a rudimentary SAR for the requisite metal-binding features of the **8-TQ** scaffold, a sublibrary of **8-TQ** derivatives with simple modifications to the scaffold was prepared in an effort to probe for possible hydrophobic (methyl groups) contacts within the active site, as well as to determine the best positions on the **8-TQ** ring to add substituents for subsequent rounds of derivatization. Therefore a series of methyl functionalized 8-TQ analogs were prepared (Figure 2-5, Scheme 2-7 and 2-8). Functionalization of the **8-TQ** fragment was achieved largely via the Skraup and Doubner-Von Miller reactions using aniline derivatives as starting materials. Compounds **28** and **29** were synthesized starting with 2-fluoroaniline with the quinoline ring forming upon addition of a methyl- $\alpha,\beta$ -unsaturated aldehyde in the presence of aqueous HCl (Scheme 2-7). The 4-methyl quinoline analog (**30**) was synthesized in similar fashion, by combining 2-fluoroaniline with an  $\alpha,\beta$ -unsaturated ketone (Scheme 2-7). Compounds **31** and **32** were obtained by starting with methyl functionalized 2-chloro or 2-fluoroaniline in the presence of glycerol utilizing nitrobenzene as the solvent and oxidant (Scheme 2-8). Substitution of the resulting methyl-8-fluoro or methyl-8-chloroquinolines to obtain the thiol functionality was obtained through a nucleophilic aromatic substitution reaction utilizing *t*-BuSH. This was followed by a deprotection reaction under refluxing concentrated HCl to yield the free thiol.

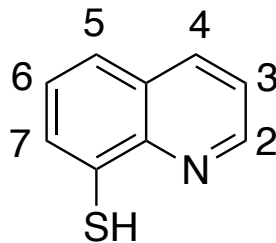
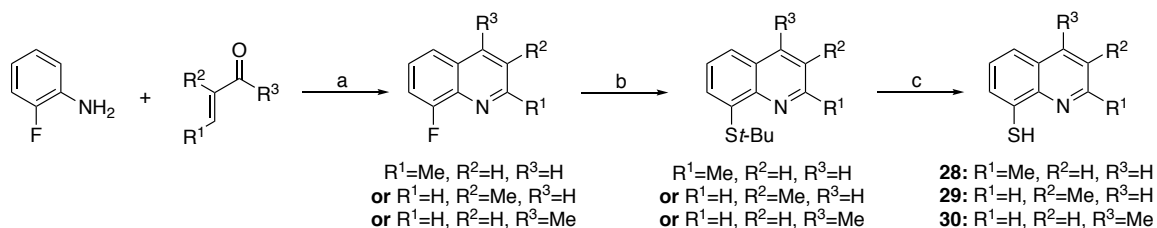
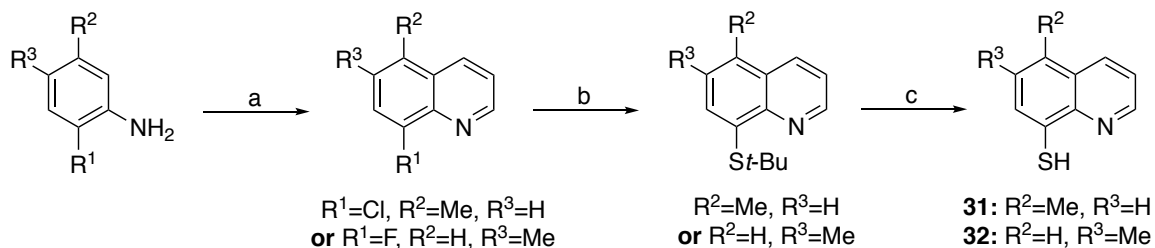


**Figure 2-5.** Structure representation of **8-TQ** with the quinoline ring positions labeled.



**Scheme 2-7.** Synthesis of 2-, 3-, and 4-methyl-8-thioquinoline. Reagents and conditions: (a) Toluene, 6M HCl, 110 °C; (b) *t*-BuSH, NaH, DMF, 140 °C; (c) 12M HCl, 100 °C.



**Scheme 2-8.** Synthesis of 5- and 6-methyl-8-thioquinoline. Reagents and conditions: (a) Glycerol, Nitrobenzene, 150 °C; (b) *t*-BuSH, NaH, DMF, 140 °C; (c) 12M HCl, 100 °C.

In addition to evaluation against Rpn11, the selectivity of these compounds (**28-32**) against off-target metalloenzymes was also examined by performing inhibition assays against a host of other metalloenzymes (Table 2-4). These off-target metalloenzymes were selected because they possess a diverse set of structures and functions, utilize a metal ion in a catalytic role, are clinically relevant targets, and have readily available assays. The metalloenzymes examined included the Zn-dependent JAMM domain enzyme Csn5, two histone deacetylases (HDAC1, HDAC6), a matrix metalloproteinase (MMP-2), carbonic anhydrase (hCAII), and a non-heme, Fe-dependent lipoxygenase (5-LO). In addition, to assess the effects of these compounds in a cellular model, a human colon carcinoma cell line (HCT 116) was utilized to measure the anti-proliferative activity of the fragments.

**Table 2-4.** Enzyme inhibition data for **8-TQ** and derivatives of this MBP hit. Data listed includes inhibitory values against off-target metalloenzymes and cytotoxicity against the HCT 116 cell line. All IC<sub>50</sub> values listed are in  $\mu$ M.

Cmpd	Structure	Rpn11	Csn5	HDAC1	HDAC6	MMP2	5-LO	hCAII	HCT116
<b>8-TQ</b>	H	2.8±0.36	10.3±2.3	>200	>200	>200	>200	>200	1.6±0.7
<b>28</b>	2-Me	>100	>100	N.D	N.D	>200	N.D	N.D	>50
<b>29</b>	3-Me	1.6±0.6	7.1±1.6	>50	>200	>200	>200	>40	2.6±0.5
<b>30</b>	4-Me	5.7±2.0	25.1±6.1	>200	>200	>200	>200	>200	>10
<b>31</b>	5-Me	2.5±1.3	2.9±1.1	>200	>200	>200	>200	>200	3.4±1.1
<b>32</b>	6-Me	0.9±0.3	1.6±0.6	>50	>50	>200	>200	>100	2.1±1.2

The results from these experiments are summarized in Table 2-4. The data demonstrate that the **8-TQ** scaffold was highly specific for the JAMM metalloproteins (Rpn11 and Csn5) over other metalloenzymes. Some discrimination between Rpn11 and Csn5 was observed, even with the relatively simple methyl substitutions, which suggests that specificity could be developed using this scaffold. Inhibition data also suggests that the Rpn11 active site was quite plastic and tolerated substitution at multiple positions on the **8-TQ** ring. Compound **28** did not inhibit the JAMM domain proteins, which correlates with loss of cytotoxicity toward the HCT 116 cell line (Table 2-4). Introduction of even a small methyl group resulted in complete loss of activity, which suggests that functionalization at the 2-position is not tolerated.

### 2.3 Conclusions

In order to discover a fragment that inhibits Rpn11, a FBDD approach using a 96- and 240-component library of MBPs led to the identification of the highly active **8-TQ** fragment. Upon identifying fragment hits **8-TQ** and **2-4**, analogs of these fragments were synthesized and evaluated. Ultimately, **8-TQ** was chosen as the lead fragment due to its high ligand efficiency, potency in an enzyme and cellular assay, and synthetic accessibility. **8-TQ** derivatives were prepared to evaluate the hypothesis that metal binding was the source of **8-TQ** activity. Indeed, the SAR obtained from compounds **21-26** (Table 2-3) indicated

that bidentate metal binding was probable for the observed inhibitory activity by **8-TQ**. Only derivative **27**, which possesses the same *N,S* donor atom set maintains some activity against Rpn11. In addition, the bioinorganic model complex [(Tp<sup>Ph,Me</sup>)Zn(**8-TQ**)] clearly supports the ability of **8-TQ** to form a ternary complex with a Zn<sup>2+</sup> ion bound in a protein-like coordination environment (Tp<sup>Ph,Me</sup>) (Figure 2-4). All of these results point to metal coordination as the mechanism of action for **8-TQ** against Rpn11. From the results obtained from this initial discovery campaign, full-length inhibitors derived from **8-TQ** were prepared and are discussed in Chapter 3.

## 2.4 Experimental

All reagents and solvents were obtained from commercial sources and used without further purification. Microwave reactions were performed in 10 mL or 35 mL microwave vials using a CEM Discover S reactor. Column chromatography was performed using a Teledyne ISCO CombiFlash Rf system with prepacked silica cartridges or High Performance Gold C18 columns.  $^1\text{H}/^{13}\text{C}$  NMR spectra were recorded at ambient temperature on a 400 or 500 Varian FT-NMR instrument located in the Department of Chemistry and Biochemistry at the U.C. San Diego. Mass spectra were obtained at the Molecular Mass Spectrometry Facility (MMSF) in the Department of Chemistry and Biochemistry at the University of California, San Diego. Further details on synthesis may be found in the Supporting Information. The purity of all compounds used in assays was determined to be >95% pure by  $^1\text{H}$  NMR spectroscopy and confirmed by high-resolution mass spectrometry (HRMS) and liquid chromatography-mass spectrometry (LC-MS) analysis using an Agilent 6230 Accurate-Mass LC-TOFMS at the MMSF (U.C. San Diego).

**3-Hydroxy-2-methyl-4*H*-pyran-4-thione (Thiomaltol, 5).** Method was adapted from previously reported procedure.<sup>27</sup> To a solution of 3-hydroxy-2-methyl-4*H*-pyran-4-one (Maltol, 5 g, 39.8 mmol) in toluene (250 mL) was added  $\text{P}_4\text{S}_{10}$  (3.2 g, 7.2 mmol) and hexamethyldisiloxane (HMDSO, 10.8 g, 66.2 mmol) and heated to

110°C for 8 h under nitrogen with the flask covered in aluminum to prevent light from reaching the solution. This was concentrated and yielded a yellow solid/sludge crude product. The crude was recrystallized from hexanes and hot vacuum filtered to remove solid waste. A yellow precipitate was observed in the filtrate solution. Precipitate was isolated via filtration to afford **7**. Yield = 3.05 g (54%). <sup>1</sup>H NMR (400 MHz, CDCl<sub>3</sub>): δ = 7.78 (br, 1H), 7.61 (d, *J* = 6.8 Hz, 1H), 7.34 (d, *J* = 6.8 Hz, 1H), 2.46 (s, 3H).

**General Procedure for compounds 2 and 6-8.** To a solution of 3-hydroxy-2-methyl-4*H*-pyran-4-thione (0.2 g, 1.4 mmol) in of H<sub>2</sub>O:EtOH (2 mL, 1:1) was added AcOH (0.25 g, 4.22 mmol) and amine (4.22 mmol) in a 10 mL reaction vessel. This was reacted by irradiating in the microwave at 165 °C, 250 psi (max pressure), and 300 W (max power) for 60 min. The resulting solution was then concentrated and purified via silica gel chromatography eluting Hexanes/0-100% EtOAc.

**3-Hydroxy-1,2-dimethylpyridine-4(1*H*)-thione (2).** Yield = 0.13 g (56%). <sup>1</sup>H NMR (400 MHz, CDCl<sub>3</sub>) δ 8.68 (br, 1H), 7.36 (d, *J* = 6.8 Hz, 1H), 7.09 (d, *J* = 6.8 Hz, 1H), 3.76 (s, 3H), 2.45 (s, 3H).

**3-Hydroxy-2-methyl-1-(thiophen-2-ylmethyl)pyridine-4(1*H*)-thione (6).** Yield = 0.13 g (57%). <sup>1</sup>H NMR (400 MHz, CDCl<sub>3</sub>) δ 8.75 (br, 1H), 7.51 (d, *J* = 6.8 Hz, 1H), 7.35 (dd, *J* = 6.4, 5.2 Hz, 1H), 7.22 (d, *J* = 6.8 Hz, 1H), 7.02-6.92 (m, 2H), 5.32 (s, 2H), 2.52 (s, 3H). ESI-MS(+): *m/z* 238.01 [M+H]<sup>+</sup>.

**1-Benzyl-3-hydroxy-2-methylpyridine-4(1*H*)-thione (7).** Yield = 0.10 g (49%). <sup>1</sup>H NMR (400 MHz, CDCl<sub>3</sub>) δ 8.77 (br, 1H), 7.53 (d, *J* = 6.7 Hz, 1H), 7.41-7.35 (m, 3H), 7.21 (d, *J* = 6.7 Hz, 1H), 7.04 (d, *J* = 6.3 Hz, 2H), 5.21 (s, 2H), 2.39 (s, 3H). ESI-MS(+): *m/z* 232.14 [M+H]<sup>+</sup>.

**3-hydroxy-2-methyl-1-phenethylpyridine-4(1*H*)-thione. (8)** Yield = 0.13 g (65%). <sup>1</sup>H NMR (400 MHz, CDCl<sub>3</sub>) δ 7.24-7.22 (m, 4H), 7.01 (d, *J* = 7.2 Hz, 2H), 6.85 (d, *J* = 6.4 Hz, 1H), 4.21 (t, *J* = 6.8, 2H), 3.02 (t, *J* = 6.8 Hz, 2H), 2.34 (s, 3H). ESI-MS(+): *m/z* 246.15 [M+H]<sup>+</sup>.

**2-Hydroxy-5-methyl-*N*-(thiophen-2-ylmethyl)benzamide (13).** Yield = 0.22 g (69%). <sup>1</sup>H NMR (400 MHz, CDCl<sub>3</sub>) δ 11.96 (s, 1H), 7.28-7.25 (m, 1H), 7.22 (d, *J* = 8.0 Hz, 1H), 7.11-6.98 (m, 3H), 6.91 (d, *J* = 8.0 Hz, 1H), 6.56 (br, 1H), 4.81 (d, *J* = 5.6 Hz, 1H), 2.26 (s, 3H). ESI-MS(+): *m/z* 248.14 [M+H]<sup>+</sup>.

***N*-Benzyl-2-hydroxy-5-methylbenzamide (14)**. Yield = 0.13 g (41%). <sup>1</sup>H NMR (400 MHz, CDCl<sub>3</sub>) δ 12.08 (s, 1H), 7.39-7.32 (m, 5H), 7.22 (d, *J* = 8.0 Hz, 1H), 7.12 (s, 1H), 6.91 (d, *J* = 8.0 Hz, 1H), 6.56 (br, 1H), 4.64 (d, *J* = 5.6 Hz, 1H), 2.26 (s, 3H). ESI-MS(+): *m/z* 242.11 [M+H]<sup>+</sup>.

**2-Hydroxy-5-methyl-*N*-phenethylbenzamide (15)**. Yield = 0.19 g (57%). <sup>1</sup>H NMR (400 MHz, CDCl<sub>3</sub>) δ 12.17 (s, 1H), 7.36-7.22 (m, 5H), 7.19 (d, *J* = 8.0 Hz, 1H), 7.03 (s, 1H), 6.89 (d, *J* = 8.0 Hz, 1H), 6.50 (br, 1H), 3.71 (dd, *J*<sub>1</sub> = 13.6 Hz, *J*<sub>2</sub> = 6.8 Hz, 2H), 2.95 (t, *J* = 6.8 Hz, 2H), 2.24 (s, 3H). ESI-MS(+): *m/z* 256.23 [M+H]<sup>+</sup>.

**Dimethyl Pyridine-2,6-dicarboxylate**. Dipicolinic acid (1 g, 5.98 mmol) was dissolved in MeOH (1 L), and concentrated H<sub>2</sub>SO<sub>4</sub> (0.5 mL) was added dropwise to the solution. The reaction mixture was heated to reflux for 24 h and monitored via TLC. Once the reaction was completed by TLC, the solvent was removed by evaporation in vacuo to afford product as a white crystalline solid. Yield = 1.16 g (100%). <sup>1</sup>H NMR (400 MHz, DMSO-*d*<sub>6</sub>): δ 8.26–8.13 (m, 3H), 3.90 (s, 6H). ESI-MS(+): *m/z* 196.09 [M+H]<sup>+</sup>.

**6-(Methoxycarbonyl)picolinic Acid.** Dimethyl pyridine-2,6- dicarboxylate (1.9 g, 9.92 mmol) was dissolved in MeOH (75 mL) and cooled to 0 °C via ice bath. Potassium hydroxide pellets (557 mg, 9.92 mmol) were added to the solution portionwise and stirred at 0 °C for an additional 4 h. Once the reaction was complete by TLC, the MeOH was removed by evaporation in vacuo. The white salt was washed with copious amounts of EtOAc to remove any remaining starting material. The salt was then dissolved in water (25 mL), and solution was acidified with 4 M HCl to pH 2. The aqueous solution was extracted with chloroform (25 mL × 3), and the combined organic layers were dried over MgSO<sub>4</sub>. MgSO<sub>4</sub> was removed by vacuum filtration and the organic layer was evaporated under vacuum to afford the product as a white powder. Yield = 1.45 g (81%). <sup>1</sup>H NMR (400 MHz, DMSO-*d*<sub>6</sub>): δ 8.23–8.14 (m, 3H), 3.90 (s, 3H). ESI-MS (-): m/z 180.09 [M-H]<sup>-</sup>.

**General Procedure for Compounds 17 and 19.** 6- (Methoxycarbonyl) picolinic acid (200 mg, 1.10 mmol), 1-ethyl-3-(3- dimethylaminopropyl) carbodiimide (EDC, 1.1 equiv), and hydroxybenzotriazole (HOBT, 1.1 equiv) were dissolved in dry DMF (10 mL), and the reaction mixture was stirred at room temperature for 30 min. The corresponding amine (1.1 equiv) was then added to the reaction mixture and allowed to react at room temperature overnight. DMF was evaporated under vacuum, and the reaction was taken up in EtOAc (10 mL) and extracted with copious amounts of saturated NaHCO<sub>3</sub> (10 mL × 3). The organic

layer was evaporated under vacuum and purified by EtOAc and hexane column chromatography. Hydrolysis was then performed by stirring the product in a solution of 1 M NaOH (4 mL) and THF (1 mL) at room temperature. Once the hydrolysis was complete by TLC, the solution was acidified with 4 M HCl to pH 4 and the precipitate was collected via vacuum filtration.

**6-((Thiophen-2-ylmethyl)carbamoyl)picolinic Acid (17).** Yield = 0.22 g (77%).

$^1\text{H}$  NMR (400 MHz,  $\text{CD}_3\text{OD}-d_4$ ):  $\delta$  8.34 (d,  $J = 7.6$  Hz, 1H), 8.30 (d,  $J = 7.6$  Hz, 1H), 8.16 (m, 1H), 7.29 (d,  $J = 4.8$  Hz, 1H), 7.08 (s, 1H), 6.96–6.94 (m, 1H), 4.79 (s, 2H). ESI-MS(-):  $m/z$  261.18  $[\text{M} - \text{H}]^-$ .

**6-(Benzylcarbamoyl)picolinic Acid (19).** Yield = 0.19 g (87%).  $^1\text{H}$  NMR (400 MHz,  $\text{CD}_3\text{OD}-d_4$ ):  $\delta$  8.34 (d,  $J = 7.2$  Hz, 1H), 8.30 (d,  $J = 7.2$  Hz, 1H), 8.15 (m, 1H), 7.38–7.23 (m, 5H), 4.63 (s, 2H). ESI-MS(-):  $m/z$  255.23  $[\text{M} - \text{H}]^-$ .

**8-(Methylthio)quinoline (25).** To a solution of 8-thioquinoline (0.07 g, 0.35 mmol) in a mixture of EtOH,  $\text{H}_2\text{O}$ , and 2M NaOH (4 mL, 2:1:1 ratio) was added  $\text{CH}_3\text{I}$  (120 mL, 1.8 mmol). The solution was stirred at room temperature for 24 h and then evaporated to dryness. The reaction mixture was then dissolved in  $\text{CH}_2\text{Cl}_2$  and washed with  $\text{H}_2\text{O}$  (3×50mL). The combined organic layers were dried and concentrated in vacuo. The crude was purified via silica gel column

chromatography eluting a gradient of 0 to 100% EtOAc in Hexanes. Yield = 0.006 g (10%).  $^1\text{H NMR}$  (500 MHz,  $\text{CDCl}_3$ ):  $\delta$  8.95 (dd,  $J = 4.2, 1.8$  Hz, 1H), 8.14 (dd,  $J = 8.3, 1.7$  Hz, 1H), 7.57 (dd,  $J = 8.2, 1.3$  Hz, 1H), 7.50 (dd,  $J = 8.1, 7.3$  Hz, 1H), 7.45 (dd,  $J = 8.2, 4.2$  Hz, 1H), 7.41 (dd,  $J = 7.4, 1.3$  Hz, 1H), 2.59 (s, 3H). ESI-MS (+):  $m/z$  176.11  $[\text{M}+\text{H}]^+$ .

**5-Chloroquinoline.** A solution of 5-Hydroxyquinoline (0.1 g, 0.68 mmol) in  $\text{POCl}_3$  (5 mL) was stirred at 100 °C for 2 h.  $\text{H}_2\text{O}$  was added slowly to the reaction mixture to neutralize  $\text{POCl}_3$  and the resulting solution was evaporated to dryness. To the resulting crude was added MeOH, which caused the formation of a white precipitate. The solid was isolated by filtration to afford product. Yield = 0.08 g (71%).  $^1\text{H NMR}$  (400 MHz,  $\text{DMSO}-d_6$ ):  $\delta$  8.93 – 8.89 (m, 1H), 8.47 (t,  $J = 6.8$  Hz, 1H), 7.78 (d,  $J = 5.5$  Hz, 1H), 7.74 – 7.67 (m, 1H), 7.60 – 7.54 (m, 1H), 7.46 (d,  $J = 6.6$  Hz, 1H). ESI-MS (+):  $m/z$  164.05  $[\text{M}+\text{H}]^+$ .

**5-(*tert*-Butylthio)quinolone.** To a solution of 5-Chloroquinoline (0.07 g, 0.43 mmol) in DMF (7 mL) was added NaH (0.035 g, 1.45 mmol) and *t*-BuSH (0.97 mL, 0.86 mmol) under nitrogen atmosphere. The reaction was stirred at 140 °C for 18 h. The resulting solution was then concentrated in vacuo and the crude material was purified by via silica gel column chromatography eluting a gradient

of 0 to 100% EtOAc in Hexanes. Yield = 0.04 g (43%).  $^1\text{H}$  NMR (400 MHz,  $\text{CD}_3\text{OD}$ ):  $\delta$  8.89 (dd,  $J = 4.3, 1.8$  Hz, 1H), 8.58 – 8.53 (m, 1H), 7.68 (d,  $J = 8.4$  Hz, 1H), 7.55 – 7.46 (m, 1H), 7.38 (dd,  $J = 8.4, 4.3$  Hz, 1H), 6.85 (d,  $J = 7.7$  Hz, 1H), 1.53 (s, 9H). ESI-MS (+):  $m/z$  218.15  $[\text{M}+\text{H}]^+$ .

**Quinoline-5-thiol (26).** A solution of 5-(*tert*-Butylthio)quinolone (0.04 g, 0.17 mmol) in conc. HCl (11 mL) was stirred at 90 °C for 19 h. The resulting solution was neutralized to pH 9-10 with NaOH and extracted twice with  $\text{CHCl}_3$  (3 $\times$ 10mL). The combined organic layers were dried and the solution was concentrated in vacuo. The crude material was then recrystallized from EtOAc. Yield = 0.01 g (48%).  $^1\text{H}$  NMR (500 MHz,  $\text{CDCl}_3$ ):  $\delta$  8.95 – 8.90 (m, 1H), 8.66 – 8.56 (m, 1H), 7.75 – 7.70 (m, 1H), 7.60 – 7.50 (m, 1H), 7.45 – 7.36 (m, 1H), 6.93 – 6.85 (m, 1H). ESI-MS (+):  $m/z$  162.10  $[\text{M}+\text{H}]^+$ .

**2,2-Dimethyl-5-((pyridin-3-ylamino)methylene)-1,3-dioxane-4,6-dione.** To a preheated (~100 °C) mixture of 3-Aminopyridine (0.37 g, 4.0 mmol) and 2,2-Dimethyl-[1,3]dioxane-4,6-dione (Meldrum's acid, 0.69 g, 4.8 mmol) was added Triethyl Orthoformate (4.0 mL, 24.0 mmol). The solution was stirred at 100 °C for 2 h. The reaction proceeded by changing color from yellow to wine red accompanying the formation of a yellow precipitate. After cooling to room

temperature, the excess liquid of Triethyl Orthoformate was removed via vacuum distillation. The resulting solid was purified via silica gel chromatography eluting a gradient of 70 to 100% EtOAc in Hexanes. Yield = 0.72 g (72%).  $^1\text{H}$  NMR (400 MHz,  $\text{CDCl}_3$ ):  $\delta$  11.25 (d,  $J = 10.4$  Hz, 1H), 8.63 (d,  $J = 14.00$  Hz, 1H), 8.61 (d,  $J = 3.2$  Hz, 1H), 8.55 (dd,  $J = 4.8$  Hz,  $J = 1.6$  Hz, 1H), 7.61 (d,  $J = 8.0$  Hz, 1H), 7.41 (dd,  $J = 8.20$ , 4.2 Hz, 1H), 1.77 (s, 6H).  $^{13}\text{C}$  NMR (100 MHz,  $\text{CDCl}_3$ ):  $\delta$  165.2, 163.0, 152.9, 147.6, 140.6, 134.6, 124.9, 124.1, 105.2, 88.5, 26.9. ESI-MS (+):  $m/z$  248.90  $[\text{M}+\text{H}]^+$ .

**1,5-Naphthyridin-4-ol.** To a flask containing 2,2-Dimethyl-5-((pyridin-3-ylamino)methylene)-1,3-dioxane-4,6-dione (2.6 g, 10.4 mmol) under nitrogen atmosphere was added Dowtherm A (150 mL) and placed in a pre-heated oil bath at 250 °C. The reaction mixture was stirred at reflux for 1 h. A color change from orange yellow to dark brown was observed. The resulting solution was cooled to room temperature and filtered to isolate solid product. The solid was rinsed with Diphenyl Ether and Acetone to give the desired product as a dark solid. Yield = 1.14 g (75%).  $^1\text{H}$  NMR (400 MHz,  $\text{CD}_3\text{OD}$  + one drop TFA):  $\delta$  9.07 (d,  $J = 4.8$  Hz, 1H), 8.72 (d,  $J = 8.8$  Hz, 1H), 8.61 (d,  $J = 7.2$  Hz, 1H), 8.22 (dd,  $J = 8.8$  Hz,  $J = 4.8$  Hz, 1H), 7.07 (d,  $J = 7.2$  Hz, 1H).  $^{13}\text{C}$  NMR (125 MHz,  $\text{CD}_3\text{OD}$  + one drop TFA):  $\delta$  172.3, 147.5, 145.5, 138.6, 134.8, 134.4, 130.1, 112.2. ESI-MS (+):  $m/z$  147.29  $[\text{M}+\text{H}]^+$ .

**4-Chloro-1,5-naphthyridine.** To a solution of 1,5-Naphthyridin-4-ol (0.8 g, 5.47 mmol) in Toluene (20 mL) was added POCl<sub>3</sub> (1.02 mL, 10.95 mmol) at room temperature. The solution was stirred at 110 °C for 2 h, then allowed to cool to room temperature, resulting in the formation of a precipitate. The solution and dark solid was quenched with sat. NaHCO<sub>3</sub> and extracted with EtOAc. The combined organic layers were dried over anhydrous Na<sub>2</sub>SO<sub>4</sub>, filtered and concentrated under reduced pressure. The residue was purified via silica gel chromatography eluting a gradient of 20 to 40% EtOAc in CH<sub>2</sub>Cl<sub>2</sub>. Yield = 0.37 g (41%). <sup>1</sup>H NMR (400 MHz, CDCl<sub>3</sub>): δ 8.92 (dd, *J* = 4.4, 1.2 Hz, 1H), 8.69 (d, *J* = 4.8 Hz, 1H), 8.26 (dd, *J* = 8.8, 1.6 Hz, 1H), 7.60 (d, *J* = 8.0 Hz, 1H), 7.56 (dd, *J* = 8.4, 4.0 Hz, 1H). ESI-MS (+): *m/z* 165.28 [M+H]<sup>+</sup>.

**4-((4-Methoxybenzyl)thio)-1,5-naphthyridine.** To a solution of 4-Chloro-1,5-naphthyridine (0.9 g, 5.47 mmol) in DMF (30 mL) was added (4-Methoxyphenyl)methanethiol (*p*-MBSH, 1.1 mL, 8.20 mmol) at room temperature. The solution was stirred for 2 h, then quenched with MeOH and concentrated in vacuo. The resulting residue was diluted with H<sub>2</sub>O and neutralized with 1N HCl to pH ~ 8. The aqueous solution was extracted with EtOAc. The combined organic layers were dried over anhydrous Na<sub>2</sub>SO<sub>4</sub>, filtered and concentrated under reduced pressure. The crude material was purified via silica gel chromatography

eluting a gradient of 25 to 70% EtOAc in Hexanes. Yield = 1.07 g (70%).  $^1\text{H}$  NMR (400 MHz,  $\text{CDCl}_3$ ):  $\delta$  8.90 (dd,  $J = 4.4, 1.6$  Hz, 1H), 8.69 (d,  $J = 4.8$  Hz, 1H), 8.33 (dd,  $J = 8.4, 1.6$  Hz, 1H), 7.63 (dd,  $J = 8.4, 4.8$  Hz, 1H), 7.39 (d,  $J = 9.2$  Hz, 2H), 7.35 (d,  $J = 4.8$  Hz, 1H), 6.86 (dd,  $J = 8.8$  Hz, 2H), 4.24 (s, 2H), 3.77 (s, 3H).  $^{13}\text{C}$  NMR (125 MHz,  $\text{CDCl}_3$ ):  $\delta$  159.2, 151.4, 150.1, 149.5, 142.6, 141.7, 137.7, 130.1, 130.1, 126.9, 125.0, 118.1, 114.3, 55.4, 34.8. ESI-MS (+):  $m/z$  283.05  $[\text{M}+\text{H}]^+$ .

**1,5-Naphthyridine-4-thiol (27).** To a solution of 4-((4-Methoxybenzyl)thio)-1,5-naphthyridine (0.7 g, 2.48 mmol) in TFA (20 mL) was added *m*-Cresol (1.3 mL, 12.41 mmol) at room temperature. The solution was then stirred at reflux for 16 h and then allowed to cool. The resulting reaction mixture was concentrated and diluted with the EtOAc. The solution was neutralized with sat.  $\text{NaHCO}_3$ , which resulted in the formation of an orange red precipitate. The precipitate was collected via vacuum filtration and washed with  $\text{H}_2\text{O}$  and Acetone to yield the desired product. Yield = 0.38 g, (94%).  $^1\text{H}$  NMR (400 MHz,  $\text{CDCl}_3$ ):  $\delta$  8.70-8.63 (m, 1H), 8.03 (dd,  $J = 7.8, 2.2$  Hz, 1H), 7.95 (d,  $J = 4.8$  Hz, 1H), 7.46 (dd,  $J = 8.2, 4.2$  Hz, 1H), 7.41 (d,  $J = 5.2$  Hz, 1H).  $^{13}\text{C}$  NMR (100 MHz,  $\text{CDCl}_3$ ):  $\delta$  174.2, 148.4, 147.2, 146.7, 143.4, 137.42, 128.2, 122.8. ESI-MS (+):  $m/z$  163.19  $[\text{M}+\text{H}]^+$ .

**8-Fluoro-2-methylquinoline.** To a solution of 2-Fluoroaniline (1 g, 9 mmol) in Toluene (40 mL) was added 6M HCl (12 mL) and Crotonaldehyde (1.47 mL, 1.8 mmol). The heterogeneous mixture was stirred at 110 °C for 2 h. The aqueous layer was separated, neutralized to pH 9, and extracted with EtOAc (3×50mL). The combined organic layers were dried over anhydrous MgSO<sub>4</sub>, filtered, and concentrated under reduced pressure. The crude material was purified via silica gel column chromatography eluting a gradient of 0 to 100% EtOAc in Hexanes. Yield = 0.71 g (49%). <sup>1</sup>H NMR (400 MHz, DMSO-*d*<sup>6</sup>): δ 8.29 (d, *J* = 9.5 Hz, 1H), 7.71 (d, *J* = 7.0 Hz, 1H), 7.56 – 7.40 (m, 3H), 2.66 (s, 3H). ESI-MS (+): *m/z* 162.2 [M+H]<sup>+</sup>.

**8-(*tert*-Butylthio)-2-methylquinoline.** To a solution of 8-Fluoro-2-methylquinoline (0.195 g, 1.21 mmol) in DMF (20 mL) was added NaH (0.097 g, 4.04 mmol) and *t*-BuSH (0.272 mL, 2.42 mmol) under nitrogen atmosphere. The solution was stirred at 140 °C for 18 h. The reaction mixture was evaporated to dryness and the crude material was purified via silica gel column chromatography eluting a gradient of 0 to 100% EtOAc in Hexanes. Yield = 0.22 g (77%). <sup>1</sup>H NMR (400 MHz, CDCl<sub>3</sub>): δ 8.74 (d, *J* = 8.3 Hz, 1H), 8.27 (dd, *J* = 7.2, 1.3 Hz, 1H), 8.17 – 8.04 (m, 1H), 7.81 (t, *J* = 7.8 Hz, 1H), 7.75 (d, *J* = 8.4 Hz, 1H), 3.59 (s, 3H), 1.43 (s, 9H). ESI-MS(+): *m/z* 231.91 [M+H]<sup>+</sup>.

**2-Methylquinoline-8-thiol (28).** A solution of 8-(*tert*-Butylthio)-2-methylquinoline (0.04 g, 0.17 mmol) in conc. HCl (11 mL) was stirred at 90 °C for 19 h. The solution was neutralized to pH 9-10 and extracted EtOAc (3×10mL). The combined organic layers were dried over anhydrous MgSO<sub>4</sub>, filtered, and concentrated under reduced pressure. The crude material was recrystallized from EtOH. Yield = 0.02 g (66%). <sup>1</sup>H NMR (500 MHz, CDCl<sub>3</sub>): δ 8.07 (d, *J* = 8.4 Hz, 1H), 7.85 (d, *J* = 7.5 Hz, 1H), 7.58 (d, *J* = 8.0 Hz, 1H), 7.41 – 7.30 (m, 2H), 2.85 (s, 3H). APCI-MS(-): *m/z* 174.10 [M-H]<sup>-</sup>.

**8-Fluoro-3-methylquinoline.** To a solution of 2-Fluoroaniline (1.0 g, 9 mmol) in Toluene (40 mL) was added 6M HCl (12 mL) and Methacrolein (1.5 mL, 1.8 mmol). The heterogeneous mixture was stirred at 110 °C for 2.5 h. The aqueous layer was separated, neutralized to pH 9 and extracted with EtOAc (3×50mL). The combined organic layers were dried over anhydrous MgSO<sub>4</sub>, filtered, and concentrated under reduced pressure. The crude material was purified via silica gel column chromatography eluting a gradient of 0 to 100% EtOAc in Hexanes. Yield = 0.65 g (45%). <sup>1</sup>H NMR (500 MHz, CDCl<sub>3</sub>): δ 8.53 (d, *J* = 2.3 Hz, 1H), 7.56 (s, 1H), 7.22 – 7.17 (m, 1H), 7.17 – 7.10 (m, 1H), 7.08 – 6.98 (m, 1H), 2.22 – 2.21 (s, 3H). ESI-MS(+): *m/z* 162.19 [M+H]<sup>+</sup>.

**8-(*tert*-Butylthio)-3-methylquinoline.** To a solution of 8-Fluoro-3-methylquinoline (0.5 g, 3.1 mmol) in DMF (50 mL) was added NaH (0.25 g, 10.3 mmol) and *t*-BuSH (0.698 mL, 6.2 mmol) under nitrogen atmosphere. The reaction mixture was stirred at 140 °C for 18 h. The resulting solution was evaporated to dryness and the crude material purified via silica gel column chromatography eluting a gradient of 0 to 100% EtOAc in Hexanes. Yield = 0.56 g (78%). <sup>1</sup>H NMR (500 MHz, CDCl<sub>3</sub>): δ 8.90 (d, *J* = 2.3 Hz, 1H), 7.96 (dd, *J* = 7.2, 1.5 Hz, 1H), 7.92 (d, *J* = 1.1 Hz, 1H), 7.74 (dd, *J* = 8.2, 1.5 Hz, 1H), 7.47 (dd, *J* = 8.1, 7.2 Hz, 1H), 2.53 (s, 3H), 1.37 (s, 9H). ESI-MS(+): *m/z* 231.92 [M+H]<sup>+</sup>.

**3-Methylquinoline-8-thiol (29).** A solution of 8-(*tert*-Butylthio)-3-methylquinoline (0.08 g, 0.35 mmol) in conc. HCl (25 mL) was stirred at 90 °C for 19 h. The reaction mixture was neutralized to pH 9 with NaOH and extracted with EtOAc (3×10mL). The combined organic layers were dried over anhydrous MgSO<sub>4</sub>, filtered, and concentrated under reduced pressure. The crude material was purified via silica gel column chromatography eluting a gradient of 0 to 100% EtOAc in Hexanes. Yield = 0.02 g (33%). <sup>1</sup>H NMR (500 MHz, CDCl<sub>3</sub>): δ 8.73 (d, *J* = 8.4 Hz, 1H), 7.85 (d, *J* = 7.5 Hz, 1H), 7.60 (d, *J* = 8.0 Hz, 1H), 7.47 – 7.45 (m, 1H), 7.35 – 7.31 (m, 1H), 5.58 (s, 1H), 2.48 (s, 3H). ESI-MS(+): *m/z* 176.16 [M+H]<sup>+</sup>.

**8-Fluoro-4-methylquinoline.** To a solution of 2-Fluoroaniline (1.0 g, 9 mmol) in Toluene (40 mL) was added 6M HCl (12 mL) and Methyl Vinyl ketone (1.5 mL, 1.8 mmol). The heterogeneous mixture was stirred at 110 °C for 16 h. The aqueous layer was separated, neutralized to pH 9 with 6M NaOH and extracted with CH<sub>2</sub>Cl<sub>2</sub> (3×50mL). The combined organic layers were dried over anhydrous MgSO<sub>4</sub>, filtered, and concentrated under reduced pressure. The crude material was purified via silica gel column chromatography eluting a gradient of 0 to 100% EtOAc in Hexanes. Yield = 0.4 g (28%). <sup>1</sup>H NMR (500 MHz, DMSO-*d*<sup>6</sup>): δ 8.74 (d, *J* = 4.4 Hz, 1H), 7.83 – 7.77 (m, 1H), 7.57 – 7.46 (m, 2H), 7.39 (dd, *J* = 4.3, 1.0 Hz, 1H), 2.61 (s, 3H). ESI-MS(+): *m/z* 162.23 [M+H]<sup>+</sup>.

**8-(*tert*-Butylthio)-4-methylquinoline.** To a solution of 8-Fluoro-4-methyl quinoline (0.26 g, 1.58 mmol) in DMF (25 mL) was added NaH (0.13 g, 5.29 mmol) and *t*-BuSH (0.356 mL, 3.16 mmol) under nitrogen atmosphere. The solution was stirred at 140 °C for 18 h. The reaction mixture was evaporated to dryness and the crude material was purified via silica gel column chromatography eluting a gradient of 0 to 100% EtOAc in Hexanes. Yield = 0.2 g (55%). <sup>1</sup>H NMR (500 MHz, CDCl<sub>3</sub>): δ 8.88 (d, *J* = 4.3 Hz, 1H), 8.05 – 7.93 (m, 2H), 7.50 (dd, *J* = 8.4, 7.2 Hz, 1H), 7.22 (dd, *J* = 4.3, 1.0 Hz, 1H), 2.69 (s, 3H), 1.36 (s, 9H). ESI-MS(+): *m/z* 231.90 [M+H]<sup>+</sup>.

**4-Methylquinoline-8-thiol (30).** A solution of 8-(*tert*-Butylthio)-4-methylquinoline (0.08 g, 0.35 mmol) in conc. HCl (25 mL) was stirred at 90 °C for 19 h. The reaction mixture was neutralized to pH 9 with NaOH and extracted with EtOAc (3×50mL). The combined organic layers were dried over anhydrous MgSO<sub>4</sub>, filtered, and concentrated under reduced pressure. The crude material was purified via silica gel column chromatography eluting a gradient of 0 to 100% EtOAc in Hexanes. Yield = 0.02 g (30%). <sup>1</sup>H NMR (500 MHz, CDCl<sub>3</sub>): δ 8.76 (d, *J* = 4.4 Hz, 1H), 7.76 – 7.66 (m, 2H), 7.39 (dd, *J* = 8.4, 7.3 Hz, 1H), 7.25 (dd, *J* = 4.4, 1.0 Hz, 1H), 2.69 (s, 3H). ESI-MS(+): *m/z* 176.17 [M+H]<sup>+</sup>.

**8-Chloro-5-methylquinoline.** To a solution of 2-Chloro-5-methylaniline (1 g, 14.1 mmol) in 75% Sulfuric acid (8 mL) was added Nitrobenzene (1.44 mL, 14.1 mmol) and Glycerol (2.06 mL, 28.2 mmol). The heterogeneous mixture was stirred at 150 °C for 2 h. This was allowed to cool, then H<sub>2</sub>O was added to the mixture and extracted with EtOAc (3×50mL). The combined organic layers were dried over anhydrous MgSO<sub>4</sub>, filtered, and concentrated under reduced pressure. The crude material was purified via silica gel column chromatography eluting a gradient of 0 to 100% EtOAc in Hexanes. Yield = 1.0 g (40%). <sup>1</sup>H NMR (500 MHz, CDCl<sub>3</sub>): δ 9.04 (dd, *J* = 4.2, 1.7 Hz, 1H), 8.32 (dd, *J* = 8.5, 1.7 Hz, 1H), 7.71 (d, *J* = 7.7 Hz, 1H), 7.49 (dd, *J* = 8.5, 4.2 Hz, 1H), 7.28 (dd, *J* = 7.8, 0.9 Hz, 1H), 2.65 (d, *J* = 1.0 Hz, 3H). ESI-MS(+): *m/z* 178.21 [M+H]<sup>+</sup>.

**8-(*tert*-Butylthio)-5-methylquinoline.** To a solution of 8-Chloro-5-methylquinoline (1 g, 5.62 mmol) in DMF (100 mL) was added NaH (0.45 g, 18.8 mmol) and *t*-BuSH (1.26 mL, 3.16 mmol) under nitrogen atmosphere. The reaction mixture was stirred at 140 °C for 18 h. The resulting solution was evaporated to dryness and the crude material purified via silica gel column chromatography eluting a gradient of 0 to 100% EtOAc in Hexanes. Yield = 0.19 g (14%). <sup>1</sup>H NMR (500 MHz, CDCl<sub>3</sub>): δ 9.05 (dd, *J* = 4.2, 1.7 Hz, 1H), 8.34 (dd, *J* = 8.5, 1.7 Hz, 1H), 7.72 (d, *J* = 7.6 Hz, 1H), 7.50 (dd, *J* = 8.5, 4.2 Hz, 1H), 7.29 (dd, *J* = 7.6, 1.0 Hz, 1H), 2.66 (d, *J* = 1.0 Hz, 3H), 1.34 (s, 9H). ESI-MS(+): *m/z* 231.91 [M+H]<sup>+</sup>.

**5-Methylquinoline-8-thiol (31).** A solution of 8-(*tert*-Butylthio)-5-methylquinoline (0.08 g, 0.35 mmol) in conc. HCl (25 mL) was stirred at 100 °C for 19 h. The resulting solution was neutralized to pH 9 with NaOH and extracted with EtOAc (3×50mL). The combined organic layers were dried and concentrated under reduced pressure. The crude material was purified via silica gel column chromatography eluting a gradient of 0 to 100% EtOAc in Hexanes. Yield = 0.05 g (81%). <sup>1</sup>H NMR (500 MHz, CDCl<sub>3</sub>): δ 8.94 (dd, *J* = 4.3, 1.8 Hz, 1H), 8.09 (dd, *J* = 8.3, 1.8 Hz, 1H), 7.79 (d, *J* = 1.8 Hz, 1H), 7.45 (dd, *J* = 8.3, 4.3 Hz, 1H), 7.38 (s, 1H), 2.39 (s, 3H). ESI-MS(+): *m/z* 176.00 [M+H]<sup>+</sup>.

**8-Fluoro-6-methylquinoline.** To a solution of 2-Fluoro-6-methylaniline (0.5 g, 4.0 mmol) in 75% Sulfuric acid (4 mL) was added Nitrobenzene (0.409 mL, 4.0 mmol) and Glycerol (588 mL, 8.0 mmol). The heterogeneous mixture was stirred at 150 °C for 3 h, then allowed to cool to room temperature. H<sub>2</sub>O was added to the reaction mixture and with EtOAc (3×50mL). The combined organic layers were dried over anhydrous MgSO<sub>4</sub>, filtered, and concentrated under reduced pressure. The crude material was purified via silica gel column chromatography eluting a gradient of 0 to 100% EtOAc in Hexanes. Yield = 0.17 g (27%). <sup>1</sup>H NMR (500 MHz, CDCl<sub>3</sub>): δ 8.79 (dd, *J* = 4.2, 1.6 Hz, 1H), 7.99 (d, *J* = 8.4 Hz, 1H), 7.92 (s, 1H), 7.34 (dd, *J* = 8.4, 4.2 Hz, 1H), 7.15 (dd, *J* = 11.5, 1.8 Hz, 1H), 2.43 (d, *J* = 1.0 Hz, 3H). ESI-MS(+): *m/z* 162.19 [M+H]<sup>+</sup>.

**8-(*tert*-Butylthio)-6-methylquinoline.** To a solution of 8-Fluoro-6-methylquinoline (0.14 g, 0.87 mmol) in DMF (14 mL) was added NaH (0.07 g, 2.91 mmol) and *t*-BuSH (0.196 mL, 1.74 mmol) under nitrogen atmosphere. The solution was stirred at 140 °C for 18 h. The resulting solution was evaporated to dryness and the crude material purified via silica gel column chromatography using a gradient of 0 to 100% EtOAc in Hexanes. Yield = 0.16 g (78% yield). <sup>1</sup>H NMR (500 MHz, CDCl<sub>3</sub>): δ 8.98 (dd, *J* = 4.2, 1.8 Hz, 1H), 8.06 (dd, *J* = 8.2, 1.8 Hz, 1H), 7.89 (d, *J* = 2.0 Hz, 1H), 7.58 (d, *J* = 1.0 Hz, 1H), 7.37 (dd, *J* = 8.2, 4.2 Hz, 1H), 2.54 (s, 3H), 1.37 (s, 9H). ESI-MS(+): *m/z* 231.91 [M+H]<sup>+</sup>.

**6-Methylquinoline-8-thiol (32).** A solution of 8-(*tert*-butylthio)-6-methylquinoline (0.08 g, 0.35 mmol) in conc. HCl (25 mL) was stirred at 100 °C for 19 h. The crude material was neutralized to pH 9 with NaOH and extracted with EtOAc (3×50mL). The combined organic layers were dried over anhydrous MgSO<sub>4</sub>, filtered, and concentrated under reduced pressure. The crude material was purified via silica gel column chromatography eluting a gradient of 0 to 100% EtOAc in Hexanes. Yield = 0.03 g (46%). <sup>1</sup>H NMR (400 MHz, CDCl<sub>3</sub>): δ 8.84 (dd, *J* = 4.3, 1.6 Hz, 1H), 8.03 (dd, *J* = 8.2, 1.6 Hz, 1H), 7.55 (d, *J* = 1.8 Hz, 1H), 7.38 (dd, *J* = 8.2, 4.2 Hz, 1H), 7.31 (d, *J* = 0.9 Hz, 1H), 5.61 (s, 1H), 2.46 (s, 3H). ESI-MS(+): *m/z* 176.17 [M+H]<sup>+</sup>.

**Synthesis of [(Tp<sup>Ph,Me</sup>)Zn(8-TQ)].** [(Tp<sup>Ph,Me</sup>)ZnOH] was synthesized as previously reported.<sup>21</sup> [(Tp<sup>Ph,Me</sup>)ZnOH] (0.1 g, 0.177 mmol) was dissolved in CH<sub>2</sub>Cl<sub>2</sub> (15 mL) to yield a colorless solution. To this was added a solution of MeOH (10 mL) containing 8-mercaptoquinoline-HCl (0.035 g, 0.177 mmol) and Et<sub>3</sub>N (25 μL, 0.177 mmol). The colorless solution obtained a bright yellow color. The reaction mixture was stirred for 20 h at room temperature under a nitrogen atmosphere. The reaction mixture was then concentrated in vacuo and yielded a bright yellow solid. The solid was dissolved in minimal amount of benzene (~5 mL). Blocks were grown out of a solution of the complex in Benzene diffused with Pentane.

**Rpn11 Activity Assay.** To measure Rpn11 activity, a synthetic peptide substrate, termed Ub4-pepOG, was engineered. This substrate consists of four linear ubiquitins connected to a short peptide sequence containing a unique cysteine to which is conjugated a single Oregon Green 488 fluorophore molecule. The peptide bond between the fourth ubiquitin and the downstream peptide is cleaved by 26S proteasome in vitro, which can be observed by SDS-PAGE and fluorescent polarization measurement. The fluorescent peptide released upon cleavage of Ub4-pepOG consists of only 30 amino acids; therefore the decrease of polarization observed in fluorescence polarization assays arose mainly from deubiquitination of the peptide and could be observed even when the proteolytic activity of the 20S CP was inhibited. The fluorescence polarization assay was performed as previously described<sup>13</sup> at 30 °C in a low-volume 384 well solid black plate. Briefly, components were added to each well in the following sequence: 1) 5 µL inhibitor compound in buffer containing 3% DMSO or 3% DMSO in buffer as a control; and 2) 5 µL of 26S proteasome (Enzo life sciences) in buffer (20 nM proteasome was pre-incubated with epoxomicin at room temperature for 1 hour, then dilute 10-fold in 1x Assay Buffer). Substrate (5 µL, 3 nM Ub4-pepOG) in buffer was then added to initiate the reaction. To evaluate the effects of Zn(cyclen)<sup>2+</sup> on Rpn11 activity, the assay was carried out in the same manner as described with the addition of 100 µM Zn(cyclen)<sup>2+</sup> in the titration reaction. Fluorescence polarization was measured using a plate reader with excitation at

480 nm and emission at 520 nm. To calculate the  $IC_{50}$  of Rpn11 inhibitors, eight to twelve-point titration was performed for each compound, up to a concentration of 100  $\mu$ M. Rpn11 activity was normalized to the DMSO control and fitted using a dose-response curve. Reported  $IC_{50}$  value represents the average value obtained from at least three independent measurements, with the standard deviation reported as the error.

**CSN5 Activity Assay.** A fluorescent substrate termed SCF<sup>skp2</sup>-Nedd8OG was engineered to measure Csn5 activity in vitro.<sup>14</sup> To produce this substrate, Nedd8 containing a unique N-terminal cysteine was labeled with Oregon Green 488, and then conjugated to SCF<sup>skp2</sup> as previously described.<sup>28</sup> This assay measures the decrease in fluorescence polarization due to the decrease in apparent molecular weight of the Oregon Green fluorophore (from the ~175 kDa substrate to ~9kDa Nedd8OG) as a result of Csn5-dependent cleavage of the isopeptide bond which links Nedd8OG to SCF<sup>skp2</sup>. Assays were performed in a low-volume 384 well solid black plate comprising equal volumes of compound, substrate (SCF<sup>skp2</sup>-Nedd8OG) and enzyme (Csn5). Fluorescence polarization was recorded using the same protocol as for the Rpn11 activity assay at 30 °C.  $IC_{50}$  was calculated as described above. Reported  $IC_{50}$  value represents the average value obtained from at least three independent measurements, with the standard deviation reported as the error.

**HDAC1 and 6 Activity Assay.** HDAC1 and 6 were purchased from BPS Bioscience (BPS Bioscience catalog #50051 and 50006) and the assay was carried out as instructed by manufacturer. The enzyme was diluted with 25 mM Tris-Cl, 137 mM NaCl, 2.7 mM KCl, 1 mM MgCl<sub>2</sub>, 0.1 mg/mL BSA, pH 8.0 buffer and its activity was measured by utilizing Substrate 3 (BPS Bioscience catalog #50037). The assays were carried out in black, low binding NUNC 96-well plates. Each well contained a volume of 50  $\mu$ L including buffer, HDAC (3.8 ng/well of HDAC-1, 50 ng/well of HDAC-6), inhibitor, and substrate (20  $\mu$ M). Prior to adding substrate, the plate was preincubated for 5 min. Upon addition of substrate, the plate was incubated at 37 °C for 30 min. At this point, HDAC assay developer (50  $\mu$ L, BPS Bioscience catalog #50030) was added to each well and the plate was incubated for 15 min at room temperature. The fluorescence was recorded with a BioTek FLx 800 microplate reader. The measured fluorescence was compared for samples versus controls containing no inhibitor (0% inhibition). Reported IC<sub>50</sub> value represents the average value obtained from at least three independent measurements, with the standard deviation reported as the error.

**MMP Activity Assay.** MMP-2 and OmniMMP fluorogenic substrate (P-126) were purchased from Enzo Life Sciences (Farmingdale, NY). The assay was carried out in white NUNC 96-well plates as previously described.<sup>29</sup> Each well

contained a volume of 90  $\mu\text{L}$  including buffer (50 mM HEPES, 10 mM  $\text{CaCl}_2$ , 0.05% Brij-35, pH 7.5), human recombinant MMP (1.16 U of MMP-2), and the fragment solution. The enzyme and inhibitor were incubated for 30 min at 37  $^\circ\text{C}$ , the reaction was then initiated by the addition of 10  $\mu\text{L}$  (100  $\mu\text{L}$  total volume of wells) of the fluorogenic OmniMMP substrate (4  $\mu\text{M}$  final concentration, Mca-Pro-Leu-Gly-Leu-Dpa-Ala-Arg- $\text{NH}_2$ -AcOH). Fluorescence measurements were recorded using a Bio-Tek FLx800 fluorescence plate reader every minute for 20 min with excitation and emission wavelengths at 320 and 400 nm, respectively. The rate of fluorescence increase was compared for samples versus negative controls (no inhibitor, arbitrarily set as 100% activity). Reported  $\text{IC}_{50}$  value represents the average value obtained from at least three independent measurements, with the standard deviation reported as the error.

**5-Lipoxygenase Activity Assay.** The assay was performed according to a literature procedure at room temperature.<sup>30</sup> Each well contained a volume of 80  $\mu\text{L}$  including buffer (50 mM Tris, 2 mM EDTA, 2 mM  $\text{CaCl}_2$ , pH 7.5), human recombinant 5-LO (0.2 U, Cayman Chemicals), reporter dye (20  $\mu\text{M}$  - dichlorofluorescein diacetate;  $\text{H}_2\text{DCFDA}$ , 10  $\mu\text{M}$ , In- vitrogen), fragment solution, arachidonic acid (AA, 3  $\mu\text{M}$ , Fischer Scientific), and adenosine triphosphate (ATP, 10  $\mu\text{M}$ , Sigma-Aldrich).  $\text{H}_2\text{DCFDA}$  and 5-LO were incubated for 5 min prior to the addition of the fragment solution. This was followed by a second incubation

for 10 min. The reaction was initiated by the addition of a substrate solution containing AA and ATP. The reaction was monitored using a Bio-Tek FLx800 fluorescence plate reader. Fluorescence measurements were recorded every minute for 20 min with excitation and emission wavelengths at 485 and 528 nm, respectively. The rate of fluorescence increase was compared for samples versus negative controls (no inhibitor, arbitrarily set as 100% activity). Reported  $IC_{50}$  value represents the average value obtained from at least three independent measurements, with the standard deviation reported as the error.

**hCAII Activity Assay.** hCAII was expressed and purified as previously reported.<sup>31</sup> Assays were carried out in 50 mM HEPES (pH 8.0). A BioTek Precision XS microplate sample processor was utilized. The compounds were incubated with protein (final concentrations of 100 nM for hCAII) for 10 min at 25 °C. A substrate (p-nitrophenylacetate; final concentration of 500  $\mu$ M) was added, and hCAII-catalyzed cleavage was monitored by the increase in absorbance at 405 nm corresponding to formation of the p-nitrophenolate anion. The initial linear reaction rate was compared to that of wells containing no inhibitor (0% inhibition) and no protein (100% inhibition). The rate of non-hCAII-catalyzed PNPA hydrolysis in the presence of inhibitor was subtracted from each trial before determination of the percent inhibition. Reported  $IC_{50}$  value represents

the average value obtained from at least three independent measurements, with the standard deviation reported as the error.

**Cytotoxicity Assay.** HCT 116 cell lines were cultured in DMEM with 10% FBS in white, clear-bottom tissue culture-treated 96-well plates. Cells were treated with different concentrations of inhibitor compounds in triplicates for 72 h at 37 °C with 5% CO<sub>2</sub> in air. CellTiter-Glo (Promega, Madison, WI) reagent was added to the 96 well plates to measure cell viability. Luminescence values were measured in PHERAstar microplate reader (BMG labtech, Ortenberg, Germany). Collected data was normalized to DMSO control and fit to a dose-response equation to determine IC<sub>50</sub> values. Reported IC<sub>50</sub> value represents the average value obtained from at least three independent measurements, with the standard deviation reported as the error.

## 2.5 Acknowledgements

Texts, schemes, and figures in the chapter are reprints of the materials published in the following paper: Christian Perez, Jing Li, Francesco Parlati, Matthieu Rouffet, Yuyong Ma, Andrew L. Mackinnon, Tsui-Fen Chou, Raymond J. Deshaies and Seth M. Cohen, "Discovery of an Inhibitor of the Proteasome Subunit Rpn11" *J. Med. Chem.* **2017**, *60*, 1343-1361. The dissertation author was the primary researcher and author. The permission to reproduce this paper was granted by the American Chemical Society. Copyright 2017, American Chemical Society.

## 2.6 References

1. Kyle, R. A.; Rajkumar, S. V., Treatment of Multiple Myeloma: A Comprehensive Review. *Clin. Lymphoma Myeloma* **2009**, *9* (4), 278-288.
2. Chai, S. C.; Ye, Q. Z., Metal-mediated inhibition is a viable approach for inhibiting cellular methionine aminopeptidase. *Bioorg. Med. Chem. Lett.* **2009**, *19* (24), 6862-4.
3. Kisselev, A. F.; van der Linden, W. A.; Overkleeft, H. S., Proteasome Inhibitors: An Expanding Army Attacking a Unique Target. *Chem. Biol.* **2012**, *19* (1), 99-115.
4. Moreau, P.; Richardson, P. G.; Cavo, M.; Orłowski, R. Z.; San Miguel, J. F.; Palumbo, A.; Harousseau, J. L., Proteasome Inhibitors in Multiple Myeloma: 10 Years Later. *Blood* **2012**, *120* (5), 947-959.
5. van der Linden, W. A.; Willems, L. I.; Shabaneh, T. B.; Li, N.; Ruben, M.; Florea, B. I.; van der Marel, G. A.; Kaiser, M.; Kisselev, A. F.; Overkleeft, H. S., Discovery of a Potent and Highly Beta 1 Specific Proteasome Inhibitor from a Focused Library of Urea-Containing Peptide Vinyl Sulfones and Peptide Epoxyketones. *Org. Biomol. Chem.* **2012**, *10* (1), 181-194.
6. Desvergne, A.; Genin, E.; Marechal, X.; Gallastegui, N.; Dufau, L.; Richy, N.; Groll, M.; Vidal, J.; Reboud-Ravaux, M., Dimerized Linear Mimics of a Natural Cyclopeptide (TMC-95A) Are Potent Noncovalent Inhibitors of the Eukaryotic 20S Proteasome. *J. Med. Chem.* **2013**, *56* (8), 3367-3378.
7. Geurink, P. P.; van der Linden, W. A.; Mirabella, A. C.; Gallastegui, N.; de Bruin, G.; Blom, A. E. M.; Voges, M. J.; Mock, E. D.; Florea, B. I.; van der Marel, G. A.; Driessen, C.; van der Stelt, M.; Groll, M.; Overkleeft, H. S.; Kisselev, A. F., Incorporation of Non-natural Amino Acids Improves Cell Permeability and Potency of Specific Inhibitors of Proteasome Trypsin-like Sites. *J. Med. Chem.* **2013**, *56* (3), 1262-1275.
8. Kawamura, S.; Unno, Y.; List, A.; Mizuno, A.; Tanaka, M.; Sasaki, T.; Arisawa, M.; Asai, A.; Groll, M.; Shuto, S., Potent Proteasome Inhibitors Derived from the Unnatural cis-Cyclopropane Isomer of Belactosin A: Synthesis, Biological Activity, and Mode of Action. *J. Med. Chem.* **2013**, *56* (9), 3689-3700.

9. Ozcan, S.; Kazi, A.; Marsilio, F.; Fang, B.; Guida, W. C.; Koomen, J.; Lawrence, H. R.; Sebti, S. M., Oxadiazole-isopropylamides as Potent and Noncovalent Proteasome Inhibitors. *J. Med. Chem.* **2013**, *56* (10), 3783-3805.
10. Cenci, S.; Oliva, L.; Cerruti, F.; Milan, E.; Bianchi, G.; Raule, M.; Mezghrani, A.; Pasqualetto, E.; Sitia, R.; Cascio, P., Pivotal Advance: Protein Synthesis Modulates Responsiveness of Differentiating and Malignant Plasma Cells to Proteasome Inhibitors. *J. Leukocyte Biol.* **2012**, *92* (5), 921-931.
11. Deshaies, R. J., Proteotoxic Crisis, the Ubiquitin-Proteasome System, and Cancer Therapy. *BMC Biol.* **2014**, *12*, 1-14.
12. Jacobsen, J. A.; Fullagar, J. L.; Miller, M. T.; Cohen, S. M., Identifying Chelators for Metalloprotein Inhibitors Using a Fragment-Based Approach. *J. Med. Chem.* **2011**, *54* (2), 591-602.
13. National Center for Biotechnology Information. PubChem BioAssay Database; AID=588493, <https://pubchem.ncbi.nlm.nih.gov/bioassay/588493>. (accessed February 23, 2018).
14. National Center for Biotechnology Information. PubChem BioAssay Database; AID=651999, <https://pubchem.ncbi.nlm.nih.gov/bioassay/651999>. (accessed February 23, 2018).
15. Li, J.; Yakushi, T.; Parlati, F.; Mackinnon, A. L.; Perez, C.; Ma, Y. Y.; Carter, K. P.; Colayco, S.; Magnuson, G.; Brown, B.; Nguyen, K.; Vasile, S.; Suyama, E.; Smith, L. H.; Sergienko, E.; Pinkerton, A. B.; Chung, T. D. Y.; Palmer, A. E.; Pass, I.; Hess, S.; Cohen, S. M.; Deshaies, R. J., Capzimin is a potent and specific inhibitor of proteasome isopeptidase Rpn11. *Nat. Chem. Biol.* **2017**, *13* (5), 486-+.
16. Dantuma, N. P.; Lindsten, K.; Glas, R.; Jellne, M.; Masucci, M. G., Short-lived green fluorescent proteins for quantifying ubiquitin/proteasome-dependent proteolysis in living cells. *Nat. Biotechnol.* **2000**, *18* (5), 538-543.
17. Hopkins, A. L.; Groom, C. R.; Alex, A., Ligand Efficiency: A Useful Metric for Lead Selection. *Drug Discov. Today* **2004**, *9* (10), 430-431.

18. Borgneczak, K.; Tjalve, H., Effect of 8-Hydroxy-Quinoline, 8-Mercapto-Quinoline and 5-Chloro-7-Iodo-8-Hydroxy-Quinoline on the Uptake and Distribution of Nickel in Mice. *Pharmacol. Toxicol.* **1994**, *74* (3), 185-192.
19. Prachayasittikul, V.; Prachayasittikul, S.; Ruchirawat, S.; Prachayasittikul, V., 8-Hydroxyquinolines: A Review of Their Metal Chelating Properties and Medicinal Applications. *Drug Des. Dev. Ther.* **2013**, *7*, 1157-1178.
20. Su, C. Y.; Liao, S.; Wanner, M.; Fiedler, J.; Zhang, C.; Kang, B. S.; Kaim, W., The Copper(I)/Copper(II) Transition in Complexes With 8-Alkylthioquinoline Based Multidentate Ligands. *Dalton Trans.* **2003**, (2), 189-202.
21. Puerta, D. T.; Cohen, S. M., Elucidating Drug-Metalloprotein Interactions with Tris(pyrazolyl)borate Model Complexes. *Inorg. Chem.* **2002**, *41* (20), 5075-5082.
22. Bridgewater, B. M.; Parkin, G., Lead Poisoning and the inactivation of 5-Aminolevulinatase Dehydratase as Modeled by the Tris(2-mercapto-1-phenylimidazolyl)hydroborato Lead Complex, {[Tm-Ph]Pb}[ClO<sub>4</sub>]. *J. Am. Chem. Soc.* **2000**, *122* (29), 7140-7141.
23. Hammes, B. S.; Carrano, C. J., Methylation of (2-Methylethanol-thiol-bis-3,5-dimethylpyrazolyl)methane Zinc Complexes and Coordination of the Resulting Thioether: Relevance to Zinc-Containing Alkyl Transfer Enzymes. *Inorg. Chem.* **2001**, *40* (5), 919-927.
24. Trofimenko, S., Recent Advances in Poly(Pyrazolyl)Borate (Scorpionate) Chemistry. *Chem. Rev.* **1993**, *93* (3), 943-980.
25. Tesmer, M.; Shu, M. H.; Vahrenkamp, H., Sulfur-Rich Zinc Chemistry: New Tris(thioimidazolyl)hydroborate Ligands and Their Zinc Complex Chemistry Related to the Structure and Function of Alcohol Dehydrogenase. *Inorg. Chem.* **2001**, *40* (16), 4022-4029.
26. Vahrenkamp, H., Transitions, Transition States, Transition State Analogues: Zinc Pyrazolylborate Chemistry Related to Zinc Enzymes. *Acc. Chem. Res.* **1999**, *32* (7), 589-596.

27. Lewis, J. A.; Puerta, D. T.; Cohen, S. M., Metal complexes of the trans-influencing ligand thiomaltol. *Inorg. Chem.* **2003**, *42* (23), 7455-7459.
28. Duda, D. M.; Borg, L. A.; Scott, D. C.; Hunt, H. W.; Hammel, M.; Schulman, B. A., Structural Insights Into NEDD8 Activation of Cullin-RING Ligases: Conformational Control of Conjugation. *Cell* **2008**, *134* (6), 995-1006.
29. Puerta, D. T.; Griffin, M. O.; Lewis, J. A.; Romero-Perez, D.; Garcia, R.; Villarreal, F. J.; Cohen, S. M., Heterocyclic Zinc-Binding Groups for Use in Next-Generation Matrix Metalloproteinase Inhibitors: Potency, Toxicity, and Reactivity. *J. Biol. Inorg. Chem.* **2006**, *11* (2), 131-138.
30. Pufahl, R. A.; Kasten, T. P.; Hills, R.; Gierse, J. K.; Reitz, B. A.; Weinberg, R. A.; Masferrer, J. L., Development of a Fluorescence-Based Enzyme Assay of Human 5-Lipoxygenase. *Anal. Biochem.* **2007**, *364* (2), 204-212.
31. Martin, D. P.; Hann, Z. S.; Cohen, S. M., Metalloprotein-Inhibitor Binding: Human Carbonic Anhydrase II as a Model for Probing Metal-Ligand Interactions in a Metalloprotein Active Site. *Inorg. Chem.* **2013**, *52* (21), 12207-12215.

**Chapter 3: Capzimin is a potent and specific inhibitor of proteasome isopeptidase Rpn11**

### 3.1 Introduction

Over the past 20 years, several proteasome inhibitors have been reported with the vast majority of inhibitors binding to the 20S CP,<sup>1-11</sup> and fewer reports of inhibitors binding to the 19S RP.<sup>12-17</sup> Currently, there are three FDA approved proteasome inhibitors, all which bind preferentially to the  $\beta$ 5 subunit of the 20S CP (Figure 1-2 and 1-3). The development of novel compounds that bind to the 19S RP may yield superior inhibitors since they in essence, alter proteasome activity via a different mechanism. As discussed in Chapter 1 and 2, Rpn11 is a subunit found in the 19S RP of the proteasome and represents a unique target for proteasome inhibition.<sup>18-22</sup> Inhibition of Rpn11 prevents hydrolysis of the polyubiquitin chain from the protein to be degraded, which completely blocks processing and cleavage of the tagged protein by all of the 20S CP catalytic subunits ( $\beta$ 1,  $\beta$ 2, and  $\beta$ 5, Figure 2-1). Therefore, Rpn11 inhibition may be an effective mechanism for proteasome inhibition.

In Chapter 2, two independent drug discovery approaches were described that identified **8-TQ** as a potent fragment that demonstrated inhibition of Rpn11 and other JAMM metalloenzymes. Rudimentary SAR around this fragment demonstrated that **8-TQ** analogs could be synthesized to gain affinity for Rpn11. In this chapter, we report the design and synthesis of a novel class of compounds based off the **8-TQ** fragment and the development of Capzimin (**CZM**), the first potent and selective Rpn11 inhibitor to be reported. The work described in this chapter demonstrates SAR of the **8-TQ** scaffold yielded several

compounds with IC<sub>50</sub> values of <300 nM, with two compounds were found to be cytotoxic in cancer cells, one of them being **CZM**. **CZM** was shown to be selective for Rpn11 over other JAMM domain containing enzymes as well as selective over other metalloenzymes.

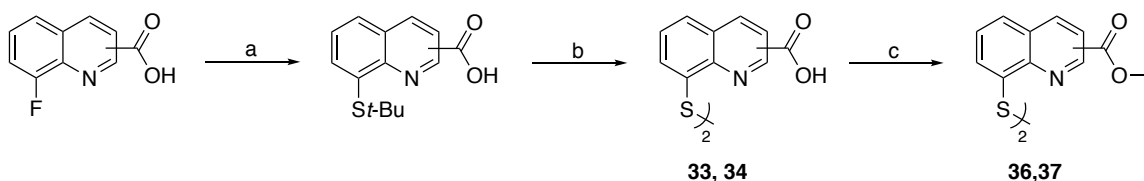
## 3.2 Results and Discussion

### 3.2.1 Synthesis of an 8-TQ Sublibrary

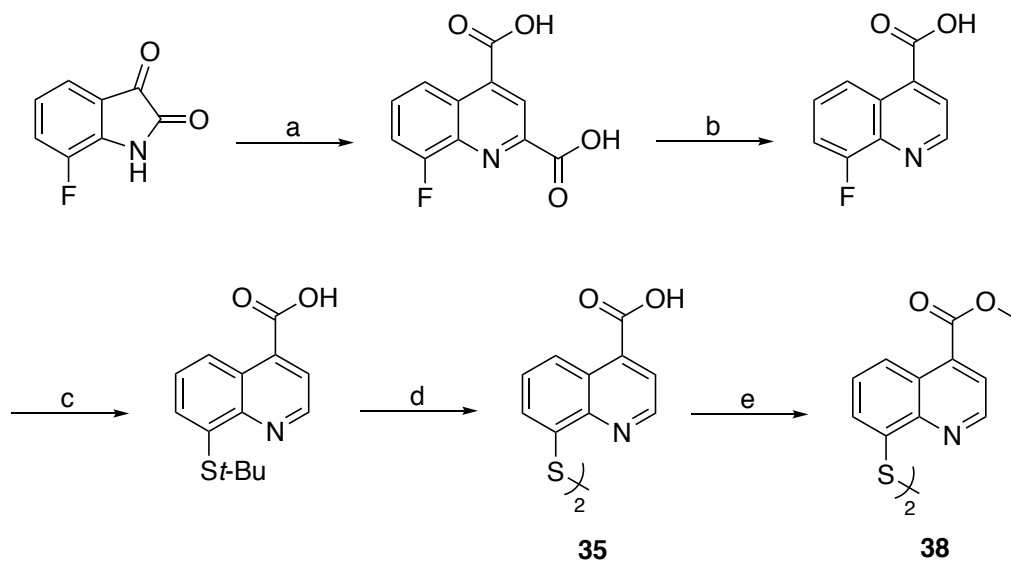
Given the high affinity of **8-TQ** toward JAMM domain proteins, derivatives were sought that could improve potency while also adding selectivity for Rpn11. Based on the results described in Chapter 2 (Table 2-4), compounds containing functional groups at the 3- and 4-positions (Figure 2-5) were primarily pursued due to their activity against Rpn11 and synthetic accessibility of these derivatives over other active compounds. In addition, derivatives of the 2-position were prepared to confirm the SAR obtained with the methyl derivatives (Table 2-4). The initial strategy involved probing for hydrophobic and hydrophilic contacts near the active site, while also examining steric limitations. The quinoline ring was initially appended with methyl groups on the 2-, 3-, 4-, 5-, and 6-positions of the ring (Scheme 2-7 and 2-8) or carboxylic acids on the 2-, 3-, and 4-positions of the ring (Figure 2-5 and Scheme 3-1).

Compounds **33** and **34** were synthesized starting from commercially available 2- or 3- carboxyl-8-fluoroquinoline as detailed in Scheme 3-1. Compound **35** was obtained via a Pfitzinger ring expansion reaction of 7-

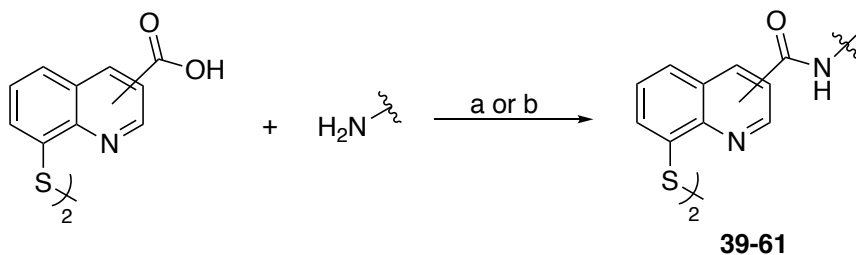
fluoroisatin and pyruvate under basic conditions to yield the dicarboxylate intermediate (Scheme 3-2). This was decarboxylated under aqueous conditions, which then yielded **35** over two steps (Scheme 3-2). The corresponding methyl ester derivatives (**36**, **37**, and **38**) were obtained via Fisher esterification (Scheme 3-1 and 3-2). Lastly, the 2-, 3-, and 4-carboxylate-8-thioquinoline compounds were coupled to amines mainly via the assistance of carbodiimidazole (CDI) or 1-[bis(dimethylamino)methylene]-1*H*-1,2,3-triazolo[4,5-*b*]pyridinium3-oxidhexafluorophosphate (HATU) coupling reagents (Scheme 3-3). Alkyl amines were coupled mainly through the use of CDI at room temperature; however, less nucleophilic amines (aromatic) were coupled using HATU with heating.



**Scheme 3-1.** Synthesis of 2- and 3-carboxyl-8-thioquinoline derivatives. Reagents and conditions: (a) *t*-BuSH, NaH, DMF, 140 °C; (b) 12M HCl, 110 °C; (c) H<sub>2</sub>SO<sub>4</sub>, MeOH, reflux.



**Scheme 3-2.** Synthesis of 4-carboxyl-8-thioquinoline. Reagents and conditions: (a) Sodium Pyruvate, 5M NaOH, 110 °C; (b) H<sub>2</sub>O, 170 °C; (c) *t*-BuSH, NaH, DMF, 140 °C; (d) 12M HCl, 110 °C; (e) H<sub>2</sub>SO<sub>4</sub>, MeOH, reflux.

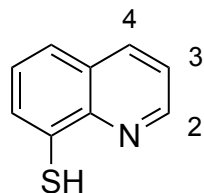


**Scheme 3-3.** Synthesis of 3-carboxamide derivatives. Reagents and conditions: (a) CDI, DMF, 25 °C; (b) HATU, Et<sub>3</sub>N, DMF, 60 °C.

It should be noted that all of the aforementioned compounds were isolated as disulfide dimers, as evidenced by mass spectrometry. Under the Rpn11 assay conditions, which contained 1 mM of dithiothreitol (DTT) as a reductant, the disulfides were reduced to the monomeric active species. Screening of the aforementioned 2-position derivatives, **33**, **36**, **63**, and **65**, (Scheme 3-1, 3-3 and Table 3-1) demonstrated that functionalization at the 2-position was not well

tolerated. All the compounds functionalized at the 2-position were consistently less active than **8-TQ** (Table 3-1). In addition, activity generally decreased with increasing functional group size at the 2-position, possibly due to a clash with the protein active site. Derivatives with 3- and 4-substituents, including methyl, carboxylate and methyl ester substituents were all well tolerated, providing a consistent SAR.

**Table 3-1.** Rpn11 inhibitory activity of **8-TQ** derivatives functionalized at the 2-, 3-, and 4-positions of the ring system. All IC<sub>50</sub> values listed are in  $\mu\text{M}$ .



Structure	Compound	Position	Inhibition
	<b>33</b>	2	>20
	<b>34</b>	3	1.1±0.1
	<b>35</b>	4	1.3±0.2
	<b>36</b>	2	>50
	<b>37</b>	3	0.9±0.1
	<b>38</b>	4	1.0±0.1
	---	2	---
	<b>45</b>	3	0.9±0.1
	<b>62</b>	4	2.2±0.6
	<b>63</b>	2	>100
	<b>46</b>	3	0.8±0.3
	<b>64</b>	4	1.0±0.2
	<b>65</b>	2	>100
	<b>54</b>	3	1.1±0.2
	---	4	---

The activity of carboxylate derivatives with aromatic substituents was also consistent with the observed SAR, with substituents at the 3- and 4- being well tolerated. Among these, comparing the same substituents at the 3- and 4-positions (**34-34**, **37-38**, **45-62**, and **46-64**) suggested that 3-position derivatives might possess marginally better activity (Table 3-1), and hence derivatives of the 3-position became the focus of this study.

Derivatization at the 3-position was consistently well tolerated. In order to confine the scope of these initial synthetic efforts, additional exploration of

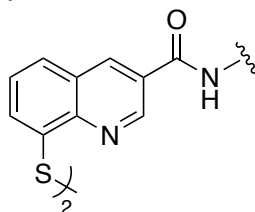
derivatives was restricted to the 3-position. To accomplish this, compound **34** was coupled to a series of amines with the assistance of CDI or HATU coupling reagents (Scheme 3-3). All of the compounds prepared via Scheme 3-3 were also isolated as disulfide dimers. A diverse set of amines, predominantly derivatives with substituted aryl groups or heterocycles with varying linker lengths (Table 3-2), was explored.

In order to identify a potent yet selective Rpn11 inhibitor, all compounds were screened in cell-free assays against Rpn11, Csn5, and AMSH. The activity of Rpn11 was measured via a fluorescence polarization assay as described in Chapter 2. Active JAMM domains are found in six other human proteins: the Csn5 subunit of the COP9-signalosome, the Brcc36 subunit of the BRCC and BRISC complexes, the closely-related AMSH and AMSH-LP proteins, MYSM1, and MPND. Of these, suitable biochemical assays are available for all but MYSM1 and MPND. AMSH is highly homologous to AMSH-LP, so we excluded this target from further consideration and focused our attention on Csn5 and AMSH as the major off-target concerns.<sup>41</sup>

To measure Csn5 activity, a fluorescent substrate termed SCF<sup>Skp2</sup>-Nedd8OG was engineered. To produce this substrate, Nedd8 containing a unique N-terminal cysteine was labeled with Oregon Green 488, and then conjugated to SCF<sup>Skp2</sup> as previously described.<sup>26</sup> For AMSH the substrate termed DiUB<sup>K63</sup>TAMRA was purchased from commercial sources. DiUB<sup>K63</sup>TAMRA is labeled with a FRET pair (TAMRA/QXL) that upon cleavage by

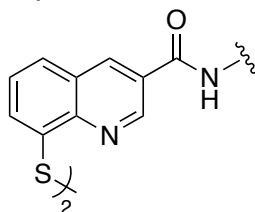
AMSH produces a fluorescent signal. The SAR obtained was used to increase activity against Rpn11 while discriminating against the other JAMM domain proteins Csn5 and AMSH. In addition, a cell-based assay was utilized to measure inhibition of the proteasome in cells. For this, a HeLa cell line that stably expresses Ub<sup>G76V</sup>-GFP (Green Fluorescent Protein) was used, which serves as a fluorescent signal for proteasome activity.<sup>27</sup> These cells were treated with  $\beta$ 5 inhibitor MG132 to accumulate Ub<sup>G76V</sup>-GFP. The MG132 was then washed out and either DMSO or one of our compounds was added, and the decay of GFP fluorescence was monitored. Under normal conditions, the accumulated Ub<sup>G76V</sup>-GFP is rapidly degraded by proteasome. However, if the proteasome function is blocked, the degradation rate of the reporter protein is reduced. The IC<sub>50</sub> values reported in Table 3-2 represent the concentration of test agent at which the degradation rate was reduced by half.

**Table 3-2.** Inhibitory activity against Rpn11, Csn5, and AMSH for 3-position substituted **8-TQ** derivatives. Cellular levels of proteasome inhibition are also listed. All IC<sub>50</sub> values listed are in μM.



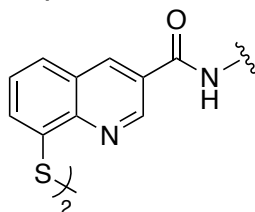
Cmpd	Structure	Rpn11	Csn5	AMSH	Ub <sup>G76V</sup> GFP Hela Cell
39	H	1.02±0.19	15.3±4.2	1.65±0.39	1.2±0.2
40	Me	1.64±0.32	67.9±14.1	4.1±1.3	2.64±0.51
41		>2	>100	2.2±0.3	>0.3
42		2.62±0.42	14.8±1.1	5.0±1.0	>10
43		0.45±0.12	19.8±2.7	4.7±1.1	1.2±0.3
44		4.64±1.35	40.7±4.9	6.76±0.48	1.0±0.2
45		0.89±0.08	<0.5	0.91±0.06	1.0±0.2
46		0.8±0.1	16±6	1.3±0.3	5±1
47		0.49±0.08	23.7±6.8	7.8±2.2	2.9±0.8

**Table 3-2.** Inhibitory activity against Rpn11, Csn5, and AMSH for 3-position substituted **8-TQ** derivatives. Cellular levels of proteasome inhibition are also listed. All IC<sub>50</sub> values listed are in  $\mu\text{M}$ , continued.



Cmpd	Structure	Rpn11	Csn5	AMSH	Ub <sup>G76V</sup> GFP Hela Cell
48		1.2±0.7	6.9±1.8	1.68±0.33	1.4±0.3
49		0.33±0.13	4.0±2.9	1.31±0.15	5.0±0.4
50 (CZM)		0.39±0.04	30.2±2.8	4.46±0.54	0.57±0.09
51		3.99±0.22	>50	16.7±2.7	>10
52		3.16±0.23	>100	3.52±0.48	>10
53		0.2±0.1	7±2	0.5±0.1	>10
54		1.1±0.1	11±4	>10	>10
55		<0.2	17.8±5.9	0.85±0.08	>10
56		0.77±0.15	>100	3.46±0.68	>10

**Table 3-2.** Inhibitory activity against Rpn11, Csn5, and AMSH for 3-position substituted **8-TQ** derivatives. Cellular levels of proteasome inhibition are also listed. All IC<sub>50</sub> values listed are in  $\mu\text{M}$ , continued.



Cmpd	Structure	Rpn11	Csn5	AMSH	Ub <sup>G76V</sup> GFP Hela Cell
57		<0.2	0.5±0.1	0.58±0.18	>10
58		0.9±0.2	7±1	<0.2	>10
59		0.82±0.26	0.34±0.2	0.89±0.25	>10
60		6.4±1.2	>100	25.4±9.3	>10
61		>5	>30	3.5±0.6	>10

Compounds with substituents at the 3-position (**34**, **37**), including carboxamide substituents, **45**, **46**, and **54**, demonstrated a small increase in activity over **8-TQ**. With this preliminary SAR, a variety of substituents were explored via an amide linkage as illustrated in Table 3-2. The introduction of 5- or 6-membered heterocyclic, aromatic rings, such as thiophene, thiazole, furan, oxazole, and pyridine (**42-53**) improved activity. In addition, compounds **42-53** all demonstrated better solubility in aqueous solution (data not shown). A trend was observed wherein the heterocycles containing a thiophene ring (**46** and **49**) demonstrated better activity than furan-based analogs (**45** and **48**). Introduction of thiazole heterocycles demonstrated similar inhibition to thiophene containing compounds; however, thiazole-containing compounds (**43**, **47**, and **50**) all demonstrated improved selectivity for Rpn11 over Csn5 and AMSH. The introduction of a phenyl (**54**) or functionalized phenyl (**55-59**) aromatic groups also improved the activity of the compounds; however, solubility in aqueous solution was poor (data not shown). Compounds **55** and **57** showed the best activity against Rpn11 ( $IC_{50}$  value <200 nM, Table 3-2); however, the phenyl substituted compounds demonstrated poor selectivity over AMSH and also failed to show any cell-based activity. A pair of saturated ring derivatives was also explored (**44** and **60**), but these compounds consistently demonstrated poor activity. From this series of aryl substituted compounds (**39-61**), compound **50** showed the best overall characteristics and performance. Compound **50** showed an  $IC_{50}$  value of 0.39  $\mu$ M in the Rpn11 biochemical assay and ~100-fold selectivity over Csn5 and

~10-fold selectivity over AMSH. Compound **50** also demonstrated cytotoxicity towards 293T and A549 cells with an IC<sub>50</sub> of 2.1 and 3.8 μM, respectively (Figure 3-1).

Evaluation of the series of compounds in Table 3-2 identified **43** and **50** as two promising leads. Both compounds showed sub-micromolar IC<sub>50</sub> values against Rpn11 in the biochemical assay and selectivity over Csn5 and AMSH. These compounds were then screened for cytotoxicity against 293T and A549 cells (Figure 3-1). Compound **43** had an IC<sub>50</sub> of 6.4 μM and 5.8 μM against 293T and A549 cells, respectively. Meanwhile compound **50** demonstrated slightly lower IC<sub>50</sub> values than **43** against both cell lines, at 2.1 μM and 3.8 μM, respectively. Ultimately, compound **50** was selected as the lead compound due to its better selectivity for Rpn11 over other JAMM proteins, efficacy in the cell-based assays, and more active cytotoxic profile. As described elsewhere, it was proposed naming **50** as 'capzimin' (**CZM**), in which the affix 'cap' stands for 19S cap and the stem 'zimin' specifies the compound class as zinc metalloisopeptidase inhibitor.<sup>23</sup> From here on, compound **50** will simply be referred to as **CZM**.

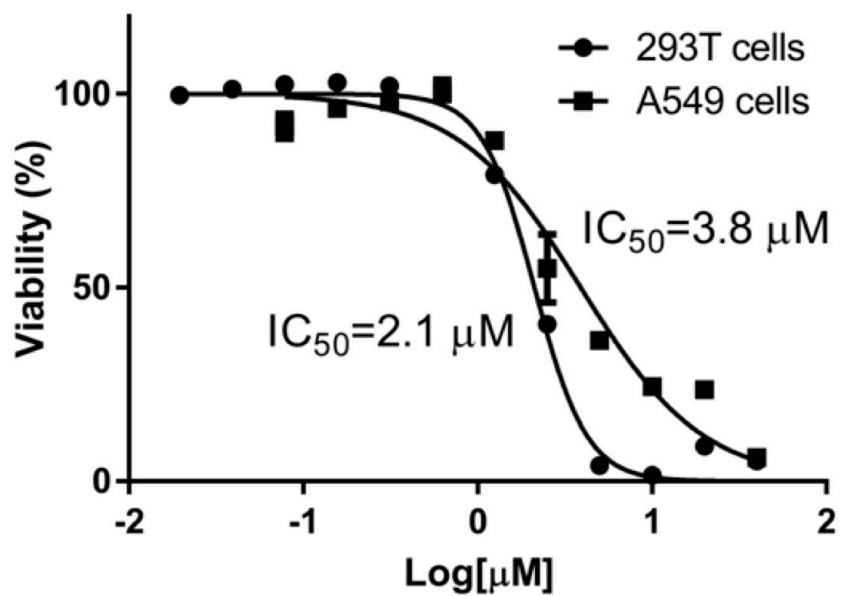
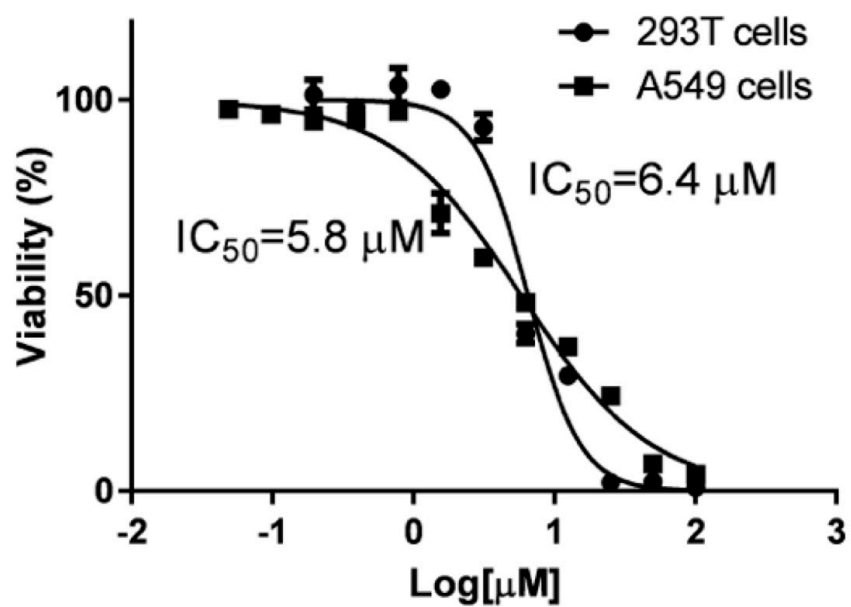


**Figure 3-1.** Cytotoxicity assay against 293T and A549 cancer cell lines with compound **43** (*top*) and **CZM** (*bottom*).

### 3.2.2 Synthesis and Evaluation of Control Compounds

A small series of control compounds (analogs of **CZM**) were synthesized (Schemes 3-4 to 3-7) to re-evaluate the role of the MBP in this lead compound. An 8-hydroxyquinoline analog (**66**) was prepared in order to determine the importance of the softer Lewis base thiol (versus the harder Lewis base oxygen donor in 8-hydroxyquinoline). Compounds **67** and **68** prevent metal coordination, as they are elaborated analogs of inactive MBP fragments. Similarly, compound **69** was prepared as an elaborated analog of the less active MBP fragment. Evaluation of these compounds yielded essentially no inhibition against Rpn11, Csn5, or AMSH (Table 3-3), recapitulating the SAR obtained with the original MBP fragments (Table 2-3).

As a final experiment to demonstrate the importance of metal coordination in this class of inhibitors, an inhibition assay was carried out utilizing compound **CZM** in the presence of a soluble, small molecule coordination compound  $\text{Zn}(\text{cyclen})^{2+}$  (cyclen = 1,4,7,10-tetraazacyclododecane). In this experiment, if metal coordination is critical for the activity of compound **CZM** then  $\text{Zn}(\text{cyclen})^{2+}$  can act as a 'decoy' of a Zn-metalloprotein active site, thereby titrating **CZM** away from Rpn11 and reducing the apparent activity of the inhibitor. When inhibition of **CZM** against Rpn11 was measured in the presence of  $\text{Zn}(\text{cyclen})^{2+}$  (100  $\mu\text{M}$ ), a significant loss in activity against Rpn11 was observed ( $\text{IC}_{50}$  = 77.4  $\mu\text{M}$  vs. 0.39  $\mu\text{M}$ , Figure 3-2). The observed  $\text{IC}_{50}$  value shift is attributed to the ability of  $\text{Zn}(\text{cyclen})^{2+}$  to compete/titrate **CZM** away from Rpn11.

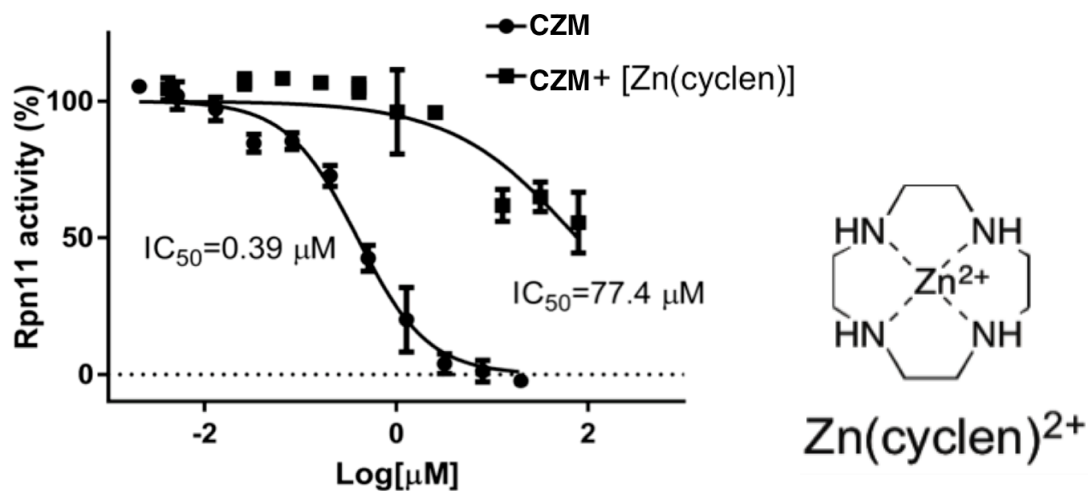
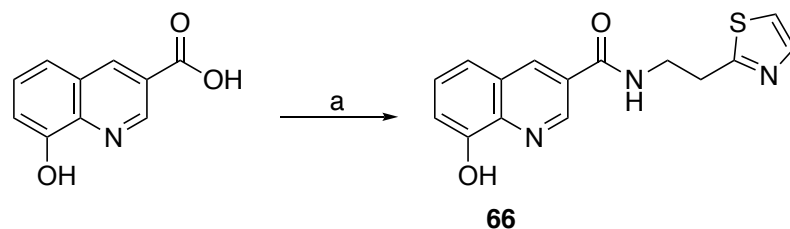
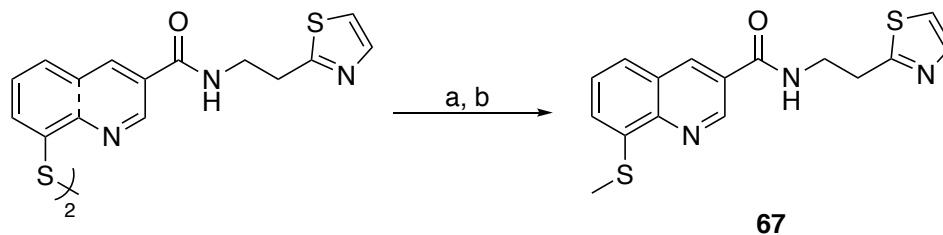


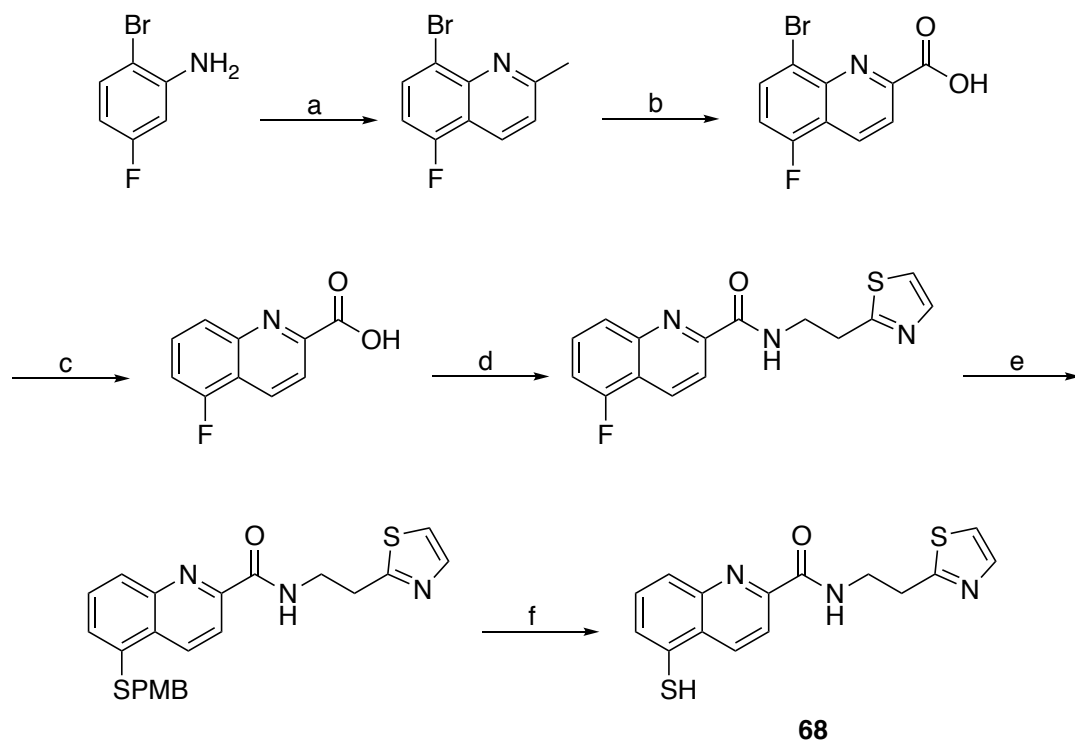
**Figure 3-2.** Inhibition of **CZM** against Rpn11 in the presence and absence of  $\text{Zn(cyclen)}^{2+}$ .



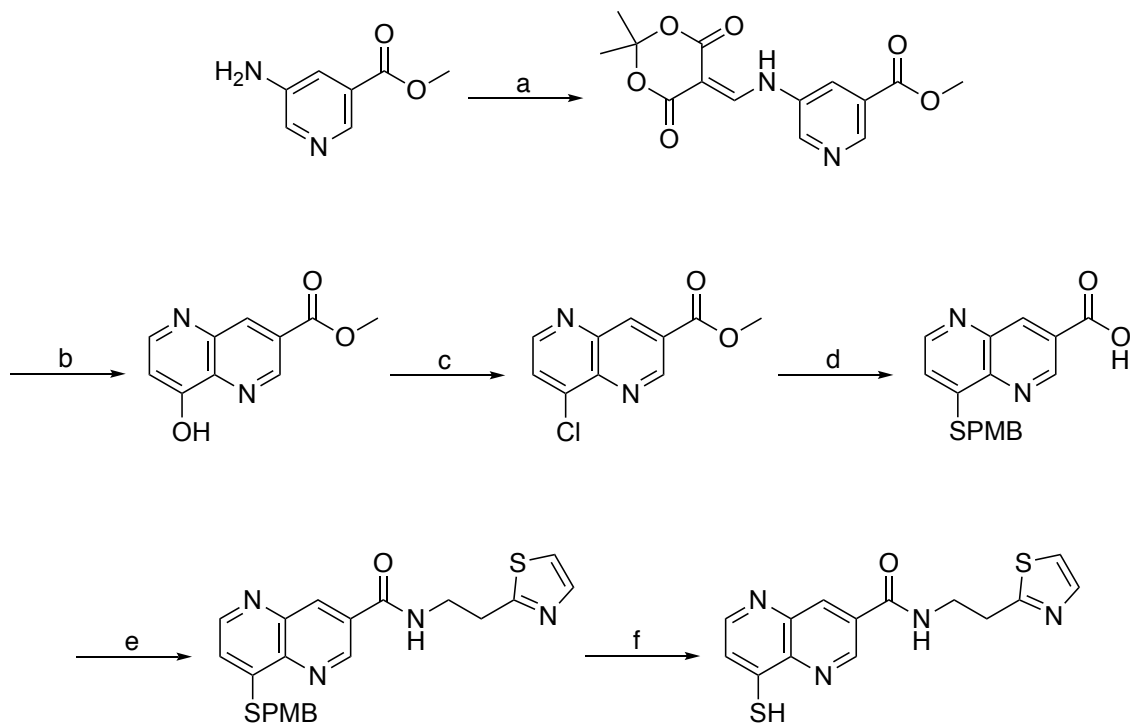
**Scheme 3-4.** Synthesis of an 8-hydroxyquinoline MBP based analog of lead compound **CZM**. Reagents and conditions: (a) 2-(Thiazol-2-yl)ethan-1-amine, HATU,  $\text{Et}_3\text{N}$ , DMF, 25 °C.



**Scheme 3-5.** Synthesis of a methylated analog of lead compound **CZM**. Reagents and conditions: (a)  $\text{NaBH}_4$ , MeOH, 25 °C; (b)  $\text{CH}_3\text{I}$ , THF, reflux.



**Scheme 3-6.** Synthesis of a structural-isomer analog of lead compound **CZM**. Reagents and conditions: (a) Crotonaldehyde, Toluene, 6M HCl, reflux; (b) SeO<sub>2</sub>, Pyridine, reflux; (c) Pd(OH)<sub>2</sub>/C, 1M NaOH, MeOH, H<sub>2</sub>, 25 °C; (d) 2-(Thiazol-2-yl)ethan-1-amine, HATU, Et<sub>3</sub>N, DMF, 25 °C; (e) *p*-MBSH, NaH, DMF, 140 °C; (f) *m*-Cresol, TFA, reflux.



69

**Scheme 3-7.** Synthesis of a MBP analog of lead compound **CZM**. Reagents and conditions: (a) Meldrum's acid, Triethylformate, 100 °C; (b) Dowtherm A, 250 °C; (c) POCl<sub>3</sub>, Toluene, 110 °C; (d) *p*-MBSH, NaH, DMF, 25 °C; (e) 2-(Thiazol-2-yl)ethan-1-amine, pyridine, EDC, HOBT, DMF, 25 °C; (f) *m*-Cresol, TFA, reflux.

**Table 3-3.** Inhibitory activity against Rpn11, Csn5, and AMSH for control compounds. Cellular levels of proteasome inhibition are also listed. All IC<sub>50</sub> values listed are in μM.

Cmpd	Rpn11	Csn5	AMSH	Ub <sup>G76V</sup> GFP Hela Cell
66	>40	>100	>100	>100
67	>40	>100	>100	>100
68	>100	35±9	>100	>100
69	82±14	>100	>100	>100

A series of **CZM** MBP analogs further validated the SAR and mode of inhibition. Compound **66** utilizes a harder Lewis base 8-hydroxyquinoline MBP that displays poor activity against Rpn11. This suggests that the soft Lewis base character of the 8-thioquinoline allows for better affinity for the active site  $Zn^{2+}$  ion. Evaluation of **67** and **68** revalidate the necessity of placing the coordinating atoms at the 1- and 8-positions. Finally, compound **69** uses the 1,5-naphthyridine-4(1*H*)-thione fragment instead of **8-TQ** as the MBP. Compound **69** showed activity against Rpn11 (~77  $\mu$ M), but was significantly less active when compared to **CZM** (0.39  $\mu$ M). This is consistent with the activity of the core scaffolds, fragments **8-TQ** and 1,5-naphthyridine-4(1*H*)-thione (Chapter 2, compound **69**, Table 2-3), where **8-TQ** shows better activity against Rpn11 than 1,5-naphthyridine-4(1*H*)-thione, again wholly consistent with metal coordination and formation of a **CZM**-Rpn11 ternary complex as the mechanism of action of these inhibitors.

Lastly, in order to determine the selectivity of **CZM** for Rpn11 over other  $Zn^{2+}$ -dependent metalloenzymes, several cross screen assays were carried out. **CZM** exhibited a 100-fold preference for inhibiting Rpn11 compared to the non-JAMM domain  $Zn^{2+}$ -dependent metalloenzymes HDAC6, MMP2, MMP12, and hCAII (Table 3-4). However, **CZM** did inhibit  $Zn^{2+}$ -dependent GLO1 with an  $IC_{50}$  of 43  $\mu$ M. Overall, **CZM** demonstrated selectivity for Rpn11 over other JAMM domain enzymes (Table 3-2) as well as other metalloenzymes (Table 3-4).

**Table 3-4.** Summary of CZM IC<sub>50</sub> on Zn<sup>2+</sup>-dependent metalloenzymes.

	<b>HDAC6</b>	<b>MMP2</b>	<b>MMP12</b>	<b>hCAII</b>	<b>GLO1</b>
<b>CZM</b>	>200	>200	>200	>200	42.8±2.2

### 3.3 Conclusions

Proteasome inhibitors represent an expanding area with a broad therapeutic potential; however, limitations with current FDA approved inhibitors have generated interest in developing novel compounds. By utilizing a FBDD approach, a first-in-class, Rpn11-selective inhibitor with sub-micromolar IC<sub>50</sub> values that is cytotoxic towards cancer cell lines has been obtained. By utilizing a modest library of 240 fragments we identified a fragment with low micromolar IC<sub>50</sub> values for Rpn11. The power of this approach was underscored by a subsequent high-throughput screen of >300,000 compounds, which yielded a thioester derivative of **8-TQ** as the only hit that satisfied all criteria.<sup>23</sup> As described in Chapter 2, a series of compounds helped establish rudimentary SAR, and from this an inhibitor that blocks proliferation of cancer cells was obtained. The findings of the synthetic campaign described in this chapter prompted an extensive biological study that is described elsewhere,<sup>23</sup> and demonstrated that **CZM** stabilizes proteasome substrates, induced an unfolded protein response, and blocked proliferation of cancer cells, including those resistant to bortezomib. Through inhibition of Rpn11 the ubiquitin tagged to the protein destined for degradation cannot be removed, thereby causing the proteasome to become inhibited. This represents a completely new mode of

action for a proteasome inhibitor and thus has potential for novel applications in the chemotherapy of cancer.

### 3.4 Experimental

**8-(*tert*-Butylthio)quinoline-2-carboxylic acid.** To a solution of 8-Fluoroquinoline-2-carboxylic acid (0.42 g, 2.19 mmol) in DMF (40 mL) was added NaH (0.18 g, 7.29 mmol) and *t*-BuSH (0.495 mL, 4.4 mmol) under nitrogen atmosphere. The solution was stirred at 140 °C for 18 h. The reaction mixture was evaporated to dryness and the crude material was taken in H<sub>2</sub>O and acidified with 1M HCl until a precipitate was formed (pH 2). The precipitate was filtered and dried under vacuum. Yield = 0.45 g (78%). <sup>1</sup>H NMR (400 MHz, CDCl<sub>3</sub>): δ 8.42 (dd, *J* = 8.5, 2.4 Hz, 1H), 8.32 (dd, *J* = 6.6, 3.7 Hz, 1H), 8.12 (d, *J* = 6.8 Hz, 1H), 7.94 (d, *J* = 7.2 Hz, 1H), 7.70 – 7.62 (m, 1H), 1.35 – 1.30 (m, 9H). ESI-MS(+): *m/z* 261.96 [M+H]<sup>+</sup>.

**8,8'-Disulfanediylbis(quinoline-2-carboxylic acid) (33).** A solution of 8-(*tert*-Butylthio)quinoline-2-carboxylic acid (0.24 g, 0.92 mmol) in conc. HCl (40 mL) was stirred at 110 °C for 12 h. The solution was neutralized to pH 9 and washed with EtOAc (3×50mL). The aqueous layer was then acidified to pH 2-3 and the precipitate was collected via vacuum filtration. The product was isolated as a disulfide dimer as evidenced by mass spectrometry. Yield = 0.15 g (80%). <sup>1</sup>H NMR (400 MHz, DMSO-*d*<sup>6</sup>): δ 8.61 (d, *J* = 8.5 Hz, 1H), 8.21 (d, *J* = 8.6 Hz, 1H), 7.92 (d, *J* = 8.0 Hz, 1H), 7.83 (d, *J* = 7.3 Hz, 1H), 7.63 (t, *J* = 7.8 Hz, 1H). ESI-MS (-): *m/z* 407.05 [M-H]<sup>-</sup>.

**Dimethyl 8,8'-disulfanediybis(quinoline-2-carboxylate) (36).** In a 10 mL microwave tube was placed **1** (0.02 g, 0.97 mmol) and MeOH (2 mL), followed by 15 drops of conc. H<sub>2</sub>SO<sub>4</sub>. The solution was placed in a microwave reactor and heated to 90 °C with stirring for 24 min. The solution was evaporated to dryness and the crude material was taken up in CHCl<sub>3</sub> and washed with a sat. NaHCO<sub>3</sub> (3×50mL). The combined organic layers were dried over anhydrous MgSO<sub>4</sub>, filtered, and concentrated under reduced pressure. Yield = 0.02 g (84%). <sup>1</sup>H NMR (400 MHz, CDCl<sub>3</sub>): δ 8.33 (dd, *J* = 8.7, 1.4 Hz, 1H), 8.26 (dd, *J* = 8.5, 1.4 Hz, 1H), 7.95 (d, *J* = 7.5 Hz, 1H), 7.68 (d, *J* = 8.2 Hz, 1H), 7.47 (td, *J* = 7.8, 1.5 Hz, 1H), 4.10 (s, 3H). ESI-MS(+): *m/z* 437.16 [M+H]<sup>+</sup>.

**8-(*tert*-Butylthio)quinoline-3-carboxylic acid.** To a solution of 8-Fluoroquinoline-3-carboxylic acid (1 g, 5.2 mmol) in DMF (40 mL) was added NaH (0.5 g, 20.8 mmol) and *t*-BuSH (2.35 mL, 20.8 mmol) under nitrogen atmosphere. The reaction mixture was stirred at 140 °C for 18 h. The solution was evaporated to dryness and the crude material was taken up in H<sub>2</sub>O and acidified with 6M HCl until a precipitate was formed (pH 2). The precipitate was filtered and dried under vacuum. Yield = 1.47 g (100%). <sup>1</sup>H NMR (400 MHz, DMSO-*d*<sup>6</sup>): δ 9.35 (d, *J* = 2.0 Hz, 1H), 8.96 (d, *J* = 1.9 Hz, 1H), 8.20 – 8.15 (m, 1H), 8.10 (d, *J* = 7.2 Hz, 1H), 7.67 (dd, *J* = 8.2, 7.2 Hz, 1H), 1.30 (s, 9H). ESI-MS(+): *m/z* 261.97 [M+H]<sup>+</sup>.

**8,8'-Disulfanediylbis(quinoline-3-carboxylic acid) (34).** A solution of 8-(tert-Butylthio)quinoline-3-carboxylic acid (0.6 g, 2.3 mmol) in conc. HCl (50 mL) was stirred at 110 °C for 12 h. The reaction mixture was neutralized to pH 9 and washed with EtOAc (3×50mL). The aqueous layer was then acidified to pH 2-3 and the observed precipitate collected via vacuum filtration. The crude material was recrystallized from EtOH. The product was isolated as a disulfide dimer as evidenced by mass spectrometry. Yield = 0.18 g (38%). <sup>1</sup>H NMR (400 MHz, DMSO-*d*<sup>6</sup>): δ 9.38 (d, *J* = 1.6 Hz, 1H), 9.02 (d, *J* = 1.6 Hz, 1H), 8.04 (d, *J* = 8.0 Hz, 1H), 7.87 (d, *J* = 8.0 Hz, 1H), 7.62 (t, *J* = 7.8 Hz, 1H). ESI-MS(+): *m/z* 409.01 [M+H]<sup>+</sup>.

**Dimethyl 8,8'-disulfanediylbis(quinoline-3-carboxylate) (37).** In a 10 mL microwave tube was placed **2** (0.020 g, 0.97 mmol) and MeOH (2 mL) followed by 15 drops of conc. H<sub>2</sub>SO<sub>4</sub>. The solution was placed in a microwave reactor and heated to 90 °C with stirring for 20 min. The solution was evaporated to dryness and the crude material was taken up in CHCl<sub>3</sub> and washed with a sat. solution of NaHCO<sub>3</sub> (3×50mL). The combined organic layers were dried over anhydrous MgSO<sub>4</sub>, filtered, and concentrated under reduced pressure. The crude material was recrystallized from EtOH. Yield = 0.004 g (19%). <sup>1</sup>H NMR (400 MHz, DMSO-*d*<sup>6</sup>): δ 9.41 (d, *J* = 2.0 Hz, 1H), 9.10 (d, *J* = 2.0 Hz, 1H), 8.08 (d, *J* = 8.1 Hz, 1H), 7.89 (d, *J* = 7.5 Hz, 1H), 7.69 – 7.59 (m, 1H), 3.98 (s, 3H). ESI-MS(+): *m/z* 437.11 [M+H]<sup>+</sup>.

**8-Fluoroquinoline-4-carboxylic acid.** To a solution of 7-Fluoroisatin (0.5 g, 3.03 mmol) in H<sub>2</sub>O (10 mL) in a 35 mL microwave tube was added 5M NaOH (2.52 mL, 15.1 mmol) and Sodium Pyruvate (0.4 g, 3.66 mmol). The mixture was placed in a microwave reactor and heated to 110 °C with stirring for 10 min. After cooling to room temperature, the suspension containing the dicarboxylic acid derivative was acidified to pH 2 and the dark solid was filtered off to afford product. A portion of the product (0.17 g) was then placed in a 10 mL microwave tube and H<sub>2</sub>O (2 mL) was added. The resulting suspension was placed in a microwave reactor and heated to 170 °C (or 280 psi) with stirring for 5 min. The brown solid was collected via vacuum filtration. Yield = 60% over 2 steps. <sup>1</sup>H NMR (400 MHz, DMSO-*d*<sup>6</sup>): δ 9.07 (d, *J* = 4.1 Hz, 1H), 8.48 (d, *J* = 7.4 Hz, 1H), 8.00 (d, *J* = 4.1 Hz, 1H), 7.73 – 7.62 (m, 2H). ESI-MS(+): *m/z* 192.27 [M+H]<sup>+</sup>.

**8-(*tert*-Butylthio)quinoline-4-carboxylic acid.** To a solution of 8-Fluoroquinoline-4-carboxylic acid (0.3 g, 1.57 mmol) in DMF (30 mL) was added NaH (0.15 g, 6.3 mmol) and *t*-BuSH (0.707 mL, 36.3 mmol) under nitrogen atmosphere. The mixture was stirred at 140 °C for 18 h. The solution was evaporated to dryness and the crude material was taken up in H<sub>2</sub>O and acidified with HCl until a precipitate formed (pH 2). The precipitate was collected via vacuum filtration and discarded. The filtrate was extracted with EtOAc (3×50mL), dried over anhydrous MgSO<sub>4</sub>, filtered, and concentrated under reduced pressure.

H<sub>2</sub>O was then added to the crude material resulting in a yellow precipitate. The precipitate was collected by vacuum filtration. Yield = 0.2 g (49% yield). <sup>1</sup>H NMR (400 MHz, DMSO-*d*<sup>6</sup>): δ 9.07 (d, *J* = 4.1 Hz, 1H), 8.60 (d, *J* = 8.6 Hz, 1H), 8.05 (d, *J* = 7.1 Hz, 1H), 7.90 (d, *J* = 4.3 Hz, 1H), 7.68 (t, *J* = 7.9 Hz, 1H), 1.30 (s, 9H). ESI-MS(+): *m/z* 261.93 [M+H]<sup>+</sup>.

**8,8'-Disulfanediylbis(quinoline-4-carboxylic acid) (35).** A solution of 8-(*tert*-Butylthio)quinoline-4-carboxylic acid (0.2 g, 0.76 mmol) in conc. HCl (18 mL) was stirred at 110 °C for 12 h. The crude material was neutralized to pH 9 and washed EtOAc (3×10mL). The aqueous layer was then acidified to pH 2-3 with HCl and the resulting precipitate was collected via vacuum filtration. The product was isolated as a disulfide dimer as evidenced by mass spectrometry. Yield = 0.09 g (58% yield). <sup>1</sup>H NMR (400 MHz, DMSO-*d*<sup>6</sup>): δ 9.13 (d, *J* = 4.5 Hz, 1H), 8.49 (d, *J* = 8.5 Hz, 1H), 8.05 (d, *J* = 4.4 Hz, 1H), 7.78 (d, *J* = 7.5 Hz, 1H), 7.61 (t, *J* = 8.0 Hz, 1H). ESI-MS(-): *m/z* 406.96 [M-H]<sup>-</sup>.

**Dimethyl 8,8'-disulfanediylbis(quinoline-4-carboxylate) (38).** In a 10 mL microwave tube was placed **3** (0.02 g, 0.97 mmol) and MeOH (2 mL), followed by 15 drops of conc. H<sub>2</sub>SO<sub>4</sub>. The reaction mixture was placed in a microwave reactor and heated to 90 °C with stirring for 20 min. The solution was evaporated to dryness and the crude material was taken up in CHCl<sub>3</sub> and washed with a sat. solution of NaHCO<sub>3</sub> (3×50mL). The collected organic layers were dried over

anhydrous MgSO<sub>4</sub>, filtered, and concentrated under reduced pressure. The crude material was recrystallized from EtOH. Yield = 0.02 g (100% yield). <sup>1</sup>H NMR (400 MHz, CDCl<sub>3</sub>): δ 8.99 (dd, *J* = 4.2, 1.7, 0.8 Hz, 1H), 8.12 (dd, *J* = 8.3, 1.7, 0.8 Hz, 1H), 7.89 (d, *J* = 8.8 Hz, 1H), 7.53 (dd, *J* = 8.3, 4.2 Hz, 1H), 7.27 (d, *J* = 1.8 Hz, 1H), 4.04 (d, *J* = 0.8 Hz, 3H). ESI-MS(+): *m/z* 437.02 [M+H]<sup>+</sup>.

**8,8'-Disulfanediylbis(quinoline-3-carboxamide) (39).** To a solution of **2** (0.05g, 0.24 mmol) in DMF (5 mL) was added CDI (0.06g, 0.37 mmol) and stirred at room temperature for ~15 min under nitrogen atmosphere. To this was added NH<sub>4</sub>OH (0.305g, 2.44 mmol) and allowed to stir for 1 h. The resulting solution was concentrated under reduced pressure and purified via reverse-phase chromatography eluting a gradient of 0 to 100% Acetonitrile in H<sub>2</sub>O. Yield = 0.016 g (32%). <sup>1</sup>H NMR (400 MHz, DMSO-*d*<sup>6</sup>): δ 9.37 (d, *J* = 2.0 Hz, 1H), 8.91 (d, *J* = 2.0 Hz, 1H), 8.38 (b, 1H), 7.94 (d, *J* = 8.4 Hz, 1H), 7.82 (m, 2H), 7.61 (t, *J* = 8.0 Hz, 1H). HR-ESI-MS calcd for [C<sub>20</sub>H<sub>15</sub>N<sub>4</sub>O<sub>2</sub>S<sub>2</sub>]<sup>+</sup>: 407.0631; Found: 407.0637.

**8,8'-Disulfanediylbis(*N*-methylquinoline-3-carboxamide) (40).** To a solution of **2** (0.05 g, 0.24 mmol) in DMF (5 mL) was added Hydroxybenzotriazole (HOBT, 0.06g, 0.37 mmol) and EDC (Ethyl-3-(3-dimethylaminopropyl)carbodiimide, 0.07g, 0.37 mmol) and stirred at room temperature for ~15 min under nitrogen atmosphere. To this reaction mixture was added Methylamine (1M THF solution,

0.49 mmol) and allowed to stir for 1 h. The resulting solution was concentrated under reduced pressure and purified via reverse-phase chromatography eluting a gradient of 0 to 100% Acetonitrile in H<sub>2</sub>O. Yield = 0.018 g (34%). <sup>1</sup>H NMR (400 MHz, DMSO-*d*<sup>6</sup>): δ 9.35 (s, 1H), 8.89 (m, 2H), 7.95 (d, *J* = 8.0 Hz, 1H), 7.83 (d, *J* = 8.0 Hz, 1H), 7.60 (t, *J* = 8.0 Hz, 1H), 2.84 (s, 3H). HR-ESI-MS calcd for [C<sub>22</sub>H<sub>19</sub>N<sub>4</sub>O<sub>2</sub>S<sub>2</sub>]<sup>+</sup>: 435.0944; Found: 435.0947.

**Dimethyl2,2'-((8,8'-disulfanediy)bis(quinoline-8,3-diyl-3-carbonyl))bis**

**(azanediyl)diacetate (41).** To a solution of **2** (0.04 g, 0.17 mmol) in DMF (4 mL) was added HATU (1-[Bis(dimethylamino)methylene]-1H-1,2,3-triazolo[4,5-b]pyridinium-3-oxidhexafluorophosphate, 0.08 g, 0.21 mmol), HOBT (0.03 g, 0.21 mmol), Et<sub>3</sub>N (0.073 mL, 0.52 mmol) and Methyl 2-aminoacetate (24 mg, 0.19 mmol) and allowed to stir at room temperature for 1 h. The resulting solution was concentrated under reduced pressure, then the crude material was then dissolved in CH<sub>2</sub>Cl<sub>2</sub> and washed with 1M HCl solution. The product, which precipitated out of the organic layer, was recrystallized from MeOH. Yield = 0.005 g (11%). <sup>1</sup>H NMR (400 MHz, DMSO-*d*<sup>6</sup>): δ 9.42 (t, *J* = 5.9 Hz, 1H, NH), 9.37 (s, 1H), 8.93 (s, 1H), 7.97 (d, *J* = 8.2 Hz, 1H), 7.85 (d, *J* = 7.5 Hz, 1H), 7.62 (t, *J* = 7.7 Hz, 1H), 4.13 (d, *J* = 5.7 Hz, 2H), 3.68 (s, 3H). HR-ESI-MS calcd for [C<sub>26</sub>H<sub>23</sub>N<sub>4</sub>O<sub>6</sub>S<sub>2</sub>]<sup>+</sup>: 551.1054; Found: 551.1052.

**Procedure for the amide coupling (Method A):** To a solution of **2** (0.2 g, 0.98 mmol) in DMF (10 mL) was added CDI (0.24 g, 1.46 mmol) and stirred at room temperature for ~15 min under nitrogen atmosphere. To this solution was added the corresponding amine (0.146 mmol) and the solution was stirred for an additional 12 h. The resulting solution was concentrated under reduced pressure, then purified via reverse-phase chromatography eluting a gradient of 0 to 100% Acetonitrile in H<sub>2</sub>O.

**Procedure for the amide coupling (Method B):** To a solution of **2** (0.2 g, 0.98 mmol) in DMF (10 mL) was added HATU (0.56 g, 1.46 mmol) and Et<sub>3</sub>N (0.204 mL, 1.46 mmol) and the mixture was stirred at 60° C for ~15 min under nitrogen atmosphere. To this solution was added the corresponding amine (0.146 mmol) and the solution was stirred for an additional 12 h. The resulting solution was concentrated under reduced pressure, then purified via reverse-phase chromatography eluting a gradient of 0 to 100% Acetonitrile in H<sub>2</sub>O.

**8,8'-Disulfanediylbis(*N*-(oxazol-2-yl)quinoline-3-carboxamide)(42).** Product afforded via Method B. Yield = 0.13 g (48%). <sup>1</sup>H NMR (400 MHz, DMSO-*d*<sup>6</sup>): δ 9.47 (s, 1H), 9.06 (d, *J* = 1.6 Hz, 1H), 8.01 (d, *J* = 8.0 Hz, 1H), 7.93 (s, 1H), 7.87 (d, *J* = 8.0 Hz, 1H), 7.64 (t, *J* = 8.0 Hz, 1H), 7.25 (s, 1H). HR-ESI-MS calcd for [C<sub>26</sub>H<sub>17</sub>N<sub>6</sub>O<sub>4</sub>S<sub>2</sub>]<sup>+</sup>: 541.0747; Found: 541.0749.

**8,8'-Disulfanediylbis(*N*-(thiazol-2-yl)quinoline-3-carboxamide) (43).** To a solution of **2** (0.2 g, 0.98 mmol) in DMF (10 mL) was added HATU (0.56 g, 1.46 mmol) and Et<sub>3</sub>N (0.204 mL, 1.46 mmol) and the mixture was stirred at 60° C for ~15 min under nitrogen atmosphere. To this solution was added the corresponding amine (0.146 mmol) and the solution was stirred for an additional 12 h. To the resulting solution was added H<sub>2</sub>O, which resulted in the formation of a precipitate. The precipitate was isolated through vacuum filtration to afford desired product. Yield = 0.12 g (43%). <sup>1</sup>H NMR (400 MHz, DMSO-*d*<sub>6</sub>): δ 9.51 (s, 1H), 9.15 (s, 1H), 7.98 (d, *J* = 8.0 Hz, 1H), 7.88 (d, *J* = 8.0 Hz, 1H), 7.64-7.59 (m, 2H), 7.32 (d, *J* = 2.4 Hz, 1H). <sup>13</sup>C NMR (100 MHz, DMSO- *d*<sub>6</sub>): δ 164.5, 159.6, 149.2, 146.6, 138.2, 137.7, 135.0, 128.7, 127.8, 127.4, 127.0, 126.8, 114.7. HR-ESI-MS calcd for [C<sub>26</sub>H<sub>16</sub>N<sub>6</sub>O<sub>2</sub>S<sub>4</sub>Na]<sup>+</sup>: 595.0110; Found: 595.0103.

**8,8'-Disulfanediylbis(*N*-((tetrahydrofuran-2-yl)methyl)quinoline-3-carboxamide) (44).** Product afforded via Method A. Yield = 0.14 g (51%). <sup>1</sup>H NMR (400 MHz, DMSO-*d*<sub>6</sub>): δ 9.43 (d, *J* = 2 Hz, 1H), 8.88 (d, *J* = 2 Hz, 1H), 7.94-7.90 (m, 3H), 7.60 (t, *J* = 8 Hz, 1H), 4.13-3.47 (m, 5H), 2.09-1.67 (m, 4H). HR-ESI-MS calcd for [C<sub>30</sub>H<sub>31</sub>N<sub>4</sub>O<sub>4</sub>S<sub>2</sub>]<sup>+</sup>: 575.1781; Found: 575.1780.

**8,8'-Disulfanediylbis(*N*-(furan-2-ylmethyl)quinoline-3-carboxamide) (45).** Product afforded via Method A. Yield = 0.084 g (30%). <sup>1</sup>H NMR (400 MHz, DMSO-*d*<sub>6</sub>): δ 9.46 (d, *J* = 2.4 Hz, 1H), 8.99 (d, *J* = 2.4 Hz, 1H), 8.50 (br, 1H), 8.35

(dd,  $J = 7.2, 1.2$  Hz, 1H), 8.28 (dd,  $J = 7.2, 1.2$  Hz, 1H), 7.84 (t,  $J = 7.6$  Hz, 1H), 7.50 (dd,  $J = 1.6, 0.8$  Hz, 1H), 6.40 (m, 2H), 4.67 (d,  $J = 5.6$  Hz, 2H). HR-ESI-MS calcd for  $[\text{C}_{30}\text{H}_{22}\text{N}_4\text{O}_4\text{S}_2\text{Na}]^+$ : 589.0975; Found: 589.0972.

**8,8'-Disulfanediylbis(*N*-(thiophen-2-ylmethyl)quinoline-3-carboxamide) (46).**

Product afforded via Method A. Yield = 0.13 g (44%).  $^1\text{H}$  NMR (400 MHz, DMSO- $d_6$ ):  $\delta$  9.58 (t,  $J = 5.6$  Hz, 1H), 9.37 (d,  $J = 2.4$  Hz, 1H), 8.91 (d,  $J = 2.4$  Hz, 1H), 7.96 (d,  $J = 8$  Hz, 1H), 7.84 (d,  $J = 8$  Hz, 1H), 7.62 (t,  $J = 8$  Hz, 1H), 7.42 (d,  $J = 6$  Hz, 1H), 7.09-6.97 (m, 2H), 4.73 (d,  $J = 5.6$  Hz, 2H). HR-ESI-MS calcd for  $[\text{C}_{30}\text{H}_{23}\text{N}_4\text{O}_2\text{S}_4]^+$ : 599.0698; Found: 599.0701.

**8,8'-Disulfanediylbis(*N*-(thiazol-2-ylmethyl)quinoline-3-carboxamide) (47).**

To a solution of **2** (0.2 g, 0.98 mmol) in DMF (10 mL) was added CDI (0.24 g, 1.46 mmol) and stirred at room temperature for ~15 min under nitrogen atmosphere. To this solution was added the corresponding amine (0.146 mmol) and the solution was stirred for an additional 12 h. To the reaction mixture was added  $\text{H}_2\text{O}$ , which resulted in the formation of a precipitate. The precipitate was isolated through vacuum filtration to afford final product. Yield = 0.035 g (12%).  $^1\text{H}$  NMR (400 MHz, DMSO- $d_6$ ):  $\delta$  9.83 (t,  $J = 5.6$  Hz, 1H), 9.40 (d,  $J = 2$  Hz, 1H), 8.95 (d,  $J = 2$  Hz, 1H), 7.97 (d,  $J = 8$  Hz, 1H), 7.86 (d,  $J = 8$  Hz, 1H), 7.76 (d,  $J = 3.2$  Hz, 1H), 7.66 (d,  $J = 3.2$  Hz, 1H), 7.63 (t,  $J = 8$  Hz, 1H), 4.86 (d,  $J = 6$  Hz, 2H). HR-ESI-MS calcd for  $[\text{C}_{28}\text{H}_{21}\text{N}_6\text{O}_2\text{S}_4]^+$ : 601.0603; Found: 601.0600.

**8,8'-Disulfanediylbis(*N*-(2-(furan-2-yl)ethyl)quinoline-3-carboxamide) (48).**

To a solution of **2** (0.2 g, 0.98 mmol) in DMF (10 mL) was added CDI (0.24 g, 1.46 mmol) and stirred at room temperature for ~15 min under nitrogen atmosphere. To this solution was added the corresponding amine (0.146 mmol) and the solution was stirred for an additional 12 h. The reaction solution was concentrated and diluted with Diethyl Ether, which resulted in the formation of a precipitate. The precipitate was isolated through vacuum filtration and purified via reverse-phase chromatography eluting a gradient of 0 to 100% Acetonitrile in H<sub>2</sub>O. Yield = 0.065 g (22%). <sup>1</sup>H NMR (400 MHz, DMSO-*d*<sub>6</sub>): δ 9.32 (d, *J* = 2 Hz, 1H), 9.04 (t, *J* = 5.2 Hz, 1H), 8.84 (d, *J* = 2 Hz, 1H), 7.94 (d, *J* = 8 Hz, 1H), 7.83 (d, *J* = 8 Hz, 1H), 7.61-7.54 (m, 2H), 6.36 (t, *J* = 2.8 Hz, 1H), 6.21 (d, *J* = 2.8 Hz, 1H), 3.62 (q, *J* = 6 Hz, 2H), 2.96 (q, *J* = 7.2 Hz, 2H). HR-ESI-MS calcd for [C<sub>32</sub>H<sub>26</sub>N<sub>4</sub>O<sub>4</sub>S<sub>2</sub>Na]<sup>+</sup>: 617.1288; Found: 617.1283

**8,8'-Disulfanediylbis(*N*-(2-(thiophen-2-yl)ethyl)quinoline-3-carboxamide)**

**(49).** To a solution of **2** (0.2 g, 0.98 mmol) in DMF (10 mL) was added CDI (0.24 g, 1.46 mmol) and stirred at room temperature for ~15 min under nitrogen atmosphere. To this solution was added the corresponding amine (0.146 mmol) and the solution was stirred for an additional 12 h. To the resulting solution was added H<sub>2</sub>O, which resulted in the formation of a precipitate. The precipitate was isolated through vacuum filtration and further purified via reverse-phase

chromatography using a gradient of 0 to 100% Acetonitrile in H<sub>2</sub>O. Yield = 0.075 g (24%). <sup>1</sup>H NMR (400 MHz, DMSO-*d*<sub>6</sub>): δ 9.35 (s, 1H), 9.10 (t, *J* = 5.2 Hz, 1H), 8.87 (s, 1H), 7.95 (d, *J* = 6.4 Hz, 1H), 7.84 (d, *J* = 6.4 Hz, 1H), 7.62 (t, *J* = 5.6 Hz, 1H), 7.34-6.96 (m, 3H), 3.60 (t, *J* = 6 Hz, 2H), 3.14 (t, *J* = 6 Hz, 2H). HR-ESI-MS calcd for [C<sub>32</sub>H<sub>27</sub>N<sub>4</sub>O<sub>2</sub>S<sub>4</sub>]<sup>+</sup>: 627.1011; Found: 627.1013.

**8,8'-Disulfanediylbis(*N*-(2-(thiazol-2-yl)ethyl)quinoline-3-carboxamide) (50).**

To a solution of **2** (0.2 g, 0.98 mmol) in DMF (10 mL) was added CDI (0.24 g, 1.46 mmol) and the mixture was stirred at room temperature for ~15 min under nitrogen atmosphere. To this solution was added the corresponding amine (0.15 mmol) and the solution was stirred for an additional ~12 h. To the resulting solution was added H<sub>2</sub>O, which resulted in the formation of a precipitate. The precipitate was isolated through vacuum to yield the final product. Yield = 0.18 g (57%). <sup>1</sup>H NMR (400 MHz, DMSO-*d*<sub>6</sub>): δ 9.33 (s, 1H), 9.11 (t, *J* = 5.2 Hz, 1H), 8.86 (s, 1H), 7.95 (d, *J* = 8 Hz, 1H), 7.84 (d, *J* = 8 Hz, 1H), 7.74 (d, *J* = 3.2 Hz, 1H), 7.62-7.58 (m, 2H), 3.74 (q, 2H), 3.34 (t, 2H). <sup>13</sup>C NMR (100 MHz, DMSO-*d*<sub>6</sub>): δ 167.7, 163.3, 148.9, 146.3, 143.0, 136.6, 134.9, 128.6, 128.6, 127.6, 127.5, 126.3, 120.4, 40.1, 32.9. HR-ESI-MS calcd for [C<sub>30</sub>H<sub>25</sub>N<sub>6</sub>O<sub>2</sub>S<sub>4</sub>]<sup>+</sup>: 629.0916; Found: 629.0913.

**8,8'-Disulfanediylbis(*N*-(pyridin-2-ylmethyl)quinoline-3-carboxamide) (51).**

Product afforded via Method B. Yield = 0.06 g (21%). <sup>1</sup>H NMR (400 MHz, DMSO-

$d_6$ ):  $\delta$  9.52 (d,  $J = 2.4$  Hz, 1H), 9.07 (d,  $J = 2.4$  Hz, 1H), 8.77-8.58 (m, 2H), 8.36 (dd,  $J = 7.2, 1.2$  Hz, 1H), 8.32 (dd,  $J = 7.2, 1.2$  Hz, 1H), 7.86-7.82 (m, 2H), 7.55 (d,  $J = 8$  Hz, 1H), 7.36 (t,  $J = 6$  Hz, 3H), 4.82 (d,  $J = 6$  Hz, 2H). HR-ESI-MS calcd for  $[\text{C}_{32}\text{H}_{25}\text{N}_6\text{O}_2\text{S}_2]^+$ : 589.1475; Found: 589.1478.

**8,8'-Disulfanediylbis(*N*-(pyridin-3-ylmethyl)quinoline-3-carboxamide) (52).**

Product afforded via Method B. Yield = 0.11 g (38%).  $^1\text{H}$  NMR (400 MHz, DMSO- $d_6$ ):  $\delta$  9.46 (d,  $J = 2.4$  Hz, 1H), 8.98 (d,  $J = 2.4$  Hz, 1H), 8.70-8.52 (m, 2H), 8.34 (dd,  $J = 7.2, 1.2$  Hz, 1H), 8.27 (dd,  $J = 7.2, 1.2$  Hz, 1H), 7.92 (d,  $J = 7.6$  Hz, 1H), 7.83 (t,  $J = 7.6$  Hz, 1H), 7.43 (dd,  $J = 7.6, 4.8$  Hz, 1H), 4.73 (d,  $J = 5.6$  Hz, 2H). HR-ESI-MS calcd for  $[\text{C}_{32}\text{H}_{25}\text{N}_6\text{O}_2\text{S}_2]^+$ : 589.1475; Found: 589.1477.

**8,8'-Disulfanediylbis(*N*-(pyridin-4-ylmethyl)quinoline-3-carboxamide) (53).**

Product afforded via Method B. Yield = 0.06 g (21%).  $^1\text{H}$  NMR (400 MHz, DMSO- $d_6$ ):  $\delta$  9.88 (t,  $J = 5.6$  Hz, 1H), 9.46 (d,  $J = 2.4$  Hz, 1H), 9.03 (d,  $J = 2.4$  Hz, 1H), 8.84-8.74 (m, 2H), 7.99 (d,  $J = 8$  Hz, 1H), 7.92-7.91 (m, 2H), 7.87 (d,  $J = 8$  Hz, 1H), 7.65 (t,  $J = 8$  Hz, 1H), 4.80 (d,  $J = 5.6$  Hz, 2H). HR-ESI-MS calcd for  $[\text{C}_{32}\text{H}_{25}\text{N}_6\text{O}_2\text{S}_2]^+$ : 589.1475; Found: 589.1477.

**8,8'-Disulfanediylbis(*N*-benzylquinoline-3-carboxamide) (54).** To a solution of **16b** (0.2 g, 0.98 mmol) in DMF (10 mL) was added HATU (0.56 g, 1.46 mmol) and  $\text{Et}_3\text{N}$  (0.204 mL, 1.46 mmol) and the mixture was stirred at 60° C for ~15 min

under nitrogen atmosphere. To this solution was added the corresponding amine (0.146 mmol) and the solution was stirred for an additional 12 h. The reaction mixture was concentrated and the crude material was dissolved in CH<sub>2</sub>Cl<sub>2</sub>. The product, which precipitated out of the organic layer, was collected via vacuum filtration. Yield = 0.03 g (42%). <sup>1</sup>H NMR (400 MHz, DMSO-*d*<sup>6</sup>): δ 9.49 (t, *J* = 5.9 Hz, 1H), 9.41 (d, *J* = 2.1 Hz, 1H), 8.95 (d, *J* = 2.2 Hz, 1H), 7.94 (s, 1H), 7.86-7.81 (m, 1H), 7.61 (t, *J* = 7.8 Hz, 1H), 7.41-7.32 (m, 4H), 7.26 (t, *J* = 7.1 Hz, 1H), 4.58 (d, *J* = 5.8 Hz, 2H). HR-ESI-MS calcd for [C<sub>34</sub>H<sub>27</sub>N<sub>4</sub>O<sub>2</sub>S<sub>2</sub>]<sup>+</sup>: 587.1570; Found: 587.1571.

**8,8'-Disulfanediylbis(N-(4-fluorobenzyl)quinoline-3-carboxamide) (55).**

Product afforded via Method A. Yield = 0.04 g (14%). <sup>1</sup>H NMR (400 MHz, DMSO-*d*<sup>6</sup>): δ 9.48 (t, *J* = 5.6 Hz, 1H), 9.39 (d, *J* = 1.6 Hz, 1H), 8.92 (d, *J* = 1.6 Hz, 1H), 7.95 (d, *J* = 8.0 Hz, 1H), 7.84 (d, *J* = 8.0 Hz, 1H), 7.61 (t, *J* = 8.0 Hz, 1H), 7.44-7.15 (m, 4H), 4.56 (d, *J* = 5.6 Hz, 2H). HR-ESI-MS calcd for [C<sub>34</sub>H<sub>25</sub>F<sub>2</sub>N<sub>4</sub>O<sub>2</sub>S<sub>2</sub>]<sup>+</sup>: 623.1382; Found: 623.1384.

**8,8'-Disulfanediylbis(N-(4-(trifluoromethyl)benzyl)quinoline-3-carboxamide)**

**(56).** Product afforded via Method A. Yield = 0.09 g (26%). <sup>1</sup>H NMR (400 MHz, DMSO-*d*<sup>6</sup>): δ 9.58 (t, *J* = 5.6 Hz, 1H), 9.40 (s, 1H), 8.94 (s, 1H), 7.96 (d, *J* = 8.0 Hz, 1H), 7.85 (d, *J* = 8.0 Hz, 1H), 7.73 (d, *J* = 8.0 Hz, 2H), 7.62-7.61 (m, 3H),

4.67 (d,  $J = 5.2$  Hz, 2H). ESI-MS(+):  $m/z$  723.25  $[M+H]^+$ . HR-ESI-MS calcd for  $[C_{36}H_{24}F_6N_4O_2S_2Na]^+$ : 745.1137; Found: 745.1141

**8,8'-Disulfanediylbis(*N*-(4-methoxybenzyl)quinoline-3-carboxamide) (57).**

Product afforded via Method A. Yield = 0.15 g (47%).  $^1H$  NMR (400 MHz, DMSO- $d_6$ ):  $\delta$  9.40-9.38 (m, 2H), 8.91 (d,  $J = 1.6$  Hz, 1H), 7.95 (d,  $J = 8.0$  Hz, 1H), 7.83 (d,  $J = 8.0$  Hz, 1H), 7.62 (t,  $J = 8.0$  Hz, 1H), 7.30 (d,  $J = 8.0$  Hz, 2H), 6.92 (d,  $J = 8.0$  Hz, 2H), 4.50 (d,  $J = 5.6$  Hz, 2H) 3.72 (s, 3H). HR-ESI-MS calcd for  $[C_{36}H_{30}N_4O_4S_2Na]^+$ : 669.1601; Found: 669.1603.

**8,8'-Disulfanediylbis(*N*-(benzo[d][1,3]dioxol-5-ylmethyl)quinoline-3-**

**carboxamide) (58).** Product afforded via Method A. Yield = 0.12 g (37%).  $^1H$  NMR (400 MHz, Acetone- $d_6$ ):  $\delta$  9.38 (s, 2H), 9.01 (s, 1H), 8.27-8.26 (m, 2H), 7.81 (d,  $J = 7.6$  Hz, 1H), 6.95 (s, 1H), 6.87-6.85 (m, 2H), 5.98 (s, 2H), 4.46 (d,  $J = 5.6$  Hz, 2H). HR-ESI-MS calcd for  $[C_{36}H_{27}N_4O_6S_2]^+$ : 675.1372; Found: 675.1374.

**8,8'-Disulfanediylbis(*N*-(4-morpholinobenzyl)quinoline-3-carboxamide) (59).**

Product afforded via Method A. Yield = 0.18 g (50%).  $^1H$  NMR (400 MHz, DMSO- $d_6$ ):  $\delta$  9.40-9.33 (m, 2H), 8.91 (s, 1H), 7.94 (d,  $J = 8.0$  Hz, 1H), 7.83 (d,  $J = 8.0$  Hz, 1H), 7.59 (t,  $J = 8.0$  Hz, 1H), 7.26 (d,  $J = 8.0$  Hz, 2H), 6.93 (d,  $J = 8.0$  Hz, 2H), 4.47 (d,  $J = 5.6$  Hz, 2H), 3.72 (t,  $J = 4.8$  Hz, 4H), 3.05 (t,  $J = 4.8$  Hz, 4H). HR-ESI-MS calcd for  $[C_{42}H_{40}N_6O_4S_2Na]^+$ : 779.2445; Found: 779.2443.

**8,8'-Disulfanediylbis(*N*-(2-morpholinoethyl)quinoline-3-carboxamide) (60).**

Product afforded via Method A. Yield = 0.07 g (24%). <sup>1</sup>H NMR (400 MHz, Acetone-*d*<sub>6</sub>): δ 9.45 (s, 1H), 8.96 (s, 1H), 8.36 (d, *J* = 8 Hz, 1H), 8.30 (d, *J* = 8 Hz, 1H), 7.86 (t, *J* = 8 Hz, 1H), 3.79-3.75 (m, 6H), 3.06(t, *J* = 6 Hz, 2H). HR-ESI-MS calcd for [C<sub>32</sub>H<sub>37</sub>N<sub>6</sub>O<sub>4</sub>S<sub>2</sub>]<sup>+</sup>: 633.2312; Found: 633.2316.

**Dibenzyl2,2'-((2,2'-((8,8'-disulfanediylbis(quinoline-8,3-diyl-3-carbonyl))bis(azanediyl))bis(acetyl))bis(azanediyl))diacetate (61).** To a solution of **2** (0.05 g, 0.24 mmol) in dry DMF (5 mL) was added HATU (0.11 g, 0.29 mmol), HOBT (0.04 g, 0.29 mmol), Et<sub>3</sub>N (0.068 mL, 0.48 mmol) and H<sub>2</sub>N-Gly-Gly-Bz (0.11 g, 0.26 mmol). The reaction was stirred at room temperature for 4 h. The resulting mixture was evaporated to dryness and the crude material was dissolved in CH<sub>2</sub>Cl<sub>2</sub> and washed with 1M HCl, H<sub>2</sub>O and then Brine. The product, which precipitated out of the organic layer, was filtered off and dried under vacuum. Yield = 0.07 g (69%). <sup>1</sup>H NMR (400 MHz, DMSO-*d*<sup>6</sup>): δ 9.40 (d, *J* = 2.1 Hz, 1H), 9.29 (t, *J* = 5.9 Hz, 1H), 8.94 (d, *J* = 2.2 Hz, 1H), 8.51 (t, *J* = 6.0 Hz, 1H), 7.96 (d, *J* = 8.0 Hz, 1H), 7.88 – 7.82 (m, 1H), 7.62 (t, *J* = 7.8 Hz, 1H), 7.37 – 7.28 (m, 5H), 5.14 (s, 2H), 4.03 (d, *J* = 5.9 Hz, 2H), 3.95 (d, *J* = 5.9 Hz, 2H). HR-ESI-MS calcd for [C<sub>42</sub>H<sub>37</sub>N<sub>6</sub>O<sub>8</sub>S<sub>2</sub>]<sup>+</sup>: 817.2109; Found: 817.2106.

**8,8'-Disulfanediylbis(*N*-(furan-2-ylmethyl)quinoline-4-carboxamide) (62).** To a solution of **3** (0.2 g, 0.98 mmol) in DMF (10 mL) was added Carbonyldimidazole (CDI, 0.24 g, 1.46 mmol) and stirred at room temperature for ~15 min under nitrogen atmosphere. To this reaction mixture was added Furan-2-ylmethanamine (0.146 mmol) and stirred for an additional 12 h. The resulting solution was concentrated under reduced pressure, then purified via silica gel column chromatography eluting a gradient of 0 to 100% EtOAc in Hexanes. Yield = 0.15 g (54%). <sup>1</sup>H NMR (400 MHz, DMSO-*d*<sup>6</sup>): δ 9.33 (t, *J* = 5.6 Hz, 1H), 9.08 (d, *J* = 4.4 Hz, 1H), 7.92 (d, *J* = 8.4 Hz, 1H), 7.76 (d, *J* = 7.6 Hz, 1H), 7.69-7.61 (m, 2H), 7.57 (t, *J* = 8.0 Hz, 1H), 6.43-6.36 (m, 2H), 4.55 (d, *J* = 5.6 Hz, 2H). ESI-MS(+): *m/z* 566.17 [M+H]<sup>+</sup>.

**8,8'-Disulfanediylbis(*N*-(thiophen-2-ylmethyl)quinoline-2-carboxamide) (63).** To a solution of **1** (0.05 g, 0.24 mmol) in dry CH<sub>2</sub>Cl<sub>2</sub> (2 mL) was added Oxalyl Chloride (0.320 mL, 2.90 mmol) and 12 drops of dry DMF under nitrogen atmosphere. The solution was stirred at room temperature for 2 h. The solution was then evaporated to dryness to remove the excess of Oxalyl Chloride. The resulting acyl chloride solution was then added to a solution of 2-Thiophenemethylamine (0.300 mL, 2.9 mmol) in dry CH<sub>2</sub>Cl<sub>2</sub> (6 mL) under nitrogen atmosphere and stirred at room temperature for 18 h. The solution was then washed with 1M HCl to remove excess of amine, dried over anhydrous MgSO<sub>4</sub>, filtered, and concentrated under reduced pressure. The crude material

was purified via silica gel column chromatography eluting a gradient of 0 to 100% EtOAc in Hexanes. Yield = 0.06 g (79%).  $^1\text{H}$  NMR (400 MHz,  $\text{CDCl}_3$ ):  $\delta$  8.59 (t,  $J$  = 6.2 Hz, 1H, NH), 8.45 – 8.40 (m, 1H), 8.39 – 8.32 (m, 1H), 7.87 (d,  $J$  = 7.6 Hz, 1H), 7.72 – 7.66 (m, 1H), 7.51 – 7.41 (m, 1H), 7.25 – 7.23 (m, 1H), 7.15 – 7.11 (m, 1H), 7.03 – 6.95 (m, 1H), 4.95 (d,  $J$  = 5.8 Hz, 2H). ESI-MS(+):  $m/z$  598.93  $[\text{M}+\text{H}]^+$ , 621.03  $[\text{M}+\text{Na}]^+$ .

**8,8'-Disulfanediylbis(*N*-(thiophen-2-ylmethyl)quinoline-4-carboxamide) (64).**

To a solution of **3** (0.05 g, 0.24 mmol) in dry  $\text{CH}_2\text{Cl}_2$  (2 mL) was added Oxalyl Chloride (0.640 mL, 5.76 mmol) and 15 drops of dry DMF under nitrogen atmosphere. The solution was stirred at room temperature for 2 h. The solution was evaporated to dryness to remove the excess of Oxalyl Chloride and dry  $\text{CH}_2\text{Cl}_2$  was added to the crude material (2 mL). The resulting acyl chloride solution was added to a solution of 2-Thiophenemethylamine (0.600 mL, 5.76 mmol) in dry  $\text{CH}_2\text{Cl}_2$  (10 mL) under nitrogen atmosphere and stirred at room temperature for 2 days. The solution was then washed with 1M HCl to remove excess of amine, dried over anhydrous  $\text{MgSO}_4$ , filtered, and concentrated under reduced pressure. The crude material was purified via silica gel column chromatography eluting a gradient of 0 to 100% EtOAc in Hexanes. Yield = 0.03 g (41% yield).  $^1\text{H}$  NMR (400 MHz,  $\text{DMSO}-d_6$ ):  $\delta$  9.47 (d,  $J$  = 5.9 Hz, 1H), 9.08 (d,  $J$  = 3.9 Hz, 1H), 7.93 (d,  $J$  = 8.4 Hz, 1H), 7.74 (d,  $J$  = 7.6 Hz, 1H), 7.67 (d,  $J$  = 4.2

Hz, 1H), 7.59 – 7.51 (m, 1H), 7.43 (d,  $J = 5.1$  Hz, 1H), 7.07 (d,  $J = 3.3$  Hz, 1H), 6.98 (s, 1H), 4.70 (d,  $J = 5.8$  Hz, 2H). ESI-MS(+):  $m/z$  599.05  $[M+H]^+$ .

**8,8'-Disulfanediylbis(*N*-benzylquinoline-2-carboxamide) (65).** To a solution of **1** (0.05 g, 0.24 mmol) in dry  $\text{CH}_2\text{Cl}_2$  (2 mL) was added Oxalyl Chloride (0.42 mL, 0.48 mmol) and 5 drops of dry DMF under nitrogen atmosphere. The solution was stirred at room temperature for 2 h. The solution was evaporated to dryness to remove the excess of Oxalyl Chloride. The resulting acyl chloride solution was then added to a solution of Benzylamine (0.319 mL, 2.9 mmol) in dry  $\text{CH}_2\text{Cl}_2$  (5 mL) under nitrogen atmosphere and the mixture was stirred at room temperature for 18 h. The solution was then washed with 1M HCl to remove excess of Benzylamine, dried over anhydrous  $\text{MgSO}_4$ , filtered, and concentrated under reduced pressure. The crude material was purified via silica gel column eluting a gradient of 0 to 100% EtOAc in Hexanes. Yield = 0.05 g (74%).  $^1\text{H}$  NMR (400 MHz,  $\text{CDCl}_3$ ):  $\delta$  8.60 (t,  $J = 6.2$  Hz, 1H, NH), 8.43 (d,  $J = 8.5$  Hz, 1H), 8.36 (d,  $J = 8.6$  Hz, 1H), 7.86 (dd,  $J = 7.5, 1.2$  Hz, 1H), 7.69 (dd,  $J = 8.2, 1.2$  Hz, 1H), 7.49 – 7.43 (m, 3H), 7.40 – 7.34 (m, 2H), 7.30 (d,  $J = 7.2$  Hz, 1H), 4.80 (d,  $J = 6.2$  Hz, 2H). ESI-MS(+):  $m/z$  587.08  $[M+H]^+$ , 609.11  $[M+\text{Na}]^+$ .

**8-Hydroxy-*N*-(2-(thiazol-2-yl)ethyl)quinoline-3-carboxamide (66).** To a solution of 8-Hydroxyquinoline-3-carboxylic acid (0.1 g, 0.529 mmol) in DMF (3 mL) was added  $\text{Et}_3\text{N}$  (0.088 mL, 0.634 mmol) and HATU (0.24 g, 0.634 mmol)

then allowed to stir at room temperature for ~15 min. To this was then added 2-(Thiazol-2-yl)ethan-1-amine (0.08 g, 0.634 mmol) and allowed to stir for 18 h. The resulting solution was concentrated in vacuo and purified via silica gel chromatography eluting a gradient of 0-20% MeOH in CH<sub>2</sub>Cl<sub>2</sub>. Yield = 0.04 g (30%). <sup>1</sup>H NMR (400 MHz, DMSO-d<sub>6</sub>): δ 9.35 (t, *J* = 3.6 Hz, 1H), 9.26 (s, 1H), 9.17 (s, 1H), 7.78 (d, *J* = 3.2 Hz, 1H), 7.66-7.63 (m, 3H), 7.40 (t, *J* = 3.6 Hz, 1H), 3.74 (q, *J* = 5.6 Hz, 2H), 3.36 (t, *J* = 6 Hz, 2H). HR-ESI-MS calcd for [C<sub>15</sub>H<sub>12</sub>N<sub>3</sub>O<sub>2</sub>S]<sup>-</sup>: 298.0656; Found: 298.0658.

**8-(Methylthio)-*N*-(2-(thiazol-2-yl)ethyl)quinoline-3-carboxamide (67).** A solution of **18** (0.1 g, 0.159 mmol) in MeOH (10 mL) was cooled down to 0 °C and placed under nitrogen atmosphere. To this was added NaBH<sub>4</sub> (0.06 g, 1.59 mmol) and allowed to stir for ~ 20 min. The solution was then allowed to heat up to room temperature and stirred for an additional 1 h. The resulting solution was then concentrated in vacuo, dissolved in THF (10 mL) and then added CH<sub>3</sub>I (0.23 g, 1.59 mmol) and allowed to stir at room temperature for 1 h. This solution was then refluxed for 18 h, concentrated and purified via silica gel chromatography eluting a gradient of 0-90% EtOAc in Hexanes. Yield = 0.23 g (22%). <sup>1</sup>H NMR (400 MHz, CDCl<sub>3</sub>): δ 9.27 (s, 1H), 8.65 (s, 1H), 7.92 (br, 1H), 7.76 (d, *J* = 1.6 Hz, 1H), 7.65 (d, *J* = 7.6 Hz, 1H), 7.56 (t, *J* = 7.6 Hz, 1H), 7.46 (d, *J* = 7.6 Hz, 1H), 7.27 (d, *J* = 1.6 Hz, 1H), 4.00 (q, *J* = 5.6 Hz, 2H), 3.39 (t, *J* = 6 Hz, 2H), 2.57 (s, 3H). HR-ESI-MS calcd for [C<sub>16</sub>H<sub>15</sub>N<sub>3</sub>OS<sub>2</sub>Na]<sup>+</sup>: 352.0549; Found: 352.0547.

**8-Bromo-5-fluoro-2-methylquinoline.** A solution of 2-Bromo-5-fluoroaniline (10 g, 52.6 mmol) in 6M HCl (50 mL) and Toluene (50 mL) was refluxed for ~30 min. To this was then added Crotonaldehyde (6.54 mL, 79 mmol) and stirred at reflux for 18 h. The resulting solution was partitioned in a separatory funnel and the organic layer was discarded. The remaining aqueous solution was made basic with 6M NaOH, then extracted with EtOAc. The organic layer was then isolated and dried with MgSO<sub>4</sub>, then filtered and purified via silica gel chromatography eluting a gradient 0-10% EtOAc in Hexanes to afford product as an off-white solid. Yield = 5.096 g (40%). <sup>1</sup>H NMR (400 MHz, CDCl<sub>3</sub>): δ 8.31 (d, *J* = 8.4 Hz, 1H), 7.94 (q, *J* = 5.6 Hz, 1H), 7.40 (d, *J* = 8.4 Hz, 1H), 7.07 (t, *J* = 8.8 Hz, 1H), 2.83 (s, 3H). ESI-MS(+): *m/z* 242.28 [M+H]<sup>+</sup>.

**8-Bromo-5-fluoroquinoline-2-carboxylic acid.** To a solution of 8-Bromo-5-fluoro-2-methylquinoline (2g, 8.33 mmol) in Pyridine (30 mL) was added selenium dioxide (2.77 g, 24.99 mmol) and heated to reflux for 16 h. The resulting solution was then concentrated in vacuo. The crude was taken up in H<sub>2</sub>O and heated to 70 °C for 30 min. The solution was hot filtered in order to remove excess SeO<sub>2</sub> byproduct and afford product as a light tan solid. Yield = 2.25 g (95%). <sup>1</sup>H NMR (400 MHz, CDCl<sub>3</sub>): δ 8.80 (d, *J* = 8.4 Hz, 1H), 8.38 (d, *J* = 8.4 Hz, 1H), 8.25 (q, *J* = 5.2 Hz, 1H), 7.52 (t, *J* = 8.8 Hz, 1H). ESI-MS(-): *m/z* 268.12 [M-H]<sup>-</sup>.

**5-Fluoroquinoline-2-carboxylic acid.** To a solution of 8-Bromo-5-fluoroquinoline-2-carboxylic acid (2.1 g, 7.90 mmol) in MeOH (30 mL) was added 1M NaOH (17.8 mL, 17.8 mmol) followed by Pd(OH)<sub>2</sub>/C (0.277 g, 0.395 mmol,) and allowed to stir at room temperature under a hydrogen atmosphere (balloon) for 2.5 h. The resulting solution was filtered over celite and rinsed with H<sub>2</sub>O and MeOH. The filtrate was recovered and concentrated in vacuo to remove organic solvent. The resulting aqueous solution was then acidified with 1M HCl to make solution slightly acidic. The acidic solution was then extracted with EtOAc. The combined organic layers were dried with MgSO<sub>4</sub> and filtered to remove solids. The filtrate was concentrated to afford product as a tan solid. Yield = 0.389 g (26%). <sup>1</sup>H NMR (400 MHz, Acetone-*d*<sub>6</sub>): δ 8.74 (d, *J* = 8.8 Hz, 1H), 8.31 (d, *J* = 8.4 Hz, 1H), 8.03 (d, *J* = 8.8 Hz, 1H), 7.92 (q, *J* = 6 Hz, 1H), 7.54 (t, *J* = 8 Hz, 1H). ESI-MS(-): *m/z* 190.22 [M-H]<sup>-</sup>.

**5-Fluoro-*N*-(2-(thiazol-2-yl)ethyl)quinoline-2-carboxamide.** To a solution of 5-Fluoroquinoline-2-carboxylic acid (0.15 g, 0.785 mmol) in DMF (5 mL) was added Et<sub>3</sub>N (0.131 mL, 0.942 mmol) followed by HATU (0.358 g, 0.942 mmol) and then 2-(Thiazol-2-yl)ethan-1-amine (0.121 g, 0.942 mmol) and allowed to stir at room temperature for 15 h. To the resulting solution was added sat. NaHCO<sub>3</sub> (aqueous) and allowed to stir for ~10 min. This was then extracted with EtOAc and dried with MgSO<sub>4</sub>, filtered, then concentrated and purified via silica gel chromatography eluting a gradient of 0-50% EtOAc in Hexanes. Yield =

0.1 g (42%). <sup>1</sup>H NMR (400 MHz, CDCl<sub>3</sub>): δ 8.73 (br, 1H), 8.59 (d, *J* = 8.8 Hz, 1H), 8.36 (d, *J* = 8.8 Hz, 1H), 7.91 (d, *J* = 8.8 Hz, 1H), 7.78 (d, *J* = 3.2 Hz, 1H), 7.71-7.66 (m, 1H), 7.30 (d, *J* = 8.8 Hz, 1H), 7.25 (d, *J* = 3.2 Hz, 1H), 4.02 (q, *J* = 6.8 Hz, 1H), 3.43 (t, *J* = 6.8 Hz, 1H). ESI-MS(+): *m/z* 302.11 [M+H]<sup>+</sup>.

**5-((4-Methoxybenzyl)thio)-*N*-(2-(thiazol-2-yl)ethyl)quinoline-2-carboxamide.**

To a solution of 5-Fluoro-*N*-(2-(thiazol-2-yl)ethyl)quinoline-2-carboxamide (0.1 g, 0.332 mmol) in DMF (5 mL) was added *p*-MBSH (0.195 mL, 1.327 mmol) and NaH (0.05 g, 1.327 mmol) then allowed to stir at 140 °C for 22 h. The resulting solution was concentrated in vacuo and purified via silica gel chromatography eluting a gradient of 0-50% EtOAc in Hexanes. Yield = 0.07 g (47%). <sup>1</sup>H NMR (400 MHz, CDCl<sub>3</sub>): δ 8.73 (br, 1H), 8.59 (d, *J* = 8.8 Hz, 1H), 8.36 (d, *J* = 8.8 Hz, 1H), 7.91 (d, *J* = 8.8 Hz, 1H), 7.78 (d, *J* = 3.2 Hz, 1H), 7.71-7.66 (m, 1H), 7.30 (d, *J* = 8.8 Hz, 1H), 7.25 (d, *J* = 3.2 Hz, 1H), 4.02 (q, *J* = 6.8 Hz, 2H), 3.43 (t, *J* = 6.8 Hz, 2H). ESI-MS(+): *m/z* 436.13 [M+H]<sup>+</sup>.

**5,5'-Disulfanediylbis(*N*-(2-(thiazol-2-yl)ethyl)quinoline-2-carboxamide) (68).**

To a solution of 5-((4-Methoxybenzyl)thio)-*N*-(2-(thiazol-2-yl)ethyl)quinoline-2-carboxamide (0.05 g, 0.115 mmol) in TFA (5 mL) was added *m*-Cresol (0.1 g, 0.956 mmol) and refluxed for 22 h. The resulting solution was concentrated in vacuo and purified via silica gel chromatography eluting a gradient of 0-50% EtOAc in Hexanes. Yield = 0.004 g (12%). <sup>1</sup>H NMR (400 MHz, DMSO-*d*<sub>6</sub>): δ 9.21

(t,  $J = 6$  Hz, 1H), 8.66 (d,  $J = 8.8$  Hz, 1H), 8.15 (d,  $J = 8$  Hz, 1H), 8.10 (d,  $J = 8.8$  Hz, 1H), 7.82-7.76 (m, 2H), 7.73 (d,  $J = 3.6$  Hz, 1H), 7.59 (d,  $J = 3.6$  Hz, 1H), 3.76 (q,  $J = 6.8$  Hz, 2H), 3.33 (t,  $J = 6.8$  Hz, 2H). HR-ESI-MS calcd for  $[\text{C}_{30}\text{H}_{24}\text{N}_6\text{O}_2\text{S}_4\text{Na}]^+$ : 651.0736; Found: 651.0736.

**Methyl-5-(((2,2-dimethyl-4,6-dioxo-1,3-dioxan-5-ylidene)methyl)amino)**

**nicotinate.** To a preheated ( $\sim 100$  °C) mixture of 3-Aminopyridine (0.61 g, 4.0 mmol) and Meldrum's acid (0.69 g, 4.8 mmol) was added Triethyl Orthoformate (4.0 mL, 24.0 mmol). The mixture was stirred at 100 °C for 2 h. The reaction proceeded by changing color from yellow to wine red accompanying the formation of yellow precipitate. After cooling to room temperature, the excess liquid of Triethyl Orthoformate was removed via vacuum distillation. The resulting solid was purified via silica gel chromatography eluting a gradient of 30 to 70% EtOAc in  $\text{CH}_2\text{Cl}_2$ . Yield = 1.6 g (88%).  $^1\text{H}$  NMR (400 MHz,  $\text{CDCl}_3$ ):  $\delta$  11.32 (d,  $J = 13.6$  Hz, 1H), 9.09 (s, 1H), 8.75 (s, 1H), 8.68 (d,  $J = 13.6$  Hz, 1H), 8.22 (s, 1H), 3.98 (s, 3H), 1.75 (s, 6H).  $^{13}\text{C}$  NMR (100 MHz,  $\text{CDCl}_3$ ):  $\delta$  165.6, 164.7, 163.1, 152.8, 148.5, 144.10, 134.9, 127.2, 125.3, 105.9, 89.7, 53.1, 27.4. ESI-MS(+):  $m/z$  306.97  $[\text{M}+\text{H}]^+$ .

**Methyl 8-hydroxy-1,5-naphthyridine-3-carboxylate.** To a solution of Methyl-5-(((2,2-dimethyl-4,6-dioxo-1,3-dioxan-5-ylidene)methyl)amino) nicotinate (0.5 g, 1.63 mmol) was added Dowtherm A (150 mL) under nitrogen atmosphere and

heated to 250 °C for 1 h. During the reaction, the color of the solution changed from orange yellow to dark brown. After cooling down to room temperature, the reaction solution was filtered to afford product. The solid was rinsed with Diphenyl Ether and Acetone. Yield = 0.15 g (45%). ESI-MS(+):  $m/z$  205.29 [M+H]<sup>+</sup>.

**Methyl 8-chloro-1,5-naphthyridine-3-carboxylate.** To a solution of Methyl 8-hydroxy-1,5-naphthyridine-3-carboxylate (0.1g, 0.49 mmol) in Toluene (10 mL) was added POCl<sub>3</sub> (0.14 mL, 1.47 mmol) at room temperature. The solution was stirred at 110 °C for 2 h, then allowed to cool to room temperature, which caused formation of a precipitate. The solution and dark solid was quenched with sat. NaHCO<sub>3</sub> and extracted with EtOAc. The combined organic layers were dried over anhydrous Na<sub>2</sub>SO<sub>4</sub>, then filtered and concentrated under reduce pressure. The residue was purified via silica gel chromatography eluting a gradient of 20 to 50% EtOAc in CH<sub>2</sub>Cl<sub>2</sub>. Yield = 0.078 g (71%). <sup>1</sup>H NMR (400 MHz, CDCl<sub>3</sub>): δ 9.49 (t,  $J$  = 2.0 Hz, 1H), 8.95 (d,  $J$  = 2.0 Hz, 1H), 8.86 (d,  $J$  = 4.8 Hz, 1H), 7.77 (d,  $J$  = 4.8 Hz, 1H), 3.99 (s, 3H). <sup>13</sup>C NMR (100 MHz, CDCl<sub>3</sub>): δ 165.0, 151.9, 151.2, 144.3, 144.0, 143.0, 140.2, 127.3, 126.2, 53.1. ESI-MS(+):  $m/z$  223.26 [M+H]<sup>+</sup>

**8-((4-Methoxybenzyl)thio)-1,5-naphthyridine-3-carboxylic acid.** To a solution of Methyl 8-chloro-1,5-naphthyridine-3-carboxylate (0.18 g, 0.81 mmol) in DMF (10 mL) was added *p*-MBSH (0.23 mL, 1.62 mmol) at room temperature. The

solution was stirred for 2 h, then acidified with 1N HCl to pH ~ 4, then concentrated under reduced pressure. The resulting residue was diluted with H<sub>2</sub>O and the solid was collected to give the desired product. Yield = 0.26 g (99%). <sup>1</sup>H NMR (400 MHz, DMSO-*d*<sup>6</sup>): δ 9.30 (s, 1H), 8.84 (d, *J* = 3.2 Hz, 1H), 8.75 (s, 1H), 7.75 (d, *J* = 3.2 Hz, 1H), 7.45 (d, *J* = 6.4 Hz, 2H), 6.92 (d, *J* = 6.4 Hz, 2H), 4.37 (s, 2H), 3.74 (s, 3H). <sup>13</sup>C NMR (125 MHz, DMSO-*d*<sup>6</sup>): δ 166.2, 159.0, 151.9, 150.9, 149.4, 143.1, 141.4, 139.2, 130.7, 128.1, 127.9, 120.5, 114.5, 55.5, 33.8. ESI-MS(+): *m/z* 325.07 [M+H]<sup>+</sup>.

**8-((4-Methoxybenzyl)thio)-*N*-(2-(thiazol-2-yl)ethyl)-1,5-naphthyridine-3-**

**carboxamide.** To a solution of 8-((4-Methoxybenzyl)thio)-1,5-naphthyridine-3-carboxylic acid (0.25 g, 0.77 mmol) in DMF (5 mL) was added 2-(Thiazol-2-yl)ethan-1-amine (0.11 g, 0.84 mmol), Pyridine (0.25 mL, 3.06 mmol), HOBT (0.24 g, 1.54 mmol) and EDC (0.3 g, 1.54 mmol) at room temperature. The solution was stirred for 2 h, then concentrated under reduced pressure. The resulting residue was diluted with H<sub>2</sub>O and extracted with EtOAc. The combined organic layers were dried over anhydrous Na<sub>2</sub>SO<sub>4</sub>, filtered and concentrated. The resulting residue was purified via silica gel chromatography eluting a gradient of 30 to 70% EtOAc in CH<sub>2</sub>Cl<sub>2</sub>. Yield = 0.17 g (51%). <sup>1</sup>H-NMR (400 MHz, DMSO-*d*<sup>6</sup>) δ 9.24 (s, 1H), 9.18 (t, *J* = 4.4 Hz, 1H), 8.83 (d, *J* = 4.0 Hz, 1H), 7.74 (d, *J* = 2.8 Hz, 1H), 7.72 (d, *J* = 4.0 Hz, 1H), 7.60 (d, *J* = 2.8 Hz, 1H), 7.45 (d, *J* = 6.8 Hz, 2H), 6.92 (d, *J* = 6.8 Hz, 2H), 4.36 (s, 2H), 3.74 (s, 3H), 3.72-3.66 (m, 2H), 3.34-

3.29 (m, 2H).  $^{13}\text{C}$  NMR (125 MHz,  $\text{DMSO-}d^6$ ):  $\delta$  167.5, 164.7, 159.0, 151.7, 150.8, 148.6, 142.8, 142.3, 141.5, 136.3, 131.0, 130.7, 127.9, 120.2, 120.1, 114.5, 55.5, 33.7, 32.7. ESI-MS(+):  $m/z$  437.07  $[\text{M}+\text{H}]^+$ .

**8-Mercapto-*N*-(2-(thiazol-2-yl)ethyl)-1,5-naphthyridine-3-carboxamide (69).**

To a solution of 8-((4-Methoxybenzyl)thio)-*N*-(2-(thiazol-2-yl)ethyl)-1,5-naphthyridine-3-carboxamide (0.14 g, 0.32 mmol) in TFA (20 mL) was added *m*-Cresol (0.17 mL, 1.60 mmol) at room temperature. The reaction was then heated at reflux for 16 h, then concentrated under reduced pressure and diluted with the EtOAc. The solution was neutralized with sat.  $\text{NaHCO}_3$ , which caused an orange red solid to precipitate. The solid was collected via filtration and washed with  $\text{H}_2\text{O}$  and Acetone to afford product. Yield = 0.087 g (86%).  $^1\text{H}$  NMR (400 MHz,  $\text{DMSO-}d^6$ ):  $\delta$  12.97 (br, 1H), 9.19 (t,  $J = 4.4$  Hz, 1H), 9.09 (s, 1H), 8.44 (s, 1H), 7.92 (d,  $J = 5.2$  Hz, 1H), 7.75 (d,  $J = 2.4$  Hz, 1H), 7.62 (d,  $J = 2.4$  Hz, 1H), 7.50 (d,  $J = 5.2$  Hz, 1H), 3.72-3.66 (m, 2H), 3.34-3.29 (m, 2H).  $^{13}\text{C}$  NMR (125 MHz,  $\text{DMSO-}d^6$ ):  $\delta$  167.4, 164.3, 147.0, 146.6, 142.8, 134.5, 133.0, 132.1, 129.1, 128.6, 120.3, 32.6. HR-ESI-MS calcd for  $[\text{C}_{14}\text{H}_{12}\text{N}_4\text{OS}_2\text{Na}]^+$ : 339.0345; Found: 339.0348.

**Rpn11 Activity Assay.** To measure Rpn11 activity, a synthetic peptide substrate, termed Ub4-pepOG, was engineered. This substrate consists of four linear ubiquitins connected to a short peptide sequence containing a unique

cysteine to which is conjugated a single Oregon Green 488 fluorophore molecule. The peptide bond between the fourth ubiquitin and the downstream peptide is cleaved by 26S proteasome in vitro, which can be observed by SDS-PAGE and fluorescent polarization measurement. The fluorescent peptide released upon cleavage of Ub4-pepOG consists of only 30 amino acids; therefore the decrease of polarization observed in fluorescence polarization assays arose mainly from deubiquitination of the peptide and could be observed even when the proteolytic activity of the 20S CP was inhibited. The fluorescence polarization assay was performed as previously described<sup>13</sup> at 30 °C in a low-volume 384 well solid black plate. Briefly, components were added to each well in the following sequence: 1) 5 µL inhibitor compound in buffer containing 3% DMSO or 3% DMSO in buffer as a control; and 2) 5 µL of 26S proteasome (Enzo life sciences) in buffer (20 nM proteasome was pre-incubated with epoxomicin at room temperature for 1 hour, then dilute 10-fold in 1x Assay Buffer). Substrate (5 µL, 3 nM Ub4-pepOG) in buffer was then added to initiate the reaction. To evaluate the effects of Zn(cyclen)<sup>2+</sup> on Rpn11 activity, the assay was carried out in the same manner as described with the addition of 100 µM Zn(cyclen)<sup>2+</sup> in the titration reaction. Fluorescence polarization was measured using a plate reader with excitation at 480 nm and emission at 520 nm. To calculate the IC<sub>50</sub> of Rpn11 inhibitors, eight to twelve-point titration was performed for each compound, up to a concentration of 100 µM. Rpn11 activity was normalized to the DMSO control and fitted using a dose-response curve. Reported IC<sub>50</sub> value represents the average value

obtained from at least three independent measurements, with the standard deviation reported as the error.

**CSN5 Activity Assay.** A fluorescent substrate termed SCF<sup>skp2</sup>-Nedd8OG was engineered to measure Csn5 activity in vitro.<sup>14</sup> To produce this substrate, Nedd8 containing a unique N-terminal cysteine was labeled with Oregon Green 488, and then conjugated to SCF<sup>skp2</sup> as previously described.<sup>28</sup> This assay measures the decrease in fluorescence polarization due to the decrease in apparent molecular weight of the Oregon Green fluorophore (from the ~175 kDa substrate to ~9kDa Nedd8OG) as a result of Csn5-dependent cleavage of the isopeptide bond which links Nedd8OG to SCF<sup>skp2</sup>. Assays were performed in a low-volume 384 well solid black plate comprising equal volumes of compound, substrate (SCF<sup>skp2</sup>-Nedd8OG) and enzyme (Csn5). Fluorescence polarization was recorded using the same protocol as for the Rpn11 activity assay at 30 °C. IC<sub>50</sub> was calculated as described above. Reported IC<sub>50</sub> value represents the average value obtained from at least three independent measurements, with the standard deviation reported as the error.

**AMSH Activity Assay.** AMSH is known to selectively cleave diubiquitin linked via K63. A substrate termed DiUb<sup>K63</sup>TAMRA was purchased from Boston Biochem to assay AMSH activity in vitro. DiUb<sup>K63</sup>TAMRA was labeled with the FRET pair TAMRA/QXL. Upon AMSH cleavage, TAMRA was separated from

the quencher QXL which resulted in an increase of TAMRA fluorescence intensity, which was monitored using a fluorescence plate reader (excitation at 540 nm and emission at 590 nm). The assay was performed in a low-volume 384 well solid black plate at 30 °C and analyzed as described above. Reported IC<sub>50</sub> value represents the average value obtained from at least three independent measurements, with the standard deviation reported as the error.

**HDAC1 and 6 Activity Assay.** HDAC1 and 6 were purchased from BPS Bioscience (BPS Bioscience catalog #50051 and 50006) and the assay was carried out as instructed by manufacturer. The enzyme was diluted with 25 mM Tris-Cl, 137 mM NaCl, 2.7 mM KCl, 1 mM MgCl<sub>2</sub>, 0.1 mg/mL BSA, pH 8.0 buffer and its activity was measured by utilizing Substrate 3 (BPS Bioscience catalog #50037). The assays were carried out in black, low binding NUNC 96-well plates. Each well contained a volume of 50 µL including buffer, HDAC (3.8 ng/well of HDAC-1, 50 ng/well of HDAC-6), inhibitor, and substrate (20 µM). Prior to adding substrate, the plate was preincubated for 5 min. Upon addition of substrate, the plate was incubated at 37 °C for 30 min. At this point, HDAC assay developer (50 µL, BPS Bioscience catalog #50030) was added to each well and the plate was incubated for 15 min at room temperature. The fluorescence was recorded with a BioTek FLx 800 microplate reader. The measured fluorescence was compared for samples versus controls containing no inhibitor (0% inhibition). Reported IC<sub>50</sub>

value represents the average value obtained from at least three independent measurements, with the standard deviation reported as the error.

**MMP Activity Assay.** MMP-2, MMP-12, and OmniMMP fluorogenic substrate (P-126) were purchased from Enzo Life Sciences (Farmingdale, NY). The assay was carried out in white NUNC 96-well plates as previously described.<sup>29</sup> Each well contained a volume of 90  $\mu$ L including buffer (50 mM HEPES, 10 mM CaCl<sub>2</sub>, 0.05% Brij-35, pH 7.5), human recombinant MMP (1.16 U of MMP-2), and the fragment solution. The enzyme and inhibitor were incubated for 30 min at 37 °C, the reaction was then initiated by the addition of 10  $\mu$ L (100  $\mu$ L total volume of wells) of the fluorogenic OmniMMP substrate (4  $\mu$ M final concentration, Mca-Pro-Leu-Gly-Leu-Dpa-Ala-Arg-NH<sub>2</sub>-AcOH). Fluorescence measurements were recorded using a Bio-Tek FLx800 fluorescence plate reader every minute for 20 min with excitation and emission wavelengths at 320 and 400 nm, respectively. The rate of fluorescence increase was compared for samples versus negative controls (no inhibitor, arbitrarily set as 100% activity). Reported IC<sub>50</sub> value represents the average value obtained from at least three independent measurements, with the standard deviation reported as the error.

**hCAII Activity Assay.** hCAII was expressed and purified as previously reported.<sup>31</sup> Assays were carried out in 50 mM HEPES (pH 8.0). A BioTek Precision XS microplate sample processor was utilized. The compounds were

incubated with protein (final concentrations of 100 nM for hCAII) for 10 min at 25 °C. A substrate (p-nitrophenylacetate; final concentration of 500 μM) was added, and hCAII-catalyzed cleavage was monitored by the increase in absorbance at 405 nm corresponding to formation of the p-nitrophenolate anion. The initial linear reaction rate was compared to that of wells containing no inhibitor (0% inhibition) and no protein (100% inhibition). The rate of non-hCAII-catalyzed PNPA hydrolysis in the presence of inhibitor was subtracted from each trial before determination of the percent inhibition. Reported IC<sub>50</sub> value represents the average value obtained from at least three independent measurements, with the standard deviation reported as the error.

**Ub<sup>G76V</sup>-GFP degradation assay.** To determine the potency of Rpn11 inhibitor in cells, a reporter degradation assay was employed. Briefly, stably transfected HeLa cells expressing Ub<sup>G76V</sup>-GFP were treated with the reversible proteasome inhibitor MG132 at 37 °C incubator with 5% CO<sub>2</sub> in air, which increased cellular levels of Ub<sup>G76V</sup>-GFP to yield a detectable fluorescent signal. After 4 h, MG132 was removed and a cycloheximide (CHX) chase was initiated with or without varying concentrations of inhibitor compound at 37 °C with 5% CO<sub>2</sub> in air. Reporter degradation, monitored by the decay of GFP fluorescence, was measured to quantify Rpn11 inhibition using high throughput microscopy. The rate of fluorescence decrease was normalized to a DMSO control and analyzed using dose-response equation. Reported IC<sub>50</sub> value represents the average

value obtained from at least three independent measurements, with the standard deviation reported as the error.

**Cytotoxicity assay.** 293T and A549 cell lines were cultured in DMEM with 10% FBS in white, clear-bottom tissue culture-treated 96-well plates. Cells were treated with different concentrations of inhibitor compounds in triplicates for 72 h at 37 °C with 5% CO<sub>2</sub> in air. CellTiter-Glo (Promega, Madison, WI) reagent was added to the 96 well plates to measure cell viability. Luminescence values were measured in PHERAstar microplate reader (BMG labtech, Ortenberg, Germany). Collected data was normalized to DMSO control and fit to a dose-response equation to determine IC<sub>50</sub> values. Reported IC<sub>50</sub> value represents the average value obtained from at least three independent measurements, with the standard deviation reported as the error.

### 3.5 Acknowledgements

Texts, schemes, and figures in the chapter are reprints of the materials published in the following paper: Christian Perez, Jing Li, Francesco Parlati, Matthieu Rouffet, Yuyong Ma, Andrew L. Mackinnon, Tsui-Fen Chou, Raymond J. Deshaies and Seth M. Cohen, "Discovery of an Inhibitor of the Proteasome Subunit Rpn11" *J. Med. Chem.* **2017**, *60*, 1343-1361. The dissertation author was the primary researcher and author. The permission to reproduce this paper was granted by the American Chemical Society. Copyright 2017, American Chemical Society.

### 3.6 References

1. Paramore, A.; Frantz, S., Bortezomib. *Nat. Rev. Drug Discov.* **2003**, *2* (8), 611-612.
2. Adams, J., The Development of Proteasome Inhibitors as Anticancer Drugs. *Cancer Cell* **2004**, *5* (5), 417-421.
3. Desvergne, A.; Genin, E.; Marechal, X.; Gallastegui, N.; Dufau, L.; Richy, N.; Groll, M.; Vidal, J.; Reboud-Ravaux, M., Dimerized Linear Mimics of a Natural Cyclopeptide (TMC-95A) Are Potent Noncovalent Inhibitors of the Eukaryotic 20S Proteasome. *J. Med. Chem.* **2013**, *56* (8), 3367-3378.
4. van der Linden, W. A.; Willems, L. I.; Shabaneh, T. B.; Li, N.; Ruben, M.; Florea, B. I.; van der Marel, G. A.; Kaiser, M.; Kisselev, A. F.; Overkleeft, H. S., Discovery of a Potent and Highly Beta 1 Specific Proteasome Inhibitor from a Focused Library of Urea-Containing Peptide Vinyl Sulfones and Peptide Epoxyketones. *Org. Biomol. Chem.* **2012**, *10* (1), 181-194.
5. Ozcan, S.; Kazi, A.; Marsilio, F.; Fang, B.; Guida, W. C.; Koomen, J.; Lawrence, H. R.; Sebt, S. M., Oxadiazole-isopropylamides as Potent and Noncovalent Proteasome Inhibitors. *J. Med. Chem.* **2013**, *56* (10), 3783-3805.
6. Kawamura, S.; Unno, Y.; List, A.; Mizuno, A.; Tanaka, M.; Sasaki, T.; Arisawa, M.; Asai, A.; Groll, M.; Shuto, S., Potent Proteasome Inhibitors Derived from the Unnatural cis-Cyclopropane Isomer of Belactosin A: Synthesis, Biological Activity, and Mode of Action. *J. Med. Chem.* **2013**, *56* (9), 3689-3700.
7. Kubiczkova, L.; Pour, L.; Sedlarikova, L.; Hajek, R.; Sevcikova, S., Proteasome inhibitors - molecular basis and current perspectives in multiple myeloma. *J. Cell. Mol. Med.* **2014**, *18* (6), 947-961.
8. Crawford, L. J.; Walker, B.; Irvine, A. E., Proteasome Inhibitors in Cancer Therapy. *J. Cell Commun. Signal.* **2011**, *5* (2), 101-110.
9. Moreau, P.; Richardson, P. G.; Cavo, M.; Orłowski, R. Z.; San Miguel, J. F.; Palumbo, A.; Harousseau, J. L., Proteasome Inhibitors in Multiple Myeloma: 10 Years Later. *Blood* **2012**, *120* (5), 947-959.

10. Kisselev, A. F.; van der Linden, W. A.; Overkleeft, H. S., Proteasome Inhibitors: An Expanding Army Attacking a Unique Target. *Chem. Biol.* **2012**, *19* (1), 99-115.
11. Kisselev, A. F.; Goldberg, A. L., Proteasome Inhibitors: From Research Tools to Drug Candidates. *Chem. Biol.* **2001**, *8* (8), 739-758.
12. Anchoori, R. K.; Karanam, B.; Peng, S. W.; Wang, J. W.; Jiang, R.; Tanno, T.; Orlowski, R. Z.; Matsui, W.; Zhao, M.; Rudek, M. A.; Hung, C. F.; Chen, X.; Walters, K. J.; Roden, R. B. S., A bis-Benzylidene Piperidone Targeting Proteasome Ubiquitin Receptor RPN13/ADRM1 as a Therapy for Cancer. *Cancer Cell* **2013**, *24* (6), 791-805.
13. Lim, H. S.; Archer, C. T.; Kodadek, T., Identification of a Peptoid Inhibitor of the Proteasome 19S Regulatory Particle. *J. Am. Chem. Soc.* **2007**, *129* (25), 7750-7751.
14. Tian, Z.; D'Arcy, P.; Wang, X.; Ray, A.; Tai, Y. T.; Hu, Y. G.; Carrasco, R. D.; Richardson, P.; Linder, S.; Chauhan, D.; Anderson, K. C., A Novel Small Molecule Inhibitor of Deubiquitylating Enzyme USP14 and UCHL5 Induces Apoptosis in Multiple Myeloma and Overcomes Bortezomib Resistance. *Blood* **2014**, *123* (5), 706-716.
15. Lim, H. S.; Cai, D.; Archer, C. T.; Kodadek, T., Periodate-Triggered Cross-Linking Reveals Sug2/Rpt4 as the Molecular Target of a Peptoid Inhibitor of the 19S Proteasome Regulatory Particle. *J. Am. Chem. Soc.* **2007**, *129* (43), 12936-12937.
16. Lauinger, L.; Li, J.; Shostak, A.; Cemel, I. A.; Ha, N. T.; Zhang, Y. R.; Merkl, P. E.; Obermeyer, S.; Stankovic-Valentin, N.; Schafmeier, T.; Wever, W. J.; Bowers, A. A.; Carter, K. P.; Palmer, A. E.; Tschochner, H.; Melchior, F.; Deshaies, R. J.; Brunner, M.; Diernfellner, A., Thiolutin is a zinc chelator that inhibits the Rpn11 and other JAMM metalloproteases. *Nat. Chem. Biol.* **2017**, *13* (7), 709-+.
17. Cromm, P. M.; Crews, C. M., The Proteasome in Modern Drug Discovery: Second Life of a Highly Valuable Drug Target. *Acs Central Sci* **2017**, *3* (8), 830-838.

18. Guterman, A.; Glickman, M. H., Complementary Roles for Rpn11 and Ubp6 in Deubiquitination and Proteolysis by the Proteasome. *J. Biol. Chem.* **2004**, *279* (3), 1729-1738.
19. Yao, T. T.; Cohen, R. E., A Cryptic Protease Couples Deubiquitination and Degradation by the Proteasome. *Nature* **2002**, *419* (6905), 403-407.
20. Ambroggio, X. I.; Rees, D. C.; Deshaies, R. J., JAMM: A Metalloprotease-like Zinc Site in the Proteasome and Signalosome. *PLOS Biol.* **2004**, *2* (1), 113-119.
21. Cope, G. A.; Suh, G. S. B.; Aravind, L.; Schwarz, S. E.; Zipursky, S. L.; Koonin, E. V.; Deshaies, R. J., Role of Predicted Metalloprotease Motif of Jab1/Csn5 in Cleavage of Nedd8 From Cul1. *Science* **2002**, *298* (5593), 608-611.
22. Verma, R.; Aravind, L.; Oania, R.; McDonald, W. H.; Yates, J. R.; Koonin, E. V.; Deshaies, R. J., Role of Rpn11 Metalloprotease in Deubiquitination and Degradation by the 26S Proteasome. *Science* **2002**, *298* (5593), 611-615.
23. Li, J.; Yakushi, T.; Parlati, F.; Mackinnon, A. L.; Perez, C.; Ma, Y. Y.; Carter, K. P.; Colayco, S.; Magnuson, G.; Brown, B.; Nguyen, K.; Vasile, S.; Suyama, E.; Smith, L. H.; Sergienko, E.; Pinkerton, A. B.; Chung, T. D. Y.; Palmer, A. E.; Pass, I.; Hess, S.; Cohen, S. M.; Deshaies, R. J., Capzimin is a potent and specific inhibitor of proteasome isopeptidase Rpn11. *Nat. Chem. Biol.* **2017**, *13* (5), 486-+.
24. National Center for Biotechnology Information. PubChem BioAssay Database; AID=588493, <https://pubchem.ncbi.nlm.nih.gov/bioassay/588493>. (accessed February 23, 2018).
25. National Center for Biotechnology Information. PubChem BioAssay Database; AID=651999, <https://pubchem.ncbi.nlm.nih.gov/bioassay/651999>. (accessed February 23, 2018).
26. Duda, D. M.; Borg, L. A.; Scott, D. C.; Hunt, H. W.; Hammel, M.; Schulman, B. A., Structural Insights Into NEDD8 Activation of Cullin-RING Ligases: Conformational Control of Conjugation. *Cell* **2008**, *134* (6), 995-1006.

27. Chou, T. F.; Deshaies, R. J., Quantitative Cell-based Protein Degradation Assays to Identify and Classify Drugs That Target the Ubiquitin-Proteasome System. *J. Biol. Chem.* **2011**, *286* (19), 16546-16554.

## **Chapter 4: Discovery of Novel Glyoxalase 1 Inhibitors**

## 4.1 Introduction

As discussed in Chapter 1, GLO1 is a homodimeric  $Zn^{2+}$ -dependent isomerase involved in the detoxification of reactive MG.<sup>1-2</sup> It was first proposed in 1971 that inhibitors of the glyoxalase system would function as antitumor agents by inducing high concentrations of MG, a GLO1 substrate.<sup>3-5</sup> During the following decades several novel GLO1 inhibitors were discovered, primarily focused for oncology indications; however, no GLO1 inhibitors have entered clinical trials.<sup>3-11</sup> Recent reports have examined GLO1 inhibitors to treat other illnesses, specifically diabetes and psychiatric conditions.<sup>12-21</sup>

Several natural products and natural product derivatives have been reported as inhibitors for GLO1. Glutathione-based inhibitors were among the first GLO1 inhibitors reported with a compound containing a hydroxamic acid MBP (**AHC-GSH**, Figure 1-6) being the first “tight-binding” inhibitor to be reported.<sup>8, 22</sup> These glutathione mimics have poor membrane permeability and need to be formulated as the ester prodrugs in order to achieve membrane penetration.<sup>4</sup> **AHC-GSH** prodrug analogs have demonstrated some efficacy in vivo, but suffer from rapid clearance (in esterase deficient mice) and have a narrow therapeutic window.<sup>23</sup> Both the hydroxamic acid MBP and glutathione origins of **AHC-GSH**, and its analogs, make these molecules unsuitable as viable drug candidates. A second class of reported inhibitors are flavonoids and flavonoid analogs which tend to coordinate the catalytic metal of GLO1 via a catechol moiety.<sup>7, 9, 24-28</sup> Methyl gerfelin (**M-GFN**) was reported as a potent

inhibitor of GLO1 within the flavonoid class (Figure 1-6).<sup>27</sup> Lastly, a N-hydroxypyridinone (**Chugai-3d**, Figure 1-6) based inhibitor reported by Chugai Pharmaceuticals shows an excellent IC<sub>50</sub> value of 11 nM.<sup>29</sup> However, no in vivo studies or clinical trials have been reported with **Chugai-3d**. The majority of GLO1 inhibitors have been designed and investigated for oncology indications and may not be suitable candidates for targets affecting diabetes or psychiatric diseases. Hence, one motivation for the work described in this chapter was to develop non-hydroxamate, non-glutathione derived GLO1 inhibitors that may be used for indications other than oncology.

Similar to the Rpn11 study discussed in Chapter 2, for the discovery of a novel GLO1 inhibitor, a FBDD approach was utilized. The MBP library was screened against GLO1 utilizing a previously reported assay.<sup>30</sup> The library was screened at two different concentrations and both screens yielded multiple hits. In this chapter, two hits identified from this screen are discussed. Additionally, the design, rationale, and synthesis of analogs of these hits is described.

## **4.2 Results and Discussion**

### **4.2.1 Screening of the MBP Library**

As described in Chapter 1 and 2, the MBP library utilized in this study is comprised of fragments which are small (MW <300 Da) and have known or predictable metal-binding motif (Figure 1-1).<sup>31</sup> To identify MBP hits that can serve as initial building blocks for GLO1 inhibitor design, a second generation

MBP library containing 240 fragments was screened against GLO1 utilizing a previously reported assay.<sup>30</sup> The assay was performed in a 96-well plate format using a colorimetric output that measures the isomerization of a hemithioacetal, formed by glutathione and methylglyoxal, to a lactic acid thioester.<sup>30</sup> The MBP library was initially screened at a fragment concentration of 200  $\mu$ M yielding >50 unique hits displaying >50% inhibition (Figure 4-1). A second assay screen at a lower fragment concentration of 50  $\mu$ M produced 25 distinct hits (Figure 4-2). From the second screen three fragments were chosen for inhibitor development (Figure 4-3).

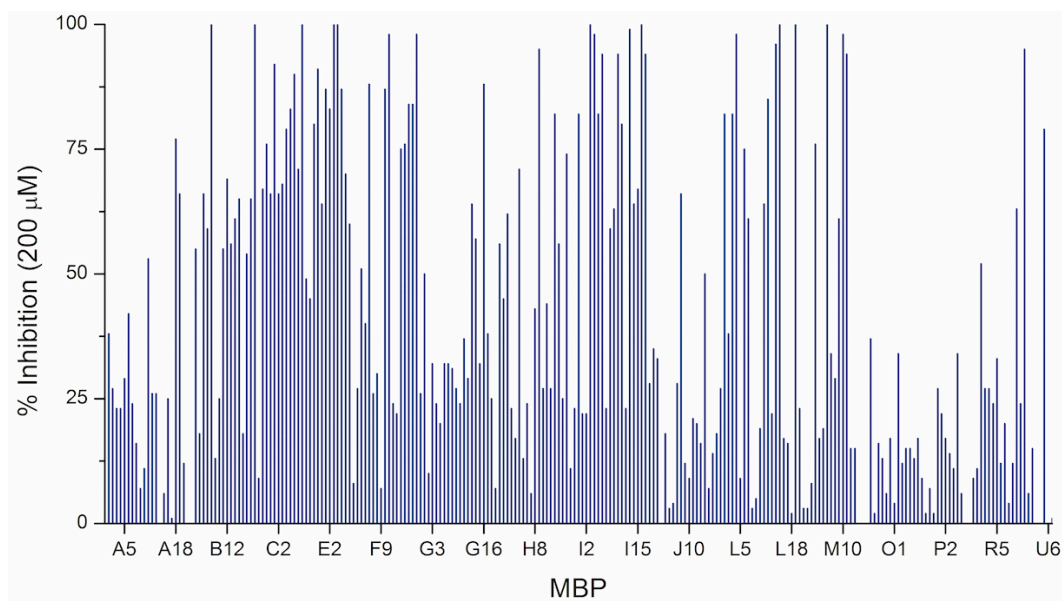
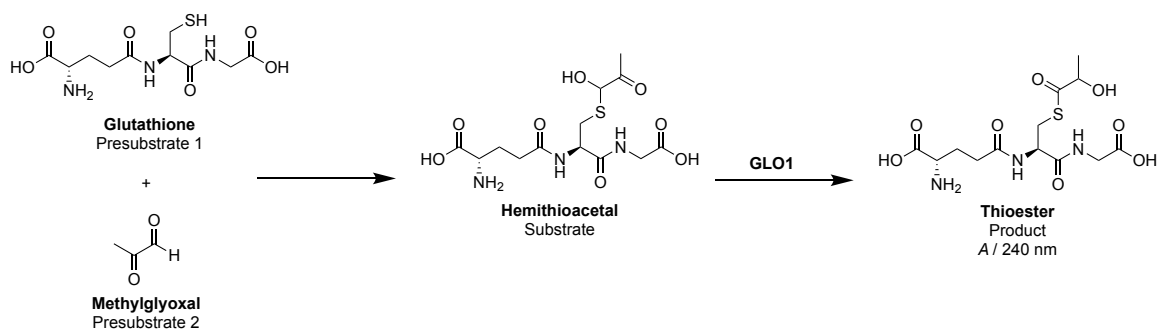


**Figure 4-1.** Reaction scheme depicting the GLO1 assay (top) screening results of the MBP library against GLO1 using a colorimetric assay (bottom). Lines represent percent enzyme inhibition for a given MBP fragment at a concentration of 200  $\mu\text{M}$ .

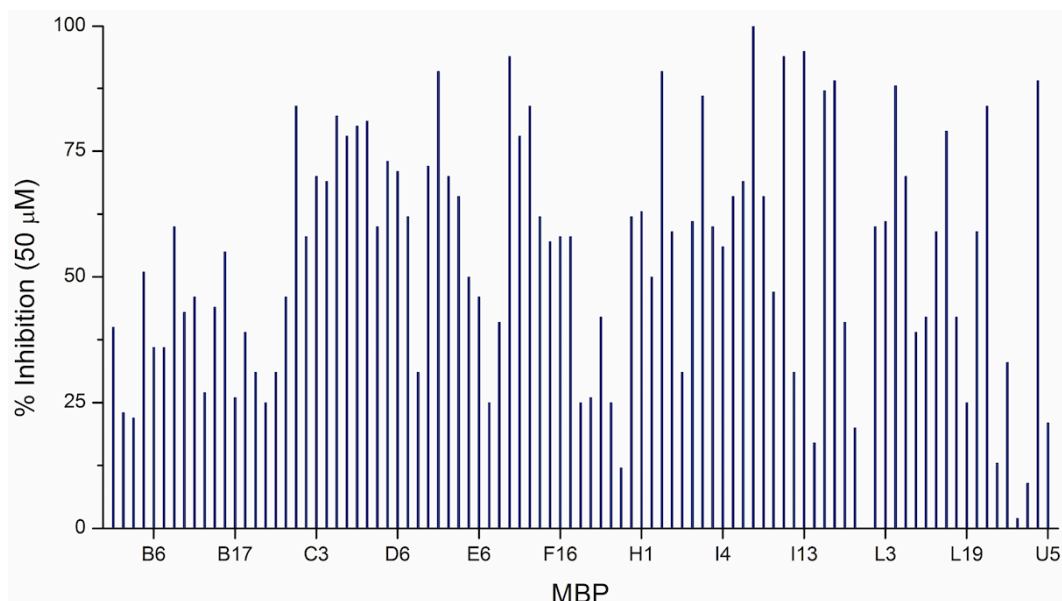


**Figure 4-2.** Screening results of the MBP library against GLO1 using a colorimetric assay. Lines represent percent enzyme inhibition for a given MBP fragment at a concentration of 50  $\mu\text{M}$ .

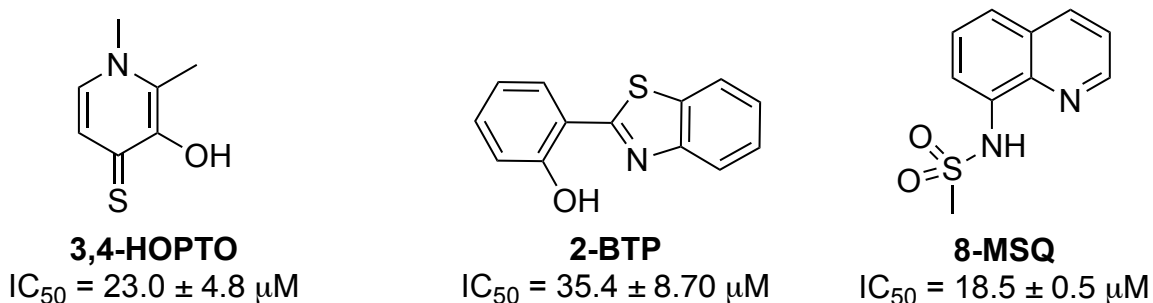


**Figure 4-3.** Molecular structures of the three lead fragment hits from the MBP library screen. MBP acronyms and  $\text{IC}_{50}$  values against GLO1 are shown.

The three fragments selected for further development were: 3-hydroxy-1,2-dimethylpyridine-4(1*H*)-thione (**3,4-HOPTO**), 2-(benzo[*d*]thiazol-2-yl)phenol (**2-BTP**), and 8-(methylsulfonyl amino)quinoline (**8-MSQ**, Chapter 5). These MBPs showed essentially complete inhibition at both 200 and 50  $\mu\text{M}$

concentrations, and were determined to have IC<sub>50</sub> values (using the same assay) of 23.0±4.8, 35.4±8.7, and 18.5±0.5 μM respectively (Figure 4-3).

#### 4.2.2 Synthesis, Computational Docking, and Evaluation of a 3,4-HOPTO Library

In order to gain insight into how the hit fragments (Figure 4-3) were binding to GLO1, a computational model was sought. Modeling studies were performed using the Molecular Operating Environment (MOE) software suite, which can account for flexible protein domains and can assist in pharmacophore modeling and SAR studies.<sup>32</sup> Using a crystal structure of GLO1 (PDB: 3VW9) an inhibitor pharmacophore model was generated. The crystal structure selected has a resolution of 1.47 Å and has the **Chugai-3d** inhibitor bound to the active site of GLO1 (Figure 1-6 and 4-4). Structural analysis of this crystal structure revealed a Zn<sup>2+</sup> metal center and two distinct pockets within the GLO1 active site: a hydrophobic and a GSH-binding pocket. The hydrophobic pocket consists of residues Cys60, Phe62, Ile88, Met179, Leu182, and Met183. The GSH-binding pocket consists of Phe67, Leu69, Met157, Phe162, as well as the conserved water network (Figure 4-4). The catalytic Zn<sup>2+</sup> has an octahedral geometry and is coordinated by Gln33, Glu99, Glu172, and His126, with the 5<sup>th</sup> and 6<sup>th</sup> coordination sites occupied by the *O,O* donor atoms of the **Chugai-3d** compound (Figure 4-4). The **Chugai-3d** binding affinity is attributed to significant contacts with both the hydrophobic and GSH-binding pockets, as well as the water network. The 6-phenyl moiety of **Chugai-3d** occupies the hydrophobic pocket

and engages in edge-to-face  $\pi$  interactions with Phe62 and additional hydrophobic contacts with Met179 and Met183 (Figure 4-4). The 7-azaindole forms an edge-to-face  $\pi$  interaction with Phe67 and a hydrophobic contact with Leu69 (Figure 4-4). Additionally, the 7-azaindole's 7-nitrogen is directly facing a water molecule and engaging in a hydrogen bond. The binding conformation and the critical contacts by **Chugai-3d** to GLO1, allowed for the development of a pharmacophore model.

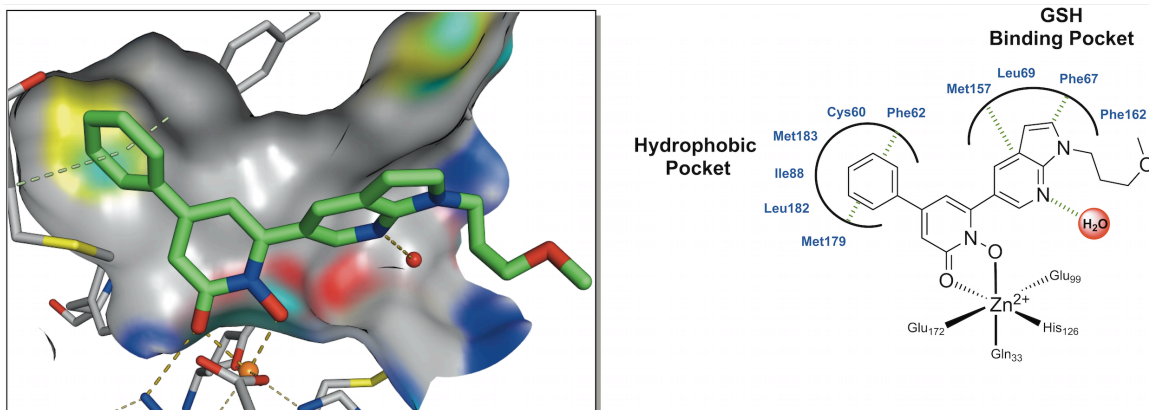


**Figure 4-4.** Superpositioned pose of **3,4-HOPTO** coordinating to the  $Zn^{2+}$  ion the GLO1 active site (*left*) and chemical illustration (*right*). A surface outlining the active site pockets is shown in gray.  $Zn^{2+}$  ion is depicted as an orange sphere and water molecule as a red sphere.

Screening of the MBP library yielded several hits, among them was **3,4-HOPTO** (Figure 4-3). This fragment is structurally very similar to the MBP found in the **Chugai-3d** compound; however, instead of an *O,O* donor set, **3,4-HOPTO** contains a *O,S* set of donor atoms. Although there is a difference in the Lewis basicity between these set of donors, it was assumed that both the **3,4-HOPTO** and **Chugai-3d** MBPs might bind the  $Zn^{2+}$  ion in a similar orientation and

geometry. The **3,4-HOPTO** fragment has several positions on the heterocycle amenable for derivatization. The optimal point(s) of attachment were determined based on computational modeling and structural studies. A binding model for **3,4-HOPTO** was obtained through superposition of the fragment into the GLO1 active site and superimposing the coordinating atoms (*O,S*) of **3,4-HOPTO** with those of the bound **Chugai-3d** (*O,O*) inhibitor (Figure 4-5). The analysis of this model prompted the design and synthesis of a library of **3,4-HOPTO** analogs. The model predicted that substitutions at the 1-position (endocyclic oxygen, Scheme 4-1 and Figure 4-5) with aromatic functional groups (Table 4-1), would facilitate interactions with Phe62, Met 179 and Met182 (similar to **Chugai-3d**) within the hydrophobic pocket. An efficient synthetic route for making analogs of the **3,4-HOPTO** fragment was achieved through a two-step route as shown in Scheme 4-1. Maltol was utilized as the starting material, where the exocyclic carbonyl oxygen was substituted to a sulfur atom in the presence of phosphorus pentasulfide to form thiomaltol. Thiomaltol underwent a dehydration reaction via irradiation in a microwave reactor under acidic conditions along with a suitable primary amine to yield compounds **70-84**.

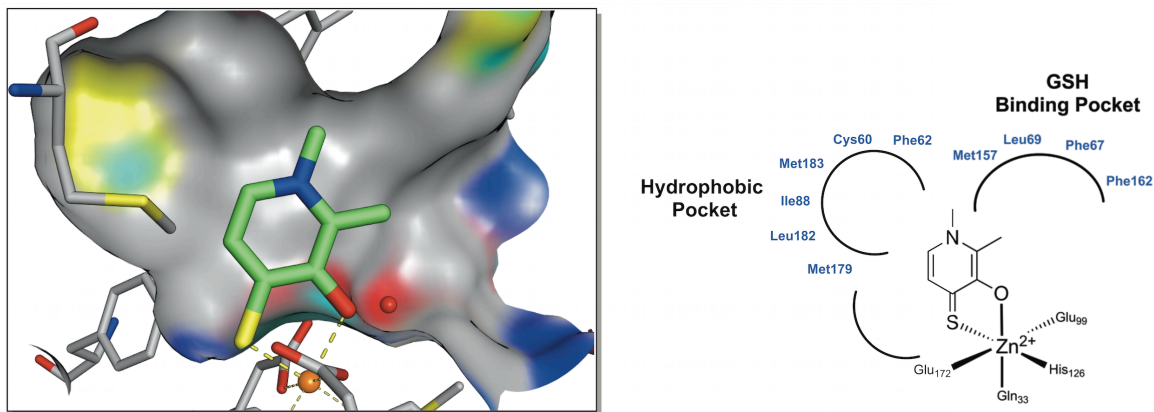
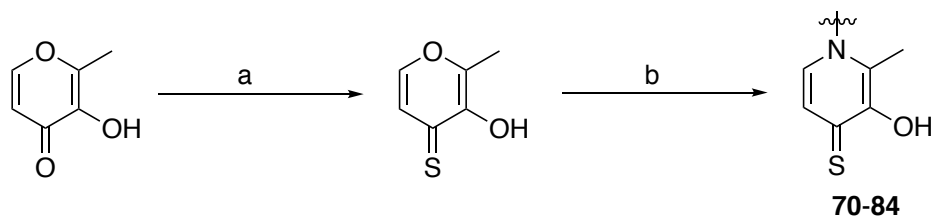
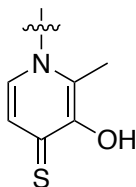


**Figure 4-5.** Superpositioned pose of **3,4-HOPTO** coordinating to the  $\text{Zn}^{2+}$  ion in the GLO1 active site (*left*) and chemical illustration (*right*). A surface outlining the active site pockets is shown in gray.  $\text{Zn}^{2+}$  ion is depicted as an orange sphere and water molecule as a red sphere.



**Scheme 4-1.** Synthetic route for 3-hydroxy-2-methylpyridine-4(1*H*)-thione analogs. Reagents and conditions: (a)  $\text{P}_2\text{S}_5$ , HMDSO, toluene, 110 °C, 8 h; (b) amine, AcOH,  $\text{H}_2\text{O}$ , EtOH, 165 °C (microwave reactor), 1 h.

**Table 4-1.** Inhibitory activity against GLO1 for **3,4-HOPTO** derivatives.



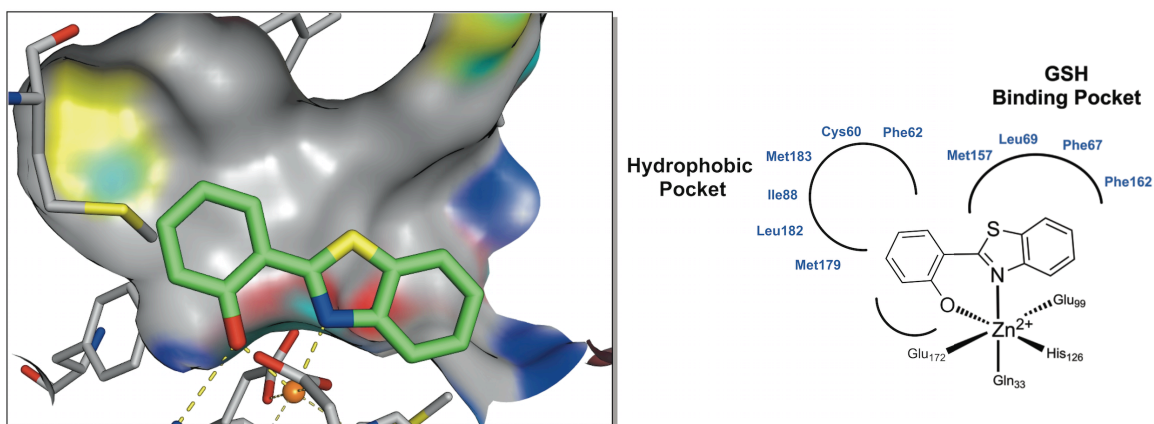
Cmpd	Structure	IC <sub>50</sub> (μM)	Cmpd	Substituent	IC <sub>50</sub> (μM)
<b>3,4-HOPTO</b>	Me	22.9 ± 4.8	<b>77</b>		3.6 ± 0.1
<b>70</b>		11.3 ± 3.1	<b>78</b>		8.4 ± 0.1
<b>71</b>		10.9 ± 0.1	<b>79</b>		12.5 ± 2.9
<b>72</b>		17.2 ± 2.5	<b>80</b>		12.4 ± 1.4
<b>73</b>		15.3 ± 1.5	<b>81</b>		5.3 ± 0.6
<b>74</b>		20.2 ± 0.6	<b>82</b>		9.1 ± 0.1
<b>75</b>		16.6 ± 1.9	<b>83</b>		11.3 ± 2.5
<b>76</b>		22.6 ± 5.0	<b>84</b>		3.8 ± 0.5

A series of aromatic amines were coupled to thiomaltol to yield compounds **70-84**. Addition of functionality at the 1-position only resulted in modest increases in activity, relative to **3,4-HOPTO** (Table 4-1). Compounds with phenyl or heterocycles (**70-76**) only increased activity moderately, with the best compounds increasing only about about 2-fold. Compounds that incorporated an extended flexible linker or fused rings system demonstrated better activity (**77-84**). Compound **77** was the best of this series. Evaluation of **77** in the computational model predicts the naphthalene group fitting best into the hydrophobic pocket. The naphthalene group forms several Van der Waals interactions with Leu172 and Met182 as well as  $\pi$ - $\pi$  interactions with Phe62. All together, this series yielded compounds with IC<sub>50</sub> values ranging 3-22  $\mu$ M and poor aqueous solubility (data not shown).

#### 4.2.3 Synthesis, Computational Docking, and Evaluation of a 2-BTP Library

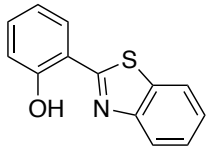
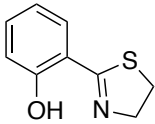
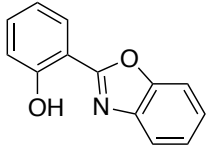
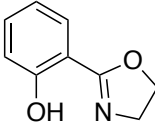
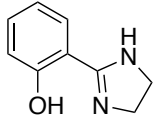
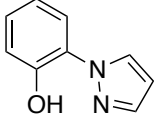
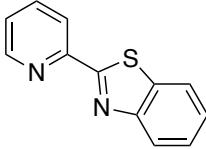
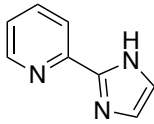
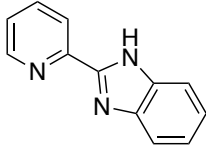
Another fragment that was explored as a GLO1 inhibitor is compound **2-BTP** (Figure 4-3). Based on the computational model developed, compound **2-BTP** is assumed to coordinate the catalytic Zn<sup>2+</sup> of GLO1 via the phenolic hydroxyl and the endocyclic nitrogen of the benzothiazole (Figure 4-6) moiety. Therefore initial efforts were made into exploring other fragments that possess this set of donor atoms (or similar) as well as isosteres of **2-BTP**. Compounds **85-93** are commercially available and were tested against GLO1 in order to find a suitable candidate for inhibitor development (Table 4-2). Besides **2-BTP** the only

fragment to demonstrate significant inhibition against GLO1 was **85** (Table 4-2). Compound **85** has a benzoxazole functional group instead of a benzothiazole group, which presumably allows for similar mode of binding. Surprisingly, compound **86** did not demonstrate any inhibition. Compounds **87-91** lack the fused ring functionality (compared to **2-BTP**) and also did not inhibit GLO1. Lastly, compounds **92** and **93** incorporate a pyridine ring instead of a phenol, and failed to inhibit GLO1.



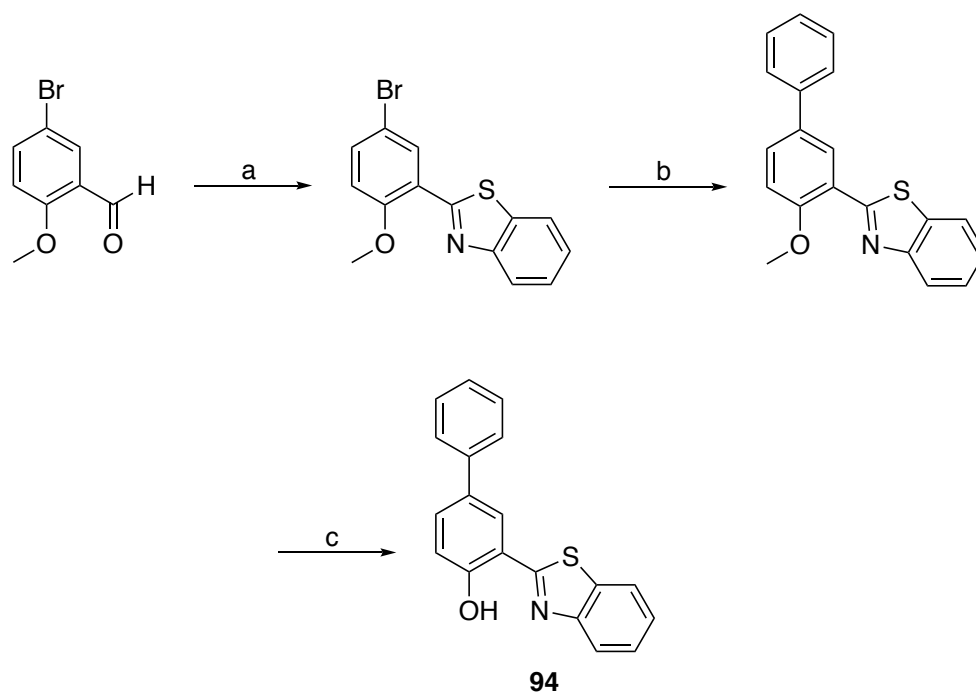
**Figure 4-6.** Superpositioned pose of **2-BTP** coordinating to the Zn<sup>2+</sup> ion the GLO1 active site (*left*) and chemical illustration (*right*). A surface outlining the active site pockets is shown in gray. Zinc is depicted as an orange sphere.

**Table 4-2.** Inhibitory activity against GLO1 for **2-BTP** derivatives.

Cmpd	Structure	IC <sub>50</sub> (μM)	Cmpd	Structure	IC <sub>50</sub> (μM)
<b>2-BTP</b>		35.4 ± 8.7	<b>89</b>		>200
<b>85</b>		49.9 ± 0.2	<b>90</b>		>200
<b>86</b>		>100	<b>91</b>		>200
<b>87</b>		>200	<b>92</b>		>200
<b>88</b>		>200	<b>93</b>		>200

The computational model developed for **3,4-HOPTO** was also utilized for **2-BTP**. For **2-BTP** only one binding pose was predicted to occur, where the benzothiazole moiety is situated in the GSH-binding pocket and the 4-position of the phenol ring is pointing directly into the hydrophobic pocket (Figure 4-6). Based on this binding conformation, it was hypothesized that adding a phenyl ring at the 4-position of the phenol ring of **2-BTP** might increase binding affinity for GLO1. Therefore compound **94** was designed. Compound **94** was synthesized as described in Scheme 4-2 starting from 5-bromo-2-methoxybenzaldehyde and underwent a condensation reaction with 2-aminobenzenethiol in the presence of sulfamic acid (Scheme 4-2). The phenyl at

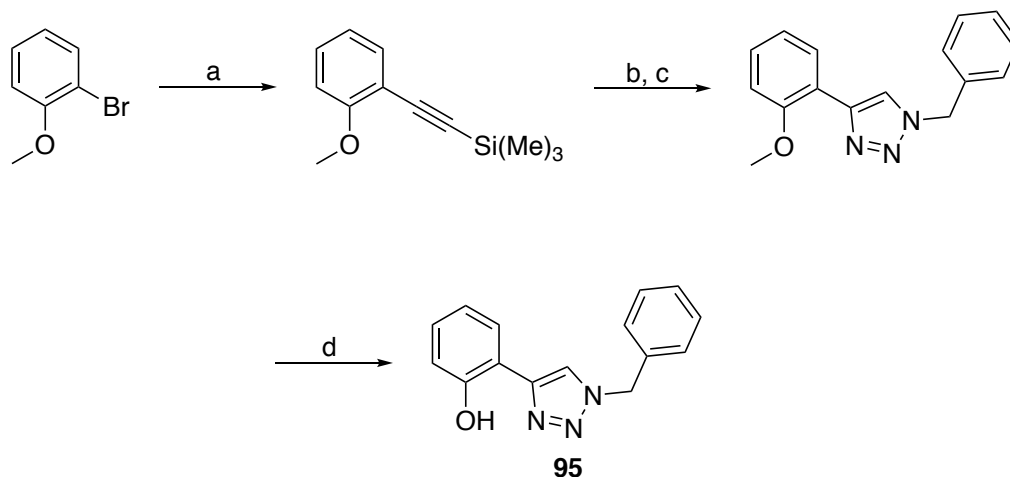
the 4-position was incorporated via a Suzuki coupling reaction. The final product was afforded via a methoxy deprotection with boron tribromide. The addition of the phenyl ring caused a 2-fold improvement in IC<sub>50</sub> value, which is attributed to a  $\pi$ - $\pi$  interaction of the phenyl with Phe62 within the hydrophobic pocket. Compound **94** also demonstrated very poor aqueous solubility, possibly due to the addition of the phenyl group.



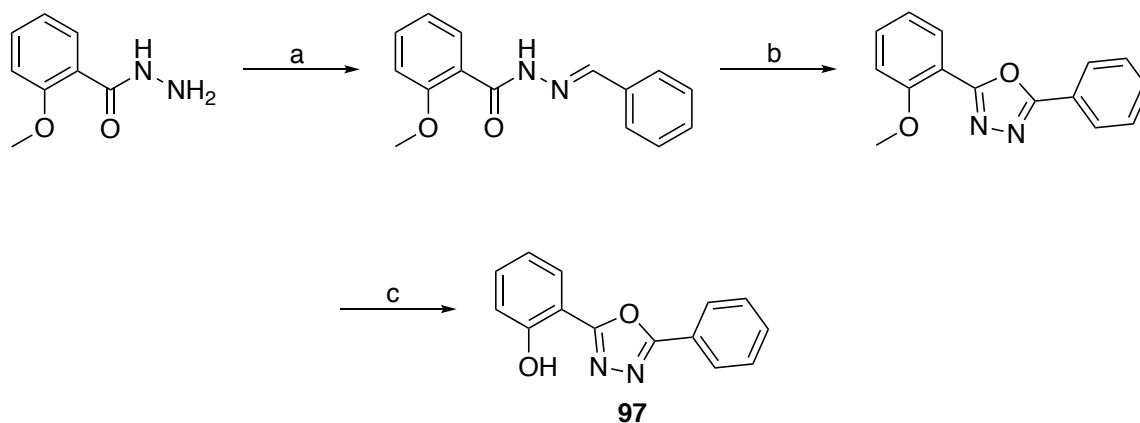
**Scheme 4-2.** Synthesis of **94**. Reagents and conditions: (a) 2-Aminobenzethiol, sulfamic acid, H<sub>2</sub>O, MeOH, Acetone, 25 °C; (b) Phenylboronic acid, DIPA, Pd(OAc)<sub>2</sub>, H<sub>2</sub>O, 100 °C; (c) BBr<sub>3</sub>, CHCl<sub>3</sub>, 25 °C.

A benzothiazole isostere ideally would help improve the solubility of **94** and offer other synthetic routes for inhibitor development. Therefore two isosteres were proposed in which the benzothiazole moiety was replaced by a triazole or

an oxadiazole functional group. Compounds **95-97** were proposed as suitable analogs of **2-BTP** that incorporate an isostere. Compound **95** was synthesized starting with 2-bromoanisole and coupling it with ethynyltrimethylsilane via a Sonogashira reaction (Scheme 4-3). This was followed by a one-pot reaction where the trimethylsilane was deprotected with tetrabutylammonium fluoride (TBAF), then reacted with benzyl azide using copper iodide as a catalyst to form the triazole ring. Lastly, the desired product was obtained via deprotection of the methoxy group with boron tribromide. Compounds **96** and **97** were afforded starting with commercially available 2-methoxybenzohydrazide combined with the corresponding aryl aldehyde to obtain the imine product (Scheme 4-4). This was followed by oxidation with Dess-Martin periodinane and deprotection with boron tribromide. Compound **95** demonstrated no inhibition of GLO1 (Table 4-3). However compounds **96** and **97** both showed similar inhibition to that of **2-BTP** (Table 4-3). These compounds demonstrated that the benzothiazole moiety could be substituted and the compounds can retain inhibition of GLO1 and affinity for the catalytic metal ion.

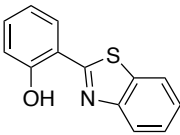
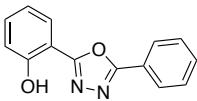
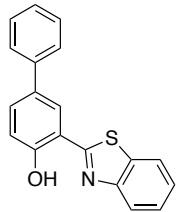
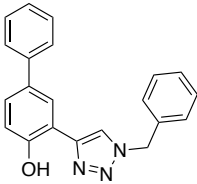
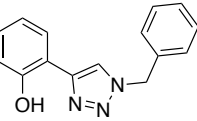
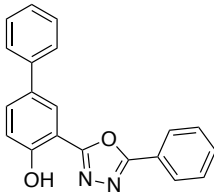
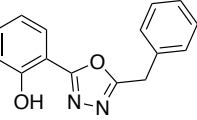
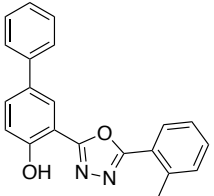


**Scheme 4-3.** Synthesis of **95**. Reagents and conditions: (a) Ethynyltrimethylsilane, Pd(dppf)Cl<sub>2</sub>, CuI, Et<sub>3</sub>N, X-Phos, Dioxane, 80 °C; (b) TBAF, H<sub>2</sub>O, DMF, 25 °C; (c) Benzyl azide, DIPA, CuI, DMF, 25 °C; (d) BBr<sub>3</sub>, CHCl<sub>3</sub>, 25 °C.



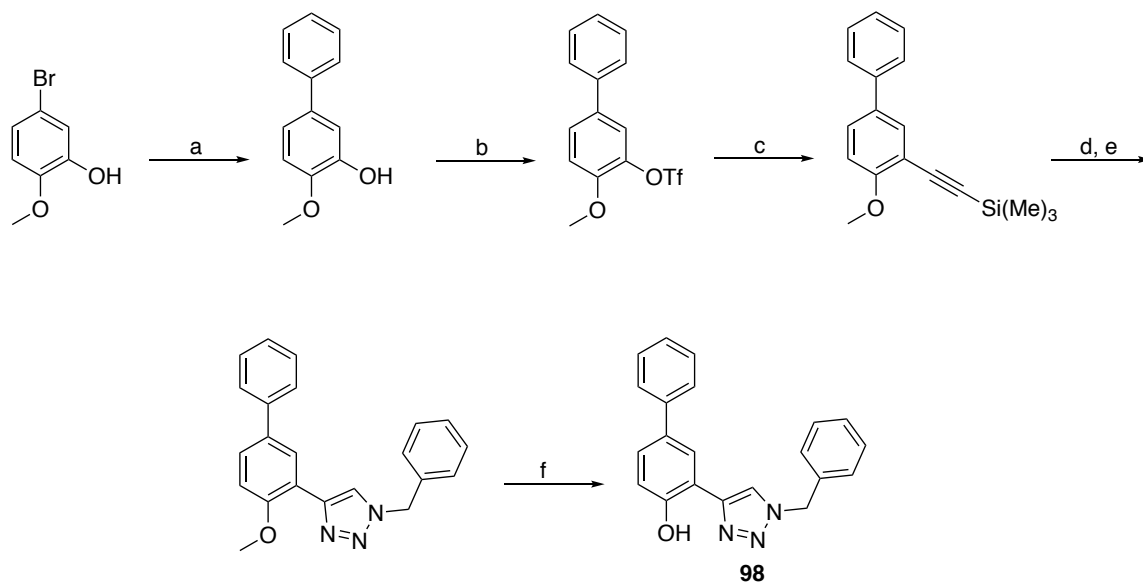
**Scheme 4-4.** Synthesis of **97**. Reagents and conditions: (a) Benzaldehyde, EtOH, reflux; (b) Dess-Martin periodinane (DMP), CH<sub>2</sub>Cl<sub>2</sub>, 25 °C; (c) BBr<sub>3</sub>, CHCl<sub>3</sub>, 25 °C.

**Table 4-3.** Inhibitory activity against GLO1 for **2-BTP** derivatives.

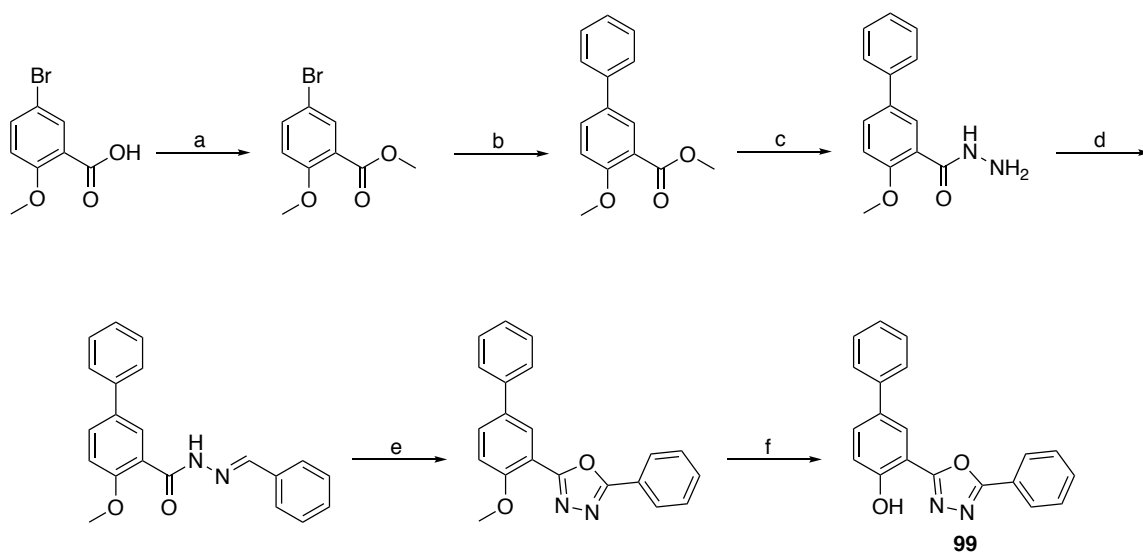
Cmpd	Structure	IC <sub>50</sub> (μM)	Cmpd	Structure	IC <sub>50</sub> (μM)
<b>2-BTP</b>		35.4 ± 8.7	<b>97</b>		47.4 ± 11.6
<b>94</b>		17.2 ± 4.5	<b>98</b>		22.1 ± 1.5
<b>95</b>		>100	<b>99</b>		17.9 ± 1.1
<b>96</b>		42.3 ± 3.5	<b>100</b>		25.1 ± 1.3

This data prompted the development of analogs of compound **94**, that incorporate a phenyl that can fit in the hydrophobic pocket, and isosteres of the benzothiazole group for improved solubility and activity. Compound **98** was synthesized starting with 5-bromo-2-methoxyphenol via coupling to phenylboronic acid (Scheme 4-5). The hydroxyl moiety was then reacted with triflate anhydride to generate the triflated hydroxyl group and a parallel synthesis to compound **95** was followed. Compounds **99** and **100** were synthesized starting with 5-bromo-2-methoxybenzoic acid (Scheme 4-6). The starting material was esterified, coupled to phenylboronic acid, then a similar synthesis to compounds **96** and **97** was followed. Similarly to compound **94**, the

addition of the phenyl ring caused a drop in IC<sub>50</sub> value (comparing **98** to **95**, **99** and **100** to **97**) which is attributed to a π-π interaction of the phenyl with Phe62 within the hydrophobic pocket (Table 4-3). The best compound from this series, **99**, demonstrated modest inhibition of GLO1 (IC<sub>50</sub> = 17.9±1.1 μM). Overall, this series of compounds failed to improve significantly the binding affinity of **2-BTP**.



**Scheme 4-5.** Synthesis of **98**. Reagents and conditions: (a) Phenylboronic acid, DIPA, Pd(OAc)<sub>2</sub>, H<sub>2</sub>O, 100 °C; (b) (CF<sub>3</sub>SO<sub>2</sub>)<sub>2</sub>O, Pyridine, CH<sub>2</sub>Cl<sub>2</sub>, 0-25 °C; (c) Ethynyltrimethylsilane, Pd(PPh<sub>3</sub>)<sub>2</sub>Cl<sub>2</sub>, CuI, Et<sub>3</sub>N, Dioxane, 80 °C; (d) TBAF, H<sub>2</sub>O, DMF, 25 °C; (e) Benzyl azide, DIPA, CuI, DMF, 25 °C; (f) BBr<sub>3</sub>, CHCl<sub>3</sub>, 25 °C.



**Scheme 4-6.** Synthesis of **99**. Reagents and conditions: (a) MeOH, H<sub>2</sub>SO<sub>4</sub>, reflux; (b) Phenylboronic acid, K<sub>2</sub>CO<sub>3</sub>, Pd(dppf)Cl<sub>2</sub>, Dioxane, reflux; (c) Hydrazine, EtOH, reflux; (d) Benzaldehyde, EtOH, reflux; (e) DMP, CH<sub>2</sub>Cl<sub>2</sub>, 25 °C; (f) BBr<sub>3</sub>, CHCl<sub>3</sub>, 25 °C.

### 4.3 Conclusions

A 240 MBP fragment library was utilized to screen for inhibitors against GLO1. The screen yielded several hits suitable for inhibitor development, of which three were chosen for hit-to-lead development (Chapters 4 and 5). Efforts to make inhibitors of GLO1 was guided by a computational model, which allowed for a pharmacophore model to be generated. With the aid of docking, analogs for two of the fragments (**3,4-HOPTO** and **2-BTP**) were synthesized and yielded novel inhibitors of GLO1 with  $IC_{50}$  values ranging 4-47  $\mu$ M. However, overall drug-likeness, synthetic accessibility, and modest inhibition activity against GLO1 in vitro did not encourage further development of these two fragments. The best hit from the initial MBP library screen was fragment **8-MSQ**. The design, rationale, and synthesis of a novel class of GLO1 inhibitors based off the **8-MSQ** hit is discussed in Chapter 5.

#### 4.4 Experimental

**Human Glyoxalase 1 Activity Assay.** Recombinant Human Glyoxalase I (GLO1) was purchased from R&D Systems (Catalog #4959-GL). Assays were carried out in 100 mM Sodium Phosphate, pH 7.0 buffer utilizing 96-well Clear UV Plate (Corning UV Transparent Microplates Catalog #3635). A fresh solution of glutathione (Pre-Substrate 1, 100 mM) as well as methylglyoxal (Pre-substrate 2, 100 mM) was prepared in deionized water. The substrate was prepared by adding 14.5 mL of buffer and 0.99 mL of each of the pre-substrate components. The substrate mixture was vortexed vigorously for 15 sec, then allowed to sit at room temperature for 20 min. Initial well volume was 50  $\mu$ L containing GLO1 (40 ng) and inhibitor. This protein and inhibitor mixture was incubated for 15-20 min prior to addition of substrate. To this was then added substrate (150  $\mu$ L) yielding a maximum amount of 5% DMSO per well. The enzyme activity was measured utilizing a Biotek Synergy HT or H4 plate reader by measuring absorbance at 240 nm every 1 min for 8 min. The rate of absorbance increase was compared for samples versus controls containing no inhibitor (100% activity). Absorbance for background wells containing DMSO, buffer and substrate (no enzyme or inhibitor) were subtracted from the rest of the wells.

**3-Hydroxy-2-methyl-4*H*-pyran-4-thione (Thiomaltol).** Method was adapted from previously reported procedure.<sup>33</sup> To a solution of 3-hydroxy-2-methyl-4*H*-pyran-4-one (Maltol, 5 g, 39.8 mmol) in toluene (250 mL) was added P<sub>4</sub>S<sub>10</sub> (3.2 g, 7.2 mmol) and hexamethyldisiloxane (HMDSO, 10.8 g, 66.2 mmol) and heated to 110°C for 8 h under nitrogen with the flask covered in aluminum to prevent light from reaching the solution. This was concentrated and yielded a yellow solid/sludge crude product. The crude was recrystallized from hexanes and hot vacuum filtered to remove solid waste. A yellow precipitate was observed in the filtrate solution. Precipitate was isolated via filtration to afford Thiomaltol. Yield = 3.05 g (54%). <sup>1</sup>H NMR (400 MHz, CDCl<sub>3</sub>): δ = 7.78 (br, 1H), 7.61 (d, *J* = 6.8 Hz, 1H), 7.34 (d, *J* = 6.8 Hz, 1H), 2.46 (s, 3H).

**General Procedure for compounds 70-84.** To a solution of 3-hydroxy-2-methyl-4*H*-pyran-4-thione (0.2 g, 1.4 mmol) in of H<sub>2</sub>O:EtOH (2 mL, 1:1) was added AcOH (0.25 g, 4.22 mmol) and amine (4.22 mmol) in a 10 mL reaction vessel. This was reacted by irradiating in the microwave at 165 °C, 250 psi (max pressure), and 300 W (max power) for 60 min. The resulting solution was then concentrated and purified via silica gel chromatography eluting Hexanes/0-100% EtOAc.

**3-Hydroxy-1,2-dimethylpyridine-4(1*H*)-thione (3,4-HOPTO).** Yield = 0.13 g (56%). <sup>1</sup>H NMR (400 MHz, CDCl<sub>3</sub>) δ 8.68 (br, 1H), 7.36 (d, *J* = 6.8 Hz, 1H), 7.09 (d, *J* = 6.8 Hz, 1H), 3.76 (s, 3H), 2.45 (s, 3H).

**3-Hydroxy-2-methyl-1-phenylpyridine-4(1*H*)-thione (70).** Yield = 0.054 g (16%). <sup>1</sup>H NMR (400 MHz, CDCl<sub>3</sub>) δ 7.57-7.55 (m, 3H), 7.51 (d, *J* = 6.4 Hz, 1H), 7.30-7.27 (m, 2H), 7.19 (d, *J* = 6.4 Hz, 1H), 2.18 (s, 3H). ESI-MS(+): *m/z* 156.13 [M+H]<sup>+</sup>.

**3-Hydroxy-2-methyl-1-(thiophen-2-ylmethyl)pyridine-4(1*H*)-thione (71).** Yield = 0.13 g (57%). <sup>1</sup>H NMR (400 MHz, CDCl<sub>3</sub>) δ 8.75 (br, 1H), 7.51 (d, *J* = 6.8 Hz, 1H), 7.35 (dd, *J* = 6.4, 5.2 Hz, 1H), 7.22 (d, *J* = 6.8 Hz, 1H), 7.02-6.92 (m, 2H), 5.32 (s, 2H), 2.52 (s, 3H). ESI-MS(+): *m/z* 238.01 [M+H]<sup>+</sup>.

**1-(Furan-2-ylmethyl)-3-hydroxy-2-methylpyridine-4(1*H*)-thione (72).** Yield = 0.071 g (37%). <sup>1</sup>H NMR (400 MHz, CDCl<sub>3</sub>) δ 7.38 (s, 1H), 7.32 (d, *J* = 7.2 Hz, 1H), 6.38 (d, *J* = 7.2 Hz, 1H), 6.34 (d, *J* = 3.2 Hz, 1H), 6.27 (d, *J* = 3.2 Hz, 1H), 4.98 (s, 2H), 2.41 (s, 3H). ESI-MS(+): 222.11 *m/z* [M+H]<sup>+</sup>.

**1-Benzyl-3-hydroxy-2-methylpyridine-4(1*H*)-thione (73).** Yield = 0.10 g (49%). <sup>1</sup>H NMR (400 MHz, CDCl<sub>3</sub>) δ 8.77 (br, 1H), 7.53 (d, *J* = 6.7 Hz, 1H), 7.41-7.35

(m, 3H), 7.21 (d,  $J = 6.7$  Hz, 1H), 7.04 (d,  $J = 6.3$  Hz, 2H), 5.21 (s, 2H), 2.39 (s, 3H). ESI-MS(+):  $m/z$  232.14 [M+H]<sup>+</sup>.

**3-Hydroxy-2-methyl-1-(pyridin-2-ylmethyl)pyridine-4(1H)-thione (74).** Yield = 0.11 g (56%). <sup>1</sup>H NMR (400 MHz, CDCl<sub>3</sub>)  $\delta$  8.67 (br, 1H), 8.54 (d,  $J = 4.7$  Hz, 1H), 7.69 (td,  $J = 7.7, 1.6$  Hz, 1H), 7.43 (d,  $J = 6.7$  Hz, 1H), 7.24-7.27(m, 2H), 7.01 (d,  $J = 7.7$  Hz, 1H), 5.28 (s, 2H), 2.36 (s, 3H). ESI-MS(+):  $m/z$  233.08 [M+H].

**3-Hydroxy-2-methyl-1-(pyridin-3-ylmethyl)pyridine-4(1H)-thione (75).** Yield = 0.13 g (62%). <sup>1</sup>H NMR (400 MHz, CDCl<sub>3</sub>)  $\delta$  8.64 (dd,  $J = 4.7, 1.6$  Hz 1H), 8.48 (d,  $J = 1.8$  Hz, 1H), 7.54 (d,  $J = 6.7$ , 1H), 7.36-7.27 (m, 2H), 7.21 (d,  $J = 6.7$  Hz, 1H), 5.24 (s, 2H), 2.40 (s, 3H). ESI-MS(+):  $m/z$  238.11 [M+H].

**3-Hydroxy-2-methyl-1-(pyridin-4-ylmethyl)pyridine-4(1H)-thione (76).** Yield = 0.12 g (58%). <sup>1</sup>H NMR (400 MHz, CDCl<sub>3</sub>)  $\delta$  8.73 (br, 1H), 8.63 (d,  $J = 5.8$  Hz, 2H), 7.48 (d,  $J = 6.7$  Hz, 1H), 7.18 (d,  $J = 6.7$ , 1H), 6.92 (d,  $J = 5.8$  Hz, 2H), 5.23 (s, 2H), 2.32 (s, 3H). ESI-MS(+):  $m/z$  233.08 [M+H].

**3-Hydroxy-2-methyl-1-(naphthalen-2-ylmethyl)pyridine-4(1H)-thione (77).** Yield = 0.084 g (32%). <sup>1</sup>H NMR (400 MHz, DMSO-*d*<sub>6</sub>)  $\delta$  8.80 (s, 1H), 8.07 (d,  $J = 8$  Hz, 1H), 8.02 (d,  $J = 8$  Hz, 1H), 7.93 (d,  $J = 8$  Hz, 1H), 7.71-7.60 (m, 3H), 7.48-

7.40 (m, 2H), 6.67 (d,  $J = 8$  Hz, 1H), 5.95 (s, 2H), 2.31 (s, 3H). ESI-MS(+):  $m/z$  280.18  $[M+H]^+$ .

**1-(Benzo[*d*][1,3]dioxol-5-ylmethyl)-3-hydroxy-2-methylpyridine-4(1*H*)-thione (78).** Yield = 0.12 g (54%).  $^1\text{H}$  NMR (400 MHz, DMSO- $d_6$ )  $\delta$  8.71 (br, 1H), 7.78 (d,  $J = 6.4$  Hz, 1H), 7.36 (d,  $J = 6.4$  Hz, 1H), 6.91 (d,  $J = 8$  Hz, 1H), 6.79 (s, 1H), 6.62 (d,  $J = 8$  Hz, 1H), 6.01 (s, 2H), 5.31 (s, 2H), 2.33 (s, 3H). ESI-MS(+):  $m/z$  275.99  $[M+H]^+$ .

**3-Hydroxy-2-methyl-1-phenethylpyridine-4(1*H*)-thione (79).** Yield = 0.13 g (65%).  $^1\text{H}$  NMR (400 MHz,  $\text{CDCl}_3$ )  $\delta$  7.24-7.22 (m, 4H), 7.01 (d,  $J = 7.2$  Hz, 2H), 6.85 (d,  $J = 6.4$  Hz, 1H), 4.21 (t,  $J = 6.8$ , 2H), 3.02 (t,  $J = 6.8$  Hz, 2H), 2.34 (s, 3H). ESI-MS(+):  $m/z$  246.15  $[M+H]^+$ .

**1-(4-Fluorophenethyl)-3-hydroxy-2-methylpyridine-4(1*H*)-thione (80).** Yield = 0.064 g (29%).  $^1\text{H}$  NMR (400 MHz,  $\text{CDCl}_3$ )  $\delta$  7.38 (d,  $J = 6.8$  Hz, 1H), 7.00-6.99 (m, 4H), 6.83 (d,  $J = 6.8$  Hz, 2H), 4.21 (t,  $J = 6.8$ , 2H), 3.05 (t,  $J = 6.8$  Hz, 2H), 2.43 (s, 3H). ESI-MS(+):  $m/z$  264.12  $[M+H]^+$ .

**1-(2-(1*H*-Indol-3-yl)ethyl)-3-hydroxy-2-methylpyridine-4(1*H*)-thione (81).** Yield = 0.11 g (41%).  $^1\text{H}$  NMR (400 MHz,  $\text{CDCl}_3$ )  $\delta$  8.76 (br, 1H), 8.12 (br, 1H), 7.53 (d,  $J = 8$  Hz, 1H), 7.42 (d,  $J = 8$  Hz, 1H), 7.29-7.24 (m, 3H), 7.20 (t,  $J = 8$  Hz,

1H), 6.75-6.70 (m, 2H), 4.30 (t,  $J = 6.8$  Hz, 1H), 3.24 (t,  $J = 6.8$  Hz, 1H), 2.44 (s, 3H). ESI-MS(+):  $m/z$  285.13  $[M+H]^+$ .

**3-Hydroxy-2-methyl-1-(3-phenylpropyl)pyridine-4(1H)-thione (82).** Yield = 0.054 g (26%).  $^1\text{H}$  NMR (400 MHz,  $\text{CDCl}_3$ )  $\delta$  8.71 (br, 1H), 7.40 (d,  $J = 6.4$  Hz, 1H), 7.32-7.15 (m, 5H) 7.06 (d,  $J = 6.4$  Hz, 1H), 3.97 (t,  $J = 6$  Hz, 2H), 2.71 (t,  $J = 6$  Hz, 2H), 2.36 (s, 3H), 2.16 (quin,  $J = 7.2$  Hz, 2H). ESI-MS(+):  $m/z$  260.14  $[M+H]^+$ .

**3-hydroxy-2-methyl-1-(4-phenylbutyl)pyridine-4(1H)-thione (83).** Yield = 0.079 g (32%).  $^1\text{H}$  NMR (400 MHz,  $\text{CDCl}_3$ )  $\delta$  7.37-7.02 (m, 7H), 3.96 (t,  $J = 6$  Hz, 2H), 2.66 (t,  $J = 6$  Hz, 2H), 2.39 (s, 3H), 1.76-1.66 (m, 4H). ESI-MS(+):  $m/z$  274.11  $[M+H]^+$ .

**1-(Biphenyl-4-ylmethyl)-3-hydroxy-2-methylpyridine-4(1H)-thione (84).** Yield = 0.11 g (24%).  $^1\text{H}$  NMR (400 MHz,  $\text{CDCl}_3$ ):  $\delta = 2.42$  (s), 5.25 (s), 7.08 (d,  $J = 8.0$  Hz, 2H), 7.23 (d,  $J = 5.6$  Hz, 1H), 7.35 (t,  $J = 7.4$  Hz, 1H), 7.43 (t,  $J = 7.4$  Hz, 2H), 7.53 (m, 3H), 7.58 (d,  $J = 8.0$  Hz, 2H), 8.77 (br, 1H). ESI-MS(+)  $m/z$  308.02  $[M+H]^+$ .

**2-(5-Bromo-2-methoxyphenyl)benzo[*d*]thiazole.** To a solution 5-Bromo-2-methoxy benzaldehyde (3 g, 13.95 mmol) in a mixture of MeOH:Acetone:Water (1:1:1, 60 mL) was added 2-Aminobenzenethiol (1.92 g, 15.35 mmol) followed by Sulfamic acid (1.49 g, 15.35 mmol) and stirred at room temperature for ~30 min. The reaction mixture was then concentrated to remove organic solvents (MeOH and Acetone). The resulting aqueous solution was diluted with water (50 mL), then extracted with EtOAc (3×50mL). The combined organic layers were dried over MgSO<sub>4</sub>, filtered, concentrated then purified via silica gel chromatography eluting 0-8% EtOAc in Hexanes. The desired product was isolated as a white solid. Yield = 2.27 g (51%). <sup>1</sup>H NMR (400 MHz, CDCl<sub>3</sub>) δ 8.68 (d, J = 2.0 Hz, 1H), 8.10 (d, J = 4.0 Hz, 1H), 7.92 (d, J = 8.0 Hz, 1H), 7.52-7.46 (m, 2H), 7.40 (d, J = 7.2 Hz, 1H), 6.87 (d, J = 8.8 Hz, 1H), 3.97 (s, 3H). ESI-MS(+): *m/z* 320.20, 322.14 [M+H]<sup>+</sup>.

**2-(4-Methoxy-[1,1'-biphenyl]-3-yl)benzo[*d*]thiazole.** To a solution of 2-(5-Bromo-2-methoxyphenyl) benzo[*d*]thiazole (0.3 g, 0.94 mmol) in H<sub>2</sub>O:Dioxane (1:1, 10 mL) was added DIPA (0.267 mL, 1.87 mmol) and Phenylboronic acid (0.171 g, 1.41 mmol) then allowed to stir at reflux. To this was then added Pd(OAc)<sub>2</sub> (0.01 g, 0.05 mmol) and allowed to reflux for an additional 2 h. The resulting aqueous solution was diluted with brine (50 mL), then extracted with EtOAc (3×50mL). The combined organic layers were dried over MgSO<sub>4</sub>, filtered through celite, concentrated then purified via silica gel chromatography

eluting 0-8% EtOAc in Hexanes. The desired product was isolated as a off-white solid. Yield = 0.13 g (44%).  $^1\text{H NMR}$  (400 MHz,  $\text{CDCl}_3$ )  $\delta$  8.82 (d,  $J = 2.0$  Hz, 1H), 8.14 (d,  $J = 8.0$  Hz, 1H), 7.96 (d,  $J = 8.0$  Hz, 1H), 7.71-7.68 (m, 3H), 7.53-7.34 (m, 5H), 7.14 (d,  $J = 8.0$  Hz, 1H), 4.09 (s, 3H). ESI-MS(+):  $m/z$  318.23  $[\text{M}+\text{H}]^+$ .

**3-(Benzo[*d*]thiazol-2-yl)-[1,1'-biphenyl]-4-ol (94).** To a solution of 2-(4-Methoxy-[1,1'-biphenyl]-3-yl)benzo[*d*]thiazole (0.13 g, 0.41 mmol) in  $\text{CHCl}_3$  (10 mL) was added  $\text{BBr}_3$  (solution in  $\text{CH}_2\text{Cl}_2$ , 2.048 mmol) and allowed to stir at room temperature under a nitrogen atmosphere overnight. The reaction mixture was then quenched by the addition of excess MeOH, then concentrated. The crude mixture was then co-evaporated with MeOH multiple times until all of the  $\text{BBr}_3$  had been consumed. The resulting solid was not further purified. The desired product was isolated as a yellow solid. Yield = 0.124 g (99%).  $^1\text{H NMR}$  (400 MHz,  $\text{CDCl}_3$ )  $\delta$  8.03 (d,  $J = 8.0$  Hz, 1H), 7.94 (d,  $J = 8.0$  Hz, 1H), 7.89 (br, 1H), 7.64-7.59 (m, 3H), 7.55-7.41 (m, 4H), 7.38 (t,  $J = 7.3$  Hz, 1H), 7.26 (d,  $J = 0.8$  Hz, 1H), 7.19 (d,  $J = 8.8$  Hz, 1H). ESI-MS(+):  $m/z$  304.39  $[\text{M}+\text{H}]^+$ .

**((2-Methoxyphenyl)ethynyl)trimethylsilane.** To a solution of 5-bromo-2-methoxyphenol (1 g, 5 mmol) in 1,4-Dioxane (5 mL) and  $\text{Et}_3\text{N}$  (5 mL) was added Ethynyltrimethylsilane (0.8 g, 8 mmol), X-Phos (0.3 g, 0.5 mmol), and  $\text{CuI}$  (0.1 g, 0.5 mmol) and degassed for ~5-10 min. To this was then added  $\text{Pd}(\text{dppf})\text{Cl}_2$  (0.4 g, 0.5 mmol) and heated to 80 °C for 17 h. The resulting mixture was filtered

through celite and then concentrated. The crude was purified via silica gel chromatography eluting 0-5% EtOAc in hexanes. Yield = 1.0 g (99%). ESI-MS(+):  $m/z$  205.45 [M+H]<sup>+</sup>.

**1-Benzyl-4-(2-methoxyphenyl)-1H-1,2,3-triazole.** To a solution of ((2-Methoxyphenyl)ethynyl)trimethylsilane (0.3 g, 1 mmol) in DMF (5 mL) was added a solution of TBAF (2 mmol) in H<sub>2</sub>O (1 mL) and allowed to stir at room temperature for ~15 min. To this was then added (azidomethyl)benzene (0.2 g, 2 mmol), DIPA (2 mmol) and CuI (0.1 mmol) and allowed to stir overnight at room temperature. The resulting mixture was filtered through celite and then concentrated. The crude was purified via silica gel chromatography eluting 0-70% EtOAc in hexanes. Yield = 0.145 g (36%). ESI-MS(+):  $m/z$  266.36 [M+H]<sup>+</sup>.

**2-(1-Benzyl-1H-1,2,3-triazol-4-yl)phenol (95).** To a solution of 1-Benzyl-4-(2-methoxyphenyl)-1H-1,2,3-triazole (0.145 g, 0.547 mmol) in CH<sub>2</sub>Cl<sub>2</sub> (5 mL) was added BBr<sub>3</sub> (1M solution in heptanes, 2.18 mmol) and stirred at room temperature overnight. To the reaction mixture was added excess MeOH to quench BBr<sub>3</sub>. The resulting solution was concentrated then purified via silica gel chromatography eluting a gradient of 0-20% MeOH in CH<sub>2</sub>Cl<sub>2</sub>. Yield = 0.13 g (95%). ESI-MS(+):  $m/z$  252.39 [M+H]<sup>+</sup>.

**2-Benzyl-5-(2-methoxyphenyl)-1,3,4-oxadiazole.** To a solution of 2-methoxybenzo hydrazide (0.2 g, 1.2 mmol) and phenylacetic acid (0.15 g, 1.2 mmol) in POCl<sub>3</sub> (2 mL) was heated to reflux for 16 h. To the reaction mixture was added excess MeOH to quench POCl<sub>3</sub>. The resulting solution was concentrated then purified via silica gel chromatography eluting a gradient of 0-40% EtOAc in hexanes. Yield = 0.12 g (42%). ESI-MS(+): *m/z* 267.22 [M+H]<sup>+</sup>.

**2-(5-Benzyl-1,3,4-oxadiazol-2-yl)phenol (96).** To a solution of 2-benzyl-5-(2-methoxyphenyl)-1,3,4-oxadiazole (0.12 g, 0.31 mmol) in CH<sub>2</sub>Cl<sub>2</sub> (5 mL) was added BBr<sub>3</sub> (1M solution in heptanes, 3.1 mmol) and stirred at room temperature overnight. To the reaction mixture was added excess MeOH to quench BBr<sub>3</sub>. The resulting solution was concentrated then purified via silica gel chromatography eluting a gradient of 0-40% EtOAc in hexanes. Yield = 0.081 g (93%). <sup>1</sup>H NMR (400 MHz, CDCl<sub>3</sub>) δ 7.69 (d, *J* = 8.0 Hz, 1H), 7.43-7.31 (m, 6H), 7.11 (d, *J* = 8.0 Hz, 1H), 6.98 (t, *J* = 8.0 Hz, 1H), 4.30 (s, 2H). ESI-MS(+): *m/z* 253.21 [M+H]<sup>+</sup>.

**2-(2-Methoxyphenyl)-5-phenyl-1,3,4-oxadiazole.** To a solution of 2-methoxybenzo hydrazide (0.2 g, 1.2 mmol) and benzoic acid (0.15 g, 1.2 mmol) in POCl<sub>3</sub> (2 mL) was heated to reflux for 16 h. To the reaction mixture was added excess MeOH to quench POCl<sub>3</sub>. The resulting solution was concentrated then

purified via silica gel chromatography eluting a gradient of 0-40% EtOAc in Hexanes. Yield = 0.106 g (36%). ESI-MS(+):  $m/z$  253.23 [M+H]<sup>+</sup>.

**2-(5-Phenyl-1,3,4-oxadiazol-2-yl)phenol (97).** To a solution of 2-(2-methoxyphenyl)-5-phenyl-1,3,4-oxadiazole (0.07 g, 0.28 mmol) in CH<sub>2</sub>Cl<sub>2</sub> (5 mL) was added BBr<sub>3</sub> (1M solution in heptanes, 2.8 mmol) and stirred at room temperature overnight. To the reaction mixture was added excess MeOH to quench BBr<sub>3</sub>. The resulting solution was concentrated then purified via silica gel chromatography eluting a gradient of 0-40% EtOAc in hexanes. Yield = 0.065 g (96%). <sup>1</sup>H NMR (400 MHz, DMSO-*d*<sub>6</sub>) δ 10.31 (br, 1H), 8.10 (m, 2H), 7.92 (d, J = 8.0 Hz, 1H), 7.64-7.60 (m, 3H), 7.49 (t, J = 8.0 Hz, 1H), 7.11 (d, J = 8.0 Hz, 1H), 7.05 (t, 7.6 Hz, 1H). ESI-MS(+):  $m/z$  239.19 [M+H]<sup>+</sup>.

**4-Methoxy-[1,1'-biphenyl]-3-ol.** To a solution of 5-bromo-2-methoxyphenol (1 g, 4.93 mmol) in H<sub>2</sub>O (10 mL) was added phenylboronic acid (1.2 g, 9.85 mmol), DIPA (1.38 mL, 9.85 mmol), and Pd(OAc)<sub>2</sub> (0.024 mmol) and heated to reflux for 16 h. To the reaction mixture was then added brine (50 mL) and extracted with EtOAc (3 X 50 mL). The combined organic layers were filtered through celite, concentrated, then purified via silica gel chromatography eluting a gradient of 0-30% EtOAc in hexanes. Yield = 0.83 g (84%). ESI-MS(+):  $m/z$  201.13 [M+H]<sup>+</sup>.

**4-Methoxy-[1,1'-biphenyl]-3-yl trifluoromethanesulfonate.** To a solution of 4-methoxy-[1,1'-biphenyl]-3-ol (0.8 g, 4.0 mmol) in CH<sub>2</sub>Cl<sub>2</sub> (20 mL) was added pyridine (1 mL) and allowed to cool to 0° C. To this was then added (CF<sub>3</sub>SO<sub>2</sub>)<sub>2</sub>O (0.74 mL, 4.39 mmol) and allowed to stir for 1 h. To the reaction mixture was then added sat. NaHCO<sub>3</sub> (aq., 50 mL) and then extracted with CH<sub>2</sub>Cl<sub>2</sub> (3 X 50 mL). The combined organic layers were dried with MgSO<sub>4</sub>, filtered, concentrated, then purified via silica gel chromatography eluting a gradient of 0-30% EtOAc in hexanes. Yield = 1.21 g (91%). ESI-MS(+): *m/z* 333.33 [M+H]<sup>+</sup>.

**((4-Methoxy-[1,1'-biphenyl]-3-yl)ethynyl)trimethylsilane.** To a solution of 4-methoxy-[1,1'-biphenyl]-3-yl trifluoromethanesulfonate (1.06 g, 3.21 mmol) in 1,4-dioxane (5 mL) and Et<sub>3</sub>N (5 mL) was added ethynyltrimethylsilane (0.69 mL, 4.81 mmol), X-Phos (0.14 g, 0.3 mmol) CuI (0.03 g, 0.16 mmol), and Pd(PPh<sub>3</sub>)<sub>2</sub>Cl<sub>2</sub> (0.11 g, 0.16 mmol) then heated to reflux for 16 h. The reaction mixture was filtered through celite, concentrated, then purified via silica gel chromatography eluting a gradient of 0-10% EtOAc in hexanes. Yield = 0.3 g (35%). ESI-MS(+): *m/z* 281.52 [M+H]<sup>+</sup>.

**1-Benzyl-4-(4-methoxy-[1,1'-biphenyl]-3-yl)-1*H*-1,2,3-triazole.** To a solution of ((4-methoxy-[1,1'-biphenyl]-3-yl)ethynyl)trimethylsilane (0.05 g, 0.17 mmol) in DMF (5 mL) was added a solution of TBAF (0.06 g, 0.19 mmol) in H<sub>2</sub>O (1 mL) and allowed to stir at room temperature for ~15 min. To the reaction mixture was

then added DIPA (0.02 mL, 0.14 mmol), (azidomethyl)benzene (0.025 mL, 0.19 mmol), and CuI (0.005 g, 0.018 mmol) then allowed to stir overnight. The resulting solution was concentrated then purified via silica gel chromatography eluting a gradient of 0-40% EtOAc in hexanes. Yield = 0.042 g (69%). ESI-MS(+):  $m/z$  342.42 [M+H]<sup>+</sup>.

**3-(1-Benzyl-1*H*-1,2,3-triazol-4-yl)-[1,1'-biphenyl]-4-ol (98).** To a solution of 1-benzyl-4-(4-methoxy-[1,1'-biphenyl]-3-yl)-1*H*-1,2,3-triazole (0.042 g, 0.12 mmol) in CH<sub>2</sub>Cl<sub>2</sub> (5 mL) was added BBr<sub>3</sub> (1M solution in CH<sub>2</sub>Cl<sub>2</sub>, 1.23 mL, 1.23 mmol) and stirred at room temperature overnight. To the reaction mixture was added excess MeOH to quench BBr<sub>3</sub>. The resulting solution was concentrated then purified via silica gel chromatography eluting a gradient of 0-20% MeOH in CH<sub>2</sub>Cl<sub>2</sub>. Yield = 0.027 g (67%). ESI-MS(+):  $m/z$  328.41 [M+H]<sup>+</sup>.

**Methyl 5-bromo-2-methoxybenzoate.** To a solution of 5-bromo-2-methoxybenzoic acid (3g, 12.98 mmol) in MeOH (500 mL) was added H<sub>2</sub>SO<sub>4</sub> (20 drops) and heated to reflux for 72 h. The reaction mixture was concentrated, washed with sat. NaHCO<sub>3</sub> (50 mL) and extracted with EtOAc (3 X 50 mL). The combined organic layers were concentrated to yield product. Product was not further purified. Yield = 2.5 g (79%). <sup>1</sup>H NMR (400 MHz, CDCl<sub>3</sub>) δ 7.89 (d, J = 2.8 Hz, 1H), 7.54 (dd, J<sub>1</sub> = 8.8 Hz, J<sub>2</sub> = 2.8 Hz, 1H), 6.85 (d, J = 8.8 Hz, 1H), 3.87 (s, 6H). ESI-MS(+):  $m/z$  246.11 [M+H]<sup>+</sup>.

**Methyl 4-methoxy-[1,1'-biphenyl]-3-carboxylate.** To a solution methyl 5-bromo-2-methoxybenzoate (2 g, 8.16 mmol) in 1,4-Dioxane (30 mL) was added phenylboronic acid (1.49 g, 12.24 mmol), K<sub>2</sub>CO<sub>3</sub> (2.26 g, 16.32 mmol), and Pd(dppf)Cl<sub>2</sub> (0.33 g, 0.41 mmol) then heated to reflux for 16 h. The reaction mixture was filtered through celite, concentrated, then purified via silica gel chromatography eluting a gradient of 0-30% EtOAc in hexanes. Yield = 1.86 g (94%). <sup>1</sup>H NMR (400 MHz, CDCl<sub>3</sub>) δ 7.57 (d, J = 8.4 Hz, 1H), 7.44 (t, J = 8.4 Hz, 1H), 7.06 (d, J = 8.4 Hz, 1H), 3.94 (s, 3H), 3.92 (s, 3H). ESI-MS(+): *m/z* 243.32 [M+H]<sup>+</sup>.

**4-Methoxy-[1,1'-biphenyl]-3-carbohydrazide.** To a solution of methyl 4-methoxy-[1,1'-biphenyl]-3-carboxylate (1.18 g, 4.87 mmol) in EtOH (20 mL) was added hydrazine (H<sub>2</sub>O solution, 30.9 mmol) and heated to reflux for 16 h. The reaction mixture was diluted with brine (50 mL), then extracted with EtOAc (3 X 50 mL). The combined organic layers were dried with MgSO<sub>4</sub>, filtered, concentrated, then purified via silica gel chromatography eluting a gradient of 0-15% MeOH in CH<sub>2</sub>Cl<sub>2</sub>. Yield = 1.16 g (98%). <sup>1</sup>H NMR (400 MHz, CDCl<sub>3</sub>) δ 7.62 (d, J = 8.0 Hz, 1H), 7.44 (t, J = 8.0 Hz, 1H), 7.07 (d, J = 8.0 Hz, 1H), 4.03 (s, 3H). ESI-MS(+): *m/z* 243.29 [M+H]<sup>+</sup>.

**(E)-N-Benzylidene-4-methoxy-[1,1'-biphenyl]-3-carbohydrazide.** To a solution of 4-methoxy-[1,1'-biphenyl]-3-carbohydrazide (0.2 g, 0.83 mmol) in

EtOH (20 mL) was added benzaldehyde (0.092 mL, 0.91 mmol) and heated to reflux overnight. The reaction mixture was diluted with brine (25 mL), then extracted with EtOAc (3 X 25 mL). The combined organic layers were dried with MgSO<sub>4</sub>, filtered, concentrated, then purified via silica gel chromatography eluting a gradient of 0-100% EtOAc in hexanes. Yield = 0.24 g (89%). ESI-MS(+): *m/z* 331.41 [M+H]<sup>+</sup>.

**2-(4-Methoxy-[1,1'-biphenyl]-3-yl)-5-phenyl-1,3,4-oxadiazole.** To a solution of (*E*)-*N*-benzylidene-4-methoxy-[1,1'-biphenyl]-3-carbohydrazide (0.24 g, 0.73 mmol) in CH<sub>2</sub>Cl<sub>2</sub> (5 mL) was added DMP (0.62 g, 1.45 mmol) and stirred at room temperature for 2.5 h. The reaction mixture was concentrated then purified via silica gel chromatography eluting a gradient of 0-40% EtOAc in hexanes. Yield = 0.089 g (37%). ESI-MS(+): *m/z* 329.38 [M+H]<sup>+</sup>.

**3-(5-Phenyl-1,3,4-oxadiazol-2-yl)-[1,1'-biphenyl]-4-ol (99).** To a solution of 2-(4-methoxy-[1,1'-biphenyl]-3-yl)-5-phenyl-1,3,4-oxadiazole (0.089 g, 0.51 mmol) in CH<sub>2</sub>Cl<sub>2</sub> (25 mL) was added BBr<sub>3</sub> (1M solution in heptanes, 5.1 mmol) and stirred at room temperature for 2.5 h. To the reaction mixture was added excess MeOH to quench BBr<sub>3</sub>. The resulting solution was concentrated then purified via silica gel chromatography eluting a gradient of 0-40% EtOAc in hexanes. Yield = 0.053 g (72%). <sup>1</sup>H NMR (400 MHz, CDCl<sub>3</sub>) δ 10.26 (br, 1H), 8.18 (d, *J* = 8.0 Hz, 1H), 8.05 (s, 1H), 7.71-7.24 (m, 11H). ESI-MS(+): *m/z* 302.31 [M+H]<sup>+</sup>.

**(E)-4-Methoxy-N-(2-methylbenzylidene)-[1,1'-biphenyl]-3-carbohydrazide.**

To a solution of 4-methoxy-[1,1'-biphenyl]-3-carbohydrazide (0.15 g, 0.06 mmol) in EtOH (20 mL) was added 2-methylbenzaldehyde (0.15 mL, 1.2 mmol) and heated to reflux overnight. The reaction mixture was diluted with brine (25 mL), then extracted with EtOAc (3×25mL). The combined organic layers were dried with MgSO<sub>4</sub>, filtered, concentrated, then purified via silica gel chromatography eluting a gradient of 0-100% EtOAc in hexanes. Yield = 0.21 g (99%). ESI-MS(+): *m/z* 345.38 [M+H]<sup>+</sup>.

**2-(4-Methoxy-[1,1'-biphenyl]-3-yl)-5-phenyl-1,3,4-oxadiazole.** To a solution of (E)-4-methoxy-N-(2-methylbenzylidene)-[1,1'-biphenyl]-3-carbohydrazide (0.21 g, 0.62 mmol) in CH<sub>2</sub>Cl<sub>2</sub> ( 5 mL) was added DMP (0.26 g, 0.62 mmol) and stirred at room temperature for 2.5 h. The reaction mixture was concentrated then purified via silica gel chromatography eluting a gradient of 0-40% EtOAc in hexanes. Yield = 0.071 g (34%). ESI-MS(+): *m/z* 343.39 [M+H]<sup>+</sup>.

**3-(5-Phenyl-1,3,4-oxadiazol-2-yl)-[1,1'-biphenyl]-4-ol (100).** To a solution of 2-(4-Methoxy-[1,1'-biphenyl]-3-yl)-5-phenyl-1,3,4-oxadiazole (0.1 g, 0.3 mmol) in CH<sub>2</sub>Cl<sub>2</sub> (25 mL) was added BBr<sub>3</sub> (1M solution in heptanes, 0.9 mmol) and stirred at room temperature for 2.5 h. To the reaction mixture was added excess MeOH to quench BBr<sub>3</sub>. The resulting solution was concentrated then purified via silica gel chromatography eluting a gradient of 0-40% EtOAc in hexanes. Yield =

0.037 g (37%).  $^1\text{H}$  NMR (400 MHz,  $\text{CDCl}_3$ )  $\delta$  10.30 (br, 1H), 8.07 (d,  $J = 8.0$  Hz, 1H), 8.04 (d,  $J = 2.0$  Hz, 1H), 7.71 ((dd,  $J_1 = 8.8$  Hz,  $J_2 = 2.0$  Hz, 1H), 7.62-7.35 (m, 8H), 7.24 (d,  $J = 8.8$  Hz, 1H), 2.79 (s, 3H). ESI-MS(+):  $m/z$  329.40  $[\text{M}+\text{H}]^+$ .

#### **4.5 Acknowledgements**

Chapter 4 highlights the work of a publication currently in preparation. The manuscript in preparation was authored by the following: Christian Perez, Benjamin Dick, Peter F. Glatt, and Seth M. Cohen with a planned title of “Metal-Binding Pharmacophore Library Yields Discovery of a Novel Glyoxalase 1 Inhibitor.” The dissertation author was the primary researcher for the data presented. The co-authors listed in these publications also participated in the research.

## 4.6 References

1. Thornalley, P. J., Glyoxalase I - structure, function and a critical role in the enzymatic defence against glycation. *Biochem. Soc. Trans.* **2003**, *31*, 1343-1348.
2. Silva, M. S.; Gomes, R. A.; Ferreira, A. E. N.; Freire, A. P.; Cordeiro, C., The glyoxalase pathway: the first hundred years ... and beyond. *Biochem. J.* **2013**, *453*, 1-15.
3. Vince, R.; Wolf, M.; Sanford, C., Glutaryl-S-(P-Bromobenzyl)-L-Cysteinylglycine - Metabolically Stable Inhibitor of Glyoxalase I. *J. Med. Chem.* **1973**, *16* (8), 951-953.
4. Creighton, D. J.; Zheng, Z. B.; Holewinski, R.; Hamilton, D. S.; Eiseman, J. L., Glyoxalase I inhibitors in cancer chemotherapy. *Biochem. Soc. Trans.* **2003**, *31*, 1378-1382.
5. Vince, R.; Wadd, W. B., Glyoxalase Inhibitors as Potential Anticancer Agents. *Biochem. Bioph. Res. Co* **1969**, *35* (5), 593-&.
6. Thornalley, P. J.; Rabbani, N., Glyoxalase in tumourigenesis and multidrug resistance. *Semin. Cell Dev. Biol.* **2011**, *22* (3), 318-325.
7. Zhang, H.; Zhai, J.; Zhang, L. P.; Li, C. Y.; Zhao, Y. N.; Chen, Y. Y.; Li, Q.; Hu, X. P., In Vitro Inhibition of Glyoxalase I by Flavonoids: New Insights from Crystallographic Analysis. *Curr. Top. Med. Chem* **2016**, *16* (4), 460-466.
8. More, S. S.; Vince, R., A metabolically stable tight-binding transition-state inhibitor of glyoxalase-I. *Bioorg. Med. Chem. Lett.* **2006**, *16* (23), 6039-6042.
9. Al-Balas, Q. A.; Hassan, M. A.; Al-Shar'i, N. A.; Mhaidat, N. M.; Almaaytah, A. M.; Al-Mahasneh, F. M.; Isawi, I. H., Novel glyoxalase-I inhibitors possessing a "zinc-binding feature" as potential anticancer agents. *Drug Des. Dev. Ther.* **2016**, *10*, 2623-2629.
10. Thornalley, P. J., Protecting the genome: defence against nucleotide glycation and emerging role of glyoxalase I overexpression in multidrug resistance in cancer chemotherapy. *Biochem. Soc. Trans.* **2003**, *31*, 1372-1377.

11. Vince, R.; Brownell, J.; Akella, L. B., Synthesis and activity of gamma-(L-gamma-azaglutamyl)-S(p-bromobenzyl)-L-cysteinylglycine: A metabolically stable inhibitor of glyoxalase I. *Bioorg. Med. Chem. Lett.* **1999**, *9* (6), 853-856.
12. Loos, M.; van der Sluis, S.; Bochdanovits, Z.; van Zutphen, I. J.; Pattij, T.; Stiedl, O.; Neuro, B. M. P. c.; Smit, A. B.; Spijker, S., Activity and impulsive action are controlled by different genetic and environmental factors. *Genes Brain Behav.* **2009**, *8* (8), 817-28.
13. Thornalley, P. J., Advances in glyoxalase research. Glyoxalase expression in malignancy, anti-proliferative effects of methylglyoxal, glyoxalase I inhibitor diesters and S-D-lactoylglutathione, and methylglyoxal-modified protein binding and endocytosis by the advanced glycation endproduct receptor. *Crit. Rev. Oncol. Hematol.* **1995**, *20* (1-2), 99-128.
14. Brownlee, M., Biochemistry and molecular cell biology of diabetic complications. *Nature* **2001**, *414* (6865), 813-20.
15. Williams, R. t.; Lim, J. E.; Harr, B.; Wing, C.; Walters, R.; Distler, M. G.; Teschke, M.; Wu, C.; Wiltshire, T.; Su, A. I.; Sokoloff, G.; Tarantino, L. M.; Borevitz, J. O.; Palmer, A. A., A common and unstable copy number variant is associated with differences in Glo1 expression and anxiety-like behavior. *PLOS One* **2009**, *4* (3), e4649.
16. Hovatta, I.; Tennant, R. S.; Helton, R.; Marr, R. A.; Singer, O.; Redwine, J. M.; Ellison, J. A.; Schadt, E. E.; Verma, I. M.; Lockhart, D. J.; Barlow, C., Glyoxalase 1 and glutathione reductase 1 regulate anxiety in mice. *Nature* **2005**, *438* (7068), 662-6.
17. Distler, M. G.; Plant, L. D.; Sokoloff, G.; Hawk, A. J.; Aneas, I.; Wuenschell, G. E.; Termini, J.; Meredith, S. C.; Nobrega, M. A.; Palmer, A. A., Glyoxalase 1 increases anxiety by reducing GABAA receptor agonist methylglyoxal. *J. Clin. Invest.* **2012**, *122* (6), 2306-15.
18. Thornalley, P. J., The glyoxalase system in health and disease. *Mol. Aspects Med.* **1993**, *14* (4), 287-371.

19. Thornalley, P. J., The glyoxalase system: new developments towards functional characterization of a metabolic pathway fundamental to biological life. *Biochem. J.* **1990**, *269* (1), 1-11.
20. McMurray, K. M.; Ramaker, M. J.; Barkley-Levenson, A. M.; Sidhu, P. S.; Elkin, P. K.; Reddy, M. K.; Guthrie, M. L.; Cook, J. M.; Rawal, V. H.; Arnold, L. A.; Dulawa, S. C.; Palmer, A. A., Identification of a novel, fast-acting GABAergic antidepressant. *Mol. Psychiatry* **2017**.
21. Distler, M. G.; Palmer, A. A., Role of Glyoxalase 1 (Glo1) and methylglyoxal (MG) in behavior: recent advances and mechanistic insights. *Front. Genet.* **2012**, *3*, 250.
22. More, S. S.; Vince, R., Inhibition of Glyoxalase I: The First Low-Nanomolar Tight-Binding Inhibitors. *J. Med. Chem.* **2009**, *52* (15), 4650-4656.
23. Sharkey, E. M.; O'Neill, H. B.; Kavarana, M. J.; Wang, H. B.; Creighton, D. J.; Sentz, D. L.; Eiseman, J. L., Pharmacokinetics and antitumor properties in tumor-bearing mice of an enediol analogue inhibitor of glyoxalase I. *Cancer Chemoth. Pharm.* **2000**, *46* (2), 156-166.
24. Yuan, M. G.; Luo, M. X.; Song, Y.; Xu, Q.; Wang, X. F.; Cao, Y.; Bu, X. Z.; Ren, Y. L.; Hu, X. P., Identification of curcumin derivatives as human glyoxalase I inhibitors: A combination of biological evaluation, molecular docking, 3D-QSAR and molecular dynamics simulation studies. *Bioorg. Med. Chem.* **2011**, *19* (3), 1189-1196.
25. Liu, M.; Yuan, M. G.; Luo, M. X.; Bu, X. Z.; Luo, H. B.; Hu, X. P., Binding of curcumin with glyoxalase I: Molecular docking, molecular dynamics simulations, and kinetics analysis. *Biophys. Chem.* **2010**, *147* (1-2), 28-34.
26. Yadav, A.; Kumar, R.; Sunkaria, A.; Singhal, N.; Kumar, M.; Sandhir, R., Evaluation of potential flavonoid inhibitors of glyoxalase-I based on virtual screening and in vitro studies. *J. Biomol. Struct. Dyn.* **2016**, *34* (5), 993-1007.
27. Kawatani, M.; Okumura, H.; Honda, K.; Kanoh, N.; Muroi, M.; Dohmae, N.; Takami, M.; Kitagawa, M.; Futamura, Y.; Imoto, M.; Osada, H., The identification of an osteoclastogenesis inhibitor through the inhibition of glyoxalase I. *P. Natl. Acad. Sci.* **2008**, *105* (33), 11691-11696.

28. Santel, T.; Pflug, G.; Hemdan, N. Y. A.; Schafer, A.; Hollenbach, M.; Buchold, M.; Hintersdorf, A.; Lindner, I.; Otto, A.; Bigl, M.; Oerlecke, I.; Hutschenreuter, A.; Sack, U.; Huse, K.; Groth, M.; Birkemeyer, C.; Schellenberger, W.; Gebhardt, R.; Platzer, M.; Weiss, T.; Vijayalakshmi, M. A.; Kruger, M.; Birkenmeier, G., Curcumin Inhibits Glyoxalase 1-A Possible Link to Its Anti-Inflammatory and Anti-Tumor Activity. *PLoS One* **2008**, *3* (10).
29. Chiba, T.; Ohwada, J.; Sakamoto, H.; Kobayashi, T.; Fukami, T. A.; Irie, M.; Miura, T.; Ohara, K.; Koyano, H., Design and evaluation of azaindole-substituted N-hydroxypyridones as glyoxalase I inhibitors. *Bioorg. Med. Chem. Lett.* **2012**, *22* (24), 7486-7489.
30. Arai, M.; Nihonmatsu-Kikuchi, N.; Itokawa, M.; Rabbani, N.; Thornalley, P. J., Measurement of glyoxalase activities. *Biochem. Soc. Trans.* **2014**, *42* (2), 491-4.
31. Jacobsen, J. A.; Fullagar, J. L.; Miller, M. T.; Cohen, S. M., Identifying chelators for metalloprotein inhibitors using a fragment-based approach. *J. Med. Chem.* **2011**, *54* (2), 591-602.
32. Molecular Operating Environment (MOE), 2013.08; Chemical Computing Group ULC, 1010 Sherbooke St. West, Suite #910, Montreal, QC, Canada, H3A 2R7, 2018.
33. Lewis, J. A.; Puerta, D. T.; Cohen, S. M., Metal complexes of the trans-influencing ligand thiomaltol. *Inorg. Chem.* **2003**, *42* (23), 7455-7459.

## **Chapter 5: Computer Aided Design of Novel Potent Glyoxalase 1 Inhibitors**

## 5.1 Introduction

As discussed in Chapter 1, anxiety and depression are the two most common psychiatric disorders in the US and affect approximately one-in-five adults at some point in their lifetime.<sup>1-2</sup> As described in Chapters 1 and 4, GLO1 is a cytosolic Zn<sup>2+</sup>-dependent isomerase that is part of the glyoxalase system, a pathway involved in the detoxification of MG.<sup>3-6</sup> MG is a reactive metabolite generated via the degradation of glycolytic intermediates and at high concentrations is capable of forming covalent adducts with proteins and nucleotides which result in AGE products, ROS, and apoptosis. Due to the role in AGE formation and cytotoxicity, GLO1 inhibitors have been investigated as potential oncogenic therapeutics, but have not had any clinical success.<sup>7-8</sup> Therefore, efforts have been made to find alternative indications for GLO1 inhibition.

In this chapter, the design, synthesis, and evaluation of a novel class of GLO1 inhibitors is reported. As described in Chapter 4, screening of a MBP library yielded **8-MSQ** as a MBP fragment that demonstrated inhibition of GLO1 (Figure 4-3). An in vitro absorbance inhibition assay and a computational molecular modeling utilizing a previously reported GLO1 crystal structure were utilized to develop SAR for **8-MSQ** against GLO1. The computational model facilitated the design of novel compounds as well as helped guide the SAR. Initially, two libraries of compounds were synthesized, each focused on finding the optimal substituents to build into the hydrophobic and GSH-binding pockets

(Figure 5-1). Lastly, the results from these libraries were utilized in a fragment-merge strategy that yielded potent GLO1 inhibitors.

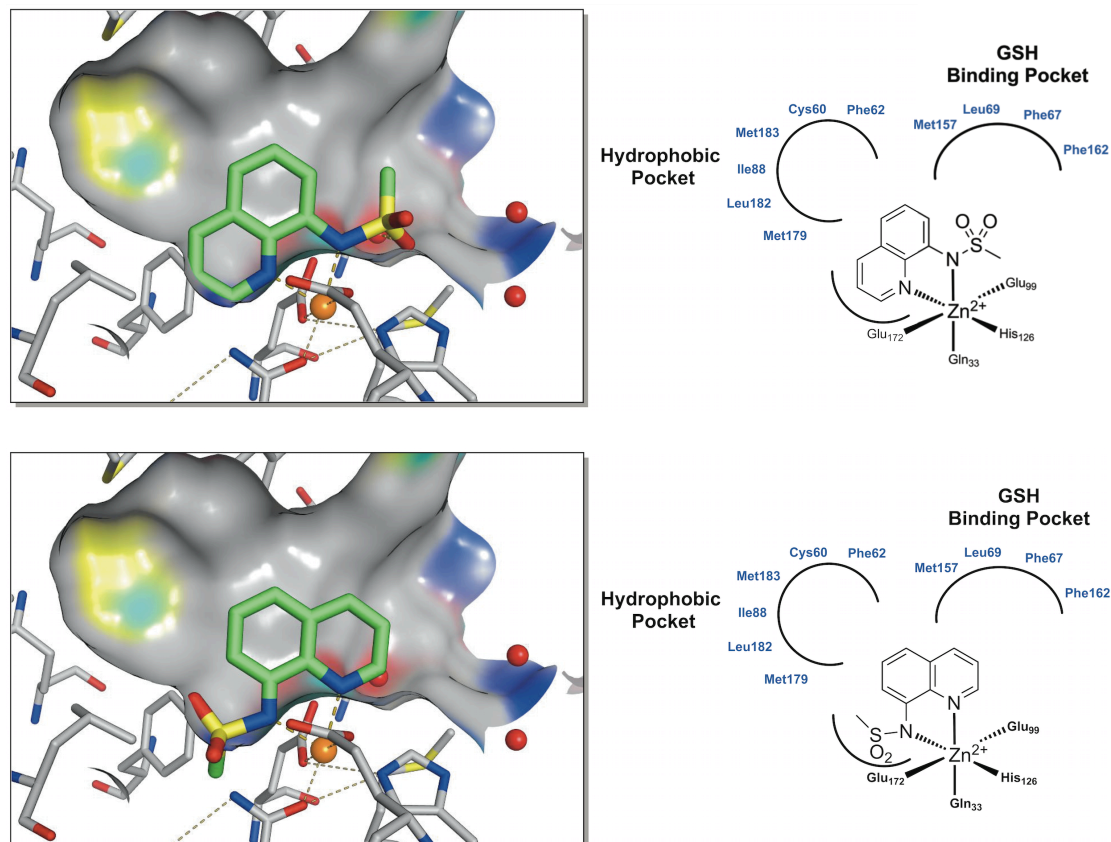


**Figure 5-1.** Superpositioned pose of **8-MSQ** coordinating to the Zn<sup>2+</sup> ion the GLO1 active site (*left*) and chemical illustration (*right*). Two possible coordinating poses are shown: pose 1 (*top*) and pose 2 (*bottom*). A surface outlining the active site pockets is shown in gray. Zinc is depicted as an orange sphere and water as a red sphere.

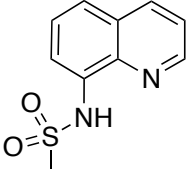
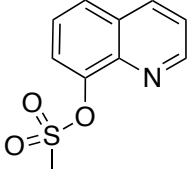
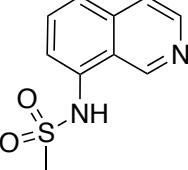
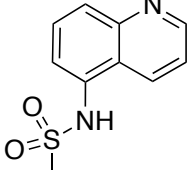
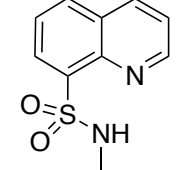
## 5.2 Results and Discussion

### 5.2.1 Investigating the Mechanism of Inhibition

The lead fragment **8-MSQ** has been previously reported as a functional group that can inhibit metalloenzymes, but has also been used as a receptor unit

in molecular sensors for biological Zn<sup>2+</sup>.<sup>9-12</sup> Based on these previous reports, it was expected that **8-MSQ** could bind to the catalytic Zn<sup>2+</sup> ion of GLO1 in a bidentate fashion through the endocyclic nitrogen and exocyclic nitrogen donor atoms (Figure 5-1). To validate this hypothesis, a series of compounds were synthesized wherein the metal-coordinating atoms were substituted or replaced (Table 5-1). Compounds **101** and **102** place the coordinating endocyclic nitrogen at different positions within the quinoline ring. Compound **103** replaces the endocyclic nitrogen with a C-H group, giving a naphthyl derivative, which is incapable of the bidentate coordination. Additionally, compound **104** replaces the sulfonamide with a sulfonate ester, while **105** replaces the sulfonamide with an amide. As highlighted by the data in Table 5-1, compounds **101-105** all showed a complete loss of activity (IC<sub>50</sub> >200 μM) against GLO1, further suggesting the importance of the bidentate binding of **8-MSQ** through the nitrogen pair of donor atoms.

**Table 5-1.** **8-MSQ** fragment derivatives used to examine the role of metal binding in GLO1 inhibition. All IC<sub>50</sub> values listed are in μM.

Cmpd	Structure	GLO1	Cmpd	Structure	GLO1
<b>8-MSQ</b>		18.46±0.50	<b>103</b>		>200
<b>101</b>		>200	<b>104</b>		>200
<b>102</b>		>200	<b>105</b>		>200

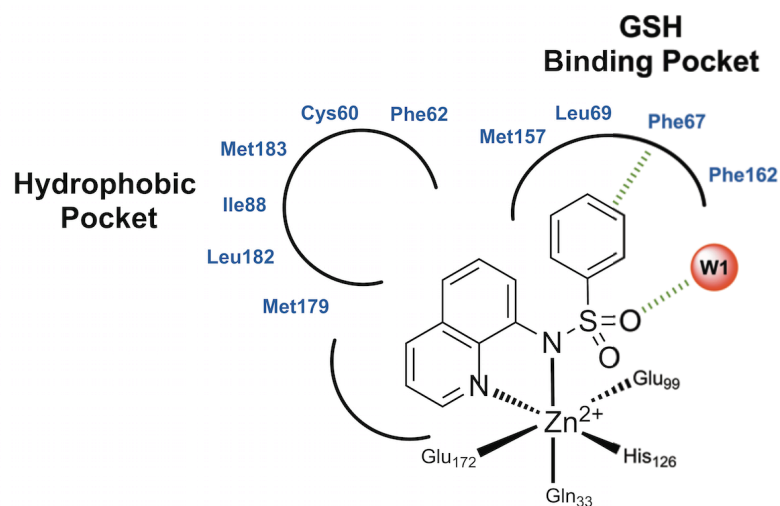
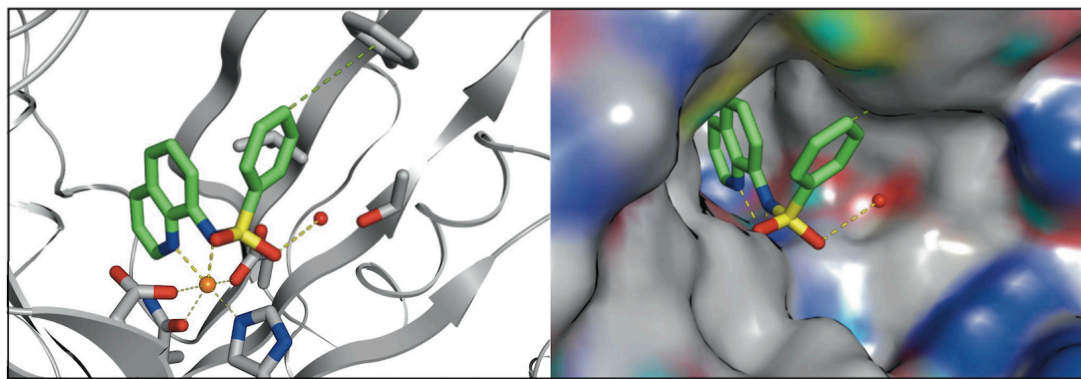
### 5.2.2 Development of a GLO1 Computational Model

The core quinoline scaffold of compound **8-MSQ** has several positions amenable for derivatization. Similar to the fragments discussed in Chapter 4, a computational model utilizing **8-MSQ** was utilized. As discussed in Chapter 4, modeling studies were performed using the MOE software suite.<sup>13</sup> Using a crystal structure of GLO1 (PDB: 3VW9) an inhibitor pharmacophore model was generated (Figure 5-1). The catalytic Zn<sup>2+</sup> has an octahedral geometry and is coordinated by Glu99, Glu172, His,126, and Gln33, with the 5<sup>th</sup> and 6<sup>th</sup> coordination sites occupied by a bound *N*-hydroxypyridinone inhibitor (**Chugai-3d**, Figure 1-6). A binding model for **8-MSQ** was obtained through docking of the fragment into the GLO1 active site and superimposing the coordinating atoms

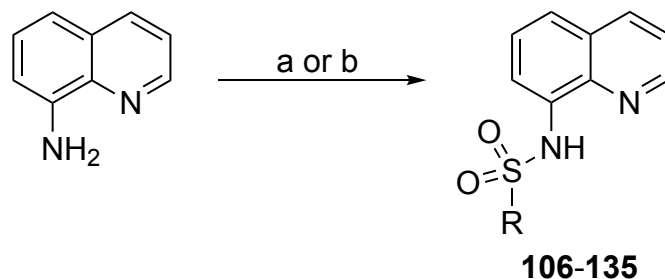
(*N,N*) of **8-MSQ** with those of the bound **Chugai-3d** inhibitor. The superposition of **8-MSQ** generated a probable binding mode in which the endocyclic nitrogen of the quinoline ring is bound at the equatorial site of the metal center and the exocyclic nitrogen of the sulfonamide functional group is bound axial of the metal center (Pose 1, Figure 5-1). The docked pose was well tolerated with no major clash predicted between the fragment and the receptor. Another mode of binding can be modeled by alternating the position of the donor set; however, modeling suggested that this alternate binding pose is likely to cause significant steric clashes with the GLO1 active site (Pose 2, Figure 5-1). Docking of pose 2 caused significant clash between the methylsulfonamide functional group of **8-MSQ** and the coordinating Gln33 (distance <1 Å). Therefore initial assessment of these two poses pointed towards pose 1 as the most likely mode of binding (Figure 5-1).

To determine whether the computational model developed in Figure 5-1 was predictive, a small set of compounds was synthesized to evaluate the computational model. Compounds **106-108** were synthesized in a straightforward, one-step manner as outlined in Scheme 5-1 starting with 8-aminoquinoline or 2-methyl-8-aminoquinoline and combining with the corresponding sulfonyl chloride. Evaluation of the inhibition of compound **106** yielded a poorer IC<sub>50</sub> value (~2-fold loss of affinity compared to **8-MSQ**) due simply to the introduction of a methyl substituent (Table 5-2). As demonstrated in pose 1 (Figure 5-1) the introduction of a methyl group generates a steric clash

with Gln33, similarly to the less favored pose 2, which is consistent with the molecular modeling study. Compound **107** incorporates a phenyl at the 8-sulfonamide position and results in a 2-fold improvement in inhibition, which also validates the computational model generated where the phenyl group can be accommodated in the glutathione binding pocket (Figure 5-2). From this docked pose, compound **107** forms a hydrogen bond between the sulfone and a water molecule (W1). An additional edge to face  $\pi$ - $\pi$  interaction between the phenyl moiety and Phe67 ( $\sim 4.5$  Å) is predicted. Lastly, a hydrophobic interaction between the phenyl and Leu69 ( $\sim 4.2$  Å) is also predicted. Compound **108** incorporates both a 2-methyl and an 8-phenylsulfonamide which results in a net slight increase in inhibition relative to **8-MSQ** but worse activity when compared with **107** (Table 5-2). Taken together these results support the predicted mode of binding (Pose 1).

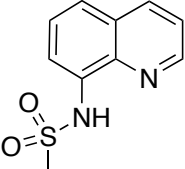
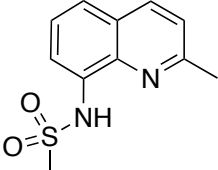
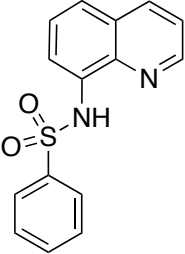
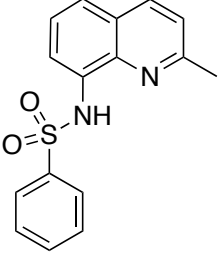


**Figure 5-2.** Superpositioned pose of compound **107** coordinating to the  $Zn^{2+}$  in the GLO1 active site. An image demonstrating the amino acid side chain residues is shown (*left*) with a surface outlining the active site GSH binding pocket is shown in gray and a chemical illustration (*bottom*). Zinc is depicted as an orange sphere and water as a red sphere.



**Scheme 5-1.** Synthesis of 8-sulfonamide derivatives. (a)  $R-SO_2Cl$ , pyridine, 25 °C; (b)  $R-SO_2Cl$ , pyridine, 25 °C.

**Table 5-2. 8-MSQ derivatives used to examine the coordination mode in the computational model. All IC<sub>50</sub> values listed are in μM.**

Compound	Structure	GLO1
8-MSQ		18.46 ± 0.50
106		42.99 ± 0.16
107		8.47 ± 1.21
108		14.49 ± 1.72

The SAR obtained from compounds **106-108** (Table 5-2) demonstrated that the computational model is a useful tool to guide the design of compounds. Additionally, based on the inhibition of compound **8**, **8-MSQ** analogs that incorporate functional groups at the sulfonamide moiety at the 8-position are well tolerated to fit in the GSH-binding pocket. Using a fixed Zn<sup>2+</sup>-coordination geometry for **8-MSQ** the SAR around the fragment was explored by making independent substitutions at 8-position.

### 5.2.3 8-Sulfonamidequinoline Analogs

The first step of our inhibitor discovery process was to find the optimal group to enhance interactions within the GSH-binding pocket. A variety of substituents were explored via a sulfonamide linkage as demonstrated in Table 5-3. The introduction of non-aromatic alkane chains lead to loss of inhibition (**109-112**). However, compounds that incorporated heterocyclic or aromatic rings, such as thiophene, furan, phenyl, and pyridine (**113-114**, **117-118**, **120-121**, **123**, **126-129**) all improved activity modestly. Three compounds incorporated fused-ring systems (**130-132**) and were among the best inhibitors of this subset of molecules. Alternatively, changing the linker between the sulfonamide functional group and the phenyl substituent (**133-135**) did not seem to change inhibition significantly. Interestingly, compounds **116** and **119** that incorporate a methoxy or nitrile at the ortho position (relative to sulfonamide) were not tolerated. Docking of these compounds within the active site predicted a major clash with a W1 and limited intramolecular rotation. Ultimately, compound **122** (Table 5-3, IC<sub>50</sub> value 1.3 μM) was the most active derivative from this group by making the best interactions within the GSH-binding pocket. Similarly to compound **107**, the 2-pyridinyl group forms an edge-to-face π interaction with Phe67 and a hydrophobic contact with Leu69 (Figure 5-3). Additionally, the 2-pyridinyl nitrogen is directly facing W1 and engaging in a hydrogen bond.

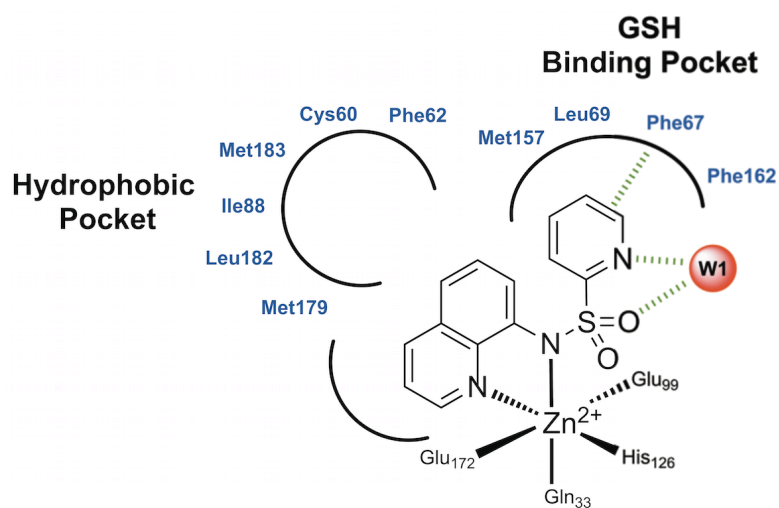
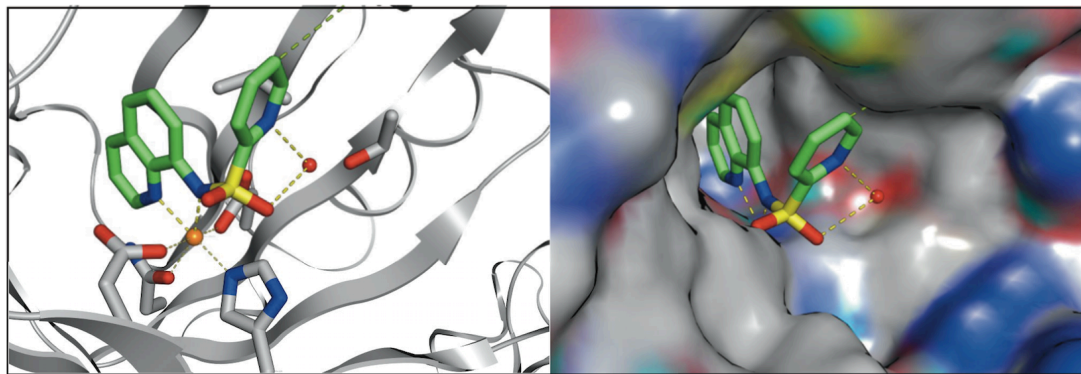
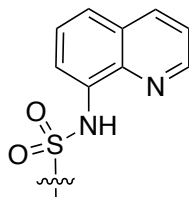


**Figure 5-3.** Superpositioned pose of compound **122** coordinating to the Zn<sup>2+</sup> ion in the GLO1 active site. An image demonstrating the amino acid side chain residues is shown (*left*) with a surface outlining the active site GSH binding pocket is shown in gray and a chemical illustration (*bottom*). Zinc is depicted as an orange sphere and water as a red sphere.

**Table 5-3. 8-MSQ fragment derivatives probing functionalization at the 8-position.** All IC<sub>50</sub> values listed are in  $\mu\text{M}$ .



Cmpd	Structure	GLO1	Cmpd	Structure	GLO1
8-MSQ		18.46 ± 0.50	122		1.31 ± 0.17
109		>20	123		11.23 ± 2.49
110		>20	124		>20
111		>20	125		4.21 ± 2.15
112		>20	126		7.50 ± 0.66
113		4.93 ± 1.51	127		5.69 ± 2.34
114		5.50 ± 3.68	128		6.12 ± 0.07
115		>20	129		6.58 ± 0.40
116		>20	130		3.62 ± 1.12

**Table 5-3.** 8-MSQ fragment derivatives probing functionalization at the 8-position. All IC<sub>50</sub> values listed are in  $\mu\text{M}$ , continued.

Cmpd	Structure	GLO1	Cmpd	Structure	GLO1
117		$6.87 \pm 0.35$	131		$3.87 \pm 0.10$
118		$6.98 \pm 1.39$	132		$3.87 \pm 0.06$
119		>20	133		$7.62 \pm 1.02$
120		$7.28 \pm 0.24$	134		$8.74 \pm 0.44$
121		$6.65 \pm 1.22$	135		$4.63 \pm 0.60$

#### 5.2.4 5-Aryl/Cyclic-8-(Methylsulfonylamino)quinoline Derivatives

A second set of compounds were pursued to explore an optimal substituent to interact within the hydrophobic pocket. Further analysis of the computational model suggests that the 5-position of the quinoline ring may be modified in order to gain interactions within the hydrophobic pocket (Figure 5-4). This series of compounds complements the study exploring the GSH-binding pocket, and taken together would be merged to find optimal groups to attach at

each position. For the synthesis of this series, 5-bromoquinoline was selectively nitrated at the 8 position yielding 5-bromo-8-nitroquinoline (Scheme 5-2). This intermediate was utilized to attach aryl or amine substituents at the 5-position via Suzuki or Buchwald coupling reactions. The products of the coupling reaction were then reduced via palladium on carbon under hydrogen atmosphere or through the use of sodium dithionite resulting in the free amine compound. Lastly, the amine was coupled with methylsulfonyl chloride under basic conditions. A set of 10 compounds was synthesized, with diverse functional groups at the 5-position (Table 5-4). Evaluation of these compounds against GLO1 gave a general trend where polar (**137** and **138**) and cycloalkanes (**144** and **145**) were not well tolerated. Only the compounds containing hydrophobic phenyl substituents resulted in better inhibition relative to **8-MSQ**. Docking of these compounds resulted in favorable interactions of the 5-phenyl substituent (**136**) within the hydrophobic pocket with predicted edge-to-face  $\pi$  interactions with Phe62 and additional hydrophobic contacts with Met179 and Met183 (Figure 5-4).

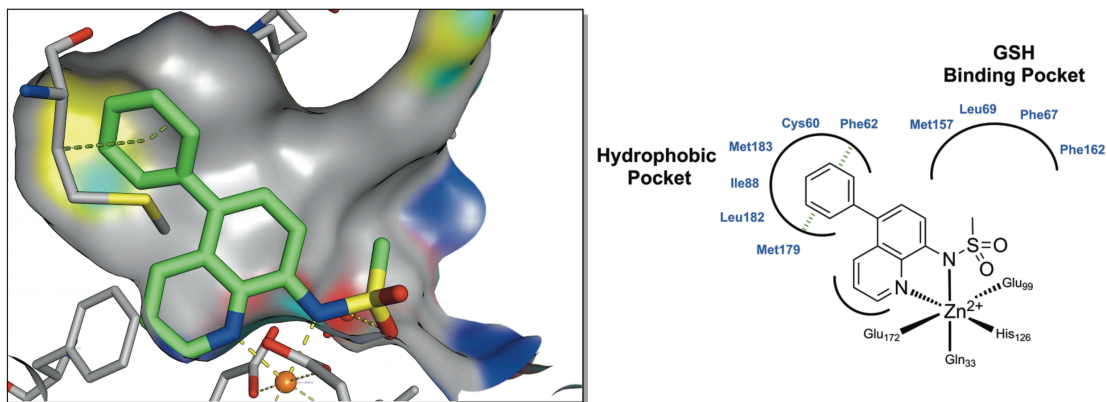
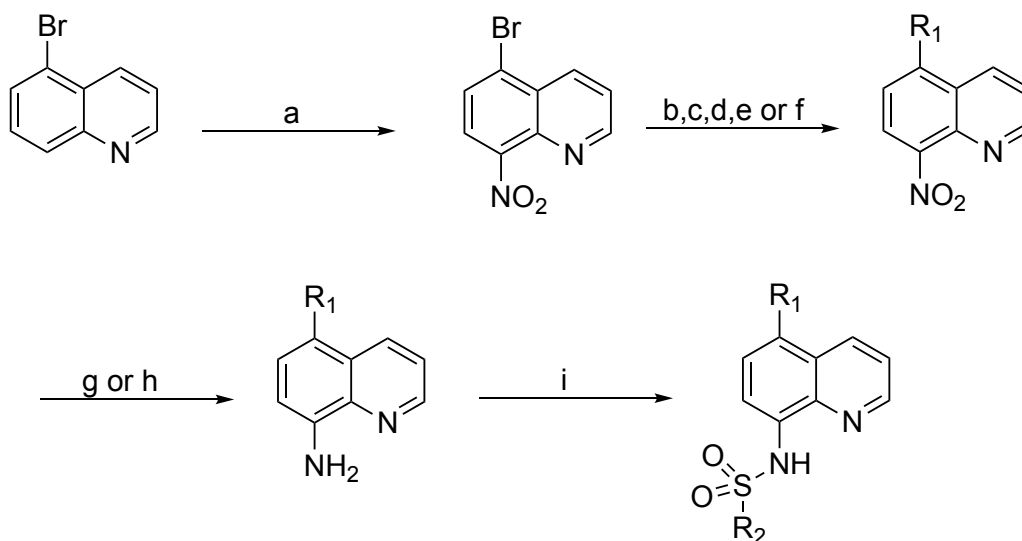
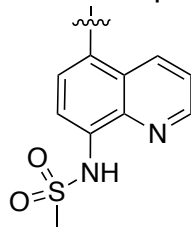


**Figure 5-4.** Superpositioned pose of **136** coordinating to the  $\text{Zn}^{2+}$  ion the GLO1 active site (*left*) and chemical illustration (*right*). A surface outlining the active site pockets is shown in gray. Zinc is depicted as an orange sphere.



**Scheme 5-2.** Synthesis 5-Aryl/Cyclic/Ethynyl-8-sulfonamide quinoline derivatives. (a)  $\text{KNO}_3$ ,  $\text{H}_2\text{SO}_4$ , 0-25 °C; (b)  $\text{R-B(OH)}_2$ ,  $\text{Pd(OAc)}_2$ , DIPA,  $\text{H}_2\text{O}$ , 100 °C; (c)  $\text{R-B(OH)}_2$ ,  $\text{Pd(PPh}_3)_4$ ,  $\text{CH}_3\text{COOK}$ , 1,4-Dioxane 100 °C; (d)  $\text{R-B(OH)}_2$ ,  $\text{Pd(dppf)Cl}_2$ , S-Phos,  $\text{K}_2\text{CO}_3$ ,  $\text{H}_2\text{O}$ , 1,4-Dioxane, 100 °C; (e)  $\text{R-Amine}$ ,  $\text{Pd}_2(\text{dba})_3$ , X-Phos,  $\text{K}_2\text{CO}_3$ , 1,4-Dioxane 100 °C; (f)  $\text{R-Ethynyl}$ ,  $\text{CuI}$ ,  $\text{Pd(dppf)Cl}_2$ , X-Phos,  $\text{Et}_3\text{N}$ , 1,4-Dioxane 90 °C; (g)  $\text{Pd/C}$ ,  $\text{H}_2$ ,  $\text{MeOH}$ , 25 °C; (h)  $\text{Na}_2\text{S}_2\text{O}_4$ ,  $\text{K}_2\text{CO}_3$ ,  $\text{H}_2\text{O}$ ,  $\text{MeOH}$ , Acetone 25 °C; (i)  $\text{R-SO}_2\text{Cl}$ , pyridine, 25 °C.

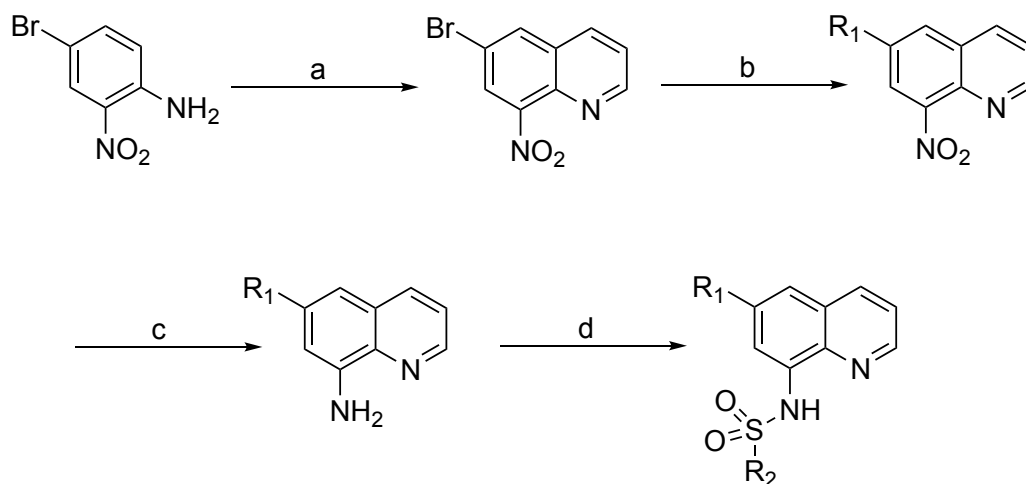
**Table 5-4.** 8-MSQ fragment derivatives used to examine the role of metal binding in GLO1 inhibition. Values shown represent IC<sub>50</sub> (μM).



Cmpd	Structure	GLO1	Cmpd	Structure	GLO1
136		11.50 ± 1.32	141		11.91 ± 0.06
137		>20	142		15.42 ± 0.21
138		>20	143		11.23 ± 1.86
139		6.17 ± 0.94	144		>100
140		13.91 ± 0.30	145		>100

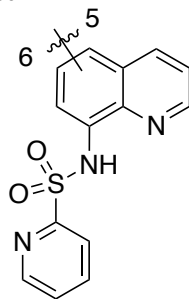
### 5.2.5 Merged Compounds

Using the optimal functional groups identified for both the 5- and 8-position, a fragment merging strategy was employed to produce a series of lead compounds. The functionality at the 8-position (2-pyridinyl sulfonamide) was maintained throughout this series, with minimal structural variation at the 5-position. Additionally, a handful of compounds were synthesized off the 6-position (Scheme 5-3). Synthesis of these compounds generally followed Scheme 5-2 where the intermediate, 5-bromo-8-nitroquinoline or 6-bromo-8-nitroquinoline, was coupled to aryl, amines, or alkynes via Suzuki, Buchwald, or Sinogashira methods. Compounds containing alkynes were reduced to alkanes in a one-pot reduction of alkyne and nitro with palladium on carbon and hydrogen (Scheme 5-2 and 5-3). Compounds containing phenyl, chlorophenyl, and fluorophenyl substituents (**146-149**, **152-153**, and **156-161**) were primarily explored based on the results from Table 5-4. Additionally, compounds **150-151**, **154-155**, and **162-163** were inspired by flavonoid GLO1 inhibitors previously reported.<sup>14-22</sup> This series of compounds yielded several inhibitors with IC<sub>50</sub> value of <1 μM, with compound **148** demonstrating the best inhibition (Table 5-5).



**Scheme 5-3.** Synthesis 5-Aryl/Cyclic/Ethynyl-8-sulfonamide quinoline derivatives. (a) Acrolein, 6M HCl, toluene, reflux; (b) R-Ethynyl, CuI, Pd(dppf)Cl<sub>2</sub>, X-Phos, Et<sub>3</sub>N, 1,4-Dioxane 90 °C; (c) Pd/C, H<sub>2</sub>, MeOH, 25 °C; (h) Na<sub>2</sub>S<sub>2</sub>O<sub>4</sub>, K<sub>2</sub>CO<sub>3</sub>, H<sub>2</sub>O, MeOH, Acetone 25 °C; (d) R-SO<sub>2</sub>Cl, pyridine, 25 °C.

**Table 5-5. 8-MSQ fragment derivatives used to examine the role of metal binding in GLO1 inhibition. All IC<sub>50</sub> values listed are in μM.**



Cmpd	Pos	Structure	GLO1	Cmpd	Pos	Structure	GLO1
146	5		0.50 ± 0.04	153	5		0.54 ± 0.20
147	5		0.48 ± 0.01	154	5		1.1 ± 0.6
148	5		0.37 ± 0.02	155	5		0.79 ± 0.13
149	5		0.72 ± 0.01	156	5		0.78 ± 0.33
150	5		0.64 ± 0.09	157	6		1.2 ± 0.1
151	5		1.0 ± 0.3	158	6		1.3 ± 0.1
152	5		0.59 ± 0.14	159	6		0.46 ± 0.06

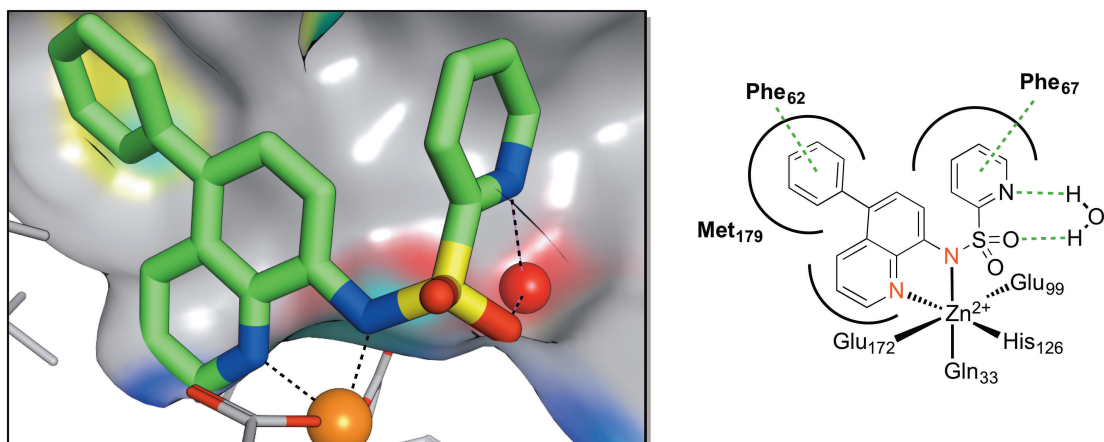


**Figure 5-5.** Binding mode of **146** within GLO1 active site (*left*) and a chemical illustration of mode of binding (*right*).

### 5.3 Conclusions

Screening of a focused MBP library yielded **8-MSQ** as a fragment hit that displayed inhibition of GLO1. Computational molecular modeling was utilized to generate a model to predict the binding mode of **8-MSQ** to GLO1. Complemented with a synthetic campaign, the computational model allowed for development of SAR, which facilitated the development of inhibitors. Compounds **148** and **162** demonstrated the most active inhibition of GLO1 (IC<sub>50</sub> value <500 nM) and are amongst the most potent GLO1 inhibitors that have been reported. This work represents the development of a novel class of GLO1 inhibitors. The non-hydroxamate and non-glutathione origins of this class of compounds makes them more drug like. Efforts to investigate these compounds as novel anti-depressants/anxiolytic compounds will be further pursued.

## 5.4 Experimental

**Human Glyoxalase 1 Activity Assay.** Recombinant Human Glyoxalase I (GLO1) was purchased from R&D Systems (Catalog #4959-GL). Assays were carried out in 100 mM Sodium Phosphate, pH 7.0 buffer utilizing 96-well Clear UV Plate (Corning UV Transparent Microplates Catalog #3635). A fresh solution of glutathione (Pre-Substrate 1, 100 mM) as well as methylglyoxal (Pre-substrate 2, 100 mM) was prepared in deionized water. The substrate was prepared by adding 14.5 mL of buffer and 0.99 mL of each of the pre-substrate components. The substrate mixture was vortexed vigorously for 15 sec, then allowed to sit at room temperature for 20 min. Initial well volume was 50  $\mu$ L containing GLO1 (40 ng) and inhibitor. This protein and inhibitor mixture was incubated for 15-20 min prior to addition of substrate. To this was then added substrate (150  $\mu$ L) yielding a maximum amount of 5% DMSO per well. The enzyme activity was measured utilizing a Biotek Synergy HT or H4 plate reader by measuring absorbance at 240 nm every 1 min for 8 min. The rate of absorbance increase was compared for samples versus controls containing no inhibitor (100% activity). Absorbance for background wells containing DMSO, buffer and substrate (no enzyme or inhibitor) were subtracted from the rest of the wells.

## Synthetic Procedures.

***N*-(Quinolin-8-yl)methanesulfonamide (8-MSQ).** To a solution of 8-aminoquinoline (0.1 g, 0.69 mmol) in Pyridine (3 mL) was added the methanesulfonyl chloride (0.161 mL, 2.08 mmol) and allowed to stir at room temperature for 12-15 h. To the resulting mixture was added H<sub>2</sub>O (50 mL) and then extracted with EtOAc (3×50mL). The combined organic layers were dried over MgSO<sub>4</sub>, then filtered, and concentrated via rotary evaporation. The resulting crude oil was purified via silica gel chromatography eluting a gradient of 0-80% EtOAc in Hexanes. Yield = 0.085 g (55%). <sup>1</sup>H NMR (400 MHz, CDCl<sub>3</sub>): δ 8.93 (br, 1H), 8.83 (dd, J<sub>1</sub> = 4.4 Hz, J<sub>2</sub> = 2 Hz, 1H), 8.20 (dd, J<sub>1</sub> = 8.4 Hz, J<sub>2</sub> = 1.6 Hz, 1H), 7.87 (dd, J<sub>1</sub> = 7.2 Hz, J<sub>2</sub> = 1.6 Hz, 1H), 7.58-7.48 (m, 3H), 3.03 (s, 3H). ESI-MS(+): *m/z* 223.08 [M+H]<sup>+</sup>, 245.04 [M+Na]<sup>+</sup>.

***N*-(Isoquinolin-8-yl)methanesulfonamide (101).** To a solution of isoquinolin-8-amine (0.2 g, 1.38 mmol) in Pyridine (3 mL) was added the methanesulfonyl chloride (0.161 mL, 2.08 mmol) and allowed to stir at room temperature for 12-15 h. To the resulting mixture was added H<sub>2</sub>O (50 mL) and then extracted with EtOAc (3×50mL). The combined organic layers were dried over MgSO<sub>4</sub>, then filtered, and concentrated via rotary evaporation. The resulting crude oil was purified via silica gel chromatography eluting a gradient of 0-20% MeOH in CH<sub>2</sub>Cl<sub>2</sub>. Yield = 0.161 g (52%). <sup>1</sup>H NMR (400 MHz, DMSO-*d*<sup>6</sup>): δ 10.75 (br, 1H),

9.92 (s, 1H), 8.70 (d, J = 6.4 Hz, 1H), 8.47 (d, J = 6.4 Hz, 1H), 8.18-8.12 (m, 2H), 7.93 (d, J = 6.8 Hz, 1H), 3.19 (s, 3H). ESI-MS(+):  $m/z$  223.08 [M+H]<sup>+</sup>.

***N*-(Quinolin-5-yl)methanesulfonamide (102).** To a solution of quinolin-5-amine (0.2 g, 1.38 mmol) in Pyridine (3 mL) was added the methanesulfonyl chloride (0.161 mL, 2.08 mmol) and allowed to stir at room temperature for 12-15 h. To the resulting mixture was added H<sub>2</sub>O (50 mL) and then extracted with EtOAc (3×50mL). The combined organic layers were dried over MgSO<sub>4</sub>, then filtered, and concentrated via rotary evaporation. The resulting crude oil was purified via silica gel chromatography eluting a gradient of 0-16% MeOH in CH<sub>2</sub>Cl<sub>2</sub>. Yield = 0.11 g (38%). <sup>1</sup>H NMR (400 MHz, CDCl<sub>3</sub>): δ 8.41 (dd, J<sub>1</sub> = 8.4 Hz. J<sub>2</sub> = 1.6 Hz, 1H), 8.29 (d, J = 8.4 Hz, 1H), 7.81 (t, J = 8.4 Hz, 1H), 7.64 (dd, J<sub>1</sub> = 8.4 Hz. J<sub>2</sub> = 1.6 Hz, 1H), 7.59 (dd, J<sub>1</sub> = 8.4 Hz. J<sub>2</sub> = 4.0 Hz, 1H), 3.51 (s, 3H). ESI-MS(+):  $m/z$  223.11 [M+H]<sup>+</sup>.

**Quinolin-8-yl methanesulfonate (103).** To a solution of 8-hydroxyquinoline (0.2 g, 1.38 mmol) in Pyridine (3 mL) was added the methanesulfonyl chloride (0.322 mL, 4.13 mmol) and allowed to stir at room temperature for 12-15 h. To the resulting mixture was added H<sub>2</sub>O (50 mL) and then extracted with EtOAc (3×50mL). The combined organic layers were dried over MgSO<sub>4</sub>, then filtered, and concentrated via rotary evaporation. The resulting crude oil was purified via silica gel chromatography eluting a gradient of 0-70% EtOAc in Hexanes. Yield =

0.085 g (34%).  $^1\text{H}$  NMR (400 MHz,  $\text{CDCl}_3$ ):  $\delta$  8.91 (dd,  $J_1 = 4$  Hz,  $J_2 = 1.6$  Hz, 1H), 8.15 (dd,  $J_1 = 8.4$  Hz,  $J_2 = 1.2$  Hz, 1H), 7.73 (d,  $J = 8$  Hz, 1H), 7.67 (d,  $J = 8$  Hz, 1H), 7.50 (t,  $J = 8$  Hz, 1H), 7.43 (dd,  $J_1 = 8.4$  Hz,  $J_2 = 4.4$  Hz, 1H), 3.40 (s, 3H). ESI-MS(+):  $m/z$  224.25  $[\text{M}+\text{H}]^+$ .

***N*-(Quinolin-8-yl)acetamide (104).** To a solution of 8-aminoquinoline (0.2 g, 1.38 mmol) in Pyridine (3 mL) was added the acetyl chloride (0.148 mL, 2.08 mmol) and allowed to stir at room temperature for 12-15 h. To the resulting mixture was added  $\text{H}_2\text{O}$  (50 mL) and then extracted with EtOAc (3 $\times$ 50mL). The combined organic layers were dried over  $\text{MgSO}_4$ , then filtered, and concentrated via rotary evaporation. The resulting crude oil was purified via silica gel chromatography eluting a gradient of 0-60% EtOAc in Hexanes. Yield = 0.076 g (32%).  $^1\text{H}$  NMR (400 MHz,  $\text{CDCl}_3$ ):  $\delta$  9.78 (br, 1H), 8.81 (dd,  $J_1 = 4$  Hz,  $J_2 = 1.6$  Hz, 1H), 8.77 (dd,  $J_1 = 8$  Hz,  $J_2 = 1.6$  Hz, 1H), 8.17 (dd,  $J_1 = 8$  Hz,  $J_2 = 1.6$  Hz, 1H), 7.55-7.48 (m, 2H), 7.47 (dd,  $J_1 = 8$  Hz,  $J_2 = 5$  Hz, 1H), 2.35 (s, 3H). ESI-MS(+):  $m/z$  187.23  $[\text{M}+\text{H}]^+$ .

***N*-Methylquinoline-8-sulfonamide (105).** To a solution of quinoline-8-sulfonyl chloride (0.2 g, 0.88 mmol) in Pyridine (3 mL) was added the methylamine (2M THF solution, 1.31 mL, 0.082 mmol) and allowed to stir at room temperature for 12-15 h. To the resulting mixture was added  $\text{H}_2\text{O}$  (50 mL) and then extracted with EtOAc (3 $\times$ 50mL). The combined organic layers were dried over  $\text{MgSO}_4$ ,

then filtered, and concentrated via rotary evaporation. The resulting crude oil was purified via silica gel chromatography eluting a gradient of 0-55% EtOAc in Hexanes. Yield = 0.11 g (43%).  $^1\text{H NMR}$  (400 MHz,  $\text{CDCl}_3$ ):  $\delta$  9.03 (d,  $J = 4$  Hz, 1H), 8.47 (d,  $J = 8$  Hz, 1H), 8.31 (d,  $J = 8$  Hz, 1H), 8.09 (d,  $J = 8$  Hz, 1H), 7.70 (t,  $J = 8$  Hz, 1H), 7.59 (dd,  $J_1 = 8$  Hz,  $J_2 = 4$  Hz, 1H), 6.26 (br, 1H), 2.59 (d,  $J = 5.6$  Hz, 3H). ESI-MS(+):  $m/z$  223.15  $[\text{M}+\text{H}]^+$ .

***N*-(2-Methylquinolin-8-yl)methanesulfonamide (106).** To a solution of 2-methylquinolin-8-amine (0.2 g, 1.26 mmol) in Pyridine (3 mL) was added Methanesulfonyl chloride (0.296 mL, 3.79 mmol) and allowed to stir at room temperature for 15 h. To the resulting mixture was added  $\text{H}_2\text{O}$  (50 mL) and then extracted with EtOAc (3 $\times$ 50mL). The combined organic layers were dried over  $\text{MgSO}_4$ , filtered, concentrated then purified via silica gel chromatography eluting 0-10% MeOH in  $\text{CH}_2\text{Cl}_2$ . The desired product was isolated as a dark brown solid. Yield = 0.191 g (64%).  $^1\text{H NMR}$  ( $\text{DMSO}-d_6$ , 400 MHz)  $\delta$  9.17 (br, 1H), 8.29 (d,  $J = 8.4$  Hz, 1H), 7.67 (m, 2H), 7.51 (m, 2H), 3.15 (s, 3H), 2.70 (s, 3H). ESI-MS(+):  $m/z$  237.07  $[\text{M}+\text{H}]^+$ , 258.98  $[\text{M}+\text{Na}]^+$ .

***N*-(Quinolin-8-yl)benzenesulfonamide (107).** Synthesized utilizing method B. Isolated as white solid. Yield = 0.179 g (91%).  $^1\text{H NMR}$  ( $\text{CDCl}_3$ , 400 MHz)  $\delta$  9.25 (br, 1H), 8.76 (d,  $J = 4.4$  Hz, 1H), 8.10 (d,  $J = 8.8$  Hz, 1H), 7.91 (d,  $J = 8$  Hz, 2H), 7.82 (dd,  $J_1 = 6.4$  Hz,  $J_2 = 2.4$  Hz, 1H), 7.41 (m, 6H). ESI-MS(+):  $m/z$

285.03 [M+H]<sup>+</sup>.

***N*-(2-Methylquinolin-8-yl)benzenesulfonamide (108).** To a solution of 2-methylquinolin-8-amine (0.2 g, 1.26 mmol) in Pyridine (3 mL) was added Benzenesulfonyl chloride (0.486 mL, 3.79 mmol) and allowed to stir at room temperature for 15 h. To the resulting mixture was added H<sub>2</sub>O (50 mL) and then extracted with EtOAc (3×50mL). The combined organic layers were dried over MgSO<sub>4</sub>, filtered, concentrated then purified via silica gel chromatography eluting 0-10% MeOH in CH<sub>2</sub>Cl<sub>2</sub>. The desired product was isolated as a light brown solid. Yield = 0.247 g (66%). <sup>1</sup>H NMR (DMSO-*d*<sup>6</sup>, 400 MHz) δ 9.76 (br, 1H), 8.18 (d, J = 8.4 Hz, 1H), 7.89 (m, 2H), 7.62-7.39 (m, 7H), 2.63 (s, 3H). ESI-MS(+): *m/z* 299.11 [M+H]<sup>+</sup>, 321.05 [M+Na]<sup>+</sup>.

*Protocol for Sulfonamide Coupling Method A* – To a solution of 8-Aminoquinoline (0.1g, 0.69 mmol) in Pyridine (3 mL) was added the corresponding Sulfonyl chloride and allowed to stir at room temperature for 12-15 h. To the resulting mixture was added H<sub>2</sub>O (50 mL) and then extracted with EtOAc (3×50mL). The combined organic layers were dried over MgSO<sub>4</sub>, then filtered, and concentrated via rotary evaporation. The resulting crude oil was purified via silica gel chromatography eluting a gradient of EtOAc in Hexanes.

*Protocol for Sulfonamide Coupling Method B* – Sulfonamides were synthesized and purified as previously reported. To a solution of 8-Aminoquinoline (0.1 g, 0.69 mmol) in Pyridine (3 mL) was added the corresponding Sulfonyl chloride (1.04 mmol). The clear solution was heated in a microwave reactor at 130 °C for 3 min (Power = 300W). The solution was then poured into H<sub>2</sub>O (12 mL) causing the product to precipitate, which was then isolated via filtration, and rinsed with water. If no precipitate was formed, the aqueous phase was extracted CH<sub>2</sub>Cl<sub>2</sub> (2×50mL). The combined organic layers were dried over MgSO<sub>4</sub>, filtered, and evaporated in vacuo to obtain a solid when co-evaporated with Et<sub>2</sub>O.

***N*-(Quinolin-8-yl)cyclopropanesulfonamide (109).** Synthesized utilizing Sulfonamide Coupling Method A. To the reaction was added 1.5 equivs, of sulfonyl chloride. Purified with a gradient of 0-30% EtOAc in Hexanes. Isolated as white solid. Yield = 0.08 g (45%). <sup>1</sup>H NMR (CDCl<sub>3</sub>, 400 MHz) δ 8.92 (br, 1H), 8.83 (dd, J<sub>1</sub> = 4.0 Hz, J<sub>2</sub> = 1.6 Hz, 1H), 8.19 (dd, J<sub>1</sub> = 8.4 Hz, J<sub>2</sub> = 1.6 Hz, 1H), 7.92 (dd, J<sub>1</sub> = 7.2 Hz, J<sub>2</sub> = 1.6 Hz, 1H), 7.57-7.47 (m, 3H), 2.57 (m, 1H), 1.29 (m, 2H), 0.90 (m, 2H). ESI-MS(+): *m/z* 249.14 [M+H]<sup>+</sup>.

***N*-(Quinolin-8-yl)propane-2-sulfonamide (110).** Synthesized utilizing Sulfonamide Coupling Method A. To the reaction was added 3.27 equivs, of sulfonyl chloride. Purified with a gradient of 0-40% EtOAc in Hexanes. Isolated as tan solid. Yield = 0.04 g (23%). <sup>1</sup>H NMR (400 MHz, CDCl<sub>3</sub>): δ 8.86 (br, 1H),

8.82 (dd,  $J_1 = 4.4$  Hz,  $J_2 = 2$  Hz, 1H), 8.18 (dd,  $J_1 = 8.4$  Hz,  $J_2 = 1.6$  Hz, 1H), 7.90 (dd,  $J_1 = 7.6$  Hz,  $J_2 = 2$  Hz, 1H), 7.54 (m, 3H), 3.37 (sept,  $J = 6.8$  Hz, 1H), 1.38 (s, 1H), 1.37 (s, 3H). ESI-MS(+):  $m/z$  251.09  $[M+H]^+$ .

***N*-(Quinolin-8-yl)butane-1-sulfonamide (111).** Synthesized utilizing Sulfonamide Coupling Method A. To the reaction was added 1.5 equivs, of sulfonyl chloride. Purified with a gradient of 0-15% EtOAc in Hexanes. Isolated as dark oil. Yield = 0.09 g (49%).  $^1\text{H}$  NMR ( $\text{CDCl}_3$ , 400 MHz)  $\delta$  8.89 (br, 1H), 8.80 (dd,  $J_1 = 4$  Hz,  $J_2 = 1.6$  Hz, 1H), 8.17 (dd,  $J_1 = 8$  Hz,  $J_2 = 1.4$  Hz, 1H), 7.84 (dd,  $J_1 = 7.2$  Hz,  $J_2 = 1.6$  Hz, 1H), 7.54-7.45 (m, 3H), 3.12 (m, 2H), 1.81 (m, 2H), 1.35 (sex,  $J = 7.2$  Hz, 2H), 0.79 (t,  $J = 7.2$  Hz, 3H). ESI-MS(+):  $m/z$  265.12  $[M+H]^+$ .

***N*-(Quinolin-8-yl)cyclohexanesulfonamide (112).** Synthesized utilizing Sulfonamide Coupling Method A. To the reaction was added 3 equivs, of sulfonyl chloride. Purified with a gradient of 0-15% EtOAc in Hexanes. Isolated as a clear oil. Yield = 0.034 g (17%).  $^1\text{H}$  NMR ( $\text{CDCl}_3$ , 400 MHz)  $\delta$  8.85 (br, 1H), 8.81 (dd,  $J_1 = 4.4$  Hz,  $J_2 = 1.6$  Hz, 1H), 8.18 (dd,  $J_1 = 8.4$  Hz,  $J_2 = 1.6$  Hz, 1H), 7.88 (dd,  $J_1 = 7.2$  Hz,  $J_2 = 1.6$  Hz, 1H), 7.53-7.46 (m, 3H), 3.09 (tt,  $J_1 = 7.2$  Hz,  $J_2 = 3.6$  Hz, 1H), 2.18-1.14 (m, 10H). ESI-MS(+):  $m/z$  291.17  $[M+H]^+$ , 313.13  $[M+Na]^+$ .

***N*-(Quinolin-8-yl)thiophene-2-sulfonamide (113).** Synthesized utilizing Sulfonamide Coupling Method B. Isolated as dark brown solid. Yield = 0.179 g (89%). <sup>1</sup>H NMR (400 MHz, CDCl<sub>3</sub>): δ 9.30 (br, 1H), 8.76 (dd, J<sub>1</sub> = 4.4 Hz, J<sub>2</sub> = 1.6 Hz, 1H), 8.12 (dd, J<sub>1</sub> = 8.4 Hz, J<sub>2</sub> = 1.6 Hz, 1H), 7.91 (dd, J<sub>1</sub> = 6.4 Hz, J<sub>2</sub> = 2.4 Hz, 1H), 7.62 (dd, J<sub>1</sub> = 3.6 Hz, J<sub>2</sub> = 1.2 Hz, 1H), 7.51 (m, 2H), 7.44 (d, J = 4.4 Hz, 1H), 7.42 (d, J = 4.0 Hz, 1H), 6.92 (t, J = 3.6 Hz, 1H). ESI-MS(+): *m/z* 291.02 [M+H]<sup>+</sup>, 312.97 [M+Na]<sup>+</sup>.

**1-Methyl-*N*-(quinolin-8-yl)-1*H*-imidazole-4-sulfonamide (114).** Synthesized utilizing Sulfonamide Coupling Method A. To the reaction was added 1.5 equivs, of sulfonyl chloride. Product precipitated as H<sub>2</sub>O was added to reaction mixture. The solid was isolated via filtration and not further purified. Isolated as pink solid. Yield = 0.089 g (48%). <sup>1</sup>H NMR (CDCl<sub>3</sub>, 400 MHz) δ 9.41 (br, 1H), 8.79 (dd, J<sub>1</sub> = 4 Hz, J<sub>2</sub> = 1.6 Hz, 1H), 8.12 (dd, J<sub>1</sub> = 8 Hz, J<sub>2</sub> = 1.6 Hz, 1H), 7.89 (t, J = 4.4 Hz, 1H), 7.54 (d, J = 1.2 Hz, 1H), 7.46-7.41 (m, 3H), 7.36 (s, 1H), 7.25 (s, 1H), 3.65 (s, 3H). ESI-MS(+): *m/z* 289.22 [M+H]<sup>+</sup>, 311.16 [M+Na]<sup>+</sup>.

**4-(1*H*-Pyrazol-1-yl)-*N*-(quinolin-8-yl)benzenesulfonamide (115).** Synthesized utilizing Sulfonamide Coupling Method B. Isolated as a white solid. Yield = 0.33 g (99%). <sup>1</sup>H NMR (CDCl<sub>3</sub>, 400 MHz) δ 9.26 (br, 1H), 8.76 (dd, J<sub>1</sub> = 4.0 Hz, J<sub>2</sub> = 1.6 Hz, 1H), 8.10 (dd, J<sub>1</sub> = 8.4 Hz, J<sub>2</sub> = 1.6 Hz, 1H), 7.98 (d, J = 9.2 Hz, 2H), 7.88 (d, J = 2.8 Hz, 1H), 7.86 (dd, J<sub>1</sub> = 6.8 Hz, J<sub>2</sub> = 2.0 Hz, 1H), 7.68 (d, J = 2.0 Hz,

1H), 7.68 (d, J = 8.8 Hz, 2H), 7.43 (m, 3H), 6.45 (dd, J<sub>1</sub> = 2.8 Hz, J<sub>2</sub> = 2.0 Hz, 1H). ESI-MS(+): *m/z* 351.08 [M+H]<sup>+</sup>, 373.06 [M+Na]<sup>+</sup>.

**2-methoxy-*N*-(quinolin-8-yl)benzenesulfonamide (116).** Synthesized utilizing Sulfonamide Coupling Method A. Purified with a gradient of 0-25% EtOAc in Hexanes. Isolated as white solid. Yield = 0.123 g (56%). <sup>1</sup>H NMR (CDCl<sub>3</sub>, 400 MHz) δ 9.70 (br, 1H), 8.79 (dd, J<sub>1</sub> = 4 Hz, J<sub>2</sub> = 1.6 Hz, 1H), 8.07 (dd, J<sub>1</sub> = 8.4 Hz, J<sub>2</sub> = 1.6 Hz, 1H), 7.98 (dd, J<sub>1</sub> = 8.4 Hz, J<sub>2</sub> = 1.6 Hz, 1H), 7.81 (dd, J<sub>1</sub> = 8.4 Hz, J<sub>2</sub> = 1.6 Hz, 1H), 7.42-7.32 (m, 3H), 6.94 (t, J = 8.4 Hz, 1H), 6.78 (t, J = 8.4 Hz, 1H), 3.81 (s, 3H). ESI-MS(+): *m/z* 315.09 [M+H]<sup>+</sup>.

**3-Methoxy-*N*-(quinolin-8-yl)benzenesulfonamide (117).** Synthesized utilizing Sulfonamide Coupling Method A. To the reaction was added 1.5 equivs, of sulfonyl chloride. Purified with a gradient of 0-25% EtOAc in Hexanes. Isolated as white solid. Yield = 0.2 g (92%). <sup>1</sup>H NMR (CDCl<sub>3</sub>, 400 MHz) δ 9.25 (br, 1H), 8.67 (dd, J<sub>1</sub> = 4 Hz, J<sub>2</sub> = 1.6 Hz, 1H), 8.00 (dd, J<sub>1</sub> = 8.4 Hz, J<sub>2</sub> = 1.6 Hz, 1H), 7.84 (m, 1H), 7.48 (m, 1H), 7.39 (m, 3H), 7.33 (dd, J<sub>1</sub> = 8.4 Hz, J<sub>2</sub> = 4.4 Hz, 1H), 7.20 (t, J<sub>1</sub> = 8 Hz, 1H), 6.88 (m, 1H), 3.63 (s, 3H). ESI-MS(+): *m/z* 315.13 [M+H]<sup>+</sup>.

**4-Methoxy-*N*-(quinolin-8-yl)benzenesulfonamide (118).** Synthesized utilizing Sulfonamide Coupling Method B. Isolated as an off-white solid. Yield = 0.117 g (54%). <sup>1</sup>H NMR (400 MHz, CDCl<sub>3</sub>): δ 9.20 (br, 1H), 8.76 (dd, J<sub>1</sub> = 4.4 Hz, J<sub>2</sub> =

1.6 Hz, 1H), 8.09 (dd,  $J_1 = 8.0$  Hz,  $J_2 = 1.6$  Hz, 1H), 7.85 (d,  $J = 8.8$  Hz, 2H), 7.80 (dd,  $J_1 = 6$  Hz,  $J_2 = 2.4$  Hz, 1H), 7.43 (m, 3H), 6.81 (d,  $J = 8.8$  Hz, 2H), 3.75 (s, 3H). ESI-MS(+):  $m/z$  315.02  $[M+H]^+$ .

**2-cyano-*N*-(quinolin-8-yl)benzenesulfonamide (119).** Synthesized utilizing Sulfonamide Coupling Method A. Purified with a gradient of 0-70% EtOAc in Hexanes. Isolated as white solid. Yield = 0.07 g (33%).  $^1\text{H}$  NMR (400 MHz,  $\text{CDCl}_3$ ):  $\delta$  8.80 (dd,  $J_1 = 4.0$  Hz,  $J_2 = 1.6$  Hz, 1H), 8.18 (dd,  $J_1 = 8.0$  Hz,  $J_2 = 1.2$  Hz, 1H), 8.09 (dd,  $J_1 = 8.4$  Hz,  $J_2 = 1.6$  Hz, 1H), 7.73-7.39 (m, 7H). ESI-MS(+):  $m/z$  310.11  $[M+H]^+$ .

**3-Cyano-*N*-(quinolin-8-yl)benzenesulfonamide (120).** Synthesized utilizing Sulfonamide Coupling Method A. To the reaction was added 1.5 equivs, of sulfonyl chloride. Purified with a gradient of 0-70% EtOAc in Hexanes. Isolated as white solid. Yield = 0.07 g (32%).  $^1\text{H}$  NMR ( $\text{CDCl}_3$ , 400 MHz)  $\delta$  9.25 (br, 1H), 8.77 (dd,  $J_1 = 4.4$  Hz,  $J_2 = 1.6$  Hz, 1H), 8.17-8.09 (m, 3H), 7.86 (dd,  $J_1 = 7.2$  Hz,  $J_2 = 1.2$  Hz, 1H), 7.70 (dd,  $J_1 = 8$  Hz,  $J_2 = 1.2$  Hz, 1H), 7.54-7.42 (m, 4H). ESI-MS(+):  $m/z$  310.11  $[M+H]^+$ .

**4-Cyano-*N*-(quinolin-8-yl)benzenesulfonamide (121).** Synthesized utilizing Sulfonamide Coupling Method B. Isolated as an orange solid. Yield = 0.106 g (99%).  $^1\text{H}$  NMR ( $\text{CDCl}_3$ , 400 MHz)  $\delta$  9.27 (br, 1H), 8.76 (dd,  $J_1 = 4.4$  Hz,  $J_2 = 1.6$

Hz, 1H), 8.12 (dd,  $J_1 = 8.4$  Hz,  $J_2 = 1.6$  Hz, 1H), 7.99 (d,  $J = 8.0$  Hz, 2H), 7.85 (dd,  $J_1 = 7.2$  Hz,  $J_2 = 1.2$  Hz, 1H), 7.63 (d,  $J = 8.0$  Hz, 2H), 7.53 (dd,  $J_1 = 8.4$  Hz,  $J_2 = 1.2$  Hz, 1H), 7.46 (m, 2H). ESI-MS(+):  $m/z$  310.07 [M+H]<sup>+</sup>.

***N*-(Quinolin-8-yl)pyridine-2-sulfonamide (122).** Synthesized utilizing Sulfonamide Coupling Method A. To the reaction was added 1.5 equivs, of sulfonyl chloride. Purified with a gradient of 0-50% EtOAc in Hexanes. Isolated as brown solid. Yield = 0.112 g (57%). <sup>1</sup>H NMR (CDCl<sub>3</sub>, 400 MHz)  $\delta$  9.94 (br, 1H), 8.85 (m, 1H), 8.59 (m, 1H), 8.37 (dd, dd,  $J_1 = 8.4$  Hz,  $J_2 = 2$  Hz, 1H), 8.09 (m, 2H), 7.76-7.48 (m, 5H). ESI-MS(+):  $m/z$  286.12 [M+H]<sup>+</sup>.

***N*-(Quinolin-8-yl)pyridine-3-sulfonamide (123).** Synthesized utilizing Sulfonamide Coupling Method A. To the reaction was added 1.1 equivs, of sulfonyl chloride. Product precipitated as H<sub>2</sub>O was added to reaction mixture. The solid was isolated via filtration and not further purified. Isolated as white solid. Yield = 0.198 g (99%). <sup>1</sup>H NMR (CDCl<sub>3</sub>, 400 MHz)  $\delta$  9.33 (br, 1H), 9.07 (dd,  $J_1 = 2.4$  Hz,  $J_2 = 0.8$  Hz, 1H), 8.70 (dd,  $J_1 = 4.4$  Hz,  $J_2 = 1.6$  Hz, 1H), 8.60 (dd,  $J_1 = 4.8$  Hz,  $J_2 = 1.6$  Hz, 1H), 8.14 (m, 1H), 8.06 (dd,  $J_1 = 8$  Hz,  $J_2 = 1.6$  Hz, 1H), 7.85 (dd,  $J_1 = 7.2$  Hz,  $J_2 = 1.6$  Hz, 1H), 7.47-7.39 (m, 2H), 7.38 (dd,  $J_1 = 8.4$  Hz,  $J_2 = 4.4$  Hz, 1H), 7.25 (m, 1H). ESI-MS(+):  $m/z$  286.10 [M+H]<sup>+</sup>, 307.99 [M+Na]<sup>+</sup>.

**6-Morpholino-*N*-(quinolin-8-yl)pyridine-3-sulfonamide (124).** Synthesized utilizing Sulfonamide Coupling Method B. Isolated as a white solid. Yield = 0.1 g (78%). <sup>1</sup>H NMR (CDCl<sub>3</sub>, 400 MHz) δ 9.20 (br, 1H), 8.76 (dd, J<sub>1</sub> = 4.4 Hz, J<sub>2</sub> = 1.6 Hz, 1H), 8.65 (m, 1H), 8.10 (dd, J<sub>1</sub> = 8.0 Hz, J<sub>2</sub> = 1.6 Hz, 1H), 7.87 (dd, J<sub>1</sub> = 9.2 Hz, J<sub>2</sub> = 2.8 Hz, 1H), 7.82 (m, 1H), 7.45 (m, 3H), 6.45 (d, J = 9.2 Hz, 1H), 3.72 (m, 4H), 3.54 (m, 4H). ESI-MS(+): *m/z* 371.10 [M+H]<sup>+</sup>, 393.17 [M+Na]<sup>+</sup>.

**4-(*tert*-Butyl)-*N*-(quinolin-8-yl)benzenesulfonamide (125).** Synthesized utilizing Sulfonamide Coupling Method B. Isolated as a white solid. Yield = 0.216 g (91%). <sup>1</sup>H NMR (CDCl<sub>3</sub>, 400 MHz) δ 9.23 (br, 1H), 8.75 (dd, J<sub>1</sub> = 4.4 Hz, J<sub>2</sub> = 2.0 Hz, 1H), 8.10 (dd, J<sub>1</sub> = 8.4 Hz, J<sub>2</sub> = 1.6 Hz, 1H), 7.83 (m, 3H), 7.43 (m, 3H), 7.37 (d, J = 8.8 Hz, 2H), 1.24 (s, 9H). ESI-MS(+): *m/z* 341.08 [M+H]<sup>+</sup>.

**4-Fluoro-*N*-(quinolin-8-yl)benzenesulfonamide (126).** Synthesized utilizing Sulfonamide Coupling Method B. Isolated as an amber solid. Yield = 0.15 g (72%). <sup>1</sup>H NMR (CDCl<sub>3</sub>, 400 MHz) δ 8.77 (dd, J<sub>1</sub> = 4.0 Hz, J<sub>2</sub> = 1.6 Hz, 1H), 8.21 (dd, J<sub>1</sub> = 8.4 Hz, J<sub>2</sub> = 1.6 Hz, 1H), 7.88-7.92 (m, 2H), 7.83 (dd, J<sub>1</sub> = 7.6 Hz, J<sub>2</sub> = 1.2 Hz, 1H), 7.58 (dd, J<sub>1</sub> = 8.0 Hz, J<sub>2</sub> = 1.2 Hz, 1H), 7.46-7.50 (m, 2H), 7.09 (t, J = 8.4 Hz, 2H). ESI-MS(+): *m/z* 303.05 [M+H]<sup>+</sup>, 324.99 [M+Na]<sup>+</sup>.

**3,4-Difluoro-*N*-(quinolin-8-yl)benzenesulfonamide (127).** Synthesized utilizing Sulfonamide Coupling Method A. To the reaction was added 1.1 equivs, of

sulfonyl chloride. Purified with a gradient of 0-20% EtOAc in Hexanes. Isolated as a brown solid. Yield = 0.1 g (46%).  $^1\text{H NMR}$  ( $\text{CDCl}_3$ , 400 MHz)  $\delta$  8.75 (dd,  $J_1 = 4.0$  Hz,  $J_2 = 1.6$  Hz, 1H), 8.11 (dd,  $J_1 = 8.0$  Hz,  $J_2 = 1.2$  Hz, 1H), 7.84 (dd,  $J_1 = 7.2$  Hz,  $J_2 = 1.2$  Hz, 1H), 7.76-7.66 (m, 2H), 7.51-7.40 (m, 3H), 7.13 (m, 1H). ESI-MS(+):  $m/z$  321.11  $[\text{M}+\text{H}]^+$ .

***N*-(Quinolin-8-yl)benzo[d][1,3]dioxole-5-sulfonamide (128).** Synthesized utilizing Sulfonamide Coupling Method B. Isolated as a dark brown solid. Yield = 0.08 g (70%).  $^1\text{H NMR}$  ( $\text{CDCl}_3$ , 400 MHz)  $\delta$  9.20 (br, 1H), 8.77 (dd,  $J_1 = 4.4$  Hz,  $J_2 = 1.6$  Hz, 1H), 8.11 (dd,  $J_1 = 8.4$  Hz,  $J_2 = 1.6$  Hz, 1H), 7.80 (dd,  $J_1 = 6.4$  Hz,  $J_2 = 2.4$  Hz, 1H), 7.50 (dd,  $J_1 = 8.0$  Hz,  $J_2 = 2.0$  Hz, 1H), 7.45 (m, 2H), 7.43 (t,  $J = 4.0$  Hz, 1H), 7.31 (d,  $J = 2.0$  Hz, 1H), 6.73 (d,  $J = 8.4$  Hz, 1H), 5.96 (s, 2H). ESI-MS(+):  $m/z$  329.09  $[\text{M}+\text{H}]^+$ .

**2-Oxo-*N*-(quinolin-8-yl)indoline-5-sulfonamide (129).** Synthesized utilizing Sulfonamide Coupling Method B. Isolated as an orange solid. Yield = 0.09 g (91%).  $^1\text{H NMR}$  ( $\text{CDCl}_3$ , 400 MHz)  $\delta$  10.72 (br, 1H), 9.80 (br, 1H), 8.86 (dd,  $J_1 = 4.0$  Hz,  $J_2 = 1.6$  Hz, 1H), 8.34 (dd,  $J_1 = 8.0$  Hz,  $J_2 = 1.6$  Hz, 1H), 7.76 (m, 2H), 7.60 (m, 3H), 7.50 (t,  $J = 8.0$  Hz, 1H), 6.82 (d,  $J = 8.8$  Hz, 1H), 3.47 (s, 2H). ESI-MS(+):  $m/z$  340.09  $[\text{M}+\text{H}]^+$ .

***N*-(Quinolin-8-yl)naphthalene-2-sulfonamide (130).** Synthesized utilizing

Sulfonamide Coupling Method B. Isolated as a white solid. Yield = 0.2 g (87%).  
 $^1\text{H}$  NMR ( $\text{CDCl}_3$ , 400 MHz)  $\delta$  9.35 (br, 1H), 8.76 (dd,  $J_1 = 4.4$  Hz,  $J_2 = 1.6$  Hz, 1H), 8.51 (d,  $J = 2.0$  Hz, 1H), 8.06 (dd,  $J_1 = 8.0$  Hz,  $J_2 = 1.6$  Hz, 1H), 7.88 (m, 3H), 7.78 (m, 2H), 7.55 (m, 2H), 7.41 (m, 3H). ESI-MS(+):  $m/z$  335.04  $[\text{M}+\text{H}]^+$ .

***N*-(Quinolin-8-yl)benzo[*d*]thiazole-6-sulfonamide (131).** Synthesized utilizing Sulfonamide Coupling Method A. To the reaction was added 1.1 equivs, of sulfonyl chloride. Purified with a gradient of 0-40% EtOAc in Hexanes. Isolated as a off-white solid. Yield = 0.11 g (45%).  $^1\text{H}$  NMR (400 MHz,  $\text{CDCl}_3$ ):  $\delta$  9.33 (br, 1H), 9.07 (s, 1H), 8.72 (d,  $J = 4.4$  Hz, 1H), 8.58 (s, 1H), 8.05 (m, 3H), 7.88 (m, 1H), 7.43 (m, 2H), 7.38 (m, 1H). ESI-MS(+):  $m/z$  342.03  $[\text{M}+\text{H}]^+$ , 363.99  $[\text{M}+\text{Na}]^+$ .

**2-(Methylthio)-*N*-(quinolin-8-yl)benzo[*d*]thiazole-6-sulfonamide (132).** Synthesized utilizing method B. Isolated as a light brown solid. Yield = 0.2 g (81%).  $^1\text{H}$  NMR ( $\text{CDCl}_3$ , 400 MHz)  $\delta$  9.28 (br, 1H), 8.74 (dd,  $J_1 = 4.4$  Hz,  $J_2 = 1.6$  Hz, 1H), 8.41 (dd,  $J_1 = 1.6$  Hz,  $J_2 = 0.4$  Hz, 1H), 8.08 (dd,  $J_1 = 8.4$  Hz,  $J_2 = 1.6$  Hz, 1H), 7.90 (dd,  $J_1 = 8.8$  Hz,  $J_2 = 1.6$  Hz, 1H), 7.90 (dd,  $J_1 = 8.4$  Hz,  $J_2 = 1.6$  Hz, 1H), 7.85 (dd,  $J_1 = 6.4$  Hz,  $J_2 = 2.8$  Hz, 1H), 7.75 (dd,  $J_1 = 8.4$  Hz,  $J_2 = 0.4$  Hz, 1H), 7.42 (m, 3H). ESI-MS(+):  $m/z$  388.05  $[\text{M}+\text{H}]^+$ .

**1-Phenyl-*N*-(quinolin-8-yl)methanesulfonamide (133).** Synthesized utilizing Sulfonamide Coupling Method B. Isolated as a yellow solid. Yield = 0.2 g (97%).

$^1\text{H}$  NMR ( $\text{CDCl}_3$ , 400 MHz)  $\delta$  8.87 (br, 1H), 8.71 (dd,  $J_1 = 4.4$  Hz,  $J_2 = 1.6$  Hz, 1H), 8.18 (dd,  $J_1 = 8.4$  Hz,  $J_2 = 1.6$  Hz, 1H), 7.80 (dd,  $J_1 = 7.6$  Hz,  $J_2 = 1.6$  Hz, 1H), 7.54 (dd,  $J_1 = 8.8$  Hz,  $J_2 = 1.2$  Hz, 1H), 7.48 (m, 2H), 7.25 (m, 1H), 7.15 (t,  $J = 8.0$  Hz, 2H), 7.08 (d,  $J = 7.2$  Hz, 2H). ESI-MS(+):  $m/z$  299.06  $[\text{M}+\text{H}]^+$ , 321.08  $[\text{M}+\text{Na}]^+$ .

**2-Phenyl-*N*-(quinolin-8-yl)ethane-1-sulfonamide (134).** Synthesized utilizing Sulfonamide Coupling Method A. To the reaction was added 1.5 equivs, of sulfonyl chloride. Purified with a gradient of 0-20% EtOAc in Hexanes. Isolated as a tan solid. Yield = 0.143 g (66%).  $^1\text{H}$  NMR ( $\text{CDCl}_3$ , 400 MHz)  $\delta$  8.96 (br, 1H), 8.81 (d,  $J = 4.0$  Hz, 1H), 8.19 (d,  $J = 8.4$  Hz, 1H), 7.90 (d,  $J = 8.4$  Hz, 1H), 7.58-7.47 (m, 3H), 7.18-7.11 (m, 3H), 6.97 (d,  $J = 8.4$  Hz, 3H), 3.40 (t,  $J = 8.0$  Hz, 2H), 3.40 (t,  $J = 8.0$  Hz, 2H), 3.16 (t,  $J = 8.0$  Hz, 2H). ESI-MS(+):  $m/z$  313.18  $[\text{M}+\text{H}]^+$ .

**3-Phenyl-*N*-(quinolin-8-yl)propane-1-sulfonamide (135).** Synthesized utilizing Sulfonamide Coupling Method A. To the reaction was added 1.1 equivs, of sulfonyl chloride. Purified with a gradient of 0-30% EtOAc in Hexanes. Isolated as a tan solid. Yield = 0.185 g (82%).  $^1\text{H}$  NMR ( $\text{CDCl}_3$ , 400 MHz)  $\delta$  9.23 (br, 1H), 8.69 (dd,  $J_1 = 4.4$  Hz,  $J_2 = 1.6$  Hz, 1H), 8.01 (dd,  $J_1 = 8.4$  Hz,  $J_2 = 1.6$  Hz, 1H), 7.83 (m, 3H), 7.39 (d,  $J = 4.8$  Hz, 2H), 7.34 (dd,  $J_1 = 8$  Hz,  $J_2 = 4$  Hz, 1H),

7.12 (d,  $J = 8.4$  Hz, 2H), 2.48 (t,  $J = 7.6$  Hz, 2H), 1.53 (sex,  $J = 7.6$  Hz, 2H), 0.81 (t,  $J = 7.2$  Hz, 3H). ESI-MS(+):  $m/z$  327.09  $[M+H]^+$ , 349.03  $[M+Na]^+$ .

**5-Bromo-8-nitroquinoline.** A solution of 5-Bromoquinoline (10 g, 48.1 mmol) in concentrated  $H_2SO_4$  (40 mL) was cooled down to 0 °C under a nitrogen atmosphere. To this was added Potassium nitrate (7.77 g, 77 mmol) slowly and portionwise. The resulting reaction mixture was then allowed to warm up to room temperature slowly and then stirred for an additional 15 h at room temperature. The resulting mixture was then poured onto ice, which caused the formation of a precipitate. The precipitate was then filtered and rinsed with excess amount of  $H_2O$ . The resulting product was not further purified. The desired product was isolated as a light yellow solid. Yield = 10.63 g (87%).  $^1H$  NMR ( $CDCl_3$ , 400 MHz)  $\delta$  9.08 (dd,  $J_1 = 4.0$  Hz,  $J_2 = 1.6$  Hz, 1H), 8.62 (dd,  $J_1 = 8.4$  Hz,  $J_2 = 1.6$  Hz, 1H), 7.90 (d,  $J_1 = 0.8$  Hz, 2H), 7.67 (dd,  $J_1 = 8.4$  Hz,  $J_2 = 4$  Hz, 1H). ESI-MS(+):  $m/z$  253.21, 255.17  $[M+H]^+$ .

**8-Nitro-5-phenylquinoline.** To a solution of 5-Bromo-8-nitroquinoline (0.4 g, 1.58 mmol) in  $H_2O$  (10 mL) was added phenylboronic acid (0.289 g, 2.37 mmol), diisopropylamine (0.443 mL, 3.16 mmol), and palladium acetate (0.018 g, 0.08 mmol) and refluxed for 16 h. To the resulting mixture was added  $H_2O$  (50 mL) and then extracted with EtOAc (3x50mL). The combined organic layers were dried over  $MgSO_4$ , filtered, concentrated then purified via silica gel

chromatography eluting 0-30% EtOAc in Hexanes. The desired product was isolated as a light tan solid. Yield = 0.297 g (75%).  $^1\text{H NMR}$  ( $\text{CDCl}_3$ , 400 MHz)  $\delta$  9.03 (d,  $J = 4.0$  Hz, 1H), 8.30 (d,  $J = 4.0$  Hz, 1H), 8.06 (d,  $J = 4.0$  Hz, 1H), 7.56-7.43 (m, 7H). ESI-MS(+):  $m/z$  251.34  $[\text{M}+\text{H}]^+$ .

*Protocol for Suzuki Coupling Method A* – To a solution of 5-Bromo-8-nitroquinoline (0.3 g, 1.18 mmol) in  $\text{H}_2\text{O}$  (10 mL) was added boronic acid (1.78 mmol), diisopropylamine (0.498 mL, 3.56 mmol), and palladium acetate (0.018 g, 0.08 mmol) and refluxed for 16 h. To the resulting mixture was added  $\text{H}_2\text{O}$  (50 mL) and then extracted with EtOAc (3 $\times$ 50mL). The resulting mixture was filtered through celite, concentrated, then purified via silica gel chromatography eluting a gradient of EtOAc in Hexanes.

*Protocol for Suzuki Coupling Method B* – To a solution of 5-Bromo-8-nitroquinoline (0.3 g, 1.18 mmol) in 1,4-Dioxane (10 mL) was added boronic acid (1.78 mmol), potassium acetate (0.233 g, 2.37 mmol), and  $\text{Pd}(\text{PPh}_3)_4$  (0.068 g, 0.06 mmol) and degassed for 5-10 mins. The solution mixture was then refluxed for 16 h under nitrogen atmosphere. The resulting mixture was filtered through celite, concentrated, then purified via silica gel chromatography eluting a gradient of EtOAc in Hexanes.

*Protocol for Suzuki Coupling Method C* – To a solution of 5-Bromo-8-nitroquinoline (0.3 g, 1.18 mmol) in H<sub>2</sub>O (5 mL) and 1,4-Dioxane (5 mL) was added boronic acid (1.78 mmol), potassium carbonate (0.328 g, 2.37 mmol), S-Phos (0.05 g, 0.12 mmol) and Pd(dppf)Cl<sub>2</sub>·CH<sub>2</sub>Cl<sub>2</sub> (0.097 g, 0.12 mmol) and degassed for 5-10 mins. The solution mixture was then refluxed for 16 h under nitrogen atmosphere. The resulting mixture was filtered through celite, concentrated, then purified via silica gel chromatography eluting a gradient of EtOAc in Hexanes or MeOH in CH<sub>2</sub>Cl<sub>2</sub>.

*Protocol for Buchwald Coupling* – To a solution of 5-Bromo-8-nitroquinoline (0.3 g, 1.18 mmol) in DMF (10 mL) was added an amine (3.56 mmol), potassium carbonate (0.492 g, 3.56 mmol), X-Phos (0.113 g, 0.24 mmol) and Pd<sub>2</sub>(dba)<sub>3</sub> (0.217 g, 0.24 mmol) and degassed for 5-10 mins. The solution mixture was then irradiated in a microwave reactor at 140 °C for 30 min. The resulting mixture filtered through celite, concentrated then purified via silica gel chromatography eluting a gradient of EtOAc in Hexanes.

*Protocol for Sonogashira Coupling* – To a solution of 5-Bromo-8-nitroquinoline (0.3 g, 1.18 mmol) in 1,4-Dioxane (10 mL) and Et<sub>3</sub>N (10 mL) was added an ethynyl (1.78 mmol), X-Phos (0.057 g, 0.12 mmol), Pd(dppf)Cl<sub>2</sub>·CH<sub>2</sub>Cl<sub>2</sub> (0.097 g, 0.12 mmol) and CuI (0.023 g, 0.12 mmol) and degassed for 5-10 mins. The solution mixture was then refluxed for 16 h under nitrogen atmosphere. The

resulting mixture was filtered through celite, concentrated, then purified via silica gel chromatography eluting a gradient of EtOAc in Hexanes.

**8-Nitro-5-(pyridin-4-yl)quinoline.** Synthesized utilizing Suzuki coupling Method C. Product was purified with a gradient of 0-15% MeOH in CH<sub>2</sub>Cl<sub>2</sub>. Yield = 0.132 g (44%). <sup>1</sup>H NMR (CDCl<sub>3</sub>, 400 MHz) δ 9.10 (dd, J<sub>1</sub> = 4 Hz, J<sub>2</sub> = 1.6 Hz, 1H), 8.81-8.80 (m, 2H), 8.23 (dd, J<sub>1</sub> = 8.8 Hz, J<sub>2</sub> = 1.6 Hz, 1H), 8.09 (d, J = 8.0 Hz, 1H), 7.59 (d, J = 8.0 Hz, 1H), 7.56 (dd, J<sub>1</sub> = 8.8 Hz, J<sub>2</sub> = 4.4 Hz, 1H), 7.40-7.39 (m, 2H). ESI-MS(+): *m/z* 252.25 [M+H]<sup>+</sup>.

**8-Nitro-5-(pyrimidin-5-yl)quinoline.** Synthesized utilizing Suzuki coupling Method C. Product was purified with a gradient of 0-15% MeOH in CH<sub>2</sub>Cl<sub>2</sub>. Yield = 0.138 g (46%). <sup>1</sup>H NMR (CDCl<sub>3</sub>, 400 MHz) δ 9.39 (s, 1H), 9.14 (d, J = 4.0 Hz, 1H), 8.90 (s, 2H), 8.17 (d, J = 8.8 Hz, 1H), 8.13 (d, J = 8 Hz, 1H), 7.63-7.60 (m, 2H). ESI-MS(+): *m/z* 253.43 [M+H]<sup>+</sup>.

**5-(4-Chlorophenyl)-8-nitroquinoline.** Synthesized utilizing Suzuki coupling Method B. Product was purified via silica gel chromatography eluting a gradient of 0-30% EtOAc in Hexanes. Yield = 0.182 g (54%). <sup>1</sup>H NMR (CDCl<sub>3</sub>, 400 MHz) δ 9.03 (d, J = 4.0 Hz, 1H), 8.30 (d, J = 4.0 Hz, 1H), 8.06 (d, J = 4.0 Hz, 1H), 7.56-7.43 (m, 7H). ESI-MS(+): *m/z* 285.43 [M+H]<sup>+</sup>.

**5-(3,4-Difluorophenyl)-8-nitroquinoline.** Synthesized utilizing Suzuki coupling Method A. Product was purified via silica gel chromatography eluting 0-40% EtOAc in Hexanes. Yield = 0.311 g (92%). <sup>1</sup>H NMR (CDCl<sub>3</sub>, 400 MHz) δ 9.09 (d, J = 4.0 Hz, 1H), 8.25 (d, J = 8.8 Hz, 1H), 8.07 (d, J = 8.0 Hz, 1H), 7.56-7.53 (m, 2H), 7.39-7.28 (m, 2H), 7.20-7.17 (m, 1H). ESI-MS(+): *m/z* 287.32 [M+H]<sup>+</sup>.

**5-(Furan-2-yl)-8-nitroquinoline.** Synthesized utilizing Suzuki coupling Method B. Product was purified via silica gel chromatography eluting a gradient of 0-30% EtOAc in Hexanes. Yield = 0.181 g (64%). <sup>1</sup>H NMR (CDCl<sub>3</sub>, 400 MHz) δ 9.04 (d, J = 4.0 Hz, 1H), 8.88 (d, J = 8.0 Hz, 1H), 8.02 (d, J = 8.0 Hz, 1H), 7.80 (d, J = 8.0 Hz, 1H), 7.68 (m, 1H), 7.57 (dd, J<sub>1</sub> = 8.0 Hz, J<sub>2</sub> = 4 Hz, 1H), 6.84 (d, J = 2.4 Hz, 1H), 6.63 (m, 1H). ESI-MS(+): *m/z* 241.31 [M+H]<sup>+</sup>.

**8-Nitro-5-(thiophen-2-yl)quinoline.** Synthesized utilizing Suzuki coupling Method B. Product was purified via silica gel chromatography eluting a gradient of 0-40% EtOAc in Hexanes. Yield = 0.3 g (99%). <sup>1</sup>H NMR (CDCl<sub>3</sub>, 400 MHz) δ 9.08 (m, 1H), 8.65 (d, J = 8.0 Hz, 1H), 8.04 (d, J = 8.0 Hz, 1H), 7.69 (d, J = 8.0 Hz, 1H), 7.55 (m, 2H), 7.27-7.24 (m, 2H). ESI-MS(+): *m/z* 257.27 [M+H]<sup>+</sup>.

**5-(Benzo[d][1,3]dioxol-5-yl)-8-nitroquinoline.** Synthesized utilizing Suzuki coupling Method A. Product was purified via silica gel chromatography eluting 0-40% EtOAc in Hexanes. Yield = 0.167 g (48%). <sup>1</sup>H NMR (CDCl<sub>3</sub>, 400 MHz) δ

9.03 (d, J = 4.0 Hz, 1H), 8.34 (d, J = 8.8 Hz, 1H), 8.03 (d, J = 8.0 Hz, 1H), 7.52-7.47 (m, 2H), 6.96 (d, J = 8.0 Hz, 1H), 6.88-6.87 (m, 2H), 6.06 (s, 2H). ESI-MS(+):  $m/z$  295.36 [M+H]<sup>+</sup>.

**8-Nitro-5-(piperidin-1-yl)quinoline.** Synthesized utilizing Buchwald coupling Method. Product was purified with a gradient of 0-25% EtOAc in Hexanes. Yield = 0.182 g (60%). <sup>1</sup>H NMR (CDCl<sub>3</sub>, 400 MHz) δ 9.04 (dd, J<sub>1</sub> = 4 Hz, J<sub>2</sub> = 1.6 Hz, 1H), 8.47 (dd, J<sub>1</sub> = 8.4 Hz, J<sub>2</sub> = 1.6 Hz, 1H), 8.11 (d, J = 8.4 Hz, 1H), 7.49 (dd, J<sub>1</sub> = 8.4 Hz, J<sub>2</sub> = 4 Hz, 1H), 7.00 (d, J = 8.4 Hz, 1H), 3.14 (t, J = 5.6 Hz, 4H), 1.88 (pent, J = 5.6 Hz, 4H), 1.72 (m, 2H). ESI-MS(+):  $m/z$  258.34 [M+H]<sup>+</sup>.

**4-(8-Nitroquinolin-5-yl)morpholine.** Synthesized utilizing Buchwald coupling Method. Product was purified with a gradient of 0-25% EtOAc in Hexanes. Yield = 0.202 g (68%). <sup>1</sup>H NMR (CDCl<sub>3</sub>, 400 MHz) δ 9.00 (dd, J<sub>1</sub> = 4 Hz, J<sub>2</sub> = 1.6 Hz, 1H), 8.49 (dd, J<sub>1</sub> = 8.4 Hz, J<sub>2</sub> = 1.6 Hz, 1H), 8.05 (d, J = 8.4 Hz, 1H), 7.50 (dd, J<sub>1</sub> = 8.4 Hz, J<sub>2</sub> = 4 Hz, 1H), 7.04 (d, J = 8.4 Hz, 1H), 3.97 (t, J = 4.4 Hz, 4H), 3.16 (t, J = 4.4 Hz, 4H). ESI-MS(+):  $m/z$  260.11 [M+H]<sup>+</sup>.

**N-(5-Phenylquinolin-8-yl)methanesulfonamide (136).** Synthesized utilizing Sulfonamide Coupling Method A. Product was purified with a gradient of 0-25% EtOAc in Hexanes. Isolated as an off-white solid. Yield = 0.033 g (24%). <sup>1</sup>H NMR (CDCl<sub>3</sub>, 400 MHz) δ 9.03 (br, 1H), 8.84 (d, J = 3.6 Hz, 1H), 8.31 (d, J = 8.4

Hz, 1H), 7.92 (d, J = 8.4 Hz, 1H), 7.51-7.43 (m, 7H), 3.08 (s, 3H). ESI-MS(+):  $m/z$  299.10 [M+H]<sup>+</sup>.

***N*-(5-(Pyridin-4-yl)quinolin-8-yl)methanesulfonamide (137).** Synthesized utilizing Sulfonamide Coupling Method A. Product was purified with a gradient of 0-10% MeOH in CH<sub>2</sub>Cl<sub>2</sub>. Isolated as an off-white solid. Yield = 0.054 g (35%). <sup>1</sup>H NMR (CDCl<sub>3</sub>, 400 MHz) δ 9.09 (br, 1H), 8.86 (d, J = 4.0 Hz, 1H), 8.74 (d, J = 5.2 Hz, 2H), 8.25 (d, J = 8.4 Hz, 1H), 7.92 (d, J = 8.4 Hz, 1H), 7.51-7.47 (m, 2H), 7.39 (m, 2H), 3.09 (s, 3H). ESI-MS(+):  $m/z$  300.14 [M+H]<sup>+</sup>.

***N*-(5-(Pyrimidin-5-yl)quinolin-8-yl)methanesulfonamide (138).** Synthesized utilizing Sulfonamide Coupling Method A. Product was purified with a gradient of 0-10% MeOH in CH<sub>2</sub>Cl<sub>2</sub>. Isolated as an off-white solid. Yield = 0.048 g (32%). <sup>1</sup>H NMR (CDCl<sub>3</sub>, 400 MHz) δ 9.29 (s, 1H), 9.12 (br, 1H), 8.88 (d, J = 4.0 Hz, 1H), 8.85 (s, 2H), 8.14 (d, J = 8.4 Hz, 1H), 7.94 (d, J = 8.4 Hz, 1H), 7.55 (dd, J<sub>1</sub> = 8.4 Hz, J<sub>2</sub> = 4.0 Hz, 1H), 7.51 (d, J = 8.4 Hz, 1H), 3.09 (s, 3H). ESI-MS(+):  $m/z$  301.10 [M+H]<sup>+</sup>.

***N*-(5-(4-Chlorophenyl)quinolin-8-yl)methanesulfonamide (139).** Synthesized utilizing Sulfonamide Coupling Method A. Product was purified with a gradient of 0-40% EtOAc in Hexanes. Isolated as an off-white solid. Yield = 0.042 g (24%). <sup>1</sup>H NMR (CDCl<sub>3</sub>, 400 MHz) δ 9.03 (br, 1H), 8.85 (dd, J<sub>1</sub> = 4.0 Hz, J<sub>2</sub> = 1.6 Hz,

1H), 8.24 (dd,  $J_1 = 4.0$  Hz,  $J_2 = 1.6$  Hz, 1H), 7.91 (d,  $J = 8.0$  Hz, 1H), 7.49-7.38 (m, 6H), 3.07 (s, 3H). ESI-MS(+):  $m/z$  333.23 [M+H]<sup>+</sup>.

***N*-(5-(3,4-Difluorophenyl)quinolin-8-yl)methanesulfonamide (140).**

Synthesized utilizing Sulfonamide Coupling Method A. Product was purified with a gradient of 0-35% EtOAc in Hexanes. Isolated as a tan solid. Yield = 0.068 g (39%). <sup>1</sup>H NMR (CDCl<sub>3</sub>, 400 MHz)  $\delta$  9.04 (br, 1H), 8.85 (dd,  $J_1 = 4.0$  Hz,  $J_2 = 1.6$  Hz, 1H), 8.23 (dd,  $J_1 = 4.0$  Hz,  $J_2 = 1.6$  Hz, 1H), 7.89 (d,  $J = 8.0$  Hz, 1H), 7.51 (dd,  $J_1 = 8.0$  Hz,  $J_2 = 4.0$  Hz, 1H), 7.46 (d,  $J = 8.0$  Hz, 1H), 7.33-7.14 (m, 3H), 3.08 (s, 3H). ESI-MS(+):  $m/z$  335.41 [M+H]<sup>+</sup>.

***N*-(5-(furan-2-yl)quinolin-8-yl)methanesulfonamide (141).** Synthesized

utilizing Sulfonamide Coupling Method A. Product was purified with a gradient of 0-25% EtOAc in Hexanes. Isolated as a red-brown oil. Yield = 0.091 g (42%). <sup>1</sup>H NMR (CDCl<sub>3</sub>, 400 MHz)  $\delta$  9.03 (br, 1H), 8.81-8.77 (m, 2H), 7.86 (d,  $J = 8.0$  Hz, 1H), 7.73 (d,  $J = 8.0$  Hz, 1H), 7.61 (d,  $J = 1.6$  Hz, 1H), 7.53 (dd,  $J_1 = 8.0$  Hz,  $J_2 = 4.0$  Hz, 1H), 6.66 (d,  $J = 3.2$  Hz, 1H), 6.58 (dd,  $J_1 = 3.2$  Hz,  $J_2 = 1.6$  Hz, 1H), 3.04 (s, 3H). ESI-MS(+):  $m/z$  289.13 [M+H]<sup>+</sup>.

***N*-(5-(Thiophen-2-yl)quinolin-8-yl)methanesulfonamide (142).** Synthesized

utilizing Sulfonamide Coupling Method A. Product was purified with a gradient of 0-55% EtOAc in Hexanes. Isolated as faint yellow crystals. Yield = 0.128 g

(68%).  $^1\text{H}$  NMR ( $\text{CDCl}_3$ , 400 MHz)  $\delta$  9.05 (br, 1H), 8.84 (dd,  $J_1 = 4.0$  Hz,  $J_2 = 1.6$  Hz, 1H), 8.58 (dd,  $J_1 = 8.0$  Hz,  $J_2 = 1.6$  Hz, 1H), 7.88 (d,  $J = 8.0$  Hz, 1H), 7.62 (d,  $J = 8.0$  Hz, 1H), 7.52 (dd,  $J_1 = 8.0$  Hz,  $J_2 = 4.0$  Hz, 1H), 7.45 (dd,  $J_1 = 4.0$  Hz,  $J_2 = 1.6$  Hz, 1H), 7.20-7.18 (m, 2H), 3.07 (s, 3H). ESI-MS(+):  $m/z$  305.33  $[\text{M}+\text{H}]^+$ .

***N*-(5-(Benzo[d][1,3]dioxol-5-yl)quinolin-8-yl)methanesulfonamide (143).**

Synthesized utilizing Sulfonamide Coupling Method A. Product was purified with a gradient of 0-50% EtOAc in Hexanes. Isolated as a faint yellow solid. Yield = 0.086 g (46%).  $^1\text{H}$  NMR ( $\text{CDCl}_3$ , 400 MHz)  $\delta$  9.00 (br, 1H), 8.83 (dd,  $J_1 = 4.0$  Hz,  $J_2 = 1.6$  Hz, 1H), 8.33 (dd,  $J_1 = 8.0$  Hz,  $J_2 = 1.6$  Hz, 1H), 7.88 (d,  $J = 8.0$  Hz, 1H), 7.47-7.44 (m, 2H), 6.95-6.87 (m, 3H), 6.05 (s, 2H), 3.06 (s, 3H). ESI-MS(+):  $m/z$  343.17  $[\text{M}+\text{H}]^+$ .

***N*-(5-(Piperidin-1-yl)quinolin-8-yl)methanesulfonamide (144).**

Synthesized utilizing Sulfonamide Coupling Method A. Product was purified with a gradient of 0-75% EtOAc in Hexanes. Isolated as a yellow solid. Yield = 0.091 g (48%).  $^1\text{H}$  NMR ( $\text{CDCl}_3$ , 400 MHz)  $\delta$  8.80 (dd,  $J_1 = 4.0$  Hz,  $J_2 = 1.6$  Hz, 1H), 8.67 (br, 1H), 8.54 (dd,  $J_1 = 8.0$  Hz,  $J_2 = 1.6$  Hz, 1H), 7.77 (d,  $J = 8.0$  Hz, 1H), 7.48 (dd,  $J_1 = 8.0$  Hz,  $J_2 = 4.0$  Hz, 1H), 7.08 (d,  $J = 8.0$  Hz, 1H), 3.03-2.95 (m, 4H), 2.94 (s, 3H), 1.85 (pent, 4H), 1.66 (br, 2H). ESI-MS(+):  $m/z$  306.11  $[\text{M}+\text{H}]^+$ .

***N*-(5-Morpholinoquinolin-8-yl)methanesulfonamide (145).** Synthesized utilizing Sulfonamide Coupling Method A. Product was purified with a gradient of 0-75% EtOAc in Hexanes. Isolated as a yellow solid. Yield = 0.101 g (51%). <sup>1</sup>H NMR (CDCl<sub>3</sub>, 400 MHz) δ 8.82 (dd, J<sub>1</sub> = 4.0 Hz, J<sub>2</sub> = 2.0 Hz, 1H), 8.72 (br, 1H), 8.56 (dd, J<sub>1</sub> = 8.4 Hz, J<sub>2</sub> = 2.0 Hz, 1H), 7.79 (d, J = 8.4 Hz, 1H), 7.50 (dd, J<sub>1</sub> = 8.4 Hz, J<sub>2</sub> = 4.0 Hz, 1H), 7.14 (d, J = 8.4 Hz, 1H), 3.97 (t, J = 4.4 Hz, 4H), 3.07 (t, J = 4.4 Hz, 4H), 2.97 (s, 3H). ESI-MS(+): *m/z* 308.54 [M+H]<sup>+</sup>.

**5-(3-Chlorophenyl)-8-nitroquinoline.** Synthesized utilizing Suzuki coupling Method B. Product was purified with a gradient of 0-35% EtOAc in Hexanes. Isolated as a tan solid. Yield = 0.222 g (65%). <sup>1</sup>H NMR (CDCl<sub>3</sub>, 400 MHz) δ 9.01 (m, 1H), 8.24 (m, 1H), 8.03 (d, J = 8.4 Hz, 1H), 7.54-7.19 (m, 6H). ESI-MS(+): *m/z* 285.24 [M+H]<sup>+</sup>.

**5-(4-Fluorophenyl)-8-nitroquinoline.** Synthesized utilizing Suzuki coupling Method C. Product was purified with a gradient of 0-35% EtOAc in Hexanes. Isolated as a brown solid. Yield = 0.167 g (53%). <sup>1</sup>H NMR (CDCl<sub>3</sub>, 400 MHz) δ 9.02 (dd, J<sub>1</sub> = 4 Hz, J<sub>2</sub> = 1.6 Hz, 1H), 8.25 (dd, J<sub>1</sub> = 8.4 Hz, J<sub>2</sub> = 1.6 Hz, 1H), 8.04 (d, J = 8.4 Hz, 1H), 7.55 (d, J = 8.4 Hz, 1H), 8.25 (dd, J<sub>1</sub> = 8.4 Hz, J<sub>2</sub> = 4 Hz, 1H), 7.43-7.40 (m, 2H), 7.24-7.20 (m, 2H). ESI-MS(+): *m/z* 269.19 [M+H]<sup>+</sup>.

**5-(4-Methoxyphenyl)-8-nitroquinoline.** Synthesized utilizing Suzuki coupling Method C. Product was purified with a gradient of 0-50% EtOAc in Hexanes. Isolated as a tan solid. Yield = 0.110 g (33%). <sup>1</sup>H NMR (CDCl<sub>3</sub>, 400 MHz) δ 9.05 (dd, J<sub>1</sub> = 4 Hz, J<sub>2</sub> = 1.6 Hz, 1H), 8.33 (dd, J<sub>1</sub> = 8.8 Hz, J<sub>2</sub> = 2 Hz, 1H), 8.06 (d, J = 8.0 Hz, 1H), 7.57 (d, J = 8.0 Hz, 1H), 7.51 (dd, J<sub>1</sub> = 8.8 Hz, J<sub>2</sub> = 4 Hz, 1H), 7.46 (t, J = 8.0 Hz, 1H), 7.06-6.97 (m, 3H), 3.86 (s, 3H). ESI-MS(+): *m/z* 281.31 [M+H]<sup>+</sup>.

**5-(3-Methoxyphenyl)-8-nitroquinoline.** Synthesized utilizing Suzuki coupling Method C. Product was purified with a gradient of 0-50% EtOAc in Hexanes. Isolated as a tan solid. Yield = 0.249 g (75%). <sup>1</sup>H NMR (CDCl<sub>3</sub>, 400 MHz) δ 9.03 (dd, J<sub>1</sub> = 4 Hz, J<sub>2</sub> = 1.6 Hz, 1H), 8.33 (dd, J<sub>1</sub> = 8.8 Hz, J<sub>2</sub> = 1.6 Hz, 1H), 8.05 (d, J = 8.0 Hz, 1H), 7.53 (d, J = 8.0 Hz, 1H), 7.49 (dd, J<sub>1</sub> = 8.8 Hz, J<sub>2</sub> = 4 Hz, 1H), 7.37 (d, J = 8.4 Hz, 1H), 7.07 (d, J = 8.4 Hz, 1H), 3.89 (s, 3H). ESI-MS(+): *m/z* 281.19 [M+H]<sup>+</sup>.

**5-(3-Chloro-4-methoxyphenyl)-8-nitroquinoline.** Synthesized utilizing Suzuki coupling Method B. Product was purified with a gradient of 0-60% EtOAc in Hexanes. Isolated as a tan solid. Yield = 0.3 g (68%). <sup>1</sup>H NMR (CDCl<sub>3</sub>, 400 MHz) δ 9.06 (dd, J<sub>1</sub> = 4 Hz, J<sub>2</sub> = 1.6 Hz, 1H), 8.30 (dd, J<sub>1</sub> = 8.4 Hz, J<sub>2</sub> = 2.0 Hz, 1H), 8.06 (d, J = 8.0 Hz, 1H), 7.54-7.46 (m, 3H), 7.33 (dd, J<sub>1</sub> = 8.4 Hz, J<sub>2</sub> = 2.0 Hz, 1H), 7.11 (d, J = 8.4 Hz, 1H), 4.00 (s, 3H). ESI-MS(+): *m/z* 315.15 [M+H]<sup>+</sup>.

**5-(3,4-Dichlorophenyl)-8-nitroquinoline.** Synthesized utilizing Suzuki coupling Method B. Product was purified with a gradient of 0-50% EtOAc in Hexanes. Isolated as a tan solid. Yield = 0.3 g (75%). ESI-MS(+):  $m/z$  319.23 [M+H]<sup>+</sup>.

**5-(3,5-Dimethoxyphenyl)-8-nitroquinoline.** Synthesized utilizing Suzuki coupling Method C. Product was purified with a gradient of 0-35% EtOAc in Hexanes. Isolated as a brown solid. Yield = 0.194 g (53%). <sup>1</sup>H NMR (CDCl<sub>3</sub>, 400 MHz)  $\delta$  9.07 (dd,  $J_1 = 4$  Hz,  $J_2 = 1.6$  Hz, 1H), 8.36 (dd,  $J_1 = 8.8$  Hz,  $J_2 = 1.6$  Hz, 1H), 8.06 (d,  $J = 8.0$  Hz, 1H), 7.58 (d,  $J = 8.0$  Hz, 1H), 7.51 (dd,  $J_1 = 8.8$  Hz,  $J_2 = 4$  Hz, 1H), 6.60-6.55 (m, 3H), 3.84 (s, 6H). ESI-MS(+):  $m/z$  311.26 [M+H]<sup>+</sup>.

**8-Nitro-5-(phenylethynyl)quinoline.** Synthesized utilizing Sonogashira coupling method. Product was purified with a gradient of 0-35% EtOAc in Hexanes. Isolated as a brown solid. Yield = 0.206 g (63%). <sup>1</sup>H NMR (CDCl<sub>3</sub>, 400 MHz)  $\delta$  9.11 (m, 1H), 8.79 (dd,  $J_1 = 8.8$  Hz,  $J_2 = 1.6$  Hz, 1H), 8.03 (d,  $J = 8.0$  Hz, 1H), 7.83 (d,  $J = 8.0$  Hz, 1H), 7.66-7.64 (m, 3H), 7.45-7.42 (m, 3H). ESI-MS(+):  $m/z$  275.21 [M+H]<sup>+</sup>.

**5-((4-Fluorophenyl)ethynyl)-8-nitroquinoline.** Synthesized utilizing Sonogashira coupling method. Product was purified with a gradient of 0-25% EtOAc in Hexanes. Isolated as an off-white solid. Yield = 0.170 g (49%). <sup>1</sup>H NMR (CDCl<sub>3</sub>, 400 MHz)  $\delta$  9.11 (dd,  $J_1 = 4$  Hz,  $J_2 = 1.6$  Hz, 1H), 8.77 (dd,  $J_1 = 8.0$  Hz,

$J_2 = 1.6$  Hz, 1H), 8.03 (d,  $J = 8.0$  Hz, 1H), 7.82 (d,  $J = 8.0$  Hz, 1H), 7.66-7.62 (m, 3H), 7.15-7.11 (m, 2H). ESI-MS(+):  $m/z$  293.21  $[M+H]^+$ .

*Protocol for Reduction A* – This method was utilized to reduce corresponding nitro compounds into amines, which were utilized in the synthesis of compounds **136-138**, **140-146**, **149-151**, and **154-163**. To a solution of 5-Aryl/Cyclic/Ethynyl-8-nitroquinoline in MeOH (25 mL) and Pd/C (10% loading, 0.05 equiv) was degassed for 5-10 mins. The solution mixture was then purged with hydrogen gas (1 atm) and stirred at room temperature for 1-2 hr. The resulting mixture was then filtered through celite and concentrated. Product was confirmed via TLC and MS and used in next step without further purification.

*Protocol for Reduction B* – This method was utilized to reduce corresponding nitro compounds into amines, which were utilized in the synthesis of compounds **139**, **147-149** and **152-153**. To a solution of Chlorophenyl-8-nitroquinoline in MeOH:Acetone:H<sub>2</sub>O (1:1:1, 15 mL) was added K<sub>2</sub>CO<sub>3</sub> (4 equiv) and sodium dithionate (4 equiv) then allowed to stir at room temperature under nitrogen overnight. The resulting solution was concentrated to remove organic solvents. The resulting aqueous solution was diluted with water (25 mL) and then extracted with EtOAc (3×50ml). The combined organic fractions were concentrated and to yield product. Product was confirmed via TLC and MS and used in next step without further purification.

***N*-(5-Phenylquinolin-8-yl)pyridine-2-sulfonamide (146).** Synthesized utilizing Sulfonamide Coupling Method A. Product was purified with a gradient of 0-40% EtOAc in Hexanes. Isolated as a white solid. Yield = 0.115 g (70%). <sup>1</sup>H NMR (CDCl<sub>3</sub>, 400 MHz) δ 9.60 (br, 1H), 8.81 (dd, J<sub>1</sub> = 4.0 Hz, J<sub>2</sub> = 1.6 Hz, 1H), 8.62-8.60 (m, 1H), 8.22 (dd, J<sub>1</sub> = 8.4 Hz, J<sub>2</sub> = 1.6 Hz, 1H), 8.14 (d, J = 8.0 Hz, 1H), 7.97 (d, J = 8.0 Hz, 1H), 7.87 (td, J<sub>1</sub> = 8.0 Hz, J<sub>2</sub> = 1.6 Hz, 1H), 7.49-7.36 (m, 8H). HR-ESI-MS calcd for [C<sub>20</sub>H<sub>16</sub>N<sub>3</sub>O<sub>2</sub>S]<sup>+</sup>: 362.0958; Found: 362.0951.

***N*-(5-(4-Chlorophenyl)quinolin-8-yl)pyridine-2-sulfonamide (147).** Synthesized utilizing Sulfonamide Coupling Method A. Product was purified with a gradient of 0-40% EtOAc in Hexanes. Isolated as a white solid. Yield = 0.061 g (79%). <sup>1</sup>H NMR (CDCl<sub>3</sub>, 400 MHz) δ 9.60 (br, 1H), 8.80 (dd, J<sub>1</sub> = 4.0 Hz, J<sub>2</sub> = 1.6 Hz, 1H), 8.60 (dd, J<sub>1</sub> = 8.0 Hz, J<sub>2</sub> = 1.6 Hz, 1H), 8.15 (m, 2H), 7.96 (d, J = 8.0 Hz, 1H), 7.87 (td, J<sub>1</sub> = 8.0 Hz, J<sub>2</sub> = 1.6 Hz, 1H), 7.44-7.29 (m, 7H). HR-ESI-MS calcd for [C<sub>20</sub>H<sub>15</sub>ClN<sub>3</sub>O<sub>2</sub>S]<sup>+</sup>: 396.0568; Found: 396.0563.

***N*-(5-(3-Chlorophenyl)quinolin-8-yl)pyridine-2-sulfonamide (148).** Synthesized utilizing Sulfonamide Coupling Method A. Product was purified with a gradient of 0-50% EtOAc in Hexanes. Isolated as a light pink solid. Yield = 0.05 g (16%). <sup>1</sup>H NMR (CDCl<sub>3</sub>, 400 MHz) δ 9.60 (br, 1H), 8.82-8.80 (m, 1H), 8.61 (dd, J<sub>1</sub> = 8.0 Hz, J<sub>2</sub> = 1.6 Hz, 1H), 8.17-8.12 (m, 2H), 7.97 (d, J = 8.0 Hz,

1H), 7.87 (td,  $J_1 = 8.0$  Hz,  $J_2 = 1.6$  Hz, 1H), 7.43-7.32 (m, 6H), 7.18 (t,  $J = 8.0$  Hz, 1H). HR-ESI-MS calcd for  $[C_{20}H_{15}ClN_3O_2S]^+$ : 396.0568; Found: 396.0565.

***N*-(5-(4-Fluorophenyl)quinolin-8-yl)pyridine-2-sulfonamide (149).**

Synthesized utilizing Sulfonamide Coupling Method A. Product was purified with a gradient of 0-45% EtOAc in Hexanes. Isolated as a light yellow solid. Yield = 0.091 g (36%).  $^1H$  NMR ( $CDCl_3$ , 400 MHz)  $\delta$  9.59 (br, 1H), 8.80-8.79 (m, 1H), 8.60 (dd,  $J_1 = 8.0$  Hz,  $J_2 = 1.6$  Hz, 1H), 8.15-8.11 (m, 2H), 7.97 (d,  $J = 8.0$  Hz, 1H), 7.88 (td,  $J_1 = 8.0$  Hz,  $J_2 = 1.6$  Hz, 1H), 7.44-7.31 (m, 5H), 7.17-7.13 (m, 2H). HR-ESI-MS calcd for  $[C_{20}H_{15}FN_3O_2S]^+$ : 380.0864; Found: 380.0866.

***N*-(5-(4-Methoxyphenyl)quinolin-8-yl)pyridine-2-sulfonamide (150).**

Synthesized utilizing Sulfonamide Coupling Method A. Product was purified with a gradient of 0-50% EtOAc in Hexanes. Isolated as a white solid. Yield = 0.12 g (43%).  $^1H$  NMR ( $CDCl_3$ , 400 MHz)  $\delta$  9.60 (br, 1H), 8.80-8.79 (m, 1H), 8.61-8.60 (m, 1H), 8.25 (dd,  $J_1 = 8.0$  Hz,  $J_2 = 1.6$  Hz, 1H), 8.14 (dd,  $J_1 = 4.0$  Hz,  $J_2 = 0.8$  Hz, 1H), 7.97 (d,  $J = 8.0$  Hz, 1H), 7.88 (td,  $J_1 = 8.0$  Hz,  $J_2 = 1.6$  Hz, 1H), 7.42-7.35 (m, 4H), 6.97-6.91 (m, 3H). HR-ESI-MS calcd for  $[C_{21}H_{18}N_3O_3S]^+$ : 392.1063; Found: 392.1061.

***N*-(5-(3-Methoxyphenyl)quinolin-8-yl)pyridine-2-sulfonamide (151).**

Synthesized utilizing Sulfonamide Coupling Method A. Product was purified with

a gradient of 0-70% EtOAc in Hexanes. Isolated as a white solid. Yield = 0.074 g (21%).  $^1\text{H}$  NMR ( $\text{CDCl}_3$ , 400 MHz)  $\delta$  9.59 (br, 1H), 8.79 (dd,  $J_1 = 4.0$  Hz,  $J_2 = 1.6$  Hz, 1H), 8.61-8.59 (m, 1H), 8.22 (dd,  $J_1 = 8.0$  Hz,  $J_2 = 1.6$  Hz, 1H), 8.13-8.11 (m, 1H), 7.95 (d,  $J = 8.0$  Hz, 1H), 7.86 (td,  $J_1 = 8.0$  Hz,  $J_2 = 1.6$  Hz, 1H), 7.41-7.29 (m, 5H), 7.01-6.00 (m, 2H). HR-ESI-MS calcd for  $[\text{C}_{21}\text{H}_{18}\text{N}_3\text{O}_3\text{S}]^+$ : 392.1063; Found: 392.1065.

***N*-(5-(3-Chloro-4-methoxyphenyl)quinolin-8-yl)pyridine-2-sulfonamide (152).**

Synthesized utilizing Sulfonamide Coupling Method A. Product was purified with a gradient of 0-100% EtOAc in Hexanes. Isolated as a white solid. Yield = 0.15 g (51%).  $^1\text{H}$  NMR ( $\text{CDCl}_3$ , 400 MHz)  $\delta$  9.59 (br, 1H), 8.82 (dd,  $J_1 = 4.4$  Hz,  $J_2 = 2.0$  Hz, 1H), 8.61-8.60 (m, 1H), 8.19 (dd,  $J_1 = 8.4$  Hz,  $J_2 = 2.0$  Hz, 1H), 8.13 (d,  $J = 8.0$  Hz, 1H), 7.96 (d,  $J = 8.0$  Hz, 1H), 7.88 (td,  $J_1 = 8.0$  Hz,  $J_2 = 1.6$  Hz, 1H), 7.43-7.39 (m, 3H), 7.36 (d,  $J = 8.0$  Hz, 1H), 7.26 (dd,  $J_1 = 8.4$  Hz,  $J_2 = 2.0$  Hz, 1H), 7.04 (d,  $J = 8.4$  Hz, 1H), 3.97 (s, 3H). HR-ESI-MS calcd for  $[\text{C}_{21}\text{H}_{16}\text{ClN}_3\text{NaO}_3\text{S}]^+$ : 448.0493; Found: 448.0491.

***N*-(5-(3,4-Dichlorophenyl)quinolin-8-yl)pyridine-2-sulfonamide (153).**

Synthesized utilizing Sulfonamide Coupling Method A. Product was purified with a gradient of 0-100% EtOAc in Hexanes. Isolated as a white solid. Yield = 0.17 g (58%).  $^1\text{H}$  NMR ( $\text{CDCl}_3$ , 400 MHz)  $\delta$  9.61 (br, 1H), 8.85 (dd,  $J_1 = 4.4$  Hz,  $J_2 = 2.0$  Hz, 1H), 8.62-8.60 (m, 1H), 8.15-8.12 (m, 2H), 7.99 (d,  $J = 8.0$  Hz, 1H), 7.89 (td,

$J_1 = 8.0$  Hz,  $J_2 = 1.6$  Hz, 1H), 7.56-7.35 (m, 5H), 7.23 (m, 1H). HR-ESI-MS calcd for  $[C_{20}H_{14}Cl_2N_3O_2S]^+$ : 430.0178; Found: 430.0180.

***N*-(5-(3,5-Dimethoxyphenyl)quinolin-8-yl)pyridine-2-sulfonamide (154).**

Synthesized utilizing Sulfonamide Coupling Method A. Product was purified with a gradient of 0-50% EtOAc in Hexanes. Isolated as an off-white solid. Yield = 0.145 g (56%).  $^1H$  NMR ( $CDCl_3$ , 400 MHz)  $\delta$  9.58 (br, 1H), 8.77-8.75 (m, 1H), 8.58-8.57 (m, 1H), 8.26 (dd,  $J_1 = 8.0$  Hz,  $J_2 = 1.6$  Hz, 1H), 8.12 (dd,  $J_1 = 8.0$  Hz,  $J_2 = 0.8$  Hz, 1H), 7.94 (dd,  $J_1 = 8.0$  Hz,  $J_2 = 1.6$  Hz, 1H), 7.86 (td,  $J_1 = 8.0$  Hz,  $J_2 = 1.6$  Hz, 1H), 7.41-7.34 (m, 3H), 6.50 (m, 3H), 3.79 (s, 6H). HR-ESI-MS calcd for  $[C_{22}H_{20}N_3O_4S]^+$ : 422.1169; Found: 422.1165.

***N*-(5-Phenethylquinolin-8-yl)pyridine-2-sulfonamide (155).** Synthesized

utilizing Sulfonamide Coupling Method A. Product was purified with a gradient of 0-100% EtOAc in Hexanes. Isolated as an off-white solid. Yield = 0.045 g (15%).  $^1H$  NMR ( $CDCl_3$ , 400 MHz)  $\delta$  9.51 (br, 1H), 8.77 (d,  $J = 2.4$  Hz, 1H), 8.57 (d,  $J = 3.6$  Hz, 1H), 8.27 (d,  $J = 8.4$  Hz, 1H), 8.07 (d,  $J = 8.4$  Hz, 1H), 7.82-7.81 (m, 2H), 7.42-7.11 (m, 8H), 3.23 (t,  $J = 8.4$  Hz, 2H), 2.95 (t,  $J = 8.4$  Hz, 2H). HR-ESI-MS calcd for  $[C_{22}H_{20}N_3O_2S]^+$ : 390.1271; Found: 390.1265.

***N*-(5-(4-Fluorophenethyl)quinolin-8-yl)pyridine-2-sulfonamide (156).**

Synthesized utilizing Sulfonamide Coupling Method A. Product was purified with

a gradient of 0-100% EtOAc in Hexanes. Isolated as an off-white solid. Yield = 0.07 g (31%).  $^1\text{H}$  NMR ( $\text{CDCl}_3$ , 400 MHz)  $\delta$  9.50 (br, 1H), 8.75 (d,  $J = 2.4$  Hz, 1H), 8.56 (d,  $J = 3.6$  Hz, 1H), 8.24 (d,  $J = 8.4$  Hz, 1H), 8.07 (d,  $J = 8.4$  Hz, 1H), 7.83-7.78 (m, 2H), 7.43-7.35 (m, 2H), 7.17 (d,  $J = 8.4$  Hz, 1H), 7.03-7.00 (m, 2H), 6.92 (m, 2H), 3.21 (t,  $J = 8.4$  Hz, 2H), 2.92 (t,  $J = 8.4$  Hz, 2H). HR-ESI-MS calcd for  $[\text{C}_{22}\text{H}_{18}\text{FN}_3\text{NaO}_2\text{S}]^+$ : 430.0996; Found: 430.0994.

**6-Bromo-8-nitroquinoline.** A solution of 4-Bromo-2-nitroaniline (5 g, 23.04 mmol) in Toluene (30 mL) and 6M HCl (30 mL) was heated to reflux for ~15 min. To this was added Acrolein (1.93 g, 34.6 mmol) and allowed to reflux for an additional 2 h. The resulting solution was then partitioned, and the organic layer was discarded. The aqueous layer was made strongly basic (pH 10-11) with 6M NaOH. The resulting basic mixture was then extracted with EtOAc (3x50mL). The combined organic layers were dried over  $\text{MgSO}_4$ , filtered, concentrated then purified via silica gel chromatography eluting 0-40% EtOAc in Hexanes. The desired product was isolated as a pink-orange solid. Yield = 1.21 g (21%).  $^1\text{H}$  NMR ( $\text{CDCl}_3$ , 400 MHz)  $\delta$  9.08 (dd,  $J_1 = 4.0$  Hz,  $J_2 = 1.6$  Hz, 1H), 8.20-8.18 (m, 2H), 8.13 (d,  $J_1 = 2.4$  Hz, 1H), 7.60 (dd,  $J_1 = 8.4$  Hz,  $J_2 = 4$  Hz, 1H). ESI-MS(+):  $m/z$  253.19  $[\text{M}+\text{H}]^+$ .

**8-Nitro-6-(phenylethynyl)quinoline.** Synthesized utilizing Sonogashira coupling method. Product was purified with a gradient of 0-40% EtOAc in

Hexanes. Isolated as an off-white solid. Yield = 0.12 g (40%).  $^1\text{H}$  NMR ( $\text{CDCl}_3$ , 400 MHz)  $\delta$  9.00 (dd,  $J_1 = 4.4$  Hz,  $J_2 = 1.6$  Hz, 1H), 8.20-8.09 (m, 3H), 7.56-7.51 (m, 3H), 7.38-7.36 (m, 3H). ESI-MS(+):  $m/z$  275.21  $[\text{M}+\text{H}]^+$ .

**6-((4-Fluorophenyl)ethynyl)-8-nitroquinoline.** Synthesized utilizing Sonogashira coupling method. Product was purified with a gradient of 0-40% EtOAc in Hexanes. Isolated as an off-white solid. Yield = 0.15 g (50%). ESI-MS(+):  $m/z$  293.11  $[\text{M}+\text{H}]^+$ .

**6-((3,5-Dimethoxyphenyl)ethynyl)-8-nitroquinoline.** Synthesized utilizing Sonogashira coupling method. Product was purified with a gradient of 0-40% EtOAc in Hexanes. Isolated as a tan solid. Yield = 0.29 g (73%).  $^1\text{H}$  NMR ( $\text{CDCl}_3$ , 400 MHz)  $\delta$  9.07 (dd,  $J_1 = 4.0$  Hz,  $J_2 = 1.6$  Hz, 1H), 8.24 (dd,  $J_1 = 4.0$  Hz,  $J_2 = 1.6$  Hz, 1H), 8.19-8.15 (m, 2H), 7.60 (dd,  $J_1 = 8.4$  Hz,  $J_2 = 4.4$  Hz, 1H), 6.73 (d,  $J = 2.4$  Hz), 6.53 (t,  $J = 2.4$  Hz), 3.82 (s, 6H). ESI-MS(+):  $m/z$  335.33  $[\text{M}+\text{H}]^+$ .

***N*-(6-Phenethylquinolin-8-yl)pyridine-2-sulfonamide (157).** Synthesized utilizing Sulfonamide Coupling Method A. Product was purified with a gradient of 0-100% EtOAc in Hexanes. Isolated as an off-white solid. Yield = 0.065 g (35%).  $^1\text{H}$  NMR ( $\text{CDCl}_3$ , 400 MHz)  $\delta$  9.48 (br, 1H), 8.71 (d,  $J = 4.4$  Hz, 1H), 8.56 (d,  $J = 4.4$  Hz, 1H), 8.06 (d,  $J = 8.0$  Hz, 1H), 7.97 (d,  $J = 8.0$  Hz, 1H), 7.85-7.77 (m, 2H),

7.37-7.34 (m, 2H), 7.24-7.11 (m, 7H), 3.05 (t, J = 8.4 Hz, 2H), 2.96 (t, J = 8.4 Hz, 2H). HR-ESI-MS calcd for  $[C_{22}H_{20}N_3O_2S]^+$ : 390.1271; Found: 390.1268.

**N-(6-(4-Fluorophenethyl)quinolin-8-yl)pyridine-2-sulfonamide (158).**

Synthesized utilizing Sulfonamide Coupling Method A. Product was purified with a gradient of 0-100% EtOAc in Hexanes. Isolated as an off-white solid. Yield = 0.075 g (36%).  $^1H$  NMR ( $CDCl_3$ , 400 MHz)  $\delta$  9.45 (br, 1H), 8.72 (d, J = 4.4 Hz, 1H), 8.56 (d, J = 4.4 Hz, 1H), 8.05 (d, J = 8.0 Hz, 1H), 7.98 (d, J = 8.0 Hz, 1H), 7.82-7.78 (m, 2H), 7.39-7.36 (m, 2H), 7.13 (s, 1H), 7.04-7.01 (m, 2H), 6.91-6.87 (m, 2H), 3.02 (t, J = 8.4 Hz, 2H), 2.94 (t, J = 8.4 Hz, 2H). HR-ESI-MS calcd for  $[C_{22}H_{18}FN_3NaO_2S]^+$ : 430.0996; Found: 430.0994.

**N-(6-(3,5-Dimethoxyphenethyl)quinolin-8-yl)pyridine-2-sulfonamide (159).**

Synthesized utilizing Sulfonamide Coupling Method A. Product was purified with a gradient of 0-100% EtOAc in Hexanes. Isolated as an off-white solid. Yield = 0.165 g (45%).  $^1H$  NMR ( $CDCl_3$ , 400 MHz)  $\delta$  9.50 (br, 1H), 8.73 (d, J = 4.4 Hz, 1H), 8.57 (d, J = 4.4 Hz, 1H), 8.07 (d, J = 8.0 Hz, 1H), 8.02 (d, J = 8.0 Hz, 1H), 7.87 (s, 1H), 7.83 (td,  $J_1 = 8.0$  Hz,  $J_2 = 1.6$  Hz, 1H), 7.41-7.35 (m, 2H), 7.21 (s, 1H), 6.32 (s, 3H), 3.74 (s, 6H), 3.06 (t, J = 8.4 Hz, 2H), 2.92 (t, J = 8.4 Hz, 2H). HR-ESI-MS calcd for  $[C_{24}H_{24}N_3O_4S]^+$ : 450.1482; Found: 450.1483.

## **5.5 Acknowledgements**

Chapter 5 highlights the work of a publication currently in preparation. The manuscript in preparation was authored by the following: Christian Perez, Benjamin Dick, Peter F. Glatt, and Seth M. Cohen with a planned title of “Metal-Binding Pharmacophore Library Yields Discovery of a Novel Glyoxalase 1 Inhibitor.” The dissertation author was the primary researcher for the data presented. The co-authors listed in these publications also participated in the research.

## 5.6 References

1. Kessler, R. C.; Chiu, W. T.; Demler, O.; Walters, E. E., Prevalence, severity, and comorbidity of 12-month DSM-IV disorders in the National Comorbidity Survey Replication. *Arch. Gen. Psychiatr.* **2005**, *62* (6), 617-627.
2. Kessler, R. C.; Petukhova, M.; Sampson, N. A.; Zaslavsky, A. M.; Wittchen, H. U., Twelve-month and lifetime prevalence and lifetime morbid risk of anxiety and mood disorders in the United States. *Int. J. Methods Psychiatr. Res.* **2012**, *21* (3), 169-184.
3. Thornalley, P. J., The glyoxalase system in health and disease. *Mol Aspects Med* **1993**, *14* (4), 287-371.
4. Thornalley, P. J., The glyoxalase system: new developments towards functional characterization of a metabolic pathway fundamental to biological life. *Biochem J* **1990**, *269* (1), 1-11.
5. Mannervik, B., Molecular enzymology of the glyoxalase system. *Drug Metabol Drug Interact* **2008**, *23* (1-2), 13-27.
6. Thornalley, P. J., Protecting the genome: defence against nucleotide glycation and emerging role of glyoxalase I overexpression in multidrug resistance in cancer chemotherapy. *Biochem Soc Trans* **2003**, *31* (Pt 6), 1372-7.
7. Creighton, D. J.; Zheng, Z. B.; Holewinski, R.; Hamilton, D. S.; Eiseman, J. L., Glyoxalase I inhibitors in cancer chemotherapy. *Biochem Soc Trans* **2003**, *31* (Pt 6), 1378-82.
8. Thornalley, P. J., Advances in glyoxalase research. Glyoxalase expression in malignancy, anti-proliferative effects of methylglyoxal, glyoxalase I inhibitor diesters and S-D-lactoylglutathione, and methylglyoxal-modified protein binding and endocytosis by the advanced glycation endproduct receptor. *Crit Rev Oncol Hematol* **1995**, *20* (1-2), 99-128.
9. Fahrni, C. J.; O'Halloran, T. V., Aqueous coordination chemistry of quinoline-based fluorescence probes for the biological chemistry of zinc. *J Am Chem Soc* **1999**, *121* (49), 11448-11458.

10. Taki, M.; Wolford, J. L.; O'Halloran, T. V., Emission ratiometric imaging of intracellular zinc: design of a benzoxazole fluorescent sensor and its application in two-photon microscopy. *J Am Chem Soc* **2004**, *126* (3), 712-3.
11. Rouffet, M.; de Oliveira, C. A.; Udi, Y.; Agrawal, A.; Sagi, I.; McCammon, J. A.; Cohen, S. M., From sensors to silencers: quinoline- and benzimidazole-sulfonamides as inhibitors for zinc proteases. *J Am Chem Soc* **2010**, *132* (24), 8232-3.
12. Chai, S. C.; Ye, Q. Z., Metal-mediated inhibition is a viable approach for inhibiting cellular methionine aminopeptidase. *Bioorg Med Chem Lett* **2009**, *19* (24), 6862-4.
13. Molecular Operating Environment (MOE), 2013.08; Chemical Computing Group ULC, 1010 Sherbooke St. West, Suite #910, Montreal, QC, Canada, H3A 2R7, 2018.
14. Liu, M.; Yuan, M. G.; Luo, M. X.; Bu, X. Z.; Luo, H. B.; Hu, X. P., Binding of curcumin with glyoxalase I: Molecular docking, molecular dynamics simulations, and kinetics analysis. *Biophys. Chem.* **2010**, *147* (1-2), 28-34.
15. Santel, T.; Pflug, G.; Hemdan, N. Y. A.; Schafer, A.; Hollenbach, M.; Buchold, M.; Hintersdorf, A.; Lindner, I.; Otto, A.; Bigl, M.; Oerlecke, I.; Hutschenreuter, A.; Sack, U.; Huse, K.; Groth, M.; Birkemeyer, C.; Schellenberger, W.; Gebhardt, R.; Platzner, M.; Weiss, T.; Vijayalakshmi, M. A.; Kruger, M.; Birkenmeier, G., Curcumin Inhibits Glyoxalase 1-A Possible Link to Its Anti-Inflammatory and Anti-Tumor Activity. *Plos One* **2008**, *3* (10).
16. Yadav, A.; Kumar, R.; Sunkaria, A.; Singhal, N.; Kumar, M.; Sandhir, R., Evaluation of potential flavonoid inhibitors of glyoxalase-I based on virtual screening and in vitro studies. *J. Biomol. Struct. Dyn.* **2016**, *34* (5), 993-1007.
17. Creighton, D. J.; Zheng, Z. B.; Holewinski, R.; Hamilton, D. S.; Eiseman, J. L., Glyoxalase I inhibitors in cancer chemotherapy. *Biochem. Soc. Trans.* **2003**, *31*, 1378-1382.
18. Kawatani, M.; Okumura, H.; Honda, K.; Kanoh, N.; Muroi, M.; Dohmae, N.; Takami, M.; Kitagawa, M.; Futamura, Y.; Imoto, M.; Osada, H., The identification

of an osteoclastogenesis inhibitor through the inhibition of glyoxalase I. *P. Natl. Acad. Sci.* **2008**, *105* (33), 11691-11696.

19. Yuan, M. G.; Luo, M. X.; Song, Y.; Xu, Q.; Wang, X. F.; Cao, Y.; Bu, X. Z.; Ren, Y. L.; Hu, X. P., Identification of curcumin derivatives as human glyoxalase I inhibitors: A combination of biological evaluation, molecular docking, 3D-QSAR and molecular dynamics simulation studies. *Bioorg. Med. Chem.* **2011**, *19* (3), 1189-1196.

20. Zhang, H.; Zhai, J.; Zhang, L. P.; Li, C. Y.; Zhao, Y. N.; Chen, Y. Y.; Li, Q.; Hu, X. P., In Vitro Inhibition of Glyoxalase I by Flavonoids: New Insights from Crystallographic Analysis. *Curr. Top. Med. Chem* **2016**, *16* (4), 460-466.

21. Al-Balas, Q. A.; Hassan, M. A.; Al-Shar'i, N. A.; Mhaidat, N. M.; Almaaytah, A. M.; Al-Mahasneh, F. M.; Isawi, I. H., Novel glyoxalase-I inhibitors possessing a "zinc-binding feature" as potential anticancer agents. *Drug Des. Dev. Ther.* **2016**, *10*, 2623-2629.

22. Takasawa, R.; Takahashi, S.; Saeki, K.; Sunaga, S.; Yoshimori, A.; Tanuma, S. I., Structure-activity relationship of human GLO I inhibitory natural flavonoids and their growth inhibitory effects. *Bioorg. Med. Chem.* **2008**, *16* (7), 3969-3975.